The role of receptor tyrosine kinase signalling in HER-2-positive cells and Trastuzumab (Herceptin) Resistance in Breast Cancer.

A Thesis submitted for the degree of Ph.D.

by Brigid Browne, BSc

October 2008

The work in this thesis was carried out under the supervision of

Dr. Norma O'Donovan,
Prof. Martin Clynes & Prof. John Crown

National Institute of Cellular Biotechnology
School of Biotechnology
Dublin City University

I hereby certify that this material, which I now submit for assessment on the programme of study leading to the award of Ph D. is entirely my own work, that I have exercised reasonable care to ensure that the work is original, and does not to the best of my knowledge breach any law of copyright, and has not been taken from the work of others save and to the extent that such work has been cited and acknowledged within the text of my work.

Signed:_____ **ID No.:** 54148791

Date:_____

Acknowledgements

First and foremost I would like to thank my supervisor, Dr. Norma O'Donovan, for all you have done for me during the last five years; for having faith in me in the first place, for the continuous support throughout the project, and for making sure I got over the final hurdles of the toughest last few months. To Prof. John Crown, thank you for giving me the opportunity to do a PhD, and for all that I have learnt from working in your group. I hope, as your first PhD student, that I have done you proud, and I certainly aspire to keep doing so. I would like to thank Prof. Martin Clynes for welcoming me into the NICB, and for the encouragement, the insights and the help with the project throughout the years.

During the years, I have been taught by expert scientists at St. Vincent's University Hospital, at UCLA and at the NICB, and I realise that I am very lucky to have had these invaluable experiences. I am very grateful for the opportunity I was given to work with Dr. Dennis Slamon at UCLA, where this PhD project began. Thanks to Dr. Slamon for welcoming me to the lab and for all that I learned while I was there. I also thank Prof. Joe Duffy in St. Vincent's Hospital, who originally took me on during my fourth year project, starting me on the road towards this PhD; thank you for your continuous support of both me and my work over the many years since then.

Many others were involved with different parts of this project. Thanks to Dr. Anne-Marie Larkin for teaching me immunohistochemistry. Thanks to Dr. Paul Dowling, who performed the proteomics work. Thanks to Dr. Finbarr O'Sullivan for help with confocal microscopy. Thank you to Salima Soualhi who helped with the new resistant cells. I would also like to thank ICORG, and Dr Susan Kennedy, Jo Ballot, Dr. Zulfi Qadir and Dr. Thamir Mahgoub in St.Vincent's, and Dr. John Kennedy and Barbara Dunne in St. James' Hospital for help with obtaining the patient samples and information. I was very lucky to be funded by the Cancer Clinical Research Trust, and the Tri-to-beat-Cancer group.

Thanks to the many others in UCLA who taught me a lot, particularly Dr. Mark Pegram and Dr. Natarajan Venkatesan, with whom I spent a lot of time. And to Dr. Neil O'Brien, you inspired me back in the St. Vincent's days, and it's been great to work (though trans-Atlantically!) with you again these past couple of years.

A very special thank you to the others in my group – particularly to Dr. Brendan Corkery and Alex Eustace, who helped me out with blots and cells in the last few months. Also to Dr. Denis Collins and Aoife Devery, who were there when it all began for me in A126. Thank you all for all the laughs, I can only imagine I haven't

been the easiest to work with the past few months when the stress really started to get to me. Thank you for putting up with the silence-in-the-clean-room rules, and for the rants about missing antibodies! I only hope others will be as patient with you as you were with me when your time comes! Denis, you've had your time already, I'm honoured to follow in your footsteps. I'd like to include Norma in this thank you too; thank you for your patience and your calming reassurances, especially through my Tourette's episodes!

On a personal note, I want to say a big thank you to everyone at the NICB – I can't name everyone, but especially the gang in the office area; Erica, Sandra, Naomi, Brendan, Raj, Ewa, Alan; thank you for the constant supply of chocolate, it was badly needed at times. To the coffee and lunch gang; to Verena for the chats and the advice along the way. To Rob and all of you in toxicology for welcoming us A126ers into the group. To Carol and Yvonne for all their help over the years and to Donnacha and Mick for solving various problems along the way. To Aisling and Eadaoin who inspired me and assured me I would get through it all alive!

An important thank you to my parents, Jim and Biddy; I hope the 'bag of weasels' times were worth it! To the rest of my family too, and to my new family, including Bernard and Patricia, thanks for your support and for the many lasagnes and cheesecakes! I also want to thank my friends, especially Leah and Laura, who have put up with my absences the last couple of years, but who were always happy to be called on when a de-stressing night out was needed. Thank you!

My last thank you is to my husband, Niall. I haven't been the most fun the last year or so; thank you for sticking by me, for listening to me, for giving me lifts, for making many many cups of tea, for supplying chocolate biscuits during the 'bad days', for hiding the chocolate biscuits during the 'healthy days', and for amazingly knowing which days where which! Most of all thank you for marrying me and for being proud of me. I look forward to many days of adventure together as Dr-Mrs-Brigid-Browne-O'Gorman!

Brigid Browne

Table of Contents

Abstract

HER-2 gene amplification or overexpression occurs in approximately 25 % of breast cancers, and trastuzumab (Tmab) is a monoclonal antibody currently used to treat patients with HER-2-overexpressing breast cancer. Signalling through alternative receptor tyrosine kinases, such as insulin-like growth factor I receptor (IGF-IR), has been implicated in resistance to Tmab. The main aim of this study was to investigate mechanisms of resistance and in particular the role of IGF-IR in resistance to Tmab.

Response to Tmab was analysed in a panel of HER-2-positive breast cancer cell lines; no correlation was found between HER-2, IGF-IR, EGFR expression or phosphorylation and response to Tmab. However, both HER-2 and phospho-HER-2 levels were found to correlate positively with phospho-IGF-IR levels (HER-2, $p = 0.16$; p-HER-2, $p = 0.002$).

Tmab (T)-resistant cells showed reduced response to Tmab compared to parental cells. T-resistant BT474 have significantly elevated HER-2, phospho-HER-2, EGFR and phospho-EGFR levels compared to parental cells, while T-resistant SKBR3 cells have significantly elevated IGF-IR levels compared to parental cells ($p = 0.026$).

Targeting IGF-IR with anti-IGF-IR siRNA or an IGF-IR tyrosine kinase inhibitor (TKI) (NVP-AEW541) inhibited the growth of both parental and T-resistant SKBR3 and BT474 cells. Combined treatment with Tmab and IGF-IR inhibitors also inhibited significantly more proliferation than single agents in T-resistant BT474 cells, and in parental and T-resistant SKBR3 cells.

SKBR3 cells were conditioned in lapatinib (a dual HER-2/EGFR TKI), and the conditioned SKBR3-L cells showed significantly reduced response to lapatinib, and to Tmab, compared to parental SKBR3 cells. Phosphoproteomic analysis revealed alterations in the levels of a number of phosphoproteins in lapatinib resistant cells.

HER-2 and IGF-IR expression were measured by immunohistochemistry in tissue microarrays (TMAs) of patient breast tumour samples. Membrane IGF-IR staining correlated inversely with HER-2 expression ($p = 0.026$).

In conclusion, these data suggest that increased signalling through alternative RTKs may play a role in acquired resistance to Tmab. The combination of anti-IGF-IR therapies with Tmab may be clinically beneficial for patients with HER-2-positive breast cancer. We have identified a number of phosphoproteins with potential involvement in trastuzumab and/or lapatinib resistance, and further analysis of these targets may lead to novel therapeutic targets in HER-2-resistant breast cancer.

Chapter 1

INTRODUCTION

1.1 HER-2 IN BREAST CANCER

A recent analysis of breast tumours has identified four distinct sub-types of tumours [1, 2]. The sub-types are classified as (i) luminal (further sub-divided into A and B) (ii) HER-2 positive/ER negative, (iii) normal-like and (iv) basal-like. The basal-like sub-type lacks expression of estrogen and progesterone receptors and HER-2. A number of studies have shown that the HER-2 positive and the basal-like sub-types have a poorer prognosis than either luminal or normal-like tumours [1-3]. Many efforts are now underway to develop and improve HER-targeted therapies. The following section will review the structure and function of HER-2 and the HER family, and describe the downstream signalling events which they activate. The role of HER-2 in cancer development, and the value of HER-2 as a prognostic and predictive marker in breast cancer will also be reviewed. Efforts to target HER-2 with targeted therapeutics will also be briefly reviewed.

1.1.1 The HER system/signalling pathway

1.1.1.1 HER family structure

The HER system consists of at least 12 ligands that interact with four known receptor tyrosine kinases (RTKs), resulting in a signalling network that regulates cellular processes such as proliferation, differentiation, cell survival, and gene transcription. The HER receptors are expressed in many tissues of epithelial, mesenchymal, and neuronal origin, where they play fundamental roles in development, proliferation and differentiation. The HER-2/neu/c-ErbB-2 proto-oncogene is located on chromosome 17q12, and encodes a 185 kilo Dalton (kd) transmembrane glycoprotein belonging to the epidermal growth factor receptor (EGFR) family [4-6]. This family includes four known members; EGFR (HER-1 or erbB1) (170 kd), HER-2 (neu or erbB2), HER-3 (erbB3) (180 kd), and HER-4 (erbB4) (180 kd). All four receptors have in common an extra-cellular ligand-binding domain, a single hydrophobic transmembrane domain, and a cytoplasmic tyrosine kinase domain. Four subdomains have been identified in the extracellular domain; subdomains I (L1) and III (L2) mediate ligand binding, while the cysteine-rich subdomains II (S1/CR1) and IV (S2/CR2) play roles in receptor dimerization [fig 1.1.1] [7].

At least 12 ligands are known to interact with the HER family, including EGF, transforming growth factor-a (TGF-a), amphiregulin, epiregulin, betacellulin, and heparin-binding EGF-like growth factor (HB-EGF), which have higher affinity for EGFR, and neuregulins 1-4, which have higher affinity for HER-3 and HER-4 [8].

In the resting state, the receptors exist as monomers which, in response to ligand-binding, form either homo- or heterodimers. The crystal structure of ligand bound EGFR shows that ligands bind EGFR in a bivalent manner, forming a 2:2 complex with EGFR dimers [9, 10]. The structure of unliganded HER-3 suggests a similar dimerization conformation [11]. No specific endogenous ligand has been identified for HER-2, but ligand binding to other members of the HER family induces receptor heterodimerization and activation of HER-2. The crystal structure of the HER-2 ectodomain was recently described, and reveals that the HER-2 ectodomain conformation is very different to that of the unliganded HER-3, but rather is similar to

the EGFR ectodomain in its liganded conformation. The potential ligand binding site in HER-2 also differs significantly from that of EGFR and HER-3, resulting in a receptor structure that is constitutively poised in an active conformation [fig 1.1.2] [12].
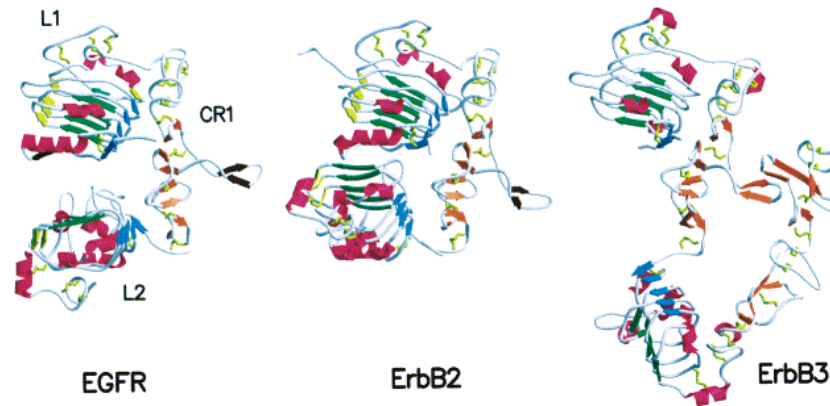
Figure 1.1.1. Ribbon structures comparing ErbB2(1–509) with sEGFR501 and sErbB3(1–621) as determined by X-ray crystallography: helices are indicated by curled, red ribbons and strands by broad arrows. The blue, green, and yellow strands depict the three prominent parallel sheets within the L1 and L2 domains. The strands in the cysteine-rich domains are coloured orange, except for those in the CR1 loop which are coloured brown. The side chains of disulfide-linked cysteine residues are depicted as yellow sticks [From Garrett *et al*, 2003].

Dimerization is accompanied by trans-phosphorylation of specific tyrosine residues within the cytoplasmic tail, which leads to the activation of numerous signalling pathways [fig 1.1.2]. The kinase domain of HER-3 is inactive [13], and its signalling functions are therefore mediated through the kinase of its heterodimeric partners. HER-2 is the preferred dimerization partner for each of the HER receptors [14, 15], and as HER-2 has the strongest kinase activity, dimers containing HER-2 generate a stronger intracellular signal than other complexes [16]. HER-2/HER-3 dimers are believed to be the most active and potent signalling heterodimers of the family. In addition, HER-2-containing dimers undergo slower dissociation and endocytosis, and are more frequently recycled back to the cell surface, prolonging the potent signals (reviewed in [7, 17]).
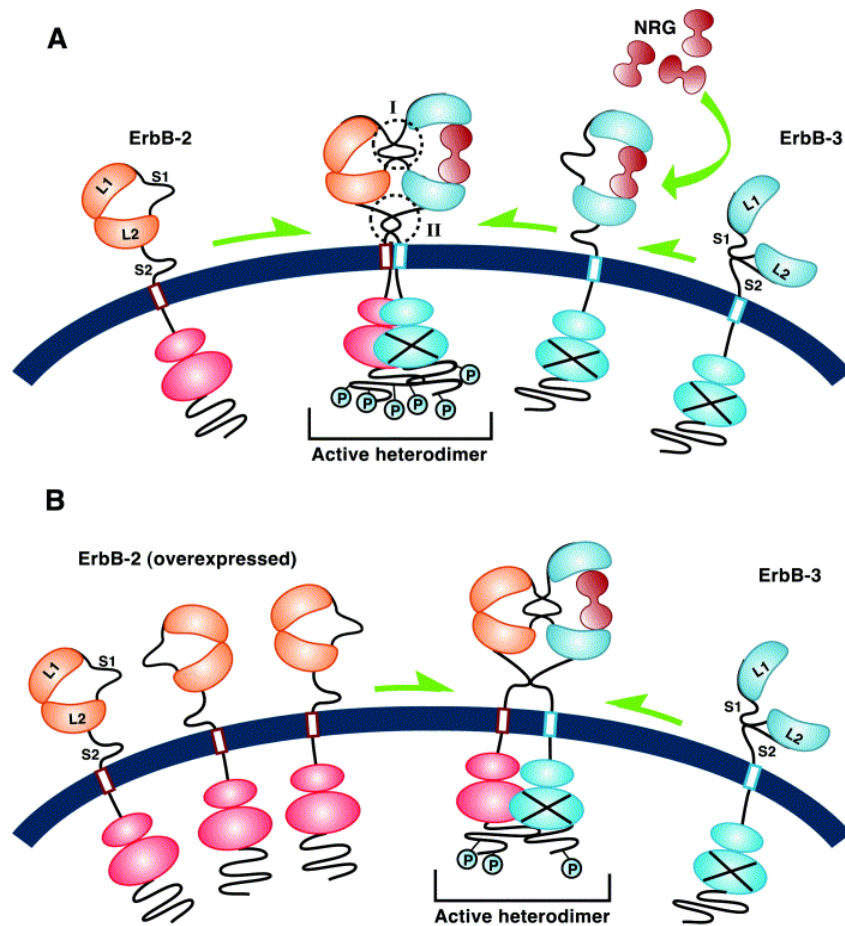
Figure 1.1.2.   HER dimerization: **A** the extracellular domains are represented by two cysteine-rich daomins (S1 and S2), and two cysteine-free, ligand-binding domains (L1 and L2). HER-2 exists on the cell surface in an active dimer conformation resulting from the interactions between S1 and S2 domains. Bivalent binding of ligands (for example neuregulin, NRG) to the L1 and L2 domains of HER-3 rearranges the conformation of the extracellular domain, leading to protrusion of the S1 dimerization loop. In the case of HER-2, the intramolecular interaction between L1 and L2 results in a preextended conformation of the S1 dimerization loop. Dimerization between a ligand-bound HER-3 and a HER-2 molecule is mediated primarily by the dimerization loop (dotted circle I), with additional possible contributions from the loop in the S2 domain (dotted circle II). Additional stabilizing interactions between the transmembrane and kinase domains may also play a role; **B** Overexpression of HER-2 at the cell surface may spontaneously recruit HER-3 into heterodimers. The formed dimers may assume the ligand-induced conformation, resulting in weak but prolonged activation. Alternatively, spontaneous homodimers formed upon overexpression of HERS-2 cannot be excluded. [From Citri *et al*, 2003].

1.1.1.2 HER signalling

The cytoplasmic tail of the HER receptors contain multiple tyrosine phosphorylation sites, varying from 19 in HER-2, to 27 sites in HER-4. These phosphorylated residues serve as docking sites for a range of signalling effector molecules containing Src homology-2 (SH2) and phosphotyrosine binding (PTB) domains. Individual receptors have distinct patterns of tyrosines, and each tyrosine residue has different affinities for different molecules. Furthermore, a given receptor can be differentially transphosphorylated in distinct dimers [18]. The specific signalling molecules recruited, therefore, and the potency of the signal initiated, depend on the identity of the stimulating ligand, the receptor to which it binds, and the second receptor of the dimer formed [19, 20]. The best characterized signalling pathways induced by the HER family are the phosphatidylinositol-3 kinase-Akt (PI3K-Akt), the Ras-mitogen-activated protein kinase (Ras-MAPK) and the phospholipase C$_?$-protein kinase C (PLC$_?$-PKC) pathways [fig. 1.1.3].

_____
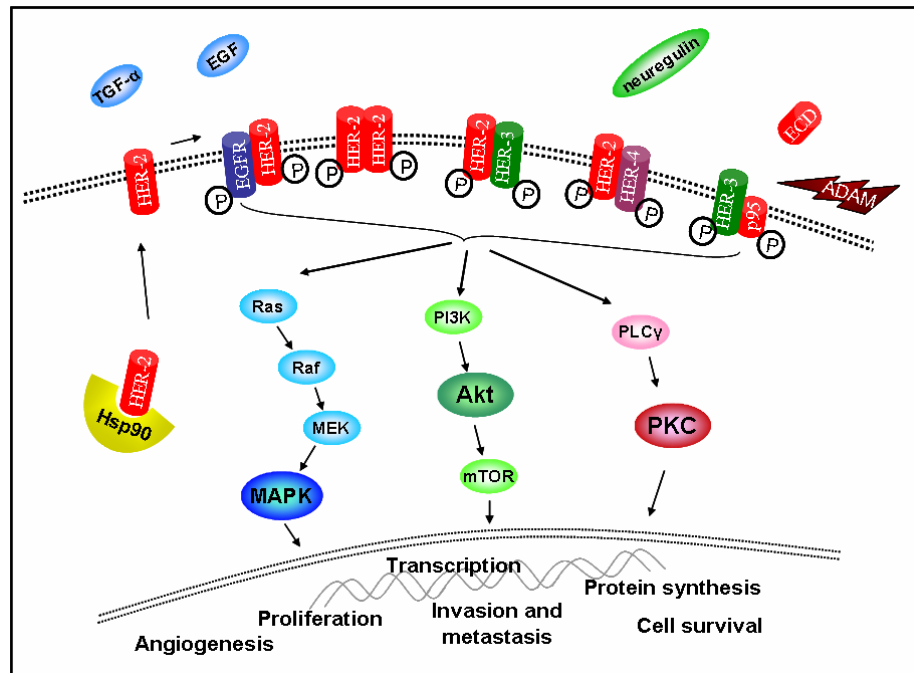
Figure 1.1.3. HER-2 signalling pathway: Ligand binding or HER-2 overexpression induces hetero- or homo-dimerization of HER-2. HER-2 phosphorylation activates Akt, MAPK and PKC signalling pathways, ultimately promoting proliferation and cell survival. Hsp90 maintains HER-2 stability and regulates its function. Cleavage of HER-2 by ADAM proteases produces an extracellular domain (ECD), which is shed, and a truncated membrane-bound p95 fragment.

_____

7

Each of the four HER proteins contains at least one docking sites for Shc (SH2-containing proto-oncogene). Of the cellular proteins that interact with HER-2, Shc is the most common, with at least five docking sites. Shc has three known isoforms, and mediates signalling from a number of other receptor tyrosine kinases (RTKs), including nerve growth factor receptor (TrkA) [21], platelet-derived growth factor receptor (PDGFR) [22] and IR [23]. Phosphorylation of Shc causes it to associate with adaptor protein Grb2 (Growth factor Receptor Bound 2). Grb2 can also bind directly to tyrosine 1139 of HER-2. In the cytosol, Grb2 is bound to the guanine nucleotide exchange factor Sos [24], and recruitment of the Grb2-Sos complex to the plasma membrane stimulates the activation of GTP-binding protein Ras, by exchanging its GDP for GTP. Ras then activates various downstream signalling cascades including the mitogen-activated protein kinase (MAPK) pathway. Ras associates with and activates the serine/threonine kinase Raf, which in turn phosphorylates MEK1 (also known as MAPK kinase). MEK1 then phosphorylates p42/44 MAPK [extracellular signal-related kinase 1 (ERK1 and ERK2)]. Once activated, MAPKs phosphorylate many cytoplasmic and nuclear substrates that include growth factor receptors, transcription factors and other proteins kinases, which mediate cellular processes such as proliferation, differentiation, cell survival and gene transcription [fig 1.1.4] [25].
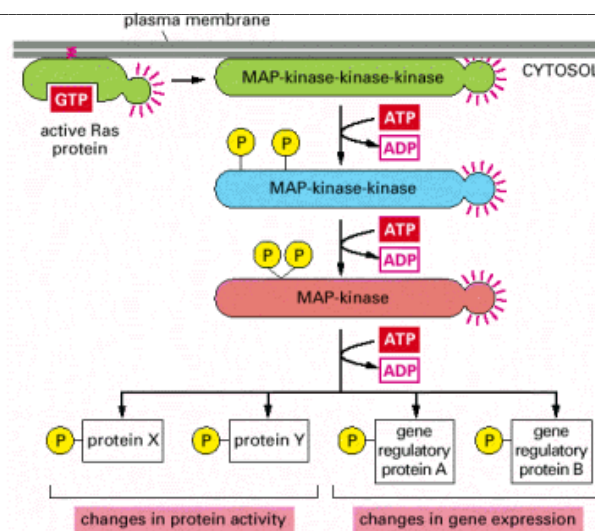
Figure 1.1.4. The MAP-kinase pathway activated by Ras. The pathway activated by Ras begins with a MAPK-kinase-kinase called *Raf,* which activates the MAPK-kinase *Mek,* which then activates the MAPK *Erk.* Erk in turn phosphorylates a variety of downstream proteins. [From Molecular Biology of the Cell, 4th Edition, Alberts *et al*, 2002].

Activation of PI3K occurs through binding of its p85 regulatory subunit to a phosphotyrosine residue on a receptor, such as those of the HER family. Activated PI3K initiates a major signalling cascade involved in promoting cell growth and survival. The p110 subunit of active PI3K phosphorylates phosphatidylinositol (PI), producing lipids such as $PI(3,4,5)P_3$ and $PI(3,4)P_2$. These lipids act as docking sites for proteins containing a pleckstrin homology (PH) domain. PH-containing proteins then transmit signals from the plasma membrane into the cell. Two such proteins are phosphatidylinositol dependant kinase-1 (PDK1) and protein kinase B (PKB/Akt). Binding of Akt to the inositol lipids causes its translocation to the plasma membrane, where its conformation is altered, enabling its phosphorylation by PDK1 [26, 27]. Active Akt is released into the cytosol, where it phosphorylates target proteins, mediating multiple biological responses, including proliferation, metabolic responses and protection from apoptosis [28]. The tumour suppressor protein PTEN (phosphatase and tensin homolog deleted on chromosome 10) is known to regulate Akt signalling by dephosphorylating PIP_2 and PIP_3, thereby preventing Akt recruitment [29]. One of the downstream substrates of Akt is BAD, a member of the Bcl-2 family of apoptotic proteins [30]. BAD neutralizes anti-apoptotic proteins Bcl-2 and Bcl-X_L, promoting cell death. Akt signalling inhibits BAD thereby protecting cells from apoptosis [31]. HER-2 and EGFR do not contain binding sites for PI3K, but active HER-3, though kinase-deficient, contains six PI3K-binding sites, and HER-2/HER-3 or EGFR/HER-3 dimers can therefore transmit potent survival signals through the Akt pathway [fig. 1.1.5] [32].

Activation of PLC? by HER-2 occurs through the recruitment of its SH2 domain to HER-2 phosphotyrosine sites, as well as through the binding of its PH-domain to PI3K products at the plasma membrane. Activated PLC? hydrolyses PIP_2 into IP_3 and diacylglycerol leading to activation of calcium/calmodulin-dependant kinases and phosphatases, and protein kinase C (PKC) (reviewed in [19]).
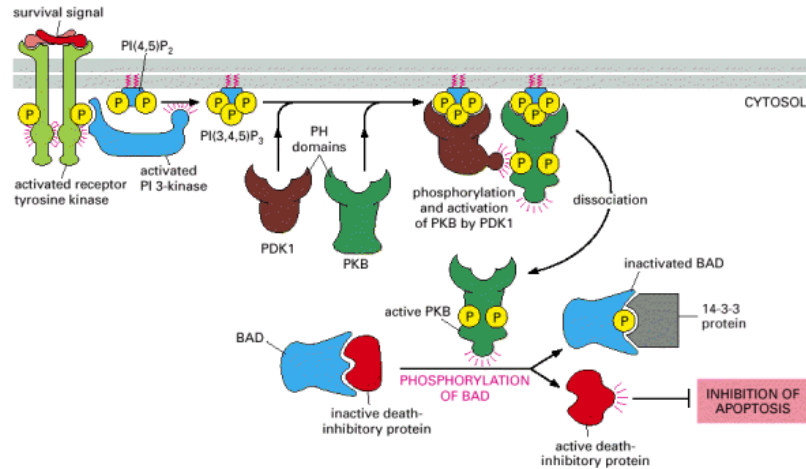
Figure 1.1.5. IGF-IR – PI 3-kinase signalling promotes cell survival. Activated IGF-IR recruits and activates PI3K. PI3K in turn phosphorylates PIP3, which serves as docking sites for PDK1 and Akt/PKB. Activated Akt dissociates from the plasma membrane and phosphorylates BAD, which regulates a number of death-inhibitory proteins. Activated BAD releases the inhibitory proteins, which block apoptosis, thereby promoting cell survival. [From Molecular Biology of the Cell, 4th Edition, Alberts *et al,* 2002].

Other important signal effectors activated by the HER family include Src tyrosine kinase, which is activated upon binding to EGFR, and phosphorylates additional tyrosine docking sites, enhancing EGFR activity. Activated Src plays a role in multiple cellular processes, including endocytosis of RTKs such as EGFR, and the re-arrangement of the cytoskeleton. Signal transducer and activator of transcription proteins 5 (STAT5), is also phosphorylated by HER proteins, and by activating protein kinases of the JAK family, is translocated to the nucleus, where it binds to specific promoter sequences in target genes. The JAK/STAT pathway regulates the transcription of many genes involved in cell proliferation, differentiation and apoptosis [19].

One of the important downstream effects of HER family signalling is the promotion of cell cycle progression and cellular survival. Cyclin D1 is a key cell cycle regulator, and is modulated by HER-2 through both the MAPK and PI3K pathways [33]. Cyclin D1 activates cyclin dependant kinases (CDKs) to promote G1/S phase cell cycle progression. Furthermore, MAPK and Akt signalling mediate additional cell cycle regulatory effects downstream of HER-2 through $p27^{kip1}$ and $p21^{waf1}$, two key regulators of CDK function [7].

1.1.1.3 HER-2 function in normal development

The HER receptors are widely expressed and functionally important in multiple tissues, particularly in mammalian development. Mice with mutated HER-2, HER-3 or neuregulin-1 proteins displayed a lack of neural crest precursor cells [34], and mouse embryos lacking HER-2, HER-3, HER-4, or neuregulins, died during embryogenesis due to severe cardiac abnormalities, as well as brain defects [35-39]. Extensive studies of Schwann cells have focused on neuregulin signalling in the development of the peripheral nervous system, and have identified that the HER-2/HER-3 dimer is activated by neuregulin in these cells [40].

Cross-talk between HER-2 signalling and other pathways has been reported during cardiac development. In a mouse model with inactive 5-hydroxytryptamine (5-HT) receptors, embryonic or neonatal death was accompanied by a specific reduction in HER-2, and cardiac malformations, suggesting that 5-HT receptors use the HER-2 signalling pathway for cardiac differentiation [41]. Another example of cross-talk was seen between neuregulin-1 and insulin-like growth factor-I (IGF-I) pathways. Hertig *et al*, reported that stimulation of cardiomyocytes with the two ligands had synergistic effects on DNA synthesis and cell growth, and this interaction was demonstrated to converge at the activation of PI3K [42]. The importance of neuregulin in promoting angiogenesis via activation of the HER receptors in endothelial cells has been demonstrated. In a rat corneal angiogenesis model, neuregulin administration led to the growth of new blood vessels, and the use of anti-vascular endothelial growth factor (VEGF) antibodies demonstrated that these anti-angiogenic effects were independent of VEGF [43].

Due to lethality *in utero*, following gene-targeting, it has been difficult to establish a role for HER proteins in normal adult tissues. In *in vivo* studies, targeted disruption of HER-2 led to a striking ductal elongation defect, and reduced branching in the pubertal adult mammary gland. However, the absence of HER-2 did not affect the ability of the animals to lactate, demonstrating the functional importance of HER-2 in the initial stages of mammary gland morphogenesis [44].

Press *et al* investigated HER-2 in a variety of normal adult and fetal tissues, and found low expression on the cell membranes of epithelial cells in the gastro-intestinal, reproductive and urinary tract, skin, breast and placenta [45]. HER-2 expression has also been found in normal ovaries and kidney [46, 47]. These studies imply that HER-2 is expressed in of a variety of epithelial cell types.

1.1.1.4 Regulation of HER-2

The levels and activity of HER-2 are regulated by a number of mechanisms. Cell surface receptor levels are down-regulated by ligand-induced receptor endocytosis, whereby receptor dimers are internalized via clathrin-coated regions of the plasma membrane which form endocytic vesicles. Receptors are then either recycled back to the cell surface, or targeted to lysosomes for degradation. There is also evidence to suggest that internalized receptors might interact with effector molecules in pre-degradative intracellular compartments, thereby activating signalling pathways distinct from those that are activated at the cell surface [48].

Heat shock protein 90 (Hsp90) plays an important regulatory role in HER-2 activity. Hsp90 and its complex of chaperone proteins promote the maturation of HER-2 from its nascent form into its stable mature form. Hsp90 then interacts with the kinase domain of HER-2, where it is responsible for maintaining the mature protein in a state competent for dimerization and activation [49]. A recent study also reported a novel interaction between surface Hsp90 and the extracellular domain (ECD) of HER-2, and suggests that this interaction promotes HER-2-mediated cytoskeletal re-arrangements [50].

Herstatin is an alternatively spliced form of HER-2 consisting of subdomains of the extracellular domain of HER-2 and a novel carboxyl-terminus domain encoded by an intron. It acts as an autoinhibitor by binding to HER-2, and blocking its activity and heterodimerization [51]. A similar type of naturally secreted protein, p85-s, composed of the extracellular domain of HER-3, binds neuregulin and inhibits activation of HER-2, HER-3 and HER-4 [52].

1.1.2 HER-2 expression in breast cancer

HER-2 overexpression occurs in 15-30 % of breast cancers [53], and this is usually due to amplification of the HER-2 gene by 2-fold to greater than 20-fold more then the number of copies in normal cells. Amplification of the HER-2 gene results in increased receptors on the cell surface; while a normal breast cell has approximately 20,000 HER-2 molecules, tumours cells have up to 2 million [54, 55].

1.1.2.1 HER-2 in transformation and tumorigenesis

Overexpression of HER-2 has been implicated in the transformation of epithelial cells, and in tumorigenesis in human tissues. Overexpression of HER-2 in NIH/3T3 cells or NR6 mouse fibroblast cells induced cell transformation and tumorigenic growth [56-58]. When simultaneously overexpressed, HER-2 and EGFR act synergistically in the transformation of NIH/3T3 cells [59]. Transformation can also be induced by co-expressing HER-2 or EGFR with HER-3 or HER-4 [60]. Overexpression of HER-2 in MCF7 breast cancer cells resulted in elevated signalling through the PI3K pathway, and enhanced tumorigenesis when implanted into nude mice [61]. In a 3-D model of MCF10A mammary epithelial acini, HER-2 overexpression enhanced proliferation, suppressed apoptosis, and promoted the formation of solid multiacinar structures, resembling those seen during the early stages of epithelial transformation [62]. Anti-apoptotic survivin is also upregulated by the coexpression of EGFR and HER-2 in MCF7, MMC-1 and HMC-2 breast cancer cells [63].

As well as playing a role in tumorigenesis, HER-2 has also been implicated in invasion, by regulating expression of integrins on the cell surface. In human mammary epithelial (HME) cells, HER-2 overexpression downregulated a4-integrin, leading to increased invasiveness of the cells. This was mediated by signalling through Rac1-p38MAPK and PI3k-Akt-PKC-d pathways [64, 65].

Overexpression of HER-2 in tumours results in increased formation of HER-2-containing heterodimers and HER-2 homodimers [66]. HER-2 homodimerization can cause constitutive activation of its kinase domain [67]. Zhan *et al* [68] compared and identified the roles of HER-2 homodimers and HER-2/EGFR heterodimers in normal

breast cell transformation and invasion, and observed that while activation of both types of dimers induced disruption of the epithelial acini-like structures, only the HER-2/EGFR heterodimers promoted invasion of cells through the extracellular matrix. The ability of the heterodimers to induce invasion required HER-2 kinase activity and was mediated through activation of PI3K, MAPK and phospholipase C?1 signalling pathways. The synergistic effects of HER-2 and EGFR may be explained, at least in part, by HER-2 increasing affinity for EGFR ligand binding and interfering with the rate of EGFR internalization, resulting in prolonged activation of downstream signalling [69].

HER-2 overexpression in breast cancer has also been implicated in the promotion of angiogenesis, another important prognostic indicator in breast cancer. In *in vitro* studies, activation of HER-2 upregulated vascular endothelial growth factor (VEGF) levels, and treatment with anti-HER-2 antibody 4D5 resulted in a dose-dependant reduction of VEGF expression [70].

1.1.2.2 Detection of HER-2 overexpression in breast cancer

Most reports find that the HER-2 gene is either amplified or overexpressed at the protein level in 15-30 % of primary invasive breast cancers [53]. Reports have varied, however, probably due to different techniques used to assess HER-2. Southern blotting was first used to assess HER-2 gene amplification [71], while other studies have used slot blot, Western blot, reverse transcriptase-polymerase chain reaction (RT-PCR), enzyme-linked immunosorbent assay (ELISA), immunohistochemistry (IHC), and fluorescent *in situ* hybridization (FISH) methods to measure gene amplification or overexpression [72]. IHC has been most commonly used, and this technique measures the amount of HER-2 protein expressed on the surface of cells, using a qualitative scoring system from 0 to 3+, with 3+ regarded as overexpression. Inconsistencies in results can occur due to variation in sample storage, fixation techniques, intensity of antigen retrieval, the type of antibody used, and scoring systems. Two commercially available HER-2 IHC tests, the HercepTest^{TM} (Dako Corporation, Denmark) and the Ventana PATHWAY^{TM} (Ventana Medical Systems, Tucson, AZ), have been approved by the US Food and Drug Administration (FDA) for use in determining the eligibility of patients to receive trastuzumab (Herceptin^{TM}), and studies have shown that when

standardized IHC techniques are used, there is excellent correlation between gene copy number and protein expression levels [72]. FISH detects amplification of the HER-2 gene and tumours are thus interpreted as negative or positive based on the number of HER-2 gene copies. This method is also commonly used, and is arguably a more sensitive and accurate method of measuring HER-2 status [73]. FISH also has the advantages of having a more objective scoring system; however, this test is also more expensive and time-consuming to run. Two FISH assay kits have been approved by the FDA; the Ventana INFORM™ (Ventana Medical Systems), and the Abbott-Vysis PathVysion™ (Abbott Laboratories, Abbott Park, IL). An approach now taken by many clinicians is to use IHC as a primary screening tool, and to use FISH to confirm HER-2 status in cases with IHC scores of 2+.

A novel method of hybridization, chromogenic *in situ* hybridization (CISH), uses a chromogen-labelled probe and offers the advantage of the ability to use a light microscope. Studies comparing CISH and FISH analysis of breast cancer samples report a strong correlation between the two techniques [74, 75]. A recent study used silver enhanced *in situ* hybridization (SISH), and reported this technique to be as accurate and reliable as FISH [76]. Another recent study combined IHC and CISH, calling the new technique 'protein and gene double staining' (PGDS), and the authors suggest that this technique will aid in improving IHC scoring, and increase the sensitivity and specificity of HER-2 testing [77].

1.1.2.3 HER-2 as a prognostic factor

HER-2 gene amplification or overexpression is reported in 15-30% of invasive human breast cancers [53]. In 1987, Slamon et al [71] reported that in 86 patients with lymph node-positive breast cancer, HER-2 amplification correlated significantly with both time to relapse and overall survival. Univariate analysis demonstrated that HER-2 amplification was equivalent to the number of lymph node metastases as a prognostic marker, but stronger than that of hormone receptors or tumour size. In multivariate analysis, the prognostic impact of HER-2 gene amplification was also significant and independent of number of metastatic axillary nodes [71].

Subsequent studies confirmed the adverse prognostic impact of HER-2 in lymph node-positive breast cancer patients. In a review of 16 different reports, Revillion *et al* [78] showed, using univariate analysis with disease-free interval as an endpoint, that overexpression of HER-2 correlated with poor outcome in 11 studies but failed to correlate in 2 reports. In the remaining 3 studies, HER-2 lacked prognostic impact in the overall population but predicted outcome in specific subgroups. In 11 studies where multivariate analysis was performed, 5 confirmed the prognostic value of HER-2 but 6 others did not. Similar conflicting results were obtained with overall survival as the endpoint [78].

In a more recent review of 81 studies, involving > 27,000 patients, 73 (90%) studies found that either HER-2 gene amplification or protein overexpression predicted patient outcome using either univariate or multivariate analysis [72]. In 52 of the 73 studies (71%) that used multivariate analysis, the adverse prognostic impact of HER-2 was found to be independent of the other variables investigated. Only 8 (10%) of the studies showed no significant association between HER-2 and patient outcome. When the breast cancer patients were separated by nodal status, most authors found that HER-2 overexpression correlated with poor outcome in node-positive patients but found conflicting results in node-negative patients [79]. The prognostic value of HER-2 in lymph node-positive breast cancer patients may be partly attributed to its ability to predict response/resistance to specific therapies.

Currently, measurement of HER-2 for determining prognosis in breast cancer is recommended by a number of expert panels including the St Gallen Consensus Group [80, 81], the National Academy of Clinical Biochemistry (NACB) (USA) [82], and the European Group of Tumour Markers (EGTM) [83].

As well as tissue levels, levels of serum HER-2 extracellular domain (ECD), have also been shown to correlate with high histological grade, lymph node involvement, hormone receptor negativity, disease recurrence, metastasis, and shortened survival [84, 85]. Most studies used ELISAs to quantify the soluble ECD of HER-2, which is cleaved from the cell surface by a matrix metalloproteinase-like protein [84].

Proteolytic shedding of the HER-2 ECD also generates an N-terminal truncated fragment p95HER-2 [86, 87]. Studies in patients have found that the presence of p95HER-2 in primary breast tumours correlates with the extent of lymph node metastasis, while the full length receptor was unrelated to nodal disease. p95HER-2 was also detected more frequently in lymph node metastasis than primary tumours, and high levels of p95HER-2 significantly correlated with reduced five-year survival in primary breast cancer patients. This truncated form of HER-2, therefore, is an independent predictor of patient outcome and may define a group of patients with HER-2-positive cancer with significantly worse outcome [86, 88].

The level of HER-2 protein does not necessarily reflect the level of activity of the receptor. Studies have been performed therefore, to examine the levels of phosphorylated HER-2 (pHER-2) in breast tumour samples, and to assess the prognostic value of pHER-2 in patients. In a study of invasive breast cancers, pHER-2 was detected in 12% of 307 HER-2-positive samples [89]. pHER-2 levels correlated with a higher percentage of HER-2 positive cells, higher number of positive lymph nodes, and elevated cellular proliferation. Both HER-2 and pHER-2 were associated with poor prognosis in node-positive patients. In a similar, though smaller, study of DCIS patients, pHER-2 was detected at a higher frequency (58%) compared to HER-2-positive invasive cancers [90]. A recent study of 70 primary breast cancers also found that pHER-2 correlated inversely with hormone receptor status, and was associated with poor clinical outcome [91]. These results suggest the potential use of phosphorylated HER-2 as a prognostic marker.

1.1.2.4 Association of HER-2 with other prognostic parameters

HER-2 overexpression has been positively correlated with other prognostic parameters such as tumour size, lymph-node infiltration, high tumour grade, DNA aneuploidy, p53 mutation, and high proliferation index [92, 93]. HER-2 amplification or overexpression correlates inversely with the presence of estrogen receptor (ER) and progesterone receptor (PR) [94]. Approximately 50% of HER-2-postive breast cancers are ER-negative, and in the other 50%, ER levels are significantly lower compared to those in ER-positive/HER-2-negative breast cancers [95]. ER stimulation decreases HER-2 protein levels, while antiestrogens, such as tamoxifen, increase HER-2

expression. Cross-talk between the ER and HER-2 signalling pathways has been demonstrated; estradiol activates the PI3K/Akt pathway in breast cancer cells, and this has been shown to be mediated by HER-2, while heregulin also activates Akt and upregulates ER activity [96, 97]. In a study of the prognostic value of combining HER-2 and ER status, patients with HER-2-positive tumours that also express ER had longer overall survival than those without ER [98].

1.1.2.5 HER-2 as a predictive marker in breast cancer

Clinical evidence demonstrates an association between HER-2 overexpression and response to a number of anti-cancer therapeutics. Amplification or overexpression of HER-2 has been implicated as a potential predictor of reduced response to the chemotherapy regimen of cyclophosphamide, methotrexate, and 5-fluorouracil (CMF), though results of different studies have been controversial [94]. A recent study examined post-adjuvant chemotherapy in 1625 primary breast cancer patients. Six hundred patients were given CMF, 600 were given CEF (epirubicin, an anthracycline, replacing methrotrexate), while 425 were given an anthracycline plus taxane regimen. In the CMF-treated patients, disease-free survival was significantly lower in HER-2-positive than in HER-2-negative patients. In the node-positive subgroup, this difference was enhanced. Compared to CMF, the anthracycline-containing regimens were significantly more effective in node-positive HER-2-overexpressing patients than in node-negative HER-2-positive patients [99]. These results confirm that HER-2-positive patients are more resistant to CMF, but sensitive to anthracycline-based or anthracycline plus taxane regimens. Previous studies have also reported the benefit of adding the anthracycline doxorubicin to chemotherapy regimens in HER-2-positive patients, and have demonstrated that HER-2-overexpressing patients benefit from higher doses compared to lower dose of CAF (cyclophosphamide, doxorubicin and 5-fluorouracil) [100].

HER-2 overexpression has also been reported to play a role in resistance to hormonal therapy. In a number of studies, HER-2-positive tumours were specifically resistant to tamoxifen treatment [98], while in others, HER-2 overexpression did not show any predictive effect [94]. In one study, HER-2-positive tumours were not only resistant to tamoxifen, but the adjuvant use of tamoxifen had an adverse effect on overall survival

compared with untreated patients [101]. In this study, HER-2 overexpression was found to be a better predictor of hormone therapy response than the hormone receptor itself. Another report also suggested that the soluble HER-2 ECD is more predictive of response to hormone therapy than the hormone receptor itself [92]. A more recent study showed that ER-positive/HER-2-positive tumours respond more favorably to aromatase inhibitors,, such as letrozole, in the neoadjuvant setting [72].

Based on studies in cell lines and animal models, it is assumed that HER-2 gene amplification or overexpression of HER-2 protein is necessary for trastuzumab to mediate its anti-cancer actions. Although not proven, clinical evidence supports the value of HER-2 in predicting response to HER-2-targeted therapy. The predictive value of HER-2 in response to trastuzumab was originally shown in patients with advanced breast cancer. In one of the first phase II trials, 46 women with HER-2 positive (2+ or 3+ by IHC) metastatic chemo-refractory breast cancers were treated with trastuzumab. Response was observed in 12% of the women, providing proof-of-principle that trastuzumab was effective in at least some HER-2 positive tumours [102]. In a phase III trial, using IHC to select patients, trastuzumab improved survival and reduced the risk of recurrence when given as a first line treatment in combination with chemotherapy in patients with metastatic breast cancer [103]. Addition of trastuzumab to chemotherapy regimens in the adjuvant setting has also improved survival, and a recent study reported a positive correlation between level of HER-2 amplification by FISH and increased complete response to trastuzumab-based neoadjuvant treatment [104]. Elevated levels of serum HER-2 ECD have also been associated with a higher response rate to trastuzumab-based therapies [72], while expression of the p95 fragment in breast tumours correlated with reduced response to trastuzumab [105]. Measurement of HER-2 is recommended by multiple expert panels for selecting patients with breast cancer for treatment with trastuzumab [80, 82, 83, 106].

Recent data also demonstrate a predictive role for HER-2 in response to lapatinib, a dual HER-2/EGFR inhibitor. In phase II/III trials, only patients with HER-2-overexpressing tumours responded to lapatinib, and preliminary data also suggest that EGFR overexpression and an intact ECD of HER-2 may also be related to response

[107]. Co-expression of phosphorylated HER-2 and HER-3 also correlated with favourable response to lapatinib in inflammatory breast cancer [108].

1.1.2.6 HER-2 targeted therapies

The discovery of HER-2 overexpression and its role in aggressive cancers led to efforts to develop agents targeting HER-2 for anti-cancer therapy. HER-2 targeted therapies that are currently in clinical use or in development can be divided into two main types, namely monoclonal antibodies and tyrosine kinase inhibitors (Table 1.1.1). Several groups developed murine monoclonal antibodies against the ectodomain of HER-2, many of which demonstrated inhibition of growth in preclinical models. One particular antibody, 4D5 was developed by Genentech (San Francisco, CA), and due to its anti-tumour effects *in vitro* and *in vivo*, this antibody was humanized for clinical use. This antibody, trastuzumab (Herceptin^{TM}, Genentech), was the first monoclonal antibody approved for breast cancer treatment. Trastuzumab demonstrated higher binding affinity for HER-2 than the murine 4D5, and potent anti-tumour effects in human tumour xenografts [109]. Trastuzumab binds to the ectodomain of HER-2, preventing its interaction with the transmembrane domain [Fig. 1.1.6]. Trastuzumab does not prevent heterodimerization of HER-2, as the specific binding site for trastuzumab is not involved in dimerization [110]. Trastuzumab will be discussed further in section 1.3.1.

A second anti-HER-2 antibody, pertuzumab (Omnitarg), was developed by Genentech and is currently in phase II clinical trials in breast cancer patients [111]. Pertuzumab has properties distinct from those of trastuzumab; its binding site on HER-2 enables it to block dimerization with other HER receptors, and in contrast to trastuzumab, pertuzumab is able to inhibit tumours with low levels of HER-2 by preventing ligand-induced activation of HER-2 heterodimers [110] [Fig. 1.1.6]. Furthermore, the combination of pertuzumab and trastuzumab synergistically inhibited the survival of BT474 breast cancer cells *in vitro*, partly due to increased apoptosis [112].
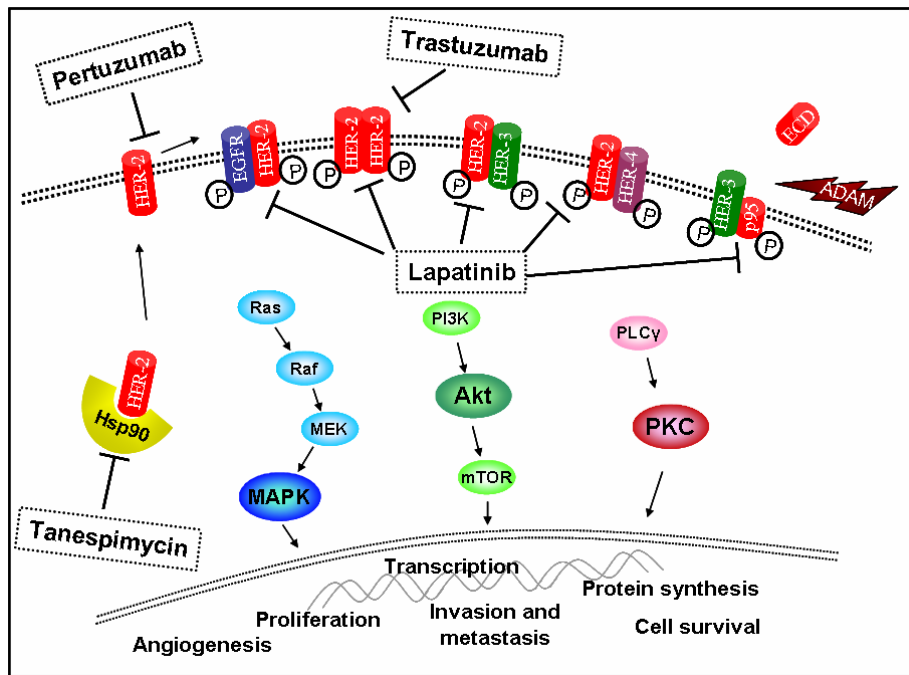
Figure 1.1.6.   Inhibition of HER-2 signalling: Trastuzumab binds the extracellular domain of HER-2 dimers and reduces HER-2 signalling; Pertuzumab also binds the extracellular domain and prevents HER-2 homo- and hetero-dimerization; Lapatinib inhibits the tyrosine kinase domain of HER-2 and EGFR; and Tanespimycin inhibits Hsp90 activity, disrupting HER-2 stability and function.

_____

Another approach to targeting HER-2 is to directly target the tyrosine kinase activity. Small molecule tyrosine kinase inhibitors (TKIs) have been developed, and one class of TKIs are the quinazolines, which mimic ATP, reversibly binding to the ATP binding site, thereby inhibiting their kinase activity. Lapatinib (GW572016, Tykerb) is a quinazoline TKI, and is a dual inhibitor of both EGFR and HER-2. Lapatinib inhibits breast cancer cell proliferation *in vitro*, and downregulates HER-2, Raf, Akt, and Erk phosphorylation. The combination of lapatinib and trastuzumab had synergistic anti-proliferative effects in HER-2-overexpressing breast cancer cell lines [113]. Lapatinib has also demonstrated activity in HER-2-positive patients [114], and was recently approved by the FDA for use in combination with capecitabine in patients with advanced metastatic breast cancer, and is also in phase III clinical trials in breast and other carcinomas (discussed further in section 1.3.2). Many other HER-2, and HER family, TKIs are being developed pre-clinically, including both reversible and irreversible TKIs (Table 1.1.1).

Other strategies under investigation for targeting HER-2 include ribozymes, antisense, small interfering RNA, and HER-2 antibodies conjugated to cellular toxins, or to chemotherapy-containing immunoliposomes [115]. Vaccines eliciting a response to HER-2 antigen are currently in clinical trials [116]. A number of other agents indirectly affect HER-2 protein expression and may prove beneficial in HER-2-overexpressing cancers, such as HSP90 inhibitors, COX-2 inhibitors, deacetylase inhibitors, or gene therapy with transcriptional factors (reviewed in [115]).

_____

Table 1.1.1.   HER-2 antagonists currently in clinical use or in pre-clinical/clinical
development.

Inhibitor	Category	Targets	Status
Trastuzumab (Herceptin)	Monoclonal antibody	HER-2	Approved for HER-2 positive metastatic breast cancer and for node positive early stage breast cancer.
Pertuzumab (Omnitarg)	Monoclonal antibody	HER-2	Phase III trials
Lapatinib (Tykerb)	TKI - Reversible	EGFR & HER-2	Approved for trastuzumab-refractory HER-2 positive metastatic breast cancer
CP-724,714	TKI - Reversible	HER-2	Phase I/II trials
TAK165	TKI - Irreversible	HER-2	Phase I trials
AEE-788	TKI - Reversible	EGFR, HER-2 & VEGFR	Phase I/II trials
BMS-599626	TKI - Reversible	EGFR & HER-2	Phase I trials
Arry-334543	TKI - Reversible	EGFR & HER-2	Phase I trials
BIBW2992	TKI - Irreversible	EGFR & HER-2	Phase II trials
HKI-272	TKI - Irreversible	EGFR & HER-2	Phase II trials
MP-412	TKI - Irreversible	EGFR & HER-2	Preclinical evaluation
CI-1033	TKI - Irreversible	Pan-HER	Phase II trials

1.2   HER-2 Targeted Therapies

1.2.1 Trastuzumab

1.2.1.1 Mechanisms of action of trastuzumab

As mentioned above trastuzumab binds to the extracellular domain of HER-2 and inhibits tumour cell growth. The mechanisms of action of trastuzumab are not yet fully understood. Several models have been proposed, some of which are discussed below.

(i) Downregulation of HER-2

It is still unclear as to whether trastuzumab causes down-modulation of HER-2. Ligand binding to EGFR family members causes ligand-receptor complexes that are internalized within endosomes. Once there, the ligand-receptor complex dissociates and the receptor can either be transported to lysosomes for degradation, or recycled back to the cell surface. When HER-2 is overexpressed, signalling is mediated preferentially by heterodimers containing HER-2 [15]. Dimers containing HER-2 preferentially result in receptor recycling, thereby efficiently sending prolonged proliferative signals to the nucleus [117]. It has been hypothesized that anti-HER-2 antibodies promote the degradation pathway for HER-2-containing endosomes [117]. This hypothesis, however, was challenged by Austin *et al* [118], who demonstrated that trastuzumab does not downregulate HER-2, but recycles passively with the receptor after endocytosis. Other groups have also demonstrated that membrane receptor levels do not change in response to trastuzumab [119, 120].

(ii) Reduced HER-2 signalling

A proposed mechanism of action is the reduction of signalling through Akt and MAPK pathways, thereby promoting apoptosis and inhibiting proliferation [119, 121] (Figure 1B). Nagata *et al* [122] demonstrated that trastuzumab specifically disrupts HER-2-Src interactions, leading to inactivation of Src. This in turn causes reduced PTEN phosphorylation, increasing PTEN phosphatase activity. This leads to rapid Akt dephosphorylation and inhibits cell proliferation.

(iii) Inhibition of HER-2 extracellular domain (ECD) shedding

When overexpressed, HER-2 undergoes proteolytic cleavage by matrix metalloproteinase-like enzymes, which results in the shedding of its ECD, and the production of a truncated membrane-bound fragment, p95 [123]. *In vitro* studies have demonstrated that this p95HER-2 fragment has kinase activity, can form heterodimers with HER-3, and can be tyrosine phosphorylated by neuregulin-1 [86, 87]. The ECD can be detected in cell culture medium, and in the serum of breast cancer patients. ECD cleavage was shown to be a ligand-independent method of HER-2 activation *in vivo* [124]. Trastuzumab inhibited ECD shedding in SKBR3 and BT474 breast cancer cell lines, by blocking matrix-metalloproteinase-mediated cleavage of the ECD [125]. Clinical studies also report a decline in serum ECD levels during trastuzumab treatment [126], and suggest that serum levels prior to treatment may be predictor of response [127, 128].

(iv) G1 arrest

One of the mechanisms of action of trastuzumab is the induction of cell cycle arrest at the G1 phase, and this is associated with reduced expression of proteins involved in sequestering the cyclin-dependent kinase (cdk) inhibitor $p27^{kip1}$, including cyclin D1. This results in the release of $p27^{kip1}$, allowing it to bind and inhibit cyclin E/cdk2 complexes [129-131]. A number of signalling pathways, including the Akt cascade, have been associated with trastuzumab-mediated induction of $p27^{kip1}$ activity [132].

(v) Induction of apoptosis

Single agent trastuzumab reduces tumour size in patients with HER-2-overexpressing metastatic breast cancer [133]. Whether this cytotoxic effect is a direct effect on the cancer cells or whether it is mediated by indirect mechanisms (by the immune system or anti-angiogenic activity) has yet to be defined. Trastuzumab-induced apoptosis has not been observed using *in vitro* models, but the situation *in vivo* is less clear. Mohsin *et al* [134] report that reduction of tumour size after three weeks of trastuzumab treatment in 35 breast cancer patients is accompanied by an average 35% increase in apoptosis. In another small pilot study (n=11), Gennari *et al* [120] found no decrease in tumour size following treatment with trastuzumab, but reported a strong increase in infiltrating lymphoid cells. The authors suggest that the response seen by Mohsin *et al* [134] may be due to an inflammation response caused by the core biopsy method used, rather than an early apoptotic response to trastuzumab [135]. Though further

investigation is required to characterize the cytotoxic effect of trastuzumab alone in cancer cells, trastuzumab has been shown to sensitize breast cancer cells to apoptosis-inducing agents. Trastuzumab sensitized cells to paclitaxel and etoposide by reducing the inhibitory phosphorylation of p34(Cdc2), down-regulating p21(Cip1), and reducing expression of anti-apoptotic Bcl-2 family member MCl-1 [136, 137]. Trastuzumab also enhanced tumour necrosis factor-related apoptosis-inducing ligand (TRAIL)-induced apoptosis, by inhibiting Akt signalling in ovarian and breast cancer cells [138].

(vi) Inhibition of angiogenesis

Overexpression of HER-2 in breast cancer cells correlates with elevated vascular endothelial growth factor (VEGF) expression and increased angiogenesis [139-141]. Trastuzumab induced normalization and regression of vasculature in a mouse model by reducing the expression of VEGF, and increasing expression of the anti-angiogenic factor thrombospondin-1 [142]. Klos *et al* [143] showed that the combination of trastuzumab and paclitaxel inhibited angiogenesis to a greater degree than either drug alone in breast cancer xenografts. This result may reflect a more efficient drug delivery to trastuzumab-normalized tumour vasculature. The HER-2/trastuzumab-regulation of VEGF activity was mediated by Akt and mTOR signalling [144].

(vii) Inhibition of DNA repair

Trastuzumab interferes with the ability of cells to repair DNA damage after platinum therapy or ionizing radiation [145-147]. Pietras *et al* [145] demonstrated that trastuzumab reduced unscheduled DNA synthesis (a measure of DNA repair) by 35-40% after cisplatin treatment of breast and ovarian cell lines, and termed this phenomenon 'receptor enhanced chemosensitivity'. Trastuzumab also decreased DNA repair by 25-44% after irradiation of MCF7-HER-2-transfected cells [148], and the combined treatment caused complete remission of MCF7-HER-2 xenograft tumours in mice. p21 is likely to be involved in trastuzumab-inhibition of DNA repair, as trastuzumab blocks cisplatin-induction of p21 [148] and blocks phosphorylation of p21 after radiation [147]. Trastuzumab also promoted DNA strand breaks in BT474 and SKBR3 breast cancer cells [149], and increased gene transcription of proteins involved in DNA repair [150]. These data suggest that trastuzumab either promotes DNA

damage independently, or inhibits its repair in association with therapeutic agents, resulting in apoptosis.

(viii) Antibody-dependant cell-mediated cytotoxicity (ADCC)

Animal studies and clinical trials have demonstrated that trastuzumab possesses cytotoxic as well as cytostatic properties, and these properties may be due to the induction of an immune response. ADCC is mainly due to the activation of natural killer (NK) cells, which express the Fcγ receptor (FcγR), and can be bound by the Fc domain of trastuzumab IgG1. Clynes *et al* [151] used FcγR-knock-out mice models with BT474 xenografts, and showed that while trastuzumab reduced tumour volume by 90% in $Fc\gamma R^{+/+}$ mice, its cytotoxic activity was significantly impaired in $Fc\gamma R^{-/-}$ mice, where it reduced tumour volume by only 29%. Mutations in the Fcγ binding domain of trastuzumab also decreased its binding, and anti-tumour activity demonstrating the importance of the Fc- FcγR interaction in mediating the ADCC effects of trastuzumab.

1.2.1.2 Trastuzumab clinical trials

Trastuzumab achieved overall responses of between 11 and 15%, as a single agent, in HER-2-positive metastatic breast cancer patients who had progressed after chemotherapy [102, 133, 152]. As a first-line treatment, trastuzumab produced response rates of 26-34% in HER-2-positive metastatic breast cancer patients [133]. The pivotal phase III trial of trastuzumab in combination with chemotherapy, in HER-2 positive metastatic breast cancer, demonstrated improved overall response rate (50% *versus* 32%), longer duration of response (time to progression: 7.4 *versus* 4.6 months), longer survival (overall survival: 25.1 *versus* 20.3 months) and a 20% reduction in risk of death, compared to chemotherapy alone [103]. Trastuzumab has been tested in combination with a variety of chemotherapy agents, including taxanes, platinum salts, vinorelbine and gemcitabine, with response rates ranging from 24% to 84% [153].

In early clinical studies with trastuzumab, cardiomyopathy was observed in a small percentage of patients. This cardiotoxicity was most notable in patients who concurrently received anthracyclines [103]. On the basis of these findings, concurrent use of anthracyclines and trastuzumab is not recommended. The trastuzumab/anthracycline-enhanced cardiotoxicity is believed to be mediated by

inhibition of neuregulin-1 growth and survival signals in cardiomyocytes. Neuregulin-1 signalling via HER-2 and HER-4 protects cardiomyocytes from anthracycline-induced cell death, therefore inhibition of HER-2 by trastuzumab may enhance the cytotoxic effects of anthracyclines in cardiomyocytes, increasing the likelihood of cardiac dysfunction [37, 154].

The most significant advancement in the treatment of HER-2-positive breast cancer came from five randomized trials demonstrating the benefit of trastuzumab treatment for early stage HER-2 positive breast cancer. Addition of trastuzumab to adjuvant therapy resulted in 39-52% reduction in disease recurrence [155]. A recent meta-analysis of the five adjuvant trials, comparing adjuvant trastuzumab plus chemotherapy versus chemotherapy alone, showed a significant reduction in mortality (p < 0.00001), recurrence (p < 0.00001) and rates of metastasis (p < 0.00001) for the trastuzumab-containing regimens [156].

In the neo-adjuvant setting, addition of trastuzumab to chemotherapy has achieved pathological complete response (pCR) rates of 12-65% and clinical complete response rates of 30-86% [153]. A randomised trial to comparing trastuzumab plus chemotherapy to chemotherapy alone in the neo-adjuvant setting was performed in 42 patients but was stopped early by the Data Monitoring Committee because of the superior results observed for the trastuzumab plus chemotherapy group (pCR 66.7% versus 25%) [157].

1.2.1.3 Mechanisms of trastuzumab resistance
Despite the proven clinical benefits of trastuzumab therapy, either as a single agent or in combination, not all patients that overexpress HER-2 respond to trastuzumab. In fact, less than 35% of patients with HER-2 overexpressing metastatic breast cancer respond to trastuzumab as a single agent [133] and the majority of those who achieve an initial response, acquire resistance within one to two years [119, 158] . Several mechanisms have been proposed in an attempt to explain both intrinsic and acquired resistance to trastuzumab. HER-2 is the preferred dimerization partner of the HER family and has been described as a non-autonomous amplifier of the HER signalling

network [17]. Alterations at any stage of this complex network may confer resistance to trastuzumab.

(i) Altered receptor-antibody binding

Trastuzumab binds to the extracellular domain (ECD) of the HER-2 receptor; disruption of this binding is therefore a potential mechanism of resistance. Nagy *et al* [159] studied the properties of trastuzumab-resistant cell line, JIMT-1, derived from a HER-2 overexpressing patient with primary resistance to trastuzumab. They found that though HER-2 expression, internalisation and down-regulation were similar to those of trastuzumab-sensitive cell lines, there was reduced number of antibody-binding sites, indicating that HER-2 was partially masked in these cells. Expression of MUC4, a membrane-associated mucin that contributes to the masking of membrane proteins, was higher in JIMT-1 cells compared to sensitive cell lines, and high levels of MUC4 correlated with decreased trastuzumab binding capacity. Thus, elevated MUC4 may promote resistance to trastuzumab by masking the antibody-binding epitopes of HER-2. Knock-down of MUC4 by RNA interference increased the binding of trastuzumab. JIMT-1 cells also had reduced phosphorylation of HER-2, suggesting that masking by MUC4 also prevents its interaction with other receptors and subsequent activation.

(ii) Cleavage of HER-2 ECD

The extent of enzymatic cleavage of HER-2 may also be a contributing factor in trastuzumab resistance. Scaltriti *et al* [105] showed in a small-scale study (n = 46), that breast cancer patients expressing p95 were less likely to respond to trastuzumab than those expressing the full length receptor, and that cells expressing p95 were not sensitive to trastuzumab but were responsive to the tyrosine kinase inhibitor lapatinib, which targets the ATP binding pocket of the intracellular domain of HER-2. There is also evidence that the metalloprotease ADAM 10 may play a role in the cleavage of the HER-2 ECD. Inhibition of ADAM 10 reduced shedding of HER-2 ECD and increased cell line sensitivity to trastuzumab [160]. Although elucidation of the role of p95 in trastuzumab resistance and breast cancer is still at an early stage, inhibiting the cleavage of HER-2 may be an attractive target for treating trastuzumab refractory tumours.

(iii) Alternative HER signalling

HER-2 is the preferred dimerization partner for each of the HER receptors. Trastuzumab does not inhibit ligand-induced heterodimerization [161, 162]. Therefore, increased activity of other ligands and receptors of the HER network could maintain HER signalling despite the presence of trastuzumab. Ritter *et al* [163] reported increased levels of EGFR ligands such as TGF-a and heparin binding EGF in trastuzumab resistant BT474 cells. Increased levels of EGFR, phospho-EGFR and EGFR/HER-2 heterodimers were also detected in the resistant cells. Co-expression of EGFR determined EGFR/HER-2 homo- and heterodimerisation in BT474 and SKBR3 cells, and was related to reduced response to trastuzumab. The modulation of response was dependant on the presence of growth factors such as EGF [164]. Other studies have also shown that increased expression of specific HER ligands, such as TGF-a, made cells less responsive to trastuzumab, and in fact TGF-a was induced by trastuzumab treatment of metastatic breast tumours [165, 166]. Furthermore, inhibition of EGFR restores sensitivity to the trastuzumab resistant cells [163, 165]. These data suggest that trastuzumab-resistance may be associated with an EGFR-related escape mechanism to HER-2 inhibition.

(iv) Aberrant Akt and PTEN signalling

Alterations in the intracellular signalling of the HER network have also been implicated in the development of trastuzumab resistance. Increased PI3K/Akt activity has been reported in trastuzumab resistant cells [167, 168]. There are a number of independent studies which suggest that loss of the protein phosphatase PTEN may be responsible for this deregulated signalling in resistant cells [122, 168, 169]. PTEN functions as a tumour suppressor gene that negatively regulates the AKT signalling pathway via direct inhibition of PI3K signalling. Downregulation of PTEN by antisense in breast cancer cells conferred resistance to trastuzumab *in vitro* and *in vivo* [122]. Inhibition of proteosomal degradation of PTEN also restored sensitivity to trastuzumab resistant cells [168]. In 47 patients with HER-2-overexpressing breast cancer, reduced PTEN levels correlated significantly with decreased response to trastuzumab-based therapy [122], and this was confirmed in another study of 17 clinical samples [168]. However, not all studies have linked PTEN loss with trastuzumab resistance. Neve *et al* [170] showed in a panel of nine HER-2 positive cell lines that there was no association between PTEN protein levels and trastuzumab

response. This discrepancy in the literature can perhaps be explained by a recent study by Berns *et al* [171]. Using an unbiased RNAi genetic screening approach, they identified knock-down of PTEN as the only gene from 8,000 screened to confer trastuzumab resistance on BT474 cells. Yet measurement of PTEN protein expression in a small group of patients (n = 51) revealed only a weak association between PTEN loss and poor trastuzumab response. Another mechanism by which increased activation of AKT signalling can occur is by activating mutations in the gene encoding the p110a subunit of PI3K. The authors measured the existence of these mutations in the same cohort of patients and again only found a weak association with poor responses to trastuzumab [171]. Data from this study and others suggests that PTEN loss and activating PI3K mutations are mutually exclusive in cancer [171, 172]. When patients were grouped as either PTEN lost or PI3K mutant there was a strong significant association with poor trastuzumab response [171]. These data suggests that increased activation of Akt signalling, either by loss of PTEN or by activating mutations in PI3K, plays a role in trastuzumab resistance.

(v) Modulation of p27^{kip1}

Activation of the Akt pathway has been shown to increase tumour cell proliferation via direct phosphorylation of the cell cycle inhibitor p27^{kip1}. Phosphorylation of p27^{kip1} by Akt prevents its translocation to the nucleus [173, 174]. Trastuzumab-mediated growth arrest is dependant on p27^{kip1}, and its inhibitory interaction with cdk2 [131]. Nahta *et al* [175] demonstrated that p27^{kip1} levels were reduced in trastuzumab-resistant SKBR3 cells, while expression of cdk2 was increased. Exogenous addition of p27^{kip1} into these cells restored sensitivity to trastuzumab. Cellular localization of p27^{kip1} may also be important for trastuzumab response, as trastuzumab-resistant BT474 cells demonstrated loss of nuclear p27^{kip1} expression [176].

(vi) Increased IGF-IR signalling

Evidence of cross-talk between IGF-IR and HER-2 signalling pathways has led to investigations of the role of IGF-IR in response or resistance to trastuzumab. Lu *et al* [177] reported that IGF-IR signalling interfered with the action of trastuzumab in breast cancer cell lines. Trastuzumab inhibited growth of HER-2 transfected MCF7/HER2-18 cell lines, which express high levels of IGF-IR, only when IGF-IR signalling was minimized by reduction of serum concentration, or treatment with IGF-

IR antibody aIR3 or with recombinant human (rh) IGFBP3. On the other hand, the growth of SKBR3 cells, which have low IGF-IR levels, was inhibited by 42% by trastuzumab. However, transfection of IGF-IR into these cells conferred almost complete resistance to trastuzumab. Again, rhIGFBP3 restored sensitivity to trastuzumab. Combining trastuzumab with reduction of IGF-IR signalling by a heat-induced dominant negative IGF-IR, 486/STOP, resulted in synergistic effects on growth inhibition in MCF7/HER2-18 cells [178].

Transfection of IGF-IR into SKBR3 cells also reduced p27^{kip1} levels [177], and IGF-I stimulation antagonised trastuzumab-induced p27^{kip1} upregulation [179]. This was accompanied by increased expression of Skp2, a ubiquitin ligase for p27^{kip1}, and by increased association of Skp2 and p27^{kip1}. Nahta *et al* [175] established trastuzumab-resistant SKBR3 cells by long-term exposure to trastuzumab. These cells were more resistant to trastuzumab, and had reduced p27^{kip1} levels. In both models, proteosome inhibitors induced p27^{kip1} expression [175, 179], suggesting that IGF-I-mediated resistance to trastuzumab involved targeting of p27^{kip1} to the proteosome degradation machinery. Akt signalling was also shown to be involved in IGF-I mediated reduction of p27^{kip1}, while MAPK inhibition had no effect [179].

Recently, Jerome *et al* [180] confirmed that rhIGFBP3 enhanced the effect of trastuzumab in MCF7/HER2-18 and SKBR3/IGF-IR cell lines. They also studied IGF-IR signalling in trastuzumab-resistant BT474 cells (BT474/HerR), which had acquired resistance through long-term exposure to trastuzumab. BT474/HerR cells had 3-fold higher expression of IGF-IR compared to parental cells, and were more resistant to trastuzumab; trastuzumab inhibited 22% of growth, compared to 40% in parental cells. The combined treatment of rhIGFBP3 and trastuzumab also had significant growth-inhibitory effects in BT474/HerR cells compared to either treatment alone, and this was associated with decreased phosphorylation of IGF-IR and its downstream signalling molecules Akt and MAPK [180]. This combined treatment also had significant anti-tumour effects on MCF7/HER2-18 xenografts.

Nahta *et al* [181] demonstrated that HER-2 and IGF-IR heterodimerize in trastuzumab-resistant SKBR3/HerR cells, and not in parental SKBR3 cells, suggesting that this heterodimerization contributes to trastuzumab resistance. IGF-I also stimulated

phosphorylation of HER-2 only the resistant cells, while a specific IGF-IR TKI, I-Ome-Ag538, decreased phosphorylated HER-2, again only in the resistant cells. Earlier studies, however, have shown that HER-2/IGF-IR heterodimers can be induced by IGF-I or heregulin in MCF7 cells [182], and that knocking out IGF-IR expression in breast cancer cells and xenografts also reduced HER-2 phosphorylation [182, 183]. Heterodimerisation and activation of HER-2 by IGF-IR, therefore, is not exclusively a characteristic of trastuzumab-resistant cells.

These data highlight the influence of IGF-IR signalling on response to trastuzumab in pre-clinical models. Kostler *et al* [184] analysed IGF-IR levels by IHC in 72 patients receiving trastuzumab for HER-2-overexpressing metastatic breast cancer. No correlation was observed between IGF-IR and any clinical or biological characteristics, including response or survival, and IGF-IR expression levels were not predictive of response to trastuzumab. The authors acknowledge, however, that the frequency of IGF-IR in this study was low, probably due to the fact that many of the tumours studied were grade 3 and hormone-negative, in which IGF-IR is usually down-regulated. This analysis, therefore, included only 39 IGF-IR-positive tumours.

Smith *et al* analyzed tissue samples from 77 patients who received trastuzumab and chemotherapy for HER-2-overexpressing metastatic breast cancer [185]. This study used tissue microarrays to measure expression and activation of a number of receptors, ligands, and downstream signaling molecules. While HER-2, EGFR and neuregulin-1 levels significantly correlated with patient outcome, IGF-IR expression alone did not. Similarly, phosphorylation of S6 ribosomal protein (pS6), which integrates signals through mTOR and p70 S6 kinase (p70S6K), did not have independent predictive value. However, the combination of low IGF-IR expression and high pS6 levels predicted a favorable patient response, and the combination of low IGF-IR, high neuregulin-1, and high pS6 levels were most strongly correlated with response to the trastuzumab-containing regimen. Though the numbers of patients in each subgroup of this study were quite small, these data suggest that elevated IGF-IR expression may contribute to resistance to trastuzumab in breast cancer patients.

Further studies with a larger cohort of HER-2 and IGF-IR expressing patients may more accurately determine the role of IGF-IR in predicting response to trastuzumab. Phosphorylated IGF-IR levels, or phosphorylation levels of its downstream signalling

mediators, such as IRS-1 or -2, Akt or MAPK, may give a more accurate indication of IGF-IR activity.

1.2.2 Lapatinib

HER-2 and EGFR are co-expressed in approximately 30% of breast cancers [186], and increased EGFR signalling may compensate for loss of HER-2 activity in trastuzumab-resistant tumours. Lapatinib (Tykerb[TM], GlaxoSmithKline) is a small molecule tyrosine kinase inhibitor of both HER-2 and EGFR, which binds reversibly to the ATP-binding site of both receptors and blocks receptor phosphorylation and activation [187]. Correlation of lapatinib response with levels of EGFR and HER-2 in 61 cell lines, from different cancer types, showed that very high levels of EGFR and/or HER-2 expression increased sensitivity to lapatinib sensitivity. However, Konecny *et al* showed that in a panel of 22 breast cancer cell lines, sensitivity to lapatinib correlates with HER-2 expression and not with EGFR expression [113].

Lapatinib inhibited the proliferation of HER-2-overexpressing breast cancer cell lines and xenografts [113], and also had synergistic inhibitory effects when combined with trastuzumab in four breast cancer cell lines, and significantly inhibited the proliferation of cell lines with acquired resistance to trastuzumab [113]. Lapatinib induces apoptosis in tumour cells *in vivo* [188] and the combination of lapatinib and trastuzumab enhanced apoptosis-induction in HER-2 overexpressing breast cancer cells *in vitro* [189]. Lapatinib in combination with tamoxifen also effectively inhibited the growth of HER-2-overexpressing tamoxifen-resistant tumour cells in a xenograft model [190].

Lapatinib inhibition of EGFR and HER-2 phosphorylation results in inhibition of phospho-Akt and phospho-Erk 1/2, both *in vitro* and in tumour xenografts [191]. Konecny *et al* showed that lapatinib response correlates with its ability to inhibit HER-2, Raf, Akt and Erk phosphorylation [113]. Lapatinib can also inhibit phosphorylation of the truncated p95 form of HER-2, which lacks the extracellular domain [87].

Lapatinib has also shown clinical efficacy in breast cancer patients [187]. In one phase II study, single agent lapatinib was evaluated in patients with relapsed or refractory inflammatory breast cancer. The patients were divided into two cohorts; cohort A included patients with HER-2-positive disease, while cohort B included patients with EGFR-positive/HER-2-negative disease. In 36 patients in total, a 62% response rate

was reported in cohort A, compared to 8% in cohort B. 75% of cohort A patients had previously treated with trastuzumab, and were either refractory or resistant to treatment, suggesting the success of targeting the HER-2 kinase domain in HER-2 resistant breast cancer. Interestingly, the frequency of expression of IGF-IR was 84% in cohort A, suggesting that elevated IGF-IR signalling may also be contributing to trastuzumab resistance in these patients [186]. In another similar phase II trial, tumours co-expressing pHER-2 and pHER-3 were more likely to respond to lapatinib, and Prior trastuzumab therapy or loss of PTEN did not preclude response to lapatinib [108]. A decrease in serum levels of HER-2 ECD has also been correlated with clinical response to lapatinib [192].

It has also been suggested that TKIs may have the advantage over antibody therapy of the ability to cross the blood brain barrier, and may therefore reduce the risk of CNS metastasis. In a study of 39 HER-2-positive advanced breast cancer patients with CNS metastatic disease, lapatinib showed clinical benefit in 5% of patients [186]; investigation with larger studies are warranted to explore this clinical benefit. Lapatinib has also shown clinical efficacy alone or in combination with trastuzumab against breast cancer in phase II and III trials [187], and a trial combining lapatinib and trastuzumab versus lapatinib alone given at progression only to HER-2-overexpressing breast cancer patients developing resistance to trastuzumab is currently underway.

Evidence from preclinical and clinical testing of lapatinib suggests that lapatinib and trastuzumab have non-overlapping mechanisms of resistance. In three cell line models of trastuzumab resistance, lapatinib retained significant activity [113]. Biomarkers studies in tumour samples from patients treated with lapatinib suggest that neither loss of PTEN nor expression of IGF-IR preclude response to lapatinib [188, 193, 194].

A recent study by Sergina *et al* [195], showed that reactivation of HER-3 mediated resistance to EGFR and HER-2 inhibition. While EGFR (gefitinib) and HER-2 (tyrophostin) selective TKIs efficiently inhibit auto-phosphorylation of EGFR, HER-2 and downstream MAPK and JNK signalling in HER-2 positive breast cancer cells, HER-3 signalling resumes after 12-24 hours of treatment. Reactivation of HER-3 leads to reactivation of Akt signalling and is believed to be mediated by Akt-driven negative feedback signalling. Concentrations of the TKIs which completely inactivate HER-2

effectively suppress HER-3 signalling, but these concentrations are not likely to be safely achievable *in vivo*. Although lapatinib was not tested in this study, the HER-3 mediated escape from EGFR and HER-2 inhibition may apply to all HER TKIs.

An *in vitro* model of acquired resistance to lapatinib was developed by chronic exposure of lapatinib-sensitive BT474 cells to lapatinib [196]. In this model, acquired resistance is attributed to a switch in cell survival dependence from HER-2 alone to co-dependence upon ER and HER-2. The increase in ER signalling was mediated, as least in part, by derepression of the transcription factor FOXO3a caused inactivation of Akt by lapatinib. Xia *et al* also showed that short-term exposure to lapatinib increased FOXO3a activity and ER signalling in breast cancer patients after 14 days of lapatinib treatment [196]. Mechanisms of acquired resistance to lapatinib in HER-2 positive, ER negative breast cancer have not yet been reported.

1.3   IGF-IR IN BREAST CANCER

The insulin-like growth factor system is a complex regulatory network of two peptides (IGF-I and IGF-II), two cell surface receptors (IGF-IR and IGF-IIR), six IGF binding proteins (IGFBPs), as well as IGF receptor-interacting proteins, such as those of the insulin-receptor-substrate (IRS) family, and IGFBP-regulating molecules such as proteases. The IGF system plays key roles in cellular growth, proliferation, differentiation, migration and apoptosis, and by regulating these cellular processes, the IGF system asserts its physiological influences on tissue formation and remodelling, bone growth, brain development, energy metabolism, and body growth and longevity [197-199]. Aberrant signalling through IGF-IR or its downstream pathways is known to contribute to human malignancy [200]. Numerous studies have reported associations between IGF-I, IGF-II and IGFBP levels and risk of developing a number of cancers [201], and overexpression of IGF-IR in cell and animal models demonstrates its role in transformation, tumour growth, and metastasis [202]. In this section, the structure and function of the IGF system components, the signalling events that they can activate and the contribution of IGF-IR signalling to the malignant phenotype will be reviewed.

1.3.1 The IGF-I/IGF-IR system/signalling pathway

1.3.1.1 IGF-I and IGF-II structure and function

IGF-I and IGF-II are single chain polypeptides of 70 and 67 amino acids respectively, and contain four domains, A, B, C, and D. The A and B domains of both are 50% homologous to those of insulin (Rinderknecht and Humbel, 1978), though the C-termini (containing the D domain) share no homology with the proinsulin C-peptide, and are not cleaved from the molecule as occurs in proinsulin processing.

The majority of circulating IGF-I is produced by the liver, and its production is strongly regulated by growth hormone (GH). However, most tissues can produce IGFs, and when circulating IGF-I concentration was reduced by 80% in a mouse model [203], the growth rate was not significantly reduced, suggesting the importance of autocrine or paracrine production of IGF-I in growth regulation. In some tissues, IGF-I gene expression is under the control of other hormones; for example, estradiol regulates IGF-I expression in the endometrium [204].

IGF-II expression is much higher in foetal development than in postnatal or adult life [205]. Disruption of the IGF-I or IGF-II gene in prenatal mice leads to a 60% decrease in birth weight, though in postnatal mice, IGF-II is no longer expressed. In humans, however, IGF-II is expressed throughout life, but cannot compensate for loss of IGF-I activity in patients with an IGF-I deficiency, which leads to severe developmental retardation [206, 207]. IGF-II is also expressed in the liver and other tissues, but is not tightly regulated by GH [208]. IGF-I and IGF-II bind with different affinities to IGF-IR, IGF-IIR and IR, and despite the significant structural similarity between the ligands, they produce very different outcomes depending on which receptor they bind.

1.3.1.2 IGF-IR structure and function

IGF-IR is related to, and structurally similar to IR, and both are transmembrane tyrosine kinase receptors (TKRs). They differ from other TKRs in that they have a covalent dimeric structure of two a and two ß chains. Both are synthesized as single chain precursors that are glycosylated on the extracellular regions, dimerized and proteolytically processed to yield the mature receptors (reviewed in [209]). The a-

subunits of IGF-IR are ~135 kiloDalton (kDa) each and are extracellular, and contain the ligand-binding domains [210, 211] [fig. 1.3.1]. The ß-subunits, which are 95 kDa each, span the membrane, and their cytoplasmic portions contain the tyrosine kinase domains [212]. The kinase domains are flanked by two regulatory regions, a juxtamembrane region used as a docking site for IRS and Shc as well as for receptor internalization, and a C-terminal tail containing two phosphotyrosine binding sites (reviewed in [213]). The kinase domains of IGF-IR and IR are 84% homologous [209].
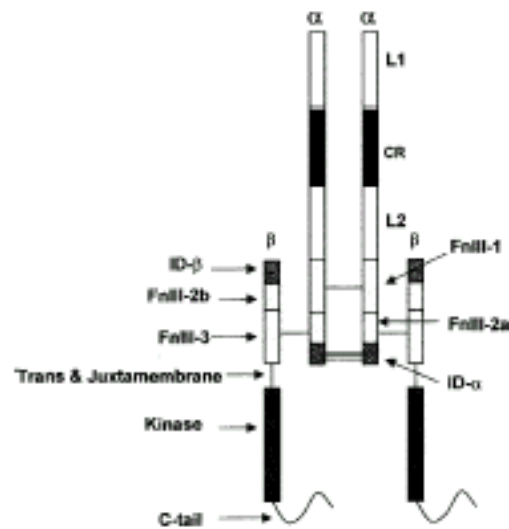
Figure 1.3.1. Structure of the IGF-IR dimer showing the distribution of domains across the a-and ß-chains and the approximate location of the a-ß disulfides and the a-a dimer disulfide bonds [From Adams *et al,* 2000. © 2000 Birkhäer Verlag, Basel].

The 3D structure of the first three domains (L1-Cys-rich-L2) of IGF-IR has been solved [Fig 1.3.2]. These domains surround a cavity large enough to accommodate a ligand molecule [214]. The cysteine-rich domain was identified as the major IGF-I binding site, and both the L1 and cys-rich domains are critical for IGF-I binding, whereas only the L1 domain is needed for IGF-II binding (reviewed in [207]). The structures of the active and inactive kinase domains of IR and the active kinase of IGF-IR have also been described [215-217]. They reveal a novel mechanism of auto-inhibition, whereby a vital tyrosine of an "activation loop" competes with protein substrates before phosphorylation, blocking the active site of the receptor until

transphosphorylation, at which point the loop becomes stabilised in an open position (reviewed in [25]).

_____
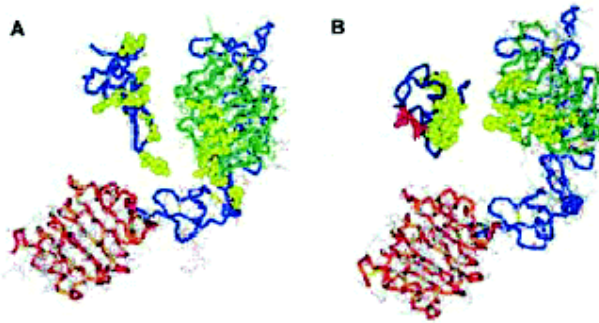
Figure 1.3.2. 3D structure of the L1-Cys-rich-L2 domain of **A** IGF-IR and **B** IR as determined by X-ray crystallography. The amino acids determined by site-directed mutagenesis to be important for ligand binding are shown in yellow as van der Waals spheres [213]. The 3D structures of IGF-I [218] and insulin [219] molecules are shown to scale.

_____

Ligand binding to the a-subunits of the extracellular region of IGF-IR or IR causes a conformational change resulting in ATP binding and tyrosine phosphorylation of the activation loop of the intracellular ß-subunits, increasing the kinase activity of the receptor [216, 220, 221]. IGF-I, IGF-II and insulin bind to IGF-IR, IGF-IIR and IR with different affinities [fig. 1.3.3]. Stimulated IGF-IR can activate signalling pathways involved in cell proliferation, differentiation, migration and protection from apoptosis [197-199]. Insulin receptor-A (IR-A) and insulin receptor-B (IR-B) have similar affinities for insulin, though IR-B activation produces the well characterised metabolic responses to insulin, while IR-A has higher affinity for IGF-I and IGF-II than IR-B [222], and its activation leads to similar cellular responses to IGF-IR activation. In cells that express both IGF-IR and IR, hybrid receptors form consisting of one half of IGF-IR and one half of either IR-A or IR-B. These heterodimers bind IGF-I with high affinity, and insulin with low affinity [223]. Their cellular or physiological roles are unknown.

IGF-IR is expressed at its highest levels during foetal and early postnatal development, but is expressed at lower levels in most adult tissues [224]. IGF-IR and IR have different, but partially overlapping physiological functions [225]. IGF-IR-deficient

mice, have severe foetal growth retardation, and die within minutes of birth, mainly due to under-developed respiratory muscles [226]. These mice also develop metabolic abnormalities. Genetic studies that knock out expression of one or both of IR and IGF-IR indicate that IGF-IR is primarily a growth promoter, mediating IGF-I and IGF-II action on prenatal growth and IGF-I action on postnatal growth, while IR mediates IGF-II-induced prenatal growth, but is mainly a mediator of the metabolic effects of insulin. Each receptor, however, has overlapping functions with the other (reviewed in [199, 225]).

_____
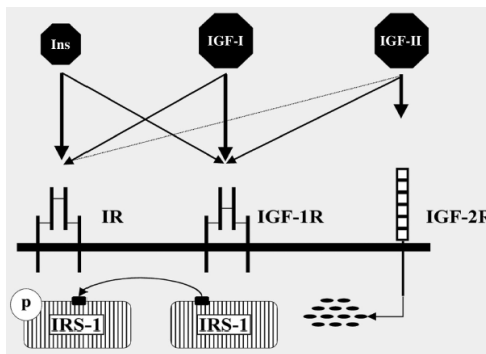
Figure 1.3.3.   Affinity of interactions of various insulin family ligands with their receptors. Insulin and IGF peptides have different affinities for IR, IGF-IR and IGF-IIR. Thickness of the arrow represents the affinity of a ligand for a receptor. IGF-I has a higher affinity for IGF-IR than for IR. Binding of the ligands to IR or IGF-IR initiates signalling pathways such as IRS-1 pathway. Binding of IGF-II to IGF-IIR leads to the degradation of this ligand. [© 2000-2005 Landes Bioscience].
_____

1.3.1.3 IGF-IIR structure and function

Unlike IGF-IR and IR, IGF-IIR (also known as cation-6-phosphate receptor) is a large single-chain peptide, with no intrinsic tyrosine kinase activity [227]. The receptor is a 300 kDa protein containing an extracellular, a transmembrane, and an intracellular domain (reviewed in [228]).

IGF-IIR binds IGF-II with high affinity, but binds IGF-I with low affinity and does not bind insulin (reviewed in [207] [fig. 1.3.2]. The majority of IGF-IIRs are located on

intracellular membranes, and their primary function is to transport IGF-II to liposomes for degradation, which occurs upon IGF-II ligand binding, preventing receptor activating interactions. IGF-IIR also binds many other ligands, including proteins containing mannose-6-phosphate, and through these interactions exerts IGF-independent effects on cell proliferation (reviewed in [229]).

1.3.1.4 IGF binding proteins

The IGFBPs are a family of six known proteins, IGFBP1 to IGFBP6, ranging in molecular weights from 22.8 – 31.3 kDa [230]. Each IGFBP has three distinct domains of approximately equal size; the N- and C-termini are highly conserved, while the middle or linker domain is the least conserved region [231-233]. Both the N and C domains are cysteine-rich and contain various disulphide bonds, and both contain IGF binding sites (reviewed in [232]. Both domains are required for wildtype IGF binding [234, 235].

IGFBP precursor proteins have secretory signal peptides, and the mature proteins are all found extracellularly. IGFBPs have higher affinity for IGFs (~0.1 nM) than does IGF-IR (~1nM); thus, by sequestering the IGFs, IGFBPs regulate their availability to receptors, thereby inhibiting, or enhancing, IGF actions. About 75% of circulating IGF is bound with IGFBP3 to form a 150 kDa complex with acid-labile-subunit (ALS) [236, 237]. The complex prolongs the half-life of IGFs and maintain them in circulation, as the complexes cannot cross the vascular endothelium. Other IGFBPs bind the remaining 20 – 25% of circulating IGFs, forming smaller complexes of 40 – 50 kDa, which can penetrate the vascular endothelium, making the IGFs available to local tissues [232, 237].

IGFBP activity is regulated by a number of proteolytic enzymes; both IGFBP-specific and non-specific proteases have been identified to cleave IGFBPs. Matrix metalloproteinases (MMPs) are a family of proteolytic enzymes involved in tissue remodelling by degradation of extracellular matrix (ECM) and are known to proteolyse IGFBPs. Prostate specific antigen (PSA) is a serine protease that specifically acts on IGFBP3. The proteolysis of IGFBPs generates protein fragments with reduced, or no affinity for IGFs, increasing free IGF levels [238].

1.3.1.5 IGF-IR activation and signal transduction

Ligand binding to IGF-IR causes a conformational change, resulting in ATP binding, and autophosphorylation of its intracellular kinase domain [216, 220, 221]. IGF-IR has fifteen tyrosine residues in total in its cytoplasmic domain; three at positions 1131, 1135 and 1136 are contained within the activation loop and are vital for ligand-stimulated activation. The subsequent phosphorylation of five other tyrosines [239, 240] provides docking sites for a wide range of intracellular proteins (summarised in table 1.3.1), which then initiate multiple signalling cascades.

Table 1.3.1. Cellular proteins interacting with the cytoplasmic domain of IGF-IR (from Adams et al, 2000).

Protein	Function
IRS-1	adaptor
IRS-2	adaptor
IRS-3	adaptor
Shc	adaptor
Grb10	adaptor
CrkII	adaptor
SH2-B	adaptor
p85	regulatory subunit of PI3K
p55?	regulatory subunit of PI3K
GAP	GTPase-activating protein
Syp/SHP-2	tyrosine phosphatase
CSK	cytoplasmic tyrosine phosphatase
Jak-1	cytoplasmic tyrosine phosphatase
SOCS-1	suppressor of cytokine receptor signalling
SOCS-2	suppressor of cytokine receptor signalling
14.3.3ß	adaptor 'scaffolding' proteins
14.3.3?	adaptor 'scaffolding' proteins
14.3.3e	adaptor 'scaffolding' proteins

The two best characterised pathways associated with IGF-IR activation are the MAPK signalling cascade, initiated by the phosphorylation of Shc, and the Akt pathway,

initiated by phosphorylation of IRSs. Shc contains a phosphotyrosine binding (PTB) domain as well as numerous tyrosine residues which can be phosphorylated by IGF-IR [24]. There are four known IRS proteins (IRS-1 – 4), and each contains a phosphotyrosine binding (PTB) domain, an N-terminal PH domain, and a C-terminal rich in tyrosine residues, but no SH2 domain. IRS-1 and IRS-2 are the best characterised. The PTB domain of IRS-1, IRS-2 and Shc bind to the same phosphotyrosine (p-Tyr 950) within the juxtamembrane region of IGF-IR, and for Shc and IRS-1 binding, a tyrosine-phosphorylated NPEY motif within the juxtamembrane domain is required [24]. The C-terminal domain of the IRSs contain multiple tyrosine phosphorylation sites, varying from 13 in IRS-3 to over 20 in IRS-1 [209], and these residues are within motifs known to favour interaction with SH2 domains [241]. Phosphorylated IRSs interact with various SH2-containing proteins such as adaptor proteins Grb2, Shc and Nck, the tyrosine phosphatase Shp2, the cytoplasmic tyrosine kinase Fyn and the p85 regulatory subunit of phosphoinositol 3-kinase (PI3K) [242, 243]. IRS-1 responds more rapidly than Shc to IGF-I stimulation; maximal phosphorylation of IRS-1 is seen within 1 – 2 minutes of simulation, while for Shc this occurs between 5 – 10 minutes [244, 245]. Receptor internalisation also seems to be required before maximal phosphorylation of Shc is achieved [244]. IRS-1 may also activate the MAPK pathway, as Grb2 can also associate with IRS-1 via its SH2 domain. IRS-2 can also bind Grb2, though this association is not linked to activation of the MAPK cascade [209]. In the absence of IRS-1, MAPK signalling provides an alternative pathway to IGF-IR-mediated protection from apoptosis, and a second alternative is through 14.3.3 protein [246].

IGF-IR signalling, through multiple pathways, mediates cell cycle progression, cell proliferation, differentiation and apoptosis, and in doing so, plays key roles in tissue formation, specific organ development, energy metabolism, and overall body growth and longevity.

Aberrant signalling through IGF-IR or its downstream pathways contributes to malignant transformation. The critical role of the ß-subunit of IGF-IR in the stimulation of cancer cell growth was elucidated using site-directed mutagenesis [220, 239, 247-250]. Cells transfected with a truncated ß-subunit, lacking the kinase domain, were completely unresponsive to IGF-I stimulation and were unable to sustain

anchorage-independent growth or form tumours in nude mice. The specific signalling roles of some of the tyrosine residues of the kinase domain have been identified: tyrosines 1131, 1135 and 1136, which are needed for signal activation, are required for induction of transformation, and mitogenesis. Mutation of tyrosine 1136 resulted in decreased colony formation in soft agar, and mutations of any two or all three, of the tyrosines blocked transformation and metastasis. Tyrosines 1250 and 1251 have been identified to have roles in the maintenance of a tumorigenic/metastatic phenotype, and may also have other functions [251].

1.3.2 The IGF-IR system in breast cancer

1.3.2.1 IGF-I ligand and IGFBP3; population studies

IGF-I levels are highest at puberty and decline afterwards, and IGF-I and IGFBP3 concentrations vary hugely between individuals. Normal adults of age 40 - 60 years have IGF-I serum levels of approximately 100– 300 ng/ml, and IGFBP3 levels of approximately 2000–6000 ng/ml [252-255]. Since 1998, several epidemiological studies have reported that higher circulating levels of IGF-I are associated with increased risk of developing breast cancer [253, 256-258]. The ratio of IGF-I to IGFBP3 has also been associated with an increased risk of cancer [259, 260]. Most of these studies divided the population into categories (tertiles, quartiles or quintiles) based on IGF-I or IGFBP3 concentrations, and compared the uppermost and lowermost categories. The results from studies of breast and other cancers have been inconsistent, probably due to varying methods of sample collection and analysis (enzyme-linked immunosorbent assay (ELISA), radioimmunoassay (RIA) or immunoradiometric assay (IRMA)). In 2004, Renehan *et al* [260] published a systematic review and analysis of published data on prostate, colorectal, breast and lung cancer. They concluded that though the associations were weaker than previously suggested, higher circulating levels of IGF-I was associated with increased risk of prostate, colorectal and premenopausal breast cancer, but not lung cancer. Higher IGFBP3 levels were related to decreased risk of lung cancer only [260]. Evidence from patients with acromegaly – a condition caused by excess production of growth hormone and resulting in IGF-I levels above the normal range – support the role of IGF-I in cancer development as patients with this condition are at an increased risk of cancer, particularly colorectal cancer [261].

Data from population studies of IGF-I and IGFBP3 levels and risk of breast cancer are inconsistent. Early studies demonstrated that IGF-I serum levels are significantly higher in breast cancer patients than normal controls [262-264]; that IGFBP3 levels are higher in breast cancer patients than controls [263, 265]; that the ratio of IGF-I to IGFBP3 is significantly elevated in premenopausal breast cancer [266]; and that high IGF-I and/or low IGFBP3 is associated with increased risk of premenopausal breast cancer [256, 264, 267]. Later studies, however, reported no association between IGF-I

levels and pre- or postmenopausal breast cancer [268, 269], while another reported positive associations between both IGF-I and IGFBP3 and risk of breast cancer [270]. There is overall consensus regarding lack of an association between either IGF-I or IGFBP3 and postmenopausal breast cancer, with the exception of a small study of African-American women with 30 postmenopausal breast cancer patients and 30 controls that found a significant association between high IGF-I levels and increased breast cancer risk [271].

Renehan *et al* [201] carried out a meta-analysis of 12 prospective cohort studies, calculating cumulative risk ratios (see table 1.3.2). They conclude that higher IGF-I levels are associated, though not as strongly as previously thought, with increased risk of pre-menopausal breast cancer (risk ratio = 1.69), or in women under 50 (risk ratio = 2.13). IGFBP3, however, is not associated (risk ratio = 1.11) with risk of pre-menopausal breast cancer. Rollison *et al* [272] recently demonstrated that high pre-menopausal levels of IGF-I (at ages 25-35) in 152 women were associated with risk of post-menopausal breast cancer. Further investigation is needed to determine the significance of these findings.

These data identify IGF-I as a risk factor for premenopausal breast cancer, and suggest that IGFBP3, either by its independent actions, or by its association with IGF-I ligand, may also influence the development of breast cancer in premenopausal women.

Table 1.3.2.   Sumamry of studies of IGF-I and IGFBP3 levels and risk of premenopausal breast cancer (NA, not available).

Study	Year	Summary of findings	Group	no. cases / controls	OR for IGF-I	OR for IGFBP3
Rinaldi *et al*	2006	Associations with IGF-I and IGFBP3 in women > 50 only.	< age 50	NA	1.03	0.92
Schernhammer *et al*	2006	No associations in pre- or post-menopausal women.	pre-meno	239/478	0.98	1.10
Rinaldi *et al*	2005	Modest associations with IGF-I and IGFBP3 in pre-menopausal women.	pre-meno	138/259	1.41	1.77
Schernhammer *et al*	2005	Modest association with only IGF-I in pre-menopausal women.	pre-meno	218/281	1.60	1.20
Allen *et al*	2005	Modest association with only IGF-I in pre-menopausal women.	pre-meno	70/209	1.71	0.49
Muti *et al*	2002	Associations with IGF-I and IGFBP3 in pre-menopausal women.	pre-meno	69/267	3.12	2.31
Krajeik *et al*	2002	Associations with IGF-I and IGFBP3 in pre-menopausal women.	pre-meno	66/66	2.01	5.28
Kaaks *et al*	2002	No associations in pre- or post-menopausal women.	< age 50	116/330	0.63	1.37
Toniolo *et al*	2000	Association with only IGF-I in pre-menopausal women.	pre-meno	172/486	1.60	1.18
Hankinson *et al*	1998	Association with IGF-I in pre-menopausal women.	pre-meno	76/105	2.88	-

1.3.2.2 Overexpression of IGF-IR in breast cancer

Studies in breast cancer in the 1990s, using ligand-binding methods (histo-autoradiographic analysis (HAA), radio-receptor assay (RRA or RIA) reported that IGF-IR is expressed in 39 – 93% of breast cancer samples [273-275], that IGF-IR expression is higher in breast cancer than normal tissues [274, 276], and that it correlates with favourable prognosis in breast cancer patients [274]. Later studies of larger numbers of cases, however, have quantified IGF-IR expression by immunohistochemistry (IHC). IGF-IR staining of breast cancer tissues is scored on a scale of 0 – 3+. Nielson *et al* [277] reported high expression (scores of 2+ - 3+) in 87% of 707 breast cancers by tissue micro-array (TMA). Interpretation of scoring may vary between studies, and two other groups reported overexpression (scores of 2+ - 3+) in 44% of 210 breast cancers by IHC [278], and 47% of 150 breast cancers by TMA [279]. Tissue studies report no correlation with survival [277, 278, 280]. Other tissue sample studies compared tumour samples to benign, adjacent or normal samples. Happerfield *et al* [273] reported either no difference between breast carcinoma and normal tissue, and a more recent, though smaller, study with paired breast cancer and adjacent non-malignant tissue also found no difference in expression (n=31 pairs) [281]. Recent studies report higher mRNA levels in normal or tumour-adjacent breast than breast cancer [280, 282, 283], and higher levels in benign breast disease (n=206) than primary breast cancer (n=508) [280]. Schnarr *et al* [284] found that IGF-IR is expressed at high levels in control samples and in well- and moderately-differentiated carcinomas, but at low levels in poorly differentiated breast cancers. Downregulation of IGF-IR correlated with tumour progression. Expression of IGF-IR was also found to be more frequent in primary breast tumours (56%) than lymph node metastasis (44%) [285]. These data suggest that progression of breast cancer is accompanied by a reduction of IGF-IR signalling.

LeRoith and Roberts [286] suggest that decreased expression of IGF-IR may protect cells from a recently described, non-apoptotic form of programmed cell death that is triggered by the unliganded IGF-IR [287].

Although IGF-IR may not be overexpressed in breast cancer to the extent that was originally suggested, there is evidence to support the role of the IGF-IR signalling

pathway in breast cancer. IGF-IR is present in most breast cancer tissue samples [273, 277, 279, 280, 288] and cell lines studied to date [289, 290].

Resnik *et al* [200] have demonstrated that IGF-I receptor activation is also enhanced in malignant breast tissue. IGF-IR/insulin receptor hybrids, which can also mediate IGF-I signalling, are also overexpressed in breast cancer [291].

Increased IRS-1 levels have also been associated with tumour development, hormone independence, and anti-estrogen resistance in breast cancer [292]. IRS-1 levels also correlated with recurrence in 195 early stage tumours [293]. Schnarr *et al* [284] found higher IRS-1 expression in normal tissue and well- and moderately-differentiated breast cancers than in poorly differentiated breast cancers, and report that downregulation of IRS-1 correlates with disease progression (n=69). Koda *et al* [294], however, found similarly high levels of IRS-1 in both primary and metastatic tumours, though in well-differentiated tumours, there was a significant correlation between IRS-1 levels in the primary and the metastatic tumours. These data seem somewhat contradictory, but perhaps the proliferative and anti-apoptotic effects of IRS-1 are required for transformation tumourigenesis, and proliferation of primary or secondary tumours, but its downregulation may be required for dedifferentiation and metastasis [295]. Its downregulation may facilitate IRS-2-mediated IGF-IR signalling. The distinct responses of IRS-1 and IRS-2 to IGF-IR activation have recently been demonstrated [296]; proliferation and anti-apoptotic responses are mediated by IRS-1 [294], while motility and metastasis correlate with increased IRS-2 activity [297].

It is also interesting that loss of heterozygosity of the IGF-IIR locus and mutations of the IGF-IIR binding domain of the remaining IGF-IIR allele are prevalent in breast cancer; perhaps the loss of ability of IGF-IIR (which has no kinase domain) to bind IGF-II allows increased interaction of IGF-II with IGF-IR, thereby increasing kinase activity and enhancing IGF-IR signalling [298].

1.3.3 IGF-IR signalling in breast cancer

1.3.3.1 Anti-apoptotic IGF-IR signalling

IGF-I/IGF-IR signalling has potent anti-apoptotic effects on cancer cells. This has been demonstrated with the use of antisense RNA technology, and a dominant negative mutant form of IGF-IR, both of which inhibited proliferation of cancer cells in monolayer and soft agar [299-301]. IGF-IR antisense also prevented the growth of C6 glioblastoma and FO-1 human melanoma cells in nude mice [299, 300], and expression of 468/STOP, a dominant negative IGF-IR, in C6, 3T3 and R- cells, induced expansive apoptosis *in vivo* [301]. Interestingly, cells expressing this mutant form were also shown to have a bystander effect, whereby they can inhibit the growth of wild-type tumours when mutant cells are co-injected with wild-type cells [302].

Overexpression of IGF-IR in MCF-10A breast cells enhanced proliferation and decreased apoptosis [303]. IGF-I signalling also protects breast cancer cells from apoptosis induced by numerous types of chemotherapies including antimetabolites (5-fluoruracil, methotrexate), antiestrogen (Tamoxifen), and topoisomerase 1 inhibitors (camptothecin) in HBL100 cells [304], and microtubule-stabilising agents (paclitaxel) and anthracyclines (doxorubicin) in MCF7 cells [305]. IGF-IR was demonstrated to exert some of its anti-apoptotic effects through transactivation of EGFR, which activates MAPK signalling and anti-apoptotic protein BAD in mammary epithelia cells [306]. Overexpression of IGF-IR in SKBR3 cells promoted resistance to the EGFR tyrosine kinase inhibitor gefitinib (Iressa), while downregulation of IGF-IR enhanced response and apoptosis-induction [307]. Overexpression of IGF-IR in MCF-10A cells upregulated phosphorylation of Ser^{473} of Akt and Ser^{2448} of mTOR [303]. Studies have shown that IGF-I rescue of MCF7 cells from chemotherapy-stimulated cell death involves at least two mechanisms; inhibition of apoptosis through PI3K/Akt, and induction of proliferation through both PI3K/Akt and MAPK signalling cascades [298, 305].

Several recent reports have demonstrated that IGFBP3 induces apoptosis in cancer cells, for example, in MCF7 breast cancer [308] cells, and can enhance ceramide-induced apoptosis in Hs578T breast cancer cells [309]. These effects may be due to sequestering of IGFs, thereby blocking their anti-apoptotic signalling through IGF-IR

[308]. However, IGFBP3 can also induce apoptosis in an IGF/IGF-R-independent manner, as was demonstrated in an IGF-IR-negative fibroblast cell line [310]. Transfection of IGFBP3 into T47D and MCF7 breast cancer cell lines also induced apoptosis, increased the ratio of pro-apoptotic to anti-apoptotic members of the Bcl-2 family, and sensitized cells to ionising radiation-induced apoptosis [311]. Furthermore, paclitaxel-induced apoptosis in Hs578T cells was accompanied by an increase in IGFBP3 levels, suggesting that IGFBP3 may be an important modulator of paclitaxel-induced apoptosis [312]. Kim *et al* [313] demonstrated that IGFBP3-induced apoptosis in MCF7 breast cancer cells is IGF-IR-independent, and is mediated via a caspase-7 and -8 pathway, with minimal release of cytochrome *c* from the mitochondria or caspase-9 activity. This suggested that IGFBP3-induced apoptosis is executed via the death receptor pathway rather than the intrinsic apoptotic pathway.

1.3.3.2 IGF-IR and PTEN signalling interactions

The protein encoded by the phosphatase and tensin homolog (PTEN) gene is a phosphatase that can regulate both protein and lipid phosphorylation. It can dephosphorylate PIP_2 and PIP_3, and in doing so, prevents PI3K-mediated activation of Akt [29]. PTEN protein thus suppresses tumour formation by restraining the PI3K/Akt pathway [314]. PTEN mutations and loss of heterozygosity (LOH) of the PTEN locus have been reported in a number of cancer cells lines and advanced cancers, including breast cancer [315]. Loss of PTEN has been reported in approximately 40% of advanced breast cancers, and is often associated with ER negativity [315-319]. In addition to suppressing downstream signalling of IGF-IR, PTEN activity downregulates IGF-IR protein expression and function in a number of human cancers, including gastric adenocarcinoma, multiple myeloma, pancreatic, lung, and prostate cancer [320-324]. PTEN can also downregulate IGF-I, IGF-II activity and upregulate IGFBP3 expression in gastric, lung and prostate cancer [325]. Loss of PTEN therefore enhances IGF-I/IGF-IR signalling by different mechanisms; increasing PI3K activity, increasing IGF-IR, and IGF ligand levels, and reducing IGFBP3 levels. The role of PTEN in regulating IGF-IR signalling in breast cancer has yet to be thoroughly examined. Weng *et al* [326, 327] demonstrated that overexpression of PTEN in MCF7 cells inhibited the phosphorylation of Akt in response to stimulation by many different growth factors, and selectively decreased ERK phosphorylation stimulated by insulin

and IGF-I, but not EGF. Inhibition of IGF-I-stimulated ERK was accompanied by decreased IRS-1 phosphorylation and reduction in its association with Grb2/Sos [326]. Insulin, IGF-I and EGF also upregulate the activity of Ets-2, a transcription factor whose function is controlled by phosphorylation, in MC7F cells. Akt inhibition had no effect on Ets-2 activity, while MEK inhibition decreased its phosphorylation. Overexpression of PTEN also decreased the phosphorylation of Ets-2 in response to insulin and IGF-I, but not EGF, stimulation [327]. These results demonstrate the role of PTEN in regulating insulin and IGF-I-mediated MAPK signalling, and that its effects influence their downstream targets such as the Ets-2 transcription factor. Moorehead *et al* [328] reported that IGF-II upregulates PTEN in the mammary gland, leading to decreased Akt signalling, epithelial proliferation, and mammary morphogenesis. Perhaps, therefore, in the absence of IGF-I, IGF-II-stimulated IGF-IR (or IR) signalling promotes apoptotic and anti-proliferative pathways, but in breast cancer, increased IGF-I levels and signalling may counteract these effects, protecting from apoptosis and enhancing proliferation of malignant cells.

1.3.3.3 IGF-IR and ER signalling

Estrogen signals through estrogen receptors (ERa and ERß), which are nuclear receptors, and members of a superfamily of ligand-inducible transcription factors [329, 330]. Estrogen signalling has been associated with increased breast cancer risk [331], and many studies of overexpression of IGF-IR in breast cancer tissues report a correlation between IGF-IR levels and positive ER status [273, 274, 279, 285]. Koda *et al* [288] also found that ERa expression correlated positively with anti-apoptotic Bcl-2 and negatively with pro-apoptotic BAX proteins in breast cancer samples. In recent years, there has been increasing evidence of cross-talk between the IGF/IGF-IR and the ER signalling pathways. Estrogens were shown to increase IGF-I binding, and IGF-IR mRNA levels in MCF7 cells by seven-fold, suggesting that a potential mechanism by which estrogens stimulate breast cancer proliferation involves sensitisation to the mitogenic effects of IGFs by enhancing IGF-IR levels [332]. IGF-IR gene transcription was recently shown to be under the control of ERa, and mediated via interactions between ERa and Sp1 [333]. Estrogen also induced protein expression of IGF-IR, IRS-1 and IRS-2, and enhanced phosphorylation of IRS-1 after IGF-I stimulation of MCF7 cells [334]. In MCF7 xenografts, estrogen increased IRS-1

levels, and withdrawal of estrogen decreased growth and dramatically reduced IRS-1 expression [334]. Oesterreich *et al* [335] established MCF7-derived cells selected for loss of ERa by long-term withdrawal of estrogen. Selected cells had reduced IGF-IR and IRS-1 mRNA and protein, decreased IGF-IR signalling, and were unresponsive to either IGF-I or estrogen stimulus. Re-expression of ERa restored the IGF-sensitive phenotype, demonstrating that ERa is a critical requirement for IGF signalling in these cells. In ERa-negative breast tumours, levels of IGF-IR and IRS-1 are often low, and IGF-I is non-mitogenic [336], and in MDA-MB-435A and MDA-MB-468 ER-negative breast cancer cell lines, which are unresponsive to IGF-I, expression and activation of IRS-1 were not sufficient to induce response to IGF-I [337], suggesting that a critical factor in the signalling loop was missing. Bartucci *et al* [338] compared IGF-IR signalling in ER-positive MCF7 and ER-negative MDA-MB-231 cells. While IGF-I activated IGF-IR in both cell lines, it did not stimulate growth or improve survival in MDA-MB-231 cells, whereas in MCF7 cells, IGF-I had mitogenic and anti-apoptotic effects.

There have also been many studies demonstrating that IGF, as well as other growth factors, upregulates ER transcriptional activity. Initial studies showed that in the absence of estradiol, IGF-I could stimulate phosphorylation of ER and induce expression of an estrogen-responsive reporter gene construct [339]. This effect was mediated via IGF-IR, and could be blocked by an anti-estrogen [339, 340]. IGF-I also increased transcriptional activity of ER in MCF7, ZR75 and T47D cell lines, and this was blocked by tamoxifen. Furthermore, IGFBP1 not only inhibited IGF-I-activation of ER, but also decreased estradiol-activation of ER [341].

The pathways involved in the cross-talk between the IGF-I and ER pathways have been examined. Phosphorylation of ER was carried out by MAPK in cells treated with IGF-I or EGF [342], while estrogen induction of IGF-IR and IRS-1 expression and phosphorylation led to enhanced MAPK activity in MCF7 cells [334]. IGF-I-simulated ERa activity was also blocked by PI3K and PKA inhibitors in MCF7 cells [343], demonstrating the involvement of the Akt pathway in cross-talk. ERa expression in MDA-MB-231 cells enhanced the stability of IRS-1 and -2 and improved cell survival through upregulation of the IRS-1/Akt/Glycogen synthase kinase 3 (GSK-3) pathway [344]. Recently Zhang *et al* [345] demonstrated, using small inhibitory RNA

molecules targeting ERa, that IGF-I dependent phosphorylation of Akt and MAPK, induction of G1-S phase progression, and enhanced expression of cyclin D1 and cyclin E are all dependent on the presence of ERa.

Cross-talk between the IGF and ER pathways thus involves receptors and ligands of both systems, survival signalling through Akt and MAPK signalling cascades, as well as regulation of transcription and activity of both receptors.

1.3.3.4 IGF-IR and EGFR/HER-2 cross-talk

Because of their common signalling pathways, possible cross-talk between EGFR or HER-2 and IGF-IR signalling has been investigated. Stimulated EGFR can transactivate IGF-IR, and IGF-IR in turn can cause transactivation of EGFR [306, 346, 347]. Blockade of EGFR signalling with the EGFR tyrosine kinase inhibitor (TKI) gefitinib (Iressa, ZD1839) decreased IGF-II-induced MAPK signalling, but not IGF-II-induced Akt signalling in HCC cells, suggesting that IGF-II/IGF-IR activation triggers proliferative signals through an EGFR-dependent pathway, while its survival signals are mediated independently of EGFR [348]. Ahmad *et al* [349] report that gefitinib also reduced IGF-I stimulated Erk activity, but not Akt, in normal mammary epithelial cells. Gefitinib had no effect on IGF-IR signalling in MCF7 and CAL-51 breast cancer cell lines, suggesting that the requirement for active EGFR in IGF-IR signalling may be lost during the malignant progression. In the same study, EGFR co-immuoprecipitated with IGF-IR, suggesting a physical interaction, or heterodimerisation, between the two receptors. This was substantiated by Morgillo *et al* [350], who reported that erlotinib (Tarceva, also an EGFR TKI) induced the heterodimerisation of IGF-IR and enhanced IGF-IR signalling, and upregulated mTOR-mediated protein synthesis of EGFR and survivin in NSCLC cells. IGF-IR conferred resistance to erlotinib in these cells, and IGF-IR has also been implicated in resistance to gefitinib in breast cancer cells [307, 351]. Jones *et al* [351] established gefitinib-resistant MCF7 cells (which were also tamoxifen resistant), and these cells had elevated IGF-IR, Akt and PKC activity, and increased migratory capacity compared to parental cells, and were more sensitive to inhibition by the IGF-IR TKI AG1024. Gefitinib and AG1024 had additive-to-synergistic effects on the proliferation of MDA-MB-231, MDA-MB-468, SKBR3 and MCF7 cells lines [307],

and AG1024 also enhanced the anti-apoptotic effects of gefitinib in these cells. Increased overexpression of IGF-IR in SKBR3 cells enhanced resistance to gefitinib [307].

Cross-talk between HER-2 and IGF-IR signalling pathways has also been reported. In 1996, Ram *et al* established a series of cell lines from a patient with intraductal and invasive ductal breast carcinoma [352]. They compared two metastatic tumour cell lines to a non-neoplastic cell line. Both metastatic cell lines had amplified and overexpressed HER-2, one having higher protein levels than the other. With three cell lines of different HER-2 protein levels, they found that increasing HER-2 levels corresponded with higher HER-2 tyrosine kinase activity, and with loss of requirement for IGF and EGF for growth in culture media. These experiments showed that constitutively active HER-2 in breast cancer directly stimulates multiple signalling pathways, and that HER-2-activated proliferative pathways can substitute for those of other growth factor receptors, including IGF-IR.

The study of heregulin and HER-2 signalling in a hormone-dependent mammary tumour model showed that heregulin enhanced the proliferation of mammary tumour primary culture cells. Knocking out HER-2 expression with an antisense molecule abolished heregulin-induced proliferation, confirming that heregulin mediates its proliferative effects through HER-2. However, an antisense molecule targeting IGF-IR also completely inhibited heregulin-induced proliferation, demonstrating that a functional IGF-IR is required for heregulin/HER-2 mitogenic activity in this model [353].

Balana *et al* [182] also used antisense technology and showed that blocking IGF-IR expression decreased the phosphorylation of HER-2, while suppression of HER-2 expression had no effect on IGF-IR phosphorylation. This suggests a hierarchical interaction, whereby IGF-IR directs HER-2 phosphorylation. Co-localisation studies also showed that the two receptors physically interact, and these heterodimers could be induced by heregulin or IGF-I stimulation in MCF7 breast cancer cells [182]. IGF-IR antisense molecules also inhibited breast tumour growth *in vivo*, and reduced HER-2 phosphorylation as well as IRS-1, Akt and MAPK activity [183].

Lu *et al* [354] investigated the molecules involved in HER-2 and IGF-IR related signalling, and found that HER-2 overexpression inhibited IGF-I-induced MAPK signalling in HER-2 transfected MCF7/HER2-18 cells [354].   Inhibition of MAPK signalling was accompanied by decreased IGF-I-induced Shc phosphorylation, decreased association of Grb2 with Shc, and decreased Raf phosphorylation. In this study, overexpression of HER-2 increased the basal levels of Shc phosphorylation and association with Grb; perhaps this resulted in less free Shc and Grb2 available upon IGF-I activation in these cells. Notably, HER-2 overexpression had no effect on IGF-I-induced phosphorylation of IGF-IR, IRS-1 or Akt.

Together, these data suggest that HER-2 can send proliferative signals via the MAPK pathway, in an IGF-IR-independent manner. HER-2 overexpression has no effect on IGF-IR/IRS-1/Akt signalling. It has also been shown that HER-2-overexpressing cells have an increased requirement for the Akt pathway in anchorage-independent growth [355], and in HER-2 overexpressing cells in culture, Akt signalling is predominantly activated by serum elements [356]. In HER-2-overexpressing cells, the unliganded HER-2 can be transactivated by IGF-IR. HER-2/Akt-mediated survival signalling in cells may therefore be directed by IGF-IR.

1.4 Strategies to target IGF-IR

1.4.1.1 Antisense oligonucleotides and small interfering RNA

Numerous approaches to blocking IGF-IR in cancer cells are being explored. IGF-IR expression can be inhibited at the translational level by the use of antisense oligonucleotides which are designed to complement messenger RNA (mRNA), causing sequence-specific inhibition of protein synthesis. ASOs are delivered into cells via transfection of antisense expressing plasmids, or via infection with antisense encoding adenoviruses. Antisense strategies have been successful at down-regulating IGF-IR protein expression in a number of cancer types in both *in vitro* and *in vivo* models [183, 299, 300, 357-365]. IGF-IR is down-regulated, and ASO treatment blocks tumour growth, and inhibits metastasis [183, 362, 365]. Down-regulation of IGF-IR also sensitized cells towards radiation and chemotherapeutic agents [362, 364]. These data suggested that antisense strategies could be useful clinically, and perhaps in combination therapy. Andrews *et al* [366] performed a pilot study on patients with malignant astrocytomas to assess the safety and feasibility of the IGF-IR antisense approach in a clinical setting. Clinical and radiographic improvement were observed in 8 out of 12 patients, and three of these were patients with distal recurrence who showed unexpected tumour regression at either the primary or the distant site [366].

Antisense strategies have limitations; they usually result in only moderately decreased IGF-IR levels, and do not produce cells which are completely deficient of the protein [367]. Some IGF-IR ASOs also cause non-specific toxicity in survival assays [358], and some have caused small but detectable suppression of IR expression [368]. An alternative to ASOs are small interfering RNAs (siRNAs), which are short sequences of 21-23 base pair duplex RNA sequences. Specific gene silencing has been demonstrated with siRNAs [369]. Bohula *et al* [368] found that the secondary structure of the IGF-IR transcript has a major effect on the efficacy of binding of ASOs and siRNAs, and identified regions within IGF-IR mRNA that would be accessible to ASOs and siRNAs. They then synthesised ASO and siRNA molecules homologous to accessible regions. Such siRNAs decreased IGF-IR expression, and inhibited survival in human and murine tumour cells [368, 370]. IGF-IR siRNAs also downregulated IGF-IR expression in lung, liver and breast cancer cells [371-374], promoted apoptosis

and increased sensitivity to chemotherapy in liver cancer cells [372], and decreased lung cancer metastasis in mice [373]. siRNA molecules seem to be more stable than ASOs, probably due to their double-stranded structure, and many chemically synthesised and plasmid-based siRNAs are being used *in vitro* [375]. RNA interference as a method of suppression of protein expression is a useful research tool as well as a potential therapeutic strategy.

1.4.1.2 Anti-IGF-IR antibodies

Several antibodies against IGF-IR have been developed. Table 1.4.1 lists anti-IGF-IR antibodies currently in clinical development. The mouse monoclonal antibody aIR-3 targets the a- domain of IGF-IR, and inhibited the proliferation of a number of cancer cells *in vitro*, including MCF7 cells [376, 377]. However, in some cases it was ineffective in blocking IGF-I-sensitive tumours in animal models [378], while in others it may have agonistic effects on IGF-IR signalling [220], and has not been developed further for clinical use.

Several other monoclonal mouse antibodies have been used experimentally. MAb 391 and mAb 4G11 reduced IGF-IR expression in a number of cancer cells, including MCF7 breast cancer cells, and downregulation of receptor was accompanied by reduced Akt and MAPK signalling [379, 380]. EM164 inhibited IGF-I-, IGF-II-, and serum-stimulated proliferation and survival of diverse human cancer cell lines *in vitro*, including breast, lung, colon, cervical, ovarian, pancreatic, melanoma, prostate, neuroblastoma, rhabdomyosarcoma, and osteosarcoma cancer cell lines [381].

To overcome immune response problems with mouse antibodies, a single-chain humanised anti-IGF-IR scFv-Fc antibody was developed which contains the Fc domain of human IgG1 fused to the Fv region of mouse monoclonal 1H7 [382]. This antibody downregulated IGF-IR expression in MCF7 cells, rendering the cells refractory to IGF-I stimulation, and also suppressed MCF7 xenograft tumour growth [383].

Burtrum *et al* [381] developed a fully human anti-IGF-IR antibody, A12, which blocked ligand binding to IGF-IR in MCF7 cells. This antibody also induced

internalization and degradation of the receptors, decreasing IGF-IR cell surface concentration, and inhibited downstream signalling through Akt and MAPK pathways. A12 significantly inhibited the growth of breast, renal and pancreatic tumour xenografts, with an increase in apoptotic tumour cells [381]. Importantly, A12 showed no cross-reactivity with IR. A12 has been combined with other anti-cancer agents experimentally, and it enhanced growth inhibition by Taxotere (docetaxel) in prostate cancer xenografts [384], and by chemotherapeutic agents melphalan and Velcade (bortezomib, a proteosome inhibitor) in multiple myeloma (MM) xenografts [384]. A12 also suppressed VEGF secretion in MM cells, and MM xenografts treated with A12 had reduced vasculature [384]. A12 is now being tested in a phase I clinical trial in patients with advanced solid tumours [377].

Wang *et al* [385] reported that fully human anti-IGF-IR antibody 19D12 inhibits ligand binding and autophosphorylation of IGF-IR homodimers and IGF-IR/IR heterodimers, but not IR homodimers. 19D12 also inhibits IRS-1 phosphorylation, and signalling through Akt and MAPK. The antibody also downregulates IGF-IR levels and inhibited the growth of an ovarian tumour xenograft [385].

CP-751,871 is a fully human anti-IGF-IR antibody that also downregulates IGF-IR expression and showed significant anti-tumour activity as a single agent or in combination with Adriamycin, 5-fluorouracil or tamoxifen in multiple tumour models [386], and is now being tested in a phase I clinical trial in multiple myeloma patients [377].

Goetsch *et al* [387] generated a humanized anti-IGF-IR antibody h7C10, which blocked phosphorylation of IGF-IR and IRS-1, and inhibited MCF7 and A549 xenograft tumour growth. h7C10 also significantly enhanced the effects of chemotherapeutic agent vinorelbine, and the anti-EGFR antibody, C225. This antibody is also being tested in a phase I trial in patients with advanced solid tumours [377].

Targeting IGF-IR activity with antibodies therefore has much potential in cancer therapy, as single agents, or more likely in combination with other agents. Lu *et al* [388] developed a bispecific antibody, or di-diabody that targets both IGF-IR and EGFR, using the variable regions from two antibodies, 11F8 to EGFR and A12 to IG-

IR. The di-diabody inhibited activation of both receptors, and decreased tumour cell proliferation. It also inhibited the growth of pancreatic and colorectal cancer xenografts [388]. This report highlights the benefits of targeting multiple receptors, and further research may validate the use of bispecific antibodies.

1.4.1.3 Dominant negative proteins

The use of dominant negative variants of IGF-IR has been investigated as a strategy to interfere with IGF-IR signalling. Some IGF-IR variants have been constructed with point mutations in the ß-subunits, which cause the formation of kinase-deficient heterodimers of mutant and wild-type receptors. Point mutations or substitutions of specific residues (e.g. lysine K1003, essential for ATP binding, or tyrosines Y1131, 1135 or 1136 of the kinase domain, or Y1250/1251 of the C-terminal domain) decreased proliferation of a number of cell lines [220, 248, 389, 390], some causing increased apoptosis [391, 392], or increasing sensitivity to chemotherapeutic agents [393]. In some studies, these mutations reduced tumour development in animals [248, 392], while in others they did not exhibit dominant negative effects [389].

Other soluble dominant negative mutants contain only a-subunits, without a transmembrane domain, and compete with wild-type receptors for ligand binding. Examples of these are 482/STOP and 486/STOP variants, which inhibited the growth of a number of cell lines, decreased Akt signalling, and induced massive apoptosis *in vivo* [301, 302, 394-396]. 486/STOP also inhibited the adhesion and invasion of MDA-MB-435 cancer cells, and decreased their metastasis *in vivo* [397]. 482/STOP and 486/STOP were also shown to have a bystander effect, inhibiting the growth of wild-type tumour cells when cells expressing the mutant protein are co-injected with wild-type cells [302, 394]. The mechanisms of action of these STOP mutants are not fully understood. Other dominant negative IGF-IRs, 950/STOP and 952/STOP, have a-domains and the juxtamembrane part of the ß-domains, but are lacking the kinase domains, and are thus anchored in the membrane. They were shown to inhibit IGF-IR signalling, tumour growth and metastasis *in vivo* [395, 396, 398, 399]. These mutant receptors probably block IGF-IR activity by dimerization with wild-type receptors.

Deletion of the C-terminus domain of IGF-IR has been shown to enhance survival, and led researchers to investigate if overexpression of the C-domain would promote apoptosis. Mini-receptors containing the last 108 amino acids of IGF-IR spliced to a membrane-targeted myristolated C-terminal (MyCF) caused death of human cancer cell types, sensitized cells to UV irradiation, and inhibited tumorigenesis in nude mice [400, 401].

1.4.1.4 Down-regulation of IGF-IR ligands

IGFBPs bind and transport IGF ligands, thereby regulating their availability to bind IGF receptors. The therapeutic potential of a number of IGFBPs is therefore being evaluated. IGFBP1 inhibits IGF–I and reduces IGF-induced proliferation and migration. IGFBP1 also abrogated estradiol-stimulated growth in MCF7 cells, and inhibited breast cancer migration independent of IGF-I presence *in vitro* [402, 403].

Increased expression of natural IGFBP3 or treatment with recombinant human IGFBP3 (rhIGFBP3) has also been shown to inhibit cancer cell growth and induce cancer cell death in a number of experimental systems (reviewed in [404]). IGFBP3 reduced cell survival and enhanced apoptosis in response to radiation in MCF7 and T47D breast cancer cells *in vitro* [311, 405]. IGFBP3 also sensitized Hs578T breast cancer cells to ceramide-induced apoptosis [406], and potentiated the effects of Taxol (paclitaxel) in this cell model [312] and in gastric carcinoma cell lines [407]. Lu *et al* [177] showed that IGF-IR signalling interfered with the growth-inhibitory effects of trastuzumab in MCF7/HER2-18 and SKBR3/IGF-IR transfected cells, and IGFBP3 treatment reduced IGF-IR signalling and restored sensitivity to trastuzumab. Jerome *et al* [180] confirmed these results in the same cell models, and also demonstrated that IGFBP3 had anti-tumour activity, and potentiated the effects of trastuzumab, in advanced-stage MCF-HER2-18 xenografts. Their study also showed that IGF-IR signalling through Akt and MAPK prevented the suppression of these pathways by trastuzumab, and that IGFBP3 restored their downregulation by trastuzumab *in vitro* and *in vivo*.

Transfection and expression of IGFBP3 in NSCLC [408, 409] and prostate cancer [410] cells also inhibited proliferation and induced apoptosis in xenograft models.

IGFBP3 overexpression also inhibited IGF-IR phosphorylation in NSCLC cells, and treatment with IGF-I or transfection of activated Akt or MAPK kinase-1 partially blocked IGFBP3-induced apoptosis in NSCLC cells [409]. This study suggests that the growth-inhibitory effects of IGFBP3 were, at least in part, due to inhibition of IGF-dependant pathways. IGFBP3 is also known to have IGF-independent functions in cells, and may induce tumour death independently of IGF binding (reviewed in [404]). IGFBP3 may also mediate the anti-proliferative effects of TNF-a, TGF-ß, retinoic acid, vitamin D analogs and p53.

Feng *et al* [411] recently reported their development of human monoclonal antibodies targeting IGF-II. They bound with high affinity to IGF-II, without cross-reacting with IGF-I or insulin, and inhibited IGF-II/IGF-IR signalling. The most potent, IGG1 m610 reduced the phosphorylation of IGF-IR, Akt and MAPK, and inhibited growth of DU145 prostate cell and MCF7 breast cancer cells. Further investigation of these and other ligand-targeting antibodies may determine their potential as therapeutic agents.

1.4.1.5 Tyrosine kinase inhibition

Another approach to inhibiting IGF-IR signalling is to target the tyrosine kinase domain with low molecular weight, or small molecule inhibitors. IGF-IR tyrosine kinase inhibitors (TKIs) currently in pre-clinical or clinical development are listed in Table 1.4.1. These TKIs inhibit activity by binding to the ATP binding site or substrate binding site in the kinase domain of the activated receptor. Earlier TKIs, such as tyrphostin AG538 or I-OMeAG inhibited IGF-IR signal transduction, but cross-reactivity with IR was also reported [412-414].

Improved IGF-IR inhibitory activity and cellular selectivity over IR have been reported for a new series of pyrrolopyrimidines derivatives, which act as ATP agonists. Two examples are NVP-AEW541 and NVP-ADW742 [415, 416]. NVP-AEW541 is 27-fold more potent towards IGF-IR compared to IR, and inhibited IGF-IR phosphorylation *in vitro* and *in vivo* [416]. This inhibitor also induced G1 cell cycle arrest in Ewing's sarcoma [417], hepatocellular carcinoma [418], and neuroblastoma [419] cell lines. The cytotoxic effects on hepatocellular carcinoma and neuroblastoma cell lines were due to induction of apoptosis, and in hepatocellular cell lines NVP-

AEW541 upregulated Bax and downregulated Bcl-2. NVP-AEW541 also enhanced the inhibitory effects of chemotherapeutic agents such as vincristine, actinomycin D, ifosfamide, doxorubicin and docetaxel, and the anti-EGFR antibody ab-3101 [417, 418]. Combined treatment of NVP-AEW541 and vincristine also significantly inhibited tumour growth of Ewing's sarcoma and neuroblastoma xenografts [417, 419]. *In vitro* NVP-EW541 downregulated VEGF mRNA, while *in vivo* NVP-AEW541 led to decreased tumour vascularization [419]. NVP-ADW742 also inhibited growth in small cell lung cancer cell lines, and enhanced the effects of imatinib (ST1571), a selective inhibitor of KIT, PDGFR and ABL tyrosine kinase activity [420, 421]. NVP-ADW742 also sensitized lung cancer cells to etoposide- and carboplatin-induced apoptosis, and treatment with NVP-ADW742 eliminated IGF-I-mediated expression of VEGF [421].

Another class of compounds, cyclolignans, inhibit IGF-IR autophosphorylation, though via a non-ATP antagonising mechanism. Picropodophyllin (PPP) has been studied in malignant melanoma cells. PPP selectively inhibited basal IGF-IR tyrosine phosphorylation, decreased phosphorylation of Akt and ERK1/2, induced apoptosis, and inhibited growth of melanoma cells [422-424]. This activity was accompanied by decreased VEGF secretion, decreased CDK1 activity, accumulation of cells in G2/M-phase, and decreased expression of mcl-1 and survivin, suggesting multiple mechanisms of action of this compound. Vasilcanu *et al* [425] showed that PPP specifically blocked tyrosine Y1136 of the activation loop of the kinase, while sparing the other two tyrosines (Y1131 and 1135). PPP also decreased tumour burden and inhibited angiogenesis in nude mice [422].

Recently, two dual-specificity tyrosine kinase inhibitors that target both IGF-IR and IR, BMS-536924 and BMS-554417 were developed, and were shown to inhibit tumour growth *in vitro* [426, 427]. BMS-554417 inhibited IGF-IR and IR signalling through the Akt and MAPK pathways, and also caused G0/G1-phase growth arrest and decreased nuclear cyclin D1 accumulation in MCF7 cells. This compound also reduced xenograft tumour growth [426]. BMS-554417 therefore represents a novel class of potent dual-kinase inhibitors.

INSM-18 is a small molecule tyrosine kinase inhibitor that has demonstrated selective inhibition of IGF-IR and HER-2. It has demonstrated anti-tumour activity in preclinical studies of breast, lung, pancreatic and prostate tumours, and is the first IGF-IR TKI to enter clinical trials. Two single dose Phase I clinical studies have been completed and report that INSM-18 was safe and well tolerated. INSM-18 is currently in a Phase I/II trial in patients with refractory prostate cancer (unpublished data, www.imsmed.com).

_____

Table 1.4.1 List of anti-IGF-IR antibodies and IGF-IR tyrosine kinase inhibitors currently beeen studied for clinical use.

Antibodies	*Development stage*
A12	Phase I in advanced solid tumours
19D12	Pre-clinical
CP-751,871	Phase I in multiple myeloma
h7C10	Phase I in advanced solid tumours
Tyrosine kinase inhibitors	
NVP-AEW541	Pre-clinical
NVP-ADW742	Pre-clinical
BMS-536924	Pre-clinical
BMS-554417	Pre-clinical
INSM-18	Phase I/II in refractory prostate cancer

_____

1.5   Study Aims

The aims of this study were as follows:

- To investigate the relationship between HER-2 and IGF-IR protein in a large panel of breast cancer cell lines;

- To determine if HER-2, EGFR and IGF-IR protein expression or phosphorylation correlate with response or resistance to trastuzumab in HER-2-positive breast cancer cells;

- To examine alterations in HER-2, EGFR and IGF-IR signalling in breast cancer cells with acquired trastuzumab-resistance;

- To investigate if inhibiting IGF-IR ligand binding, receptor expression or tyrosine kinase activity restores sensitivity to trastuzumab in trastuzumab-resistant cells:

- To determine if trastuzumab-resistant HER-2 positive breast cancer cells display cross-resistance to lapatinib;

- To investigate the development of resistance to HER-2 antagonists, and to examine global alterations in protein phosphorylation in resistant cells compared to parental cells, and

- To analyse the relationship between HER-2 and IGF-IR expression in breast cancer patient samples.

Chapter 2

MATERIALS AND METHODS

2.1   Cell lines, cell culture and reagents

Twenty-seven human breast cancer cell lines were used in this study, including a panel of 21 established cell lines, four HER-2 transfected and empty vector control transfected cell line pairs, and two trastuzumab-conditioned HER-2 overexpressing breast cancer cell lines selected for long-term growth in trastuzumab-containing medium. The cell lines BT474, CAMA-1, HCC1419, HCC1937, HCC1954, MCF-7, MDA-MB-175, MDA-MB- 231, MDA-MB-361, MDA-MB-435, MDA-MB-468, MDA-MB-453, SKBR3, T47D, UACC-812, and ZR-75-1 were obtained from the American Type Culture Collection (ATCC). CAL51, EFM-19 and KPL-1 were obtained from the German Tissue Repository DSMZ. SUM190 and SUM225 were obtained from the University of Michigan, USA. CAMA-1 cells were grown in Minimum Essential Medium (MEM) supplemented with 10% foetal calf serum (FCS); MDA-MB-175 and UACC-812 cells were grown in Leibovitz's L-15 medium with 15% FCS; CAL51 and KPL1 cells were cultured in Dulbecco's Modified Eagle Medium (DMEM) with 10% FCS; SUM190 and SUM225 cells were cultured in Ham's F-12 supplemented with 5% heat-inactivated foetal calf serum (FCS), 5 mg/mL insulin, and 1 mg/mL hydrocortisone; all other cell lines were maintained in RPMI 1640 medium supplemented with 10% FCS, including HCC-2218 and ZR-75-30 cells, which were also supplemented with 1 mM sodium pyruvate. T47D, MCF-7, MDA-MB-231 and ZR-75-1 cells were stably transfected with a full-length cDNA of the HER-2 gene as previously described [56]. Trastuzumab-conditioned cell lines BT474/Tr and SKBR3/Tr were generated by continuously culturing cells for a minimum of 10 months in RPMI supplemented with 1.4 µM trastuzumab (Genentech). All cells were routinely tested for the presence of Mycoplasma.

2.2   Preparation of cell lysates

Cells were grown in 100 mm petri dishes and whole cell lysates were prepared as follows: cells were washed twice with cold PBS and 100-500 µl RIPA buffer (5 mM Tris-HCl pH 7.4, 1% NP-40, 0.1% SDS, 150 mM NaCl, 1% Triton x-100) containing 1x Protease Inhibitor cocktail (Calbiochem), 2 mM PMSF (Sigma), and 1 mM Sodium Orthovanadate (Sigma), was added and cells were incubated on ice for 10 minutes. Lysates were collected and centrifuged at 14,000 revolutions per minute (rpm) for 10

minutes at 4°C. The pellets were discarded and the supernatants collected and stored at -80°C. Protein quantification was performed using the BCA quantitation kit (Pierce Biotechnology).

2.3   *Immunoprecipitation (IP)*

500 µg of protein lysate was diluted in 900 µl RIPA buffer and incubated with 3 µg antibody (monoclonal anti-a-HER-2 (Calbiochem) or polyclonal anti-IGF-IRß (Santa Cruz Biotechnology)) at 4 ^{o}C, shaking, for 30 minutes. 50 µl of packed Protein-G agarose beads (Santa Cruz Biotechnology) were added and the samples incubated overnight, shaking, at 4 ^{o}C. The samples were centrifuged at 14,000 rpm for 25 seconds, the supernatants removed and the pellets washed with IP wash buffer (mild lysis buffer (Cell Signaling Technology) with protease inhibitors). The wash was repeated twice and the samples were centrifuged for 35 seconds. The supernatants were removed and the pellets resuspended in 50 µl denaturing buffer and denatured at 95 ^{o}C for five minutes. Denatured samples were then centrifuged at 14,000 rpm for 3 minutes and the supernatants collected and stored at -20°C.

2.4   *Western Blot analysis*

5-50 µg protein or 20-25 µl immunoprecipitated sample were electrophoretically resolved on denaturing polyacrylamide gels (Lonza Workingham Ltd), transferred to nitrocellulose membranes (Amersham), which were blocked with either bovine serum albumin (BSA) (Sigma) or skimmed-milk powder (Bio-Rad) in PBS-tween (0.1%), and incubated overnight at 4°C with primary antibodies: monoclonal anti-a-HER-2 (Calbiochem); polyclonal anti-EGFR (Lab Instruments); polyclonal anti-phosphorylated HER-2/EGFR (Cell Signaling Technology); polyclonal anti-IGF-IRß (Santa Cruz Biotechnology); monoclonal anti-survivin (Novus Biologicals), monoclonal anti-a-tubulin (Sigma); polyclonal anti-Akt, anti-MAPK, anti-phosphorylated Akt and MAPK antibodies (Cell Signalling Technology); or monoclonal anti-phosphotyrosine antibody (Upstate). Proteins were visualised using horseradish peroxidase-conjugated anti-mouse (Sigma) or anti-rabbit antibodies (Sigma) and Luminol reagent (Santa Cruz Biotechnology). Protein bands were semi-

quantified by densitometry, and protein levels were calculated relative to a-tubulin levels.

2.5 Enzyme-linked immunosorbant assays (ELISAs)

Total HER-2 protein levels were measured in protein lysates using commercially available quantitative ELISA (Calbiochem), according to the manufacturer's instructions. 0.5 µg of each protein lysate was used and HER-2 protein levels were calculated as nanogram (ng) HER-2 per milligram (mg) of total protein. Total IGF-IR and EGFR, and phosphorylated HER-2, IGF-IR and EGFR protein content were measured using ELISAs (R&D Systems), according to the manufacturer's instructions. 50 – 100 µg of protein lysate was used for IGF-IR, and 30 µg used for EGFR measurement, and protein levels were calculated as ng/mg of total protein. 7 µg, 140 µg and 30 µg were used for phosphorylated HER-2, phosphorylated IGF-IR, and phosphorylated EGFR measurements, respectively, and absorbance was measured at 570 nm. For the phospho-ELISAs, values were expressed relative to the sample with the highest level of the phosphorylated protein.

2.6 Proliferation assays

1 - 1.5x10^4 and 2.5 - 3.75x10^3 cells were plated in wells of 24-well and 96-well plates respectively. After 24 hours, cells were treated with the appropriate media supplemented with 2, 5, or 10 % FCS, with or without 10 or 100 nM trastuzumab, 1 µg/ml anti-IGF-IR antibody aIR3 (Calbiochem), 1 µg/ml IGF-binding-protein 3 (IGFBP3) (Sigma), 0-3 µM IGF-IR TKI NVP-AEW541 (Novartis) or 0-3 µM TKI BMS-536924 (Bristol-Myers Squibb). Proliferation was measured after three and/or five days. Cell counting was used to measure proliferation in the 24-well plate assays; wells were rinsed with PBS, incubated in trypsin-EDTA (Gibco) (trypsinized), and cells were either resuspended in isoton and counted using a Beckman Coulter Counter (Beckman Coulter), or resuspended in RPMI containing Guava Viacount reagent and counted using a Guava EasyCyte (Guava Technologies). Cell counting, acid phosphatase assays or the crystal violet assay was used to measure proliferation of cells in 96-well plates. For the acid phosphatase assay, media was removed and each well rinsed with PBS; 100 µl of acid phosphatase substrate (10 mM p-nitrophenol

phosphate (Sigma) in 0.1 M sodium acetate (Sigma), 0.1% triton X-100 (BDH), pH 5.5) was then added to each well followed by incubation at $37^{o}C$ for 45 minutes, at which time 50 µl of NaOH (Sigma) was added to each well and the absorbance was read at 405 nm with 620 nm as a reference. For the crystal violet assay, media was removed from the wells, each well rinsed with PBS, and incubated in 50 µl 0.1% crystal violet (Sigma) in methanol for 15 minutes, rinsed three times in H_2O, dried overnight, and incubated in 100 µl Sorenson's buffer (0.1 Msodium citrate and citric acid in ethanol and H_2O, pH 4.2) for 20 minutes, after which absorbance was read at 540 nm. Proliferation or inhibition of proliferation was calculated relative to untreated controls. Each assay was carried out in triplicate.

2.7   *Small interfering RNA (siRNA) transfection*

A validated siRNA molecule targeting exon 2, and two pre-designed siRNA molecules targeting exons 2 and 4 of the IGF-IR gene were obtained from Ambion [Table 2.1]. A siRNA molecule targeting kinesin, and a scrambled sequence siRNA molecule (Ambion) were used as transfection controls. Each siRNA molecule was transfected at a final concentration of 30 nM. $6.5 - 8x10^3$ and $3 - 3.5x10^5$ cells were resuspended in 10% RPMI for 96-well and 6-well plates respectively. Each siRNA and NeoFX^{TM} transfection agent was diluted in Gibco^{TM} Opti-MEM reduced serum medium (Invitrogen), and incubated at room temperature (RT) for 10 minutes. Diluted NeoFX was then added to each diluted siRNA and incubated for a further 10 minutes at RT. The transfection mix was then added to the wells followed by the addition of the cell suspension. After 24 hours, the transfection media was replaced with 10 % RPMI with or without 15 µg/ml trastuzumab. 6-well plates were used to prepare lysates after 72 hours. Cells in 96-well plates were harvested after four days trastuzumab treatment and counted using the Guava EasyCyte.

Table 2.1. Sequences of three anti-IGF-IR siRNA molecules, with the Ambion siRNA ID number, and the number (1-3) assigned to each in this study.

ID	No.	Sense	Antisense
103301	1	GGUCUGUGAGGAAGAAAAGtt	CUUUUCUUCCUCACAGACCtt
74	2	GGAUUGAGAAAAAUGCUGAtt	UCAGCAUUUUUCUCAAUCCtg
144648	3	GCUCACGGUCAUUACCGAGtt	CUCGGUAAUGACCGUGAGCtt

2.8   *Terminal DNA transferase-mediated dUTP nick end labelling (TUNEL) assay*

$3 – 5 \times 10^4$ cells were plated in wells of 24-well plates, in media containing 5 % FCS. After 24 hours, cells were treated with trastuzumab (10 nM), NVP-AEW541 (1 µM), or both, in 2 % FCS. Dimethyl sulfoxide (DMSO) control wells were included in each assay, and lapatinib (2.5 µM) was used as a positive control for apoptosis induction. After 48 (MCF7), or 72 hours (SKBR3 and SKBR3/Tr), media was collected into microcentrifuge tubes and the wells were washed with PBS, which was also collected. Cells were trypsinized and added to the media collected for each sample. The tubes were centrifuged at 300 x g for 5 minutes and the media was aspirated. The cell pellets were re-suspended in PBS, and the cell suspension of two wells were transferred to one well of a round bottomed 96 well plate. 50 µL of 4% para-formaldehyde-PBS was added to the wells and mixed, and the plate was incubated at 4 ^{o}C for 60 minutes. The plate was centrifuged at 300 x g for 5 minutes and the supernatant aspirated leaving approximately 15 µL in each well. The remaining volume was used to resuspend the cells and 200 µL of ice cold 70 % ethanol was added gradually to each well. The plates were then stored at -20 ^{o}C overnight. The fixed cells were stained according to the protocol for the TUNEL assay (Guava Technologies). Cells were analysed on the Guava EasyCyte machine using the CytoSoft TUNEL assay software (Guava Technologies). Positive and negative controls supplied with the TUNEL assay kit were run with each assay.

2.9   Cell Cycle Assays

$3 - 5x10^4$ cells were plated in wells of 24-well plates, in media containing 5 % FCS. After 24 hours, cells were treated with trastuzumab (10 nM), NVP-AEW541 (1 µM), or both, in 2 % FCS. Dimethyl sulfoxide (DMSO) control wells were included in each assay, and gefitinb (Iressa, AstraZeneca) (1 µM) was used as a positive control for cell cycle arrest. After 48 (MCF7), or 72 hours (SKBR3 and SKBR3/Tr), media was collected into microcentrifuge tubes and the wells were washed with PBS, which was also collected. Cells were trypsinized and added to the media collected for each sample. The tubes were centrifuged at 300 x g for 5 minutes and the media was aspirated. The cell pellets were re-suspended in PBS, and each cell suspension was transferred to a well of a round bottomed 96 well plate. The plate was centrifuged at 450 x g for 5 minutes and the supernatant aspirated leaving approximately 15 µL in each well. The remaining volume was used to resuspend the cells and 200 µL of ice cold 70 % ethanol was added gradually to each well. The plates were then stored at 4 ^{o}C overnight. After fixing the cells were stained according to the protocol for the Guava PCA-96 cell cycle assay (Guava Technologies). Cells were analysed on the Guava EasyCyte machine and the data was analysed using the Modfit LT software (Verity Software House).

2.10   Lapatinib and Trastuzumab conditioning of cells

Trastuzumab-sensitive SKBR3, and trastuzumab-resistant SKBR3/Tr and HCC1419 cells were selected to be conditioned in lapatinib (Tykerb, GW572016, GlaxoSmithKline) and/or trastuzumab- containing growth media. 96-well dose response proliferation assays were performed in 0 – 600 nM lapatinib in order to select an appropriate concentration for conditioning. Each cell line was grown in duplicate flasks containing either control media or conditioned media, and media was replaced twice weekly for 6 months. SKBR3 cells were conditioned in trastuzumab (10 µg/ml (68 nM)) alone, lapatinib (200 nM) alone, or combined trastuzumab (5 µg/ml (34 nM)) and lapatinib (100 nM); SKBR3/Tr cells were conditioned in lapatinib (400 nm), and HCC1419 cells were conditioned in lapatinib (250 nM). After two months, the lapatinib concentration for SKBR3 cells was increased to 250 nM. After three and six months of conditioning, dose-response assays were performed to monitor alterations in response to lapatinib and trastuzumab.

2.11 Doubling time assays

$3.x10^3$ cells were plated in wells of 48-well plates. After 24 hours, cells were treated with and without 100 nM trastuzumab or 100 nM lapatinib. The Guava EasyCyte was used to count cell numbers at days 0, 3, 5 and 7. Doubling times were calculated between days 3 and 7 using the formula

$$\text{Doubling time} \; = \; \frac{(T_t - T_0) \, (\text{Log2})}{(\text{Log}T_t - \text{Log}T_0)} \; ,$$

where T_t is the end timepoint and T_0 is the beginning timepoint (days), which in this case were 7 and 3, respectively. Each assay was performed in triplicate.

2.12 Phosphoprotein preparation

Cells were grown in 175 cm^2 flasks, and treated for 24 hours with control growth media (RPMI + 10 % FCS), or media containing trastuzumab (10 µg/ml (68 nM)) or lapatinib (1 µM). Triplicate samples of each treatment were prepared. Total protein was extracted and the phosphoprotein fragments were concentrated using the Pierce^{TM} Phosphoprotein Enrichment Kit (Pierce Biotechnology). Using this kit, cells were washed twice with cold HEPES buffer (50 mM, pH 7), and lysed using the Lysis/Binding/Wash buffer provided, supplemented with CHAPS (0.25%), 1X Halt Protease Inhibitor EDTA-free and 1X Halt Phosphatase Inhibitor Cocktail (Pierce Biotechnology). Cells were scraped into microcentrifuge tubes, and placed on ice for 45 minutes, vortexing periodically. The lysed cells were centrifuged at 10,000 x g for 20 minutes at 4 ^{o}C and the supernatant collected and stored at -80 ^{o}C. After protein quantification, the concentration of each lysate was adjusted to 0.5 mg/ml and the phosphoprotein fraction of each was enriched using columns supplied with the kit, according to the protocol provided. The eluted phosphoprotein fractions were then concentrated according to the protocol, yielding 150-200 µl of concentrated phosphoprotein for each sample. The samples were then stored at -80°C.

2.13 Phosphoproteomic analysis

2.13.1 Protein labelling and two-dimensional differential gel electrophoresis (DIGE)

All proteomic analysis detailed in this thesis was carried out by Dr. Paul Dowling. DIGE was performed using three CyDye DIGE Fluor Minimal dyes Cy3, Cy5 and Cy2

(GE Healthcare) [428]. In this technique, 25 µg of each phosphoprotein sample was added to microcentrifuge tubes and labelled with Cy3 or Cy5 dye (200 pico mole (pmol) in 1 µl anhydrous dimethylformamide (DMF)). Each tube was mixed by vortexing, and placed on ice for 30 minutes in the dark. Under these conditions approximately 1% of the lysine residues of the protein are covalently conjugated to the CyDyes. The reaction was quenched by the addition of a 50-fold molar excess of free lysine to the dye for 10 minutes on ice in the dark. The labelled samples were stored at $-80\,^{\circ}$C.

Each gel compared two samples, one labelled with Cy3 and the other with Cy5 [Table 2.2]. Triplicate gels were run for each comparison. A Cy2-labelled pool was prepared containing 12.5 µg of protein from each of the 18 samples. This pool was used on all gels as an internal standard to allow for accurate quantification [428]. A mix of each sample was also prepared to run on a preparative gel to facilitate protein identification after electrophoresis. An equal volume of 2x sample buffer (2.5 ml rehydration buffer stock solution (7 M urea, 2 M thiourea, 4 % CHAPS), pharmalyte broad range pH 4-7 (2%) (GE Healthcare), DTT (2%)) (Sigma) was added to the labelled protein samples. The mixture was left on ice for 10 minutes before the next step.

The protein samples were then passively rehydrated into immobiline 24-cm linear pH gradient strips (IPG, pH 3-11) (GE Healthcare) using rehydration buffer solution (7 M urea, 2 M thiourea, 4 % CHAPS, 0.5% IPG buffer, 50 mM DTT). Each strip was overlaid with 3 ml IPG Cover Fluid (GE Healthcare) and allowed to rehydrate overnight at RT. Isoelectric focussing (IEF) was then performed using the IPGphor apparatus (40 kv/hr @ 20 $^{\circ}$C with resistance set at 50mA) (GE Healthcare).

Table 2.2. DIGE experimental design, showing gel number and the Cy dye used for each sample. Triplicate gels were run for each comparison. Gel no.s 3, 6 and 9 are examples of reverse labelling, and are introduced to avoid any slight bias caused because of the different molecular weights of the Cy dyes.

Gel no.	Cy2	Cy3	Cy5
1	Cy2 pool	SKBR3 (C)	SKBR3-L (C)
2	Cy2 pool	SKBR3 (C)	SKBR3-L (C)
3	Cy2 pool	SKBR3-L (C)	SKBR3 (C)
4	Cy2 pool	SKBR3 (T)	SKBR3-L (T)
5	Cy2 pool	SKBR3 (T)	SKBR3-L (T)
6	Cy2 pool	SKBR3-L (T)	SKBR3 (T)
7	Cy2 pool	SKBR3 (L)	SKBR3-L (L)
8	Cy2 pool	SKBR3 (L)	SKBR3-L (L)
9	Cy2 pool	SKBR3-L (L)	SKBR3 (L)

For second dimension separation, the strips were equilibrated by incubating in equilibrium solution (50 mM Tris-HCL, pH 8.8, 6 M urea, 30% glycerol, 1% SDS) containing 65 mM DTT for 20 minutes, followed by 20 minutes incubation in the same buffer containing 240 mM iodoacetamide (both at RT). 12.5 % acrylamide gel solutions (acrylamide/bis 40 %, 1.5 M Tris pH 8.8, 10 % SDS) were prepared, and prior to pouring, 10 % ammonium persulfate and 100 µl neat TEMED were added. The gels were overlaid with 1 ml saturated butanol, and left to set for at least three hours at RT. Equilibrated IPG strips were transferred onto 24 cm 12.5% uniform polyacrylamide gels poured between low fluorescence glass plates. Strips were overlaid with 0.5% low melting point agarose in running buffer containing bromophenol blue. Gels were run at 2.5 W/gel for 30 min and then 100 W total at 10 ^{o}C until the dye front had run off the bottom of the gels.

2.13.2 Gel Imaging

All of the gels were scanned using the Typhoon 9400 Variable Mode Imager (GE Heathcare) to generate gel images at the appropriate excitation and emission

wavelengths from the Cy2-, Cy3- and Cy5-labelled samples. The resultant gel images were cropped using the ImageQuant software tool and imported into Decyder 6.5 software. The biological variation analysis (BVA) module of Decyder 6.5 was used to compare the control versus test samples to generate lists of differentially expressed proteins.

2.13.3 Spot digestion

Preparative gels containing 400 mg of protein were fixed and then poststained with colloidal CBB stain (Sigma). The subsequent gels were scanned using the Typhoon 9400 Variable Mode Imager (GE Heathcare) to generate gel images at the appropriate excitation and emission wavelengths for the colloidal CBB stain. Preparative gel images were then matched to the Master gel image generated from the DIGE experiment. Spots of interest were selected and a pick list was generated and imported into the software of the Ettan Spot Picker robot (GE Healthcare). Gel plugs were placed into presiliconised microtitre plate and stored at 47C until digestion. Tryptic digestions were performed using the Ettan Digestor robot (GE Healthcare). Excess liquid was removed from each plug, and washed for three cycles of 20 min using 50 mM NH4HCO3 in 50% methanol solution. The plugs were then washed for two cycles of 15 min using 70% ACN and left to air dry for 1 h. Lyophilised sequencing grade tryspin (Promega) was reconstituted with 50 mM acetic acid as a stock solution and then diluted to a working solution with 40 mM NH4HCO3 in 10% ACN solution, to a concentration of 12.5 ng trypsin per mL. Samples were digested at 37ºC overnight and were then extracted twice with 50% ACN and 0.1% TFA solution for 20 min each. All extracts were pooled and concentrated by SpeedVac (Thermo Scientific) for 40 min.

2.13.4 MALDI ToF/ToF Mass Spectrometry and Protein Identification

One fifth of the peptide extract solution from the digest was added to a 384 spot MALDI sample plate (Applied Biosystems) and supplemented with 0.5 µl of a 5 mg/ml solution of recrystalised α-cyano-4-hydroxy-trans-cinnamic acid matrix (Laser Biolabs) plus 10mM NH4H2PO4 in 50% acetonitrile/water containing 0.1% TFA and allowed to air dry prior to analysis. MALDI mass spectra were generated using a 4800 TOF/TOF Proteomics Analyzer instrument (Applied Biosystems). An internal sample mix, Pep4 (Laser Biolabs) was also spotted onto target slides and used as an internal

calibrant. All MS and MS/MS experiments were carried out in positive reflectron mode. Ten precursor ions for MS/MS were selected automatically on the basis of intensity from the MS spectra. The MS and MS/MS data were combined and searched against a number of databases using GPS Explorer software (Applied Biosystems) and a local MASCOT (Matrix Science) search engine for protein identification. A mass window of 20 ppm was set for database searching on all precursors.

2.14 Tissue Micro-Array (TMA) construction

Formalin-fixed paraffin-embedded tumour samples were obtained from 230 HER-2-overexpressing patients; 150 were obtained from St. Vincent's University Hospital, Dublin, and 68 were obtained from St. James' Hospital, Dublin. Ethical approval was obtained from the ethics committees of both hospitals. The samples were collected between 1994 and 2006. All patients were treated with trastuzumab. Relevant clinicopathologic features, treatment and follow-up were compiled for all patients by Dr. Zulfi Qadir and Dr Thamir Mahgoub. Slides of each tumour sample were prepared, and Haematoxylin and Eosin (H&E) staining was performed by Deirdre McMahon in St. Vincent's University Hospital. The tumour-containing area of each sample was identified and marked by Dr. Susan Kennedy. TMAs were then constructed using a Tissue Arrayer (Beecher) [Fig. 2.1]: Four cores (6mm) were taken from each sample and placed into empty cores of a recipient paraffin block. An array map is used to log the position of each sample, and cores of paraffin-embedded liver sample are placed around the perimeter of each TMA in a unique pattern for easy distinguishing of each TMA. Approximately 30 patient samples were included in each TMA.   TMAs were also obtained from Dr Susan Kennedy which contained cores from unselected breast tumours and in some cases corresponding normal tissues.

Figure 2.1 Construction of tissue microarrays using the Beecher TMA arrayer: One needle is used to punch a hole in the recipient block, and a second needle is used to remove a core of tumour from a donor paraffin block and place it in the hole made in the recipient block.

___

2.15 Immunohistochemistry

All immunohistochemical staining was performed using the DAKO Autostainer (DAKO). Deparaffinization and antigen retrieval was performed using Epitope Retrieval 3-in-1 Solution (pH 6) (DAKO) and the PT Link system (DAKO), whereby slides are heated to 97 ^{o}C for 40 minutes, then cooled to 65 ^{o}C. The slides are then immersed in wash buffer (DAKO). HER-2 staining was performed using the HercepTest^{TM} (DAKO). A control slide supplied with the HercepTest^{TM} kit was included in each staining run; this slide contains three pelleted, formalin-fixed, paraffin-embedded human breast cancer cell lines with staining intensity scores of 0, 1+ and 3+. A positive control 3+ patient sample slide, and a negative control score 0 patient sample slide were also included in each run. Each slide was also run with Negative Control Reagent, supplied with the kit, in place of the primary antibody, to allow evaluation of non-specific staining and allow better interpretation of specific staining at the antigen site. IGF-IR staining was performed using rabbit anti-IGF-IRß antibody (Cell Signalling technology). All slides were counterstained with haematoxylin (Sigma) for 5 minutes, and rinsed with deionised water, followed by wash buffer. All slides were then dehydrated in graded alcohols (2 x 3 minutes each

in 70% IMS, 90% IMS and 100% IMS), and cleared in xylene (2 x 5 minutes), and mounted with coverslips using DPX mountant (Sigma). Protein expression levels were assessed by Dr. Susan Kennedy. HER-2 levels were scored using the HercepTest^{TM} scoring guidelines, which assigns scores of 0, 1+ (both HER-2 negative), 2+ (weakly positive) or 3+ (strongly positive) based on membrane staining intensity. IGF-IR cytoplasmic staining was assigned the following scores based on staining intensity: and scored as negative (0), weak (1+), moderate (2+), strong (3+). Membrane IGF-IR staining was scored as either positive or negative, with membrane staining only recorded as positive when it clearly exceeded the cytoplasmic level of staining [273].

2.16   Statistical Analysis

Analysis of the difference of comparisons in protein levels and response to treatment was performed using student t-tests (two-tailed with unequal variance). Chi-square tests, parametric Pearson's correlation analysis and nonparametric Mann-Whitney U and Kruskal-Wallis tests were performed using StatView 5.0.1 (SAS Institue Inc.). $P<0.05$ was regarded as statistically significant.

Chapter 3

CHARACTERISATION OF BREAST CANCER CELL LINE PANEL

3.1   HER-2, IGF-IR AND SURVIVIN PROTEIN LEVELS IN BREAST CANCER CELL LINE PANEL

HER-2, IGF-IR and survivin protein levels were measured by western blot in a panel of 23 breast cancer cell lines, including four HER-2-transfected cell lines and their corresponding control-transfected cells [Fig. 3.1]. HER-2 and IGF-IR expression levels were semi-quantified by densitometry [Table 3.1].   Analysis by student's t-test confirmed that HER-2 expression levels are significantly higher in HER-2-amplified cell lines compared to non-amplified cell lines (p = 0.0006), while no significant difference was observed in IGF-IR levels between HER-2-amplified and non-amplified cells. No direct correlations were observed between levels of HER-2, IGF-IR and survivin [Fig. 3.2]. IGF-IR expression was elevated by over 50% in two out of four, and reduced by 44% in one HER-2-transfected cell line compared to control-transfected cells. Survivin protein expression was also reduced in three out of four HER-2-transfected cell lines [Fig. 3.3].
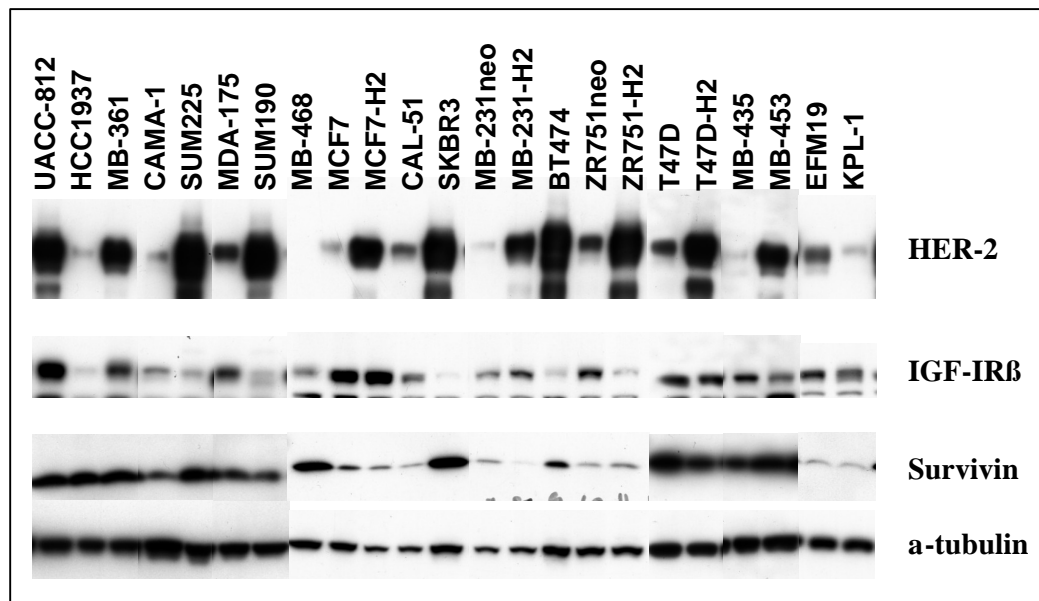
Figure 3.1. Western blot of HER-2, IGF-IRß and survivin expression levels in 23 breast cancer cell lines. a-tubulin was used as a loading control.

_____

83

Table 3.1. HER-2 and IGF-IRß levels in breast cancer cell lines. HER-2 amplification status was obtained from UCLA. Protein levels were measured by western blotting and semi-quantified relative to a-tubulin using ImageQuant densitometry software (Amersham). Protein levels are expressed as arbitrary units; the highest of each protein level is assigned a value of 1 and all others are expressed relative to this.

Cell line	HER-2 Amplified	HER-2	IGF-IR
T47D-HER2	+	1.00	0.85
UACC-812	+	0.88	0.56
ZR751-HER2	+	0.88	0.43
SKBR3	+	0.65	0.32
BT474	+	0.59	0.20
SUM190	+	0.58	0.14
SUM225	+	0.45	0.33
MCF7-HER2	+	0.33	0.68
MDA-MB-361	+	0.16	0.29
MDA-MB-231-HER2	+	0.12	0.25
ZR751neo	-	0.11	0.77
MDA-MB-175	+	0.08	0.26
MDA-MB-453	+	0.06	0.36
T47Dneo	-	0.04	0.48
EFM-19	-	0.03	0.34
CAL-51	-	0.02	0.25
HCC1937	-	0.01	0.16
MCF7neo	-	0.01	0.61
MDA-MB-231neo	-	0.01	0.15
CAMA-1	-	0.00	0.53
MDA-MB-468	-	0.00	1.00
MDA-MB-435	-	0.00	0.56
KPL-1	-	0.00	0.18
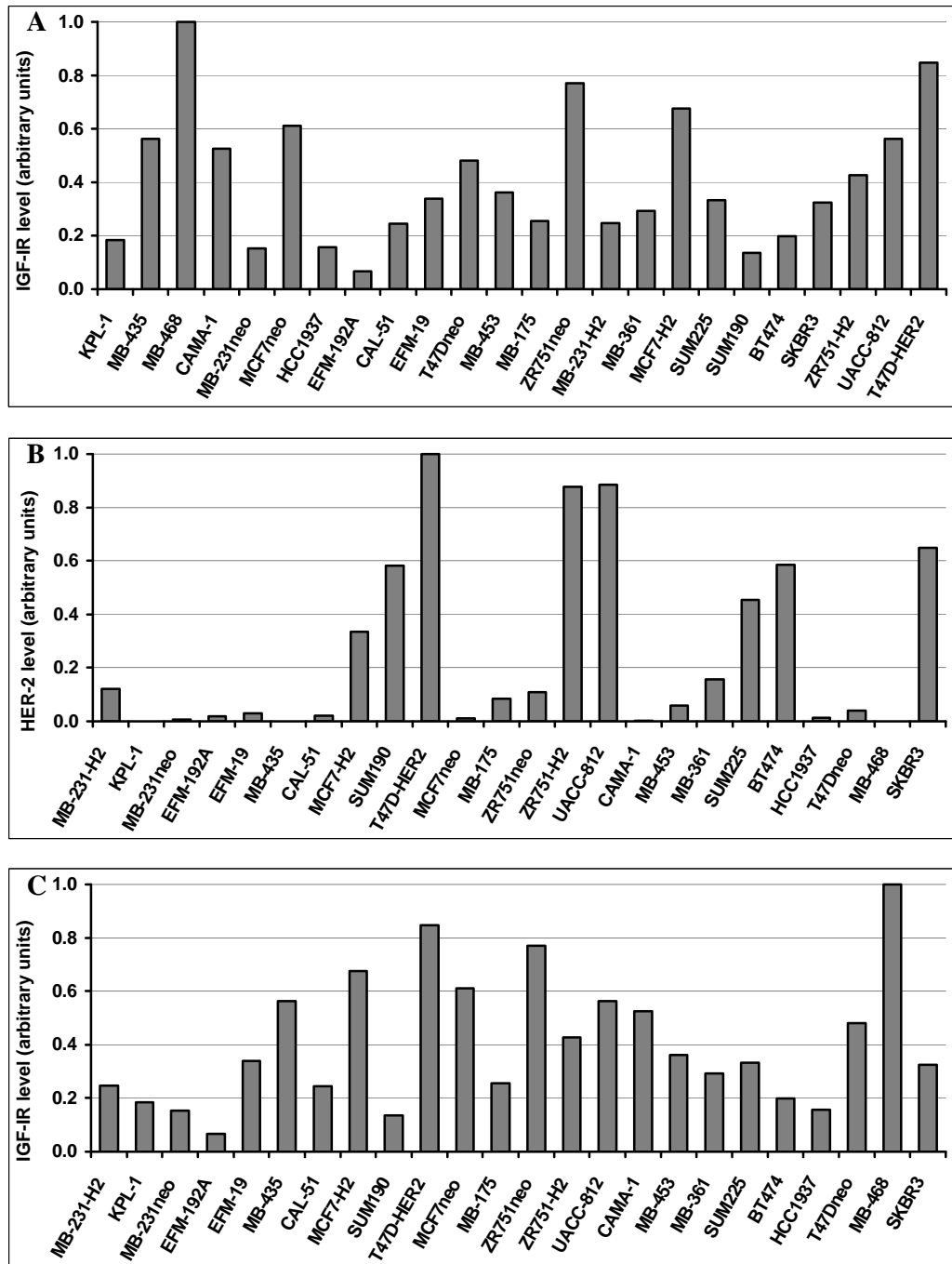
Figure 3.2 Relationships between HER-2, IGF-IRß and survivin protein levels in breast cancer cell lines. Levels were measured by western blotting and semi-quantified relative to a-tubulin using ImageQuant densitometry software (Amersham). Protein levels are expressed as arbitrary units; the highest of each protein level is assigned a value of 1 and all others are expressed relative to this. **A**. IGF-IRß levels in cell lines arranged from left to right with increasing HER-2 expression. **B**. HER-2 levels in cell lines arranged from left to right with increasing survivin expression. **C**. IGF-IRß levels in cell lines arranged from left to right with increasing survivin expression.
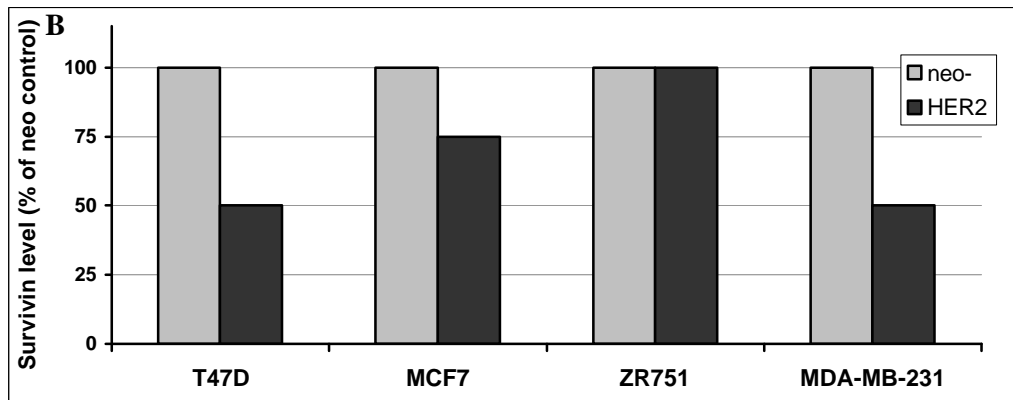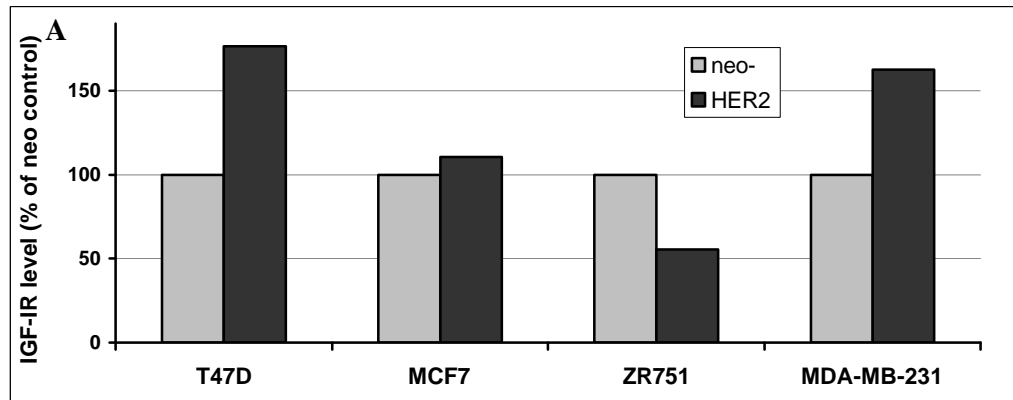
Figure 3.3 IGF-IRß and survivin expression in HER-2- and control empty vector-transfected (neo) breast cancer cell lines. Protein levels were measured by western blotting and semi-quantified relative to a-tubulin using ImageQuant densitometry software (Amersham). Levels of (**A**) IGF-IRß and (**B**) survivin are expressed as percentage of expression in control transfected cells.

_____

3.2 RESPONSE TO TRASTUZUMAB IN HER-2-POSITIVE BREAST CANCER CELL LINES

Response to trastuzumab was investigated in 14 HER-2-overexpressing cell lines [Fig. 3.4]. BT474 was the most sensitive cell line (59 ± 5 % inhibition), while ZR751-HER-2 was the most resistant cell line (0.5 ± 0.7 % inhibition). None of the three HER-2 transfected cell lines (ZR751-H2, T47D-H2, MCF7-H2) showed significant response to trastuzumab treatment in the proliferation assay.
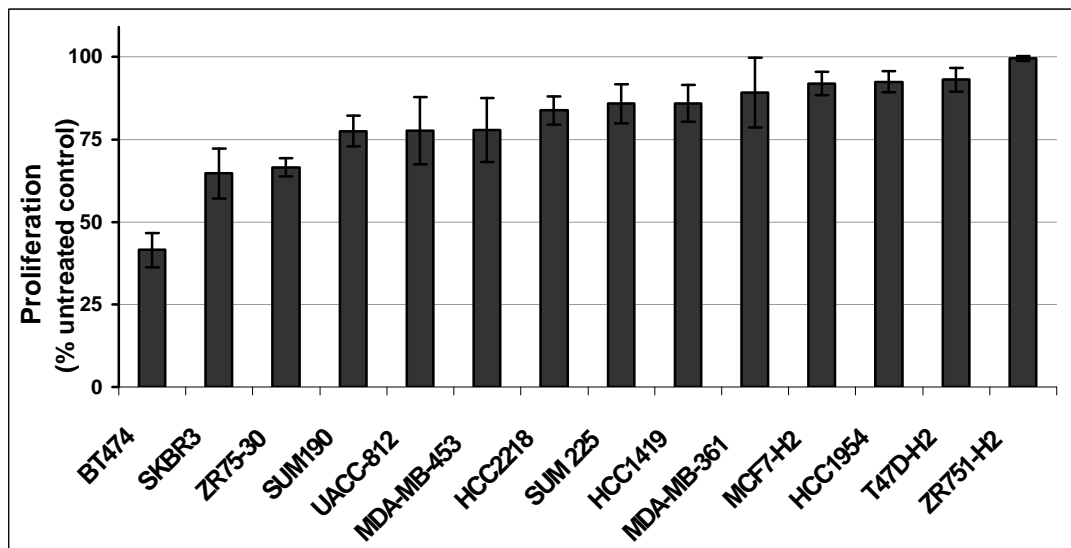
Figure 3.4. Percentage proliferation of HER-2-overexpressing breast cancer cell lines treated with trastuzumab (100 nM). Proliferation was measured after 5 days by cell counting and is expressed relative to untreated control. Error bars represent standard deviation of triplicate experiments.

_____

3.3 RELATIONSHIP BETWEEN HER-2, P-HER-2, IGF-IR, P-IGF-IR, EGFR AND P-EGFR AND RESPONSE TO TRASTUZUMAB

HER-2, IGF-IR, EGFR, and phosphorylated HER-2, IGF-IR, and EGFR were quantified by ELISA in the panel of HER-2-overexpressing cell lines [Table 3.2 and Figs. 3.5 – 3.7]. While the ELISAs for the total proteins are quantitative and give a value in nanogram per milligram of total protein, the phospho-protein ELISAs give an arbitrary optical density value. Thus for the phospho-protein ELISAs the values for each cell line were expressed relative to the cell line with the highest level of that phospho-protein.

Statistical analyses were performed to analyse the relationships between total protein expression and phosphorylation level of each receptor. Using Pearson's correlation analysis, no correlation was observed between receptor expression and phosphorylation of HER-2, IGF-IR or EGFR [Table 3.3]. However, both HER-2 and phospho-HER-2 correlate positively with phospho-IGF-IR levels (HER-2, $p = 0.16$, $r = 0.628$; p-HER-2 $p = 0.002$, $r = 0.742$) [Fig. 3.10]. A positive trend was also observed between IGF-IR and phospho-EGFR levels, but did not reach statistical significance ($p = 0.079$, $r = 0.551$) [Fig. 3.10].

Statistical analyses were also performed to assess the relationships between protein level, or phosphorylation level, and response to trastuzumab *in vitro*. No significant correlations were observed between protein expression levels, or phosphorylation levels of any of the three receptors, and response to trastuzumab [Fig. 3.8 and Fig. 3.9].

Table 3.2. Total and phosphorylated HER-2, IGF-IR and EGFR levels in 14 HER-2-overexpressing breast cancer cell lines. Protein levels were measured by ELISA; phospho-HER-2, phospho-IGF-IR and phospho-EGFR levels are expressed as arbitrary units, relative to the cell line with the highest ELISA optical density reading, which was assigned a value of 1 ($\pm$ standard error).

	HER-2 ng/mg	IGF-IR ng/mg	EGFR ng/mg	p-HER-2	p-IGF-IR	p-EGFR
HCC1419	577.6 $\pm$ 64.7	3.02 $\pm$ 0.35	0.00 $\pm$ 0.00	1.00 $\pm$ 0.00	1.00 $\pm$ 0.00	0.20 $\pm$ 0.05
SUM 190	406.6 $\pm$ 82.1	4.10 $\pm$ 0.53	5.97 $\pm$ 0.18	0.22 $\pm$ 0.04	0.53 $\pm$ 0.08	0.22 $\pm$ 0.01
HCC2218	392.9 $\pm$ 94.1	1.83 $\pm$ 0.26	2.45 $\pm$ 0.31	0.55 $\pm$ 0.02	0.43 $\pm$ 0.04	0.23 $\pm$ 0.01
SUM 225	354.2 $\pm$ 97.8	1.35 $\pm$ 0.09	5.90 $\pm$ 0.17	0.44 $\pm$ 0.06	0.36 $\pm$ 0.06	0.21 $\pm$ 0.01
SKBR3	228.1 $\pm$ 37.6	0.71 $\pm$ 0.06	2.41 $\pm$ 0.22	0.34 $\pm$ 0.02	0.30 $\pm$ 0.04	0.57 $\pm$ 0.01
ZR75-30	205.7 $\pm$ 41.6	2.04 $\pm$ 0.07	0.00 $\pm$ 0.00	0.76 $\pm$ 0.10	0.42 $\pm$ 0.02	0.10 $\pm$ 0.02
T47D-H2	172.1 $\pm$ 30.8	7.10 $\pm$ 0.43	ND	0.92 $\pm$ 0.08	0.55 $\pm$ 0.02	ND
BT474	147.9 $\pm$ 13.3	3.65 $\pm$ 0.51	3.18 $\pm$ 0.13	0.44 $\pm$ 0.05	0.50 $\pm$ 0.03	0.37 $\pm$ 0.01
MDA-MB-361	141.0 $\pm$ 35.8	0.67 $\pm$ 0.12	0.00 $\pm$ 0.00	0.10 $\pm$ 0.00	0.16 $\pm$ 0.02	0.04 $\pm$ 0.01
HCC1954	132.2 $\pm$ 18.2	3.09 $\pm$ 0.35	7.60 $\pm$ 0.57	0.32 $\pm$ 0.04	0.52 $\pm$ 0.09	0.23 $\pm$ 0.02
ZR751-H2	131.1 $\pm$ 29.2	4.88 $\pm$ 0.41	ND	0.09 $\pm$ 0.01	0.38 $\pm$ 0.13	ND
UACC-812	104.0 $\pm$ 9.1	7.96 $\pm$ 0.87	3.60 $\pm$ 0.50	0.90 $\pm$ 0.05	0.56 $\pm$ 0.04	0.62 $\pm$ 0.02
MCF7-H2	27.0 $\pm$ 8.2	6.76 $\pm$ 0.29	ND	0.37 $\pm$ 0.04	0.40 $\pm$ 0.04	ND
MDA-MB-453	26.0 $\pm$ 1.6	1.57 $\pm$ 0.19	0.00 $\pm$ 0.00	0.01 $\pm$ 0.00	0.10 $\pm$ 0.02	0.03 $\pm$ 0.01

ND; not determined

Table 3.3. Pearson's correlation analysis of the relationship between HER-2, IGF-IR and EGFR expression and phosphorylation in HER-2-overexpressing cell lines. (r; Pearson's correlation coefficient; p, significance (2-tailed)).

		p-HER-2	IGF-IR	p-IGFIR	EGFR	p-EGFR
HER-2	*r*	*0.392*	*-0.293*	***0.628***	*0.044*	*-0.065*
	p	0.166	0.309	**0.016**	0.899	0.850
p-HER-2	*r*		*0.410*	***0.742***	*-0.136*	*0.378*
	p		0.145	**0.002**	0.690	0.252
IGF-IR	*r*			*0.380*	*0.309*	***0.551***
	p			0.180	0.356	**0.079**
p-IGFIR	*r*				*0.123*	*0.246*
	p				0.719	0.467
EGFR	*r*					*0.314*
	p					0.347
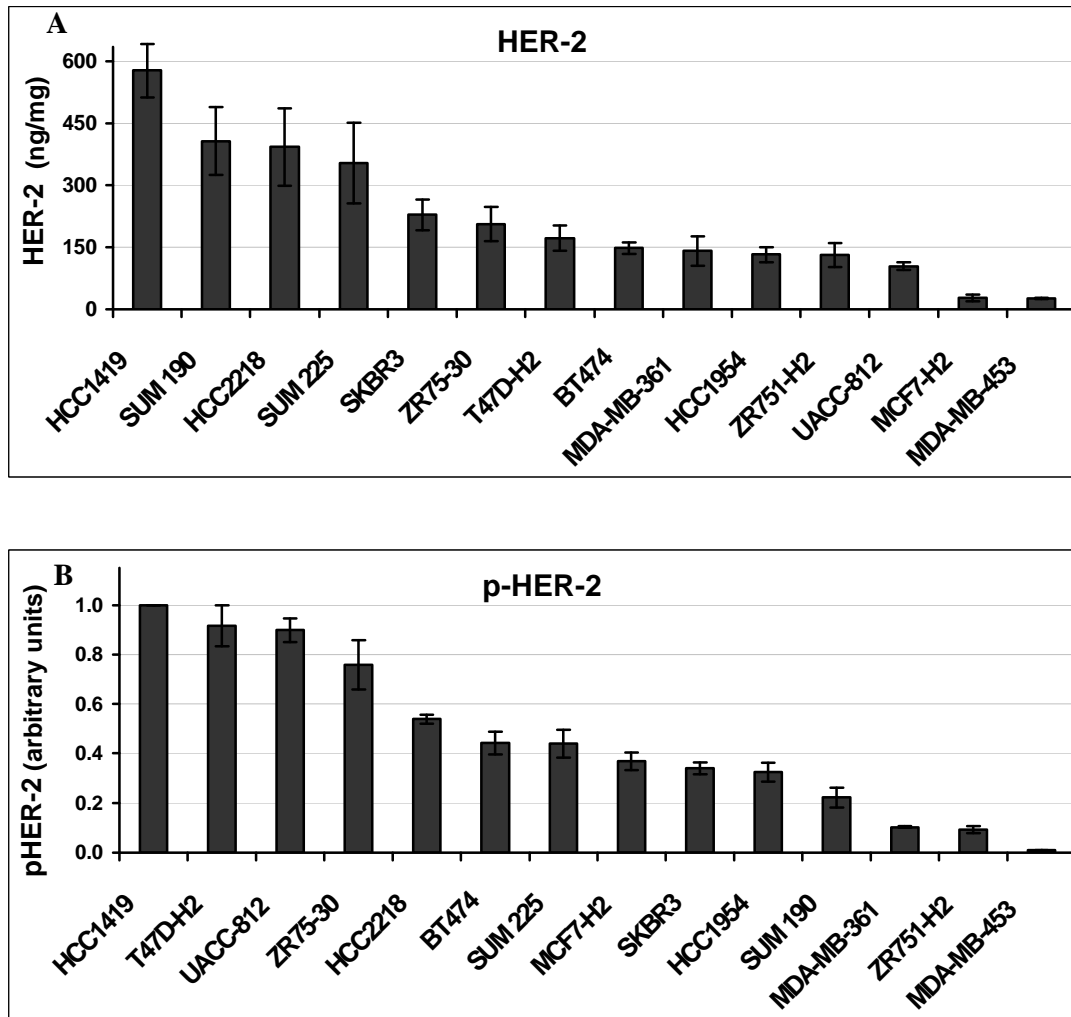
Figure 3.5. **A.** HER-2 and **B.** phospho-HER-2 protein levels in 14 HER-2-overexpressing breast cancer cell lines. HER-2 is expressed as ng/mg total protein; p-HER-2 is expressed as arbitrary units, relative to the cell line with the highest optical density reading, which was assigned a value of 1. Error bars represent standard error of triplicate experiments.

_____
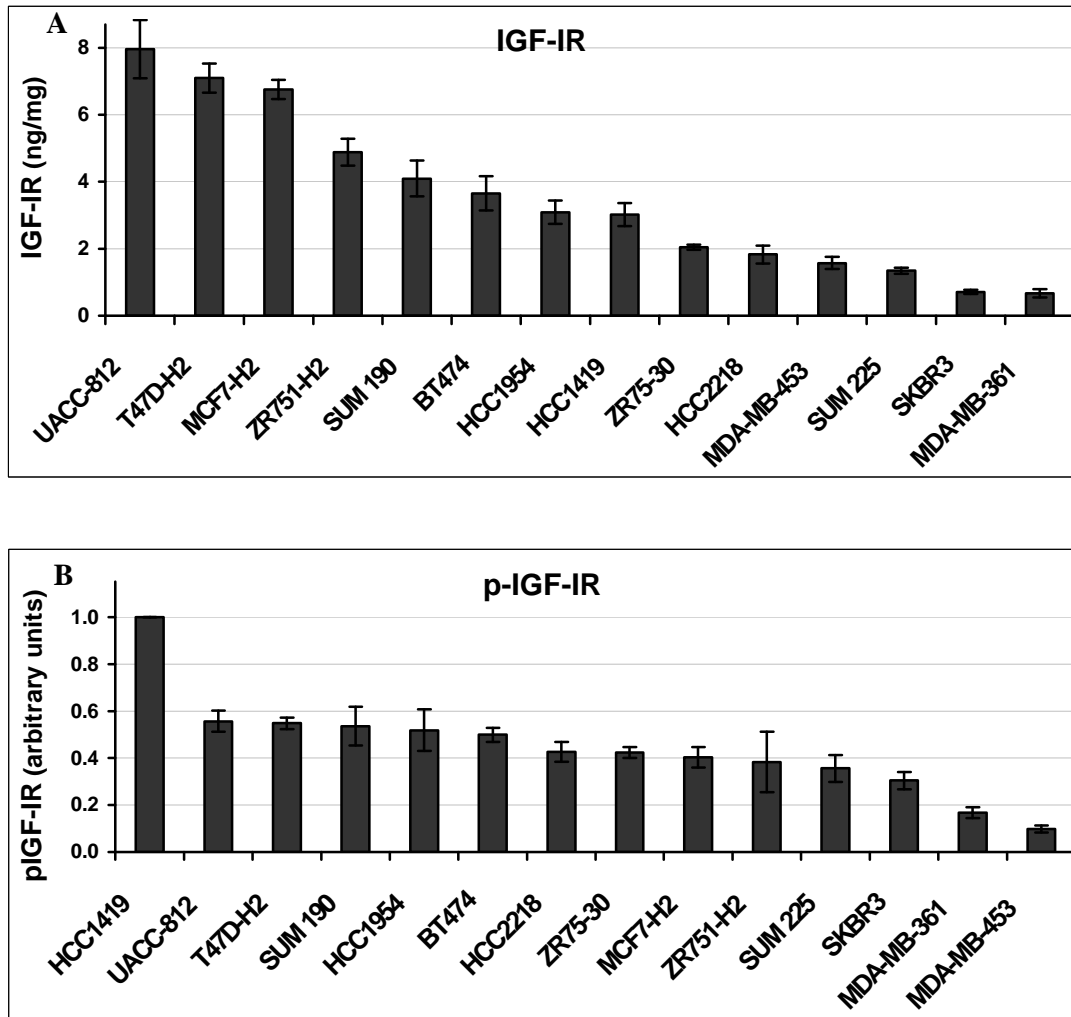
Figure 3.6. **A.** IGF-IR and **B.** phospho-IGF-IR protein levels in 14 HER-2-
overexpressing breast cancer cell lines. IGF-IR is expressed as ng/mg total protein; p-
IGF-IR is expressed as arbitrary units, relative to the cell line with the highest optical
density reading, which was assigned a value of 1. Error bars represent standard error of
triplicate experiments.

_____
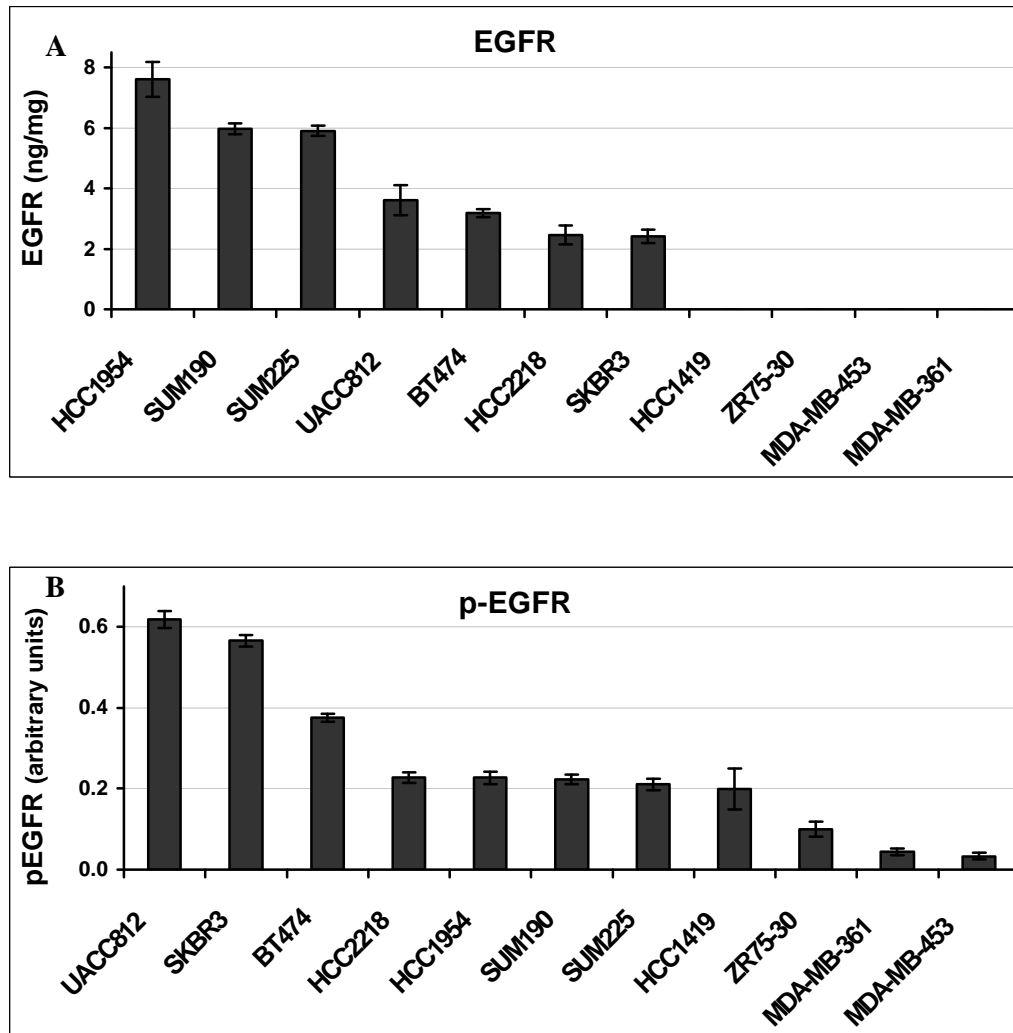
Figure 3.7. **A.** EGFR and **B.** phospho-EGFR protein levels in 11 HER-2-overexpressing breast cancer cell lines. EGFR is expressed as ng/mg total protein; p-EGFR is expressed as arbitrary units, relative to the cell line with the highest optical density reading, which was assigned a value of 1. Error bars represent standard error of triplicate experiments.
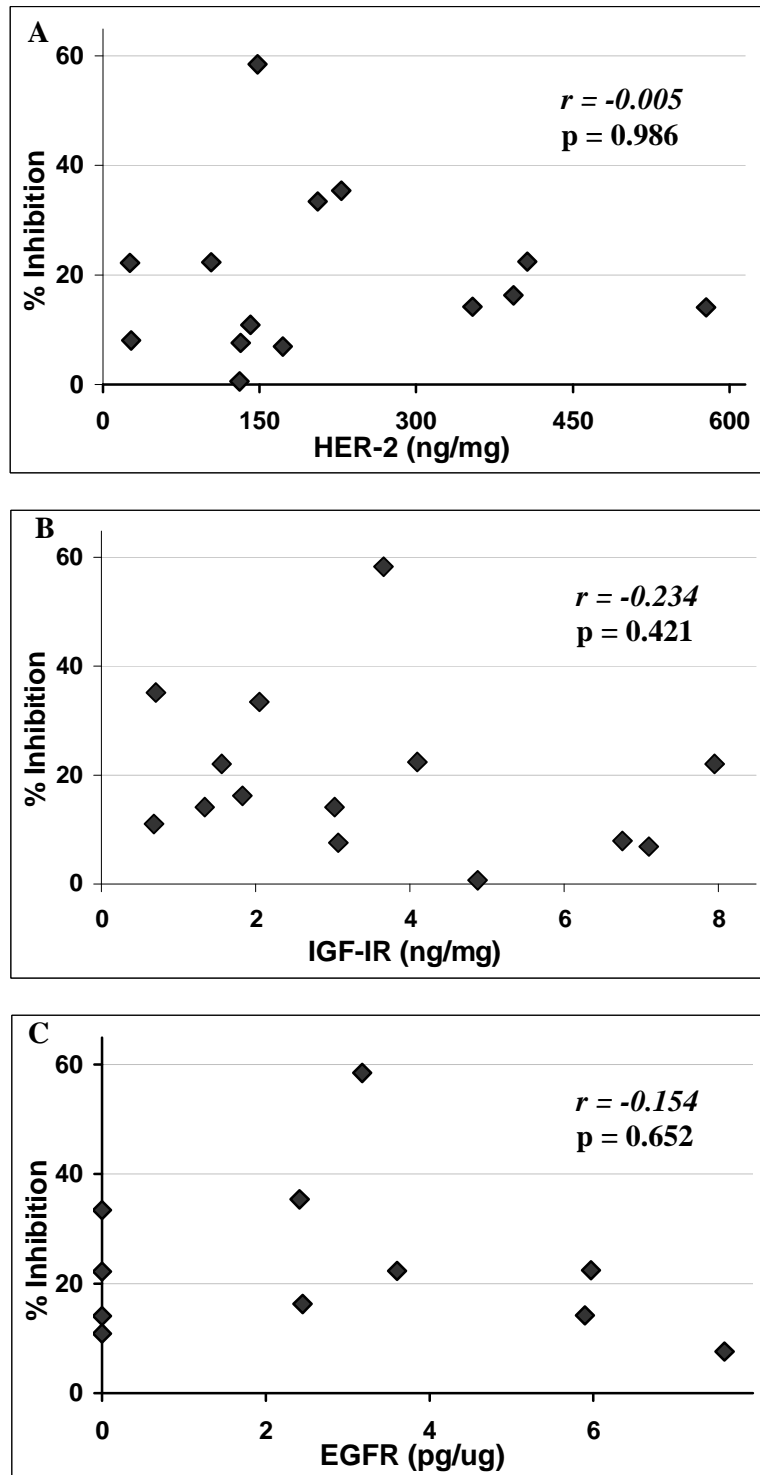
Figure 3.8. Scatterplots relating **A.** HER-2, **B.** IGF-IR and **C.** EGFR levels to percentage inhibition by trastuzumab in the HER-2-overexpressing breast cancer cell lines. Proliferation was measured by cell counting after 5 days, and % inhibition is expressed relative to untreated control. Protein levels were quantified by ELISA. Correlations were analysed by calculating Pearson's correlation coefficient (r).

_____
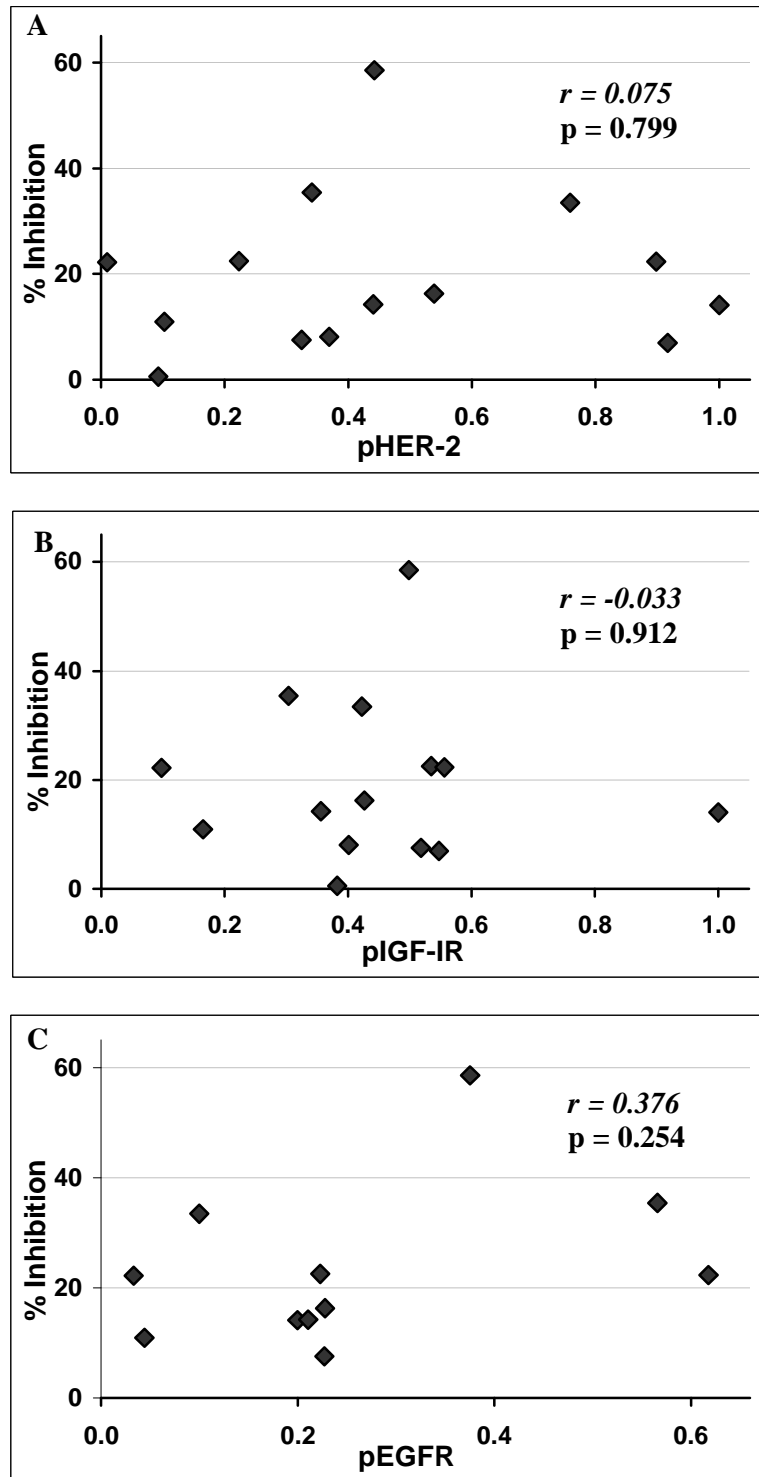
Figure 3.9. Scatterplots relating **A.** p-HER-2, **B.** p-IGF-IR and **C.** p-EGFR levels to percentage inhibition by trastuzumab in the HER-2-overexpressing breast cancer cell lines. Proliferation was measured by cell counting after 5 days, and % inhibition is expressed relative to untreated control. Protein levels were quantified by ELISA. Correlations were analysed by calculating Pearson's correlation coefficient (r).
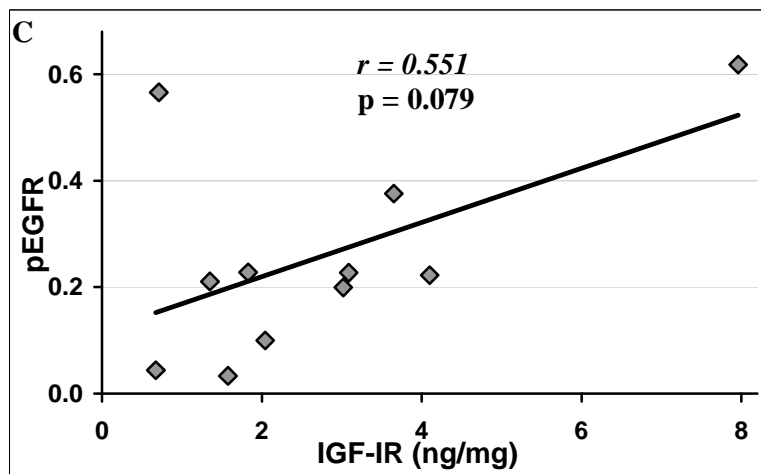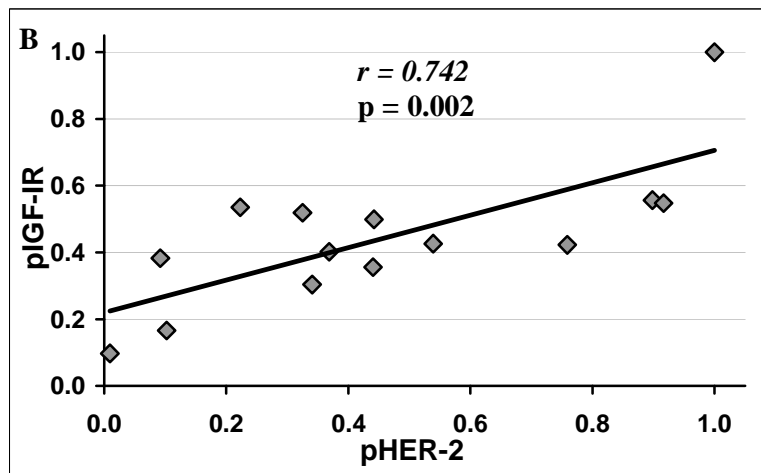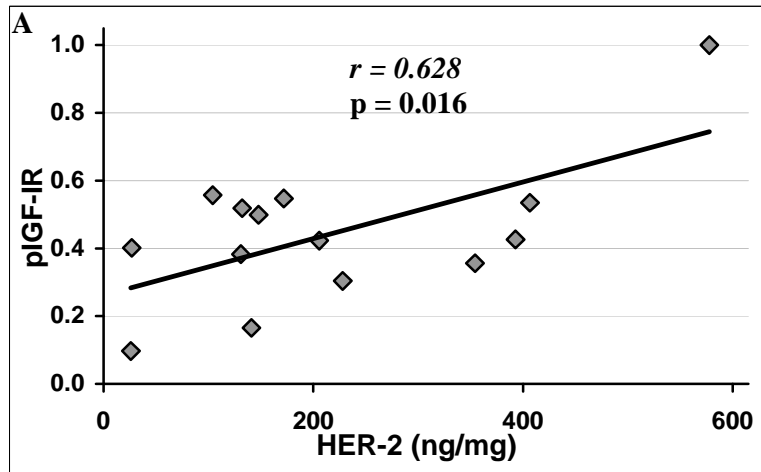
Figure 3.10. Scatterplots relating **A.** HER-2 to p-IGF-IR, **B.** p-HER-2 to p-IGF-IR and **C.** IGF-IR to p-EGFR expression levels in the HER-2-overexpressing breast cancer cell lines, as measured by ELISA. Correlations were analysed by calculating Pearson's correlation coefficient (r).

_____

Chapter 4

CHARACTERISATION OF TRASTUZUMAB RESISTANCE

4.1 REDUCED IGF-I STIMULATION DOES NOT CONFER SENSITIVITY TO TRASTUZUMAB

It has previously been reported that IGF/IGF-IR signalling interferes with trastuzumab inhibition in HER-2-transfected MCF7/HER2-18 cells, and that reduction of IGF-IR stimulation of cells by reducing the serum content of the growth media restores sensitivity to trastuzumab in these cells [177]. We found that reduction of serum in the growth media of MCF7-HER2 cells did not sensitise these cells to trastuzumab, nor did IGF-I stimulation affect the growth in 1 %, 5 % or 10 % serum [Fig. 4.1]. These assays were performed at varied conditions: proliferation was measured at different time-points up to six days; serum concentration was varied between 0 – 10 %; IGF-I concentration was used at 40, 80 and 100 ng/ml. Response to trastuzumab was not enhanced at any of these conditions (results not shown).
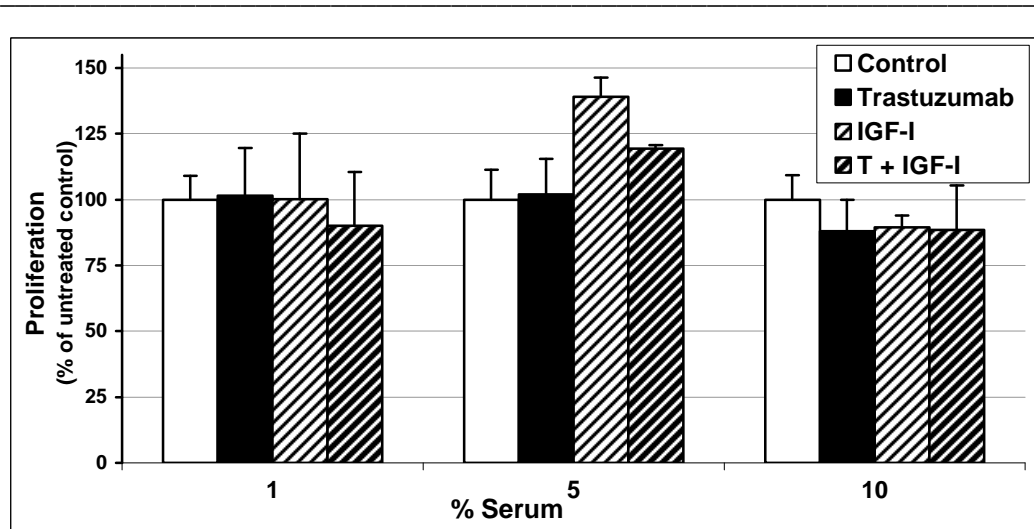
Figure 4.1. Proliferation of MCF7-HER2 cells treated with and without trastuzumab (T) (100 nM) and IGF-I (40 ng/ml) in varying serum concentrations. Proliferation was measured by cell counting after 5 days, and is expressed relative to untreated control. Error bars represent standard deviation of three experiments.

4.2 ELEVATED HER-2 SIGNALLING INTERFERES WITH IGF-I-INDUCED MAPK SIGNALLING

Transfection of HER-2 into MCF7 cells causes elevated HER-2 signalling, and HER-2-transfected MCF7 cells have elevated Akt activity compared to control-transfected cells grown in serum-free or serum-containing growth media [Fig. 4.2]. IGF-I treatment causes phosphorylation of Akt in both MCF7neo and MCF7-HER2 cells. Elevated HER-2 signalling, however, interferes with IGF-I-induced MAPK signalling; MCF7-HER2 cells have reduced MAPK phosphorylation in response to IGF-I compared to MCF7neo cells. This suggests that HER-2 and IGF-IR may have independent pathways for signalling through Akt, but may share common signalling molecules in the MAPK pathway.
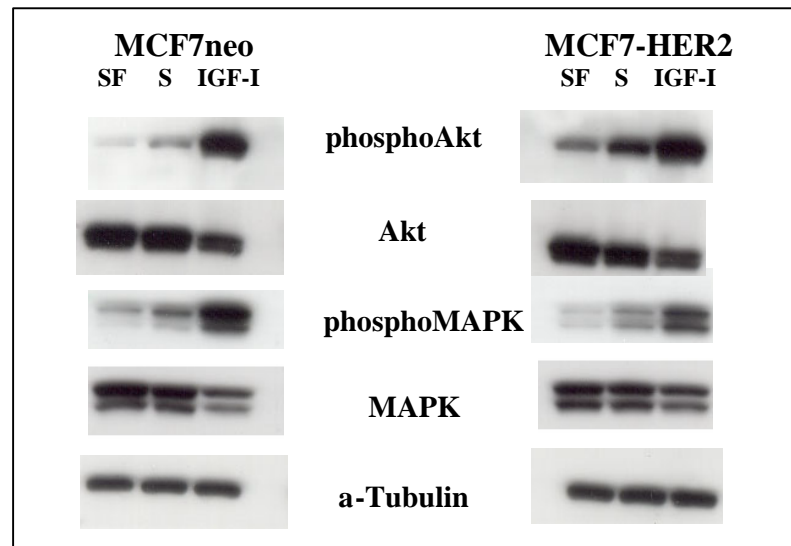
Figure 4.2 Western blot of phosphorylated Akt and MAPK in MCF7neo and MCF7-HER2 cells. Cells were serum-starved for 24 hours and treated with serum-free (SF) media, serum-containing (S) media, or SF media with IGF-I (100 ng/ml) for 10 minutes. a-tubulin was used as a loading control.

4.3   TRASTUZUMAB TREATMENT ANTAGONISES IGF-I-STIMULATED AKT SIGNALLING

Trastuzumab treatment of MCF7-HER2 cells results in a slight elevation of Akt phosphorylation, which returns to almost basal levels within two hours [Fig 4.3]. IGF-I stimulation caused an increase in phosphorylated Akt levels after two hours of treatment and this effect was reduced by trastuzumab [Fig. 4.3]. After two hours, trastuzumab reduced the IGF-I-stimulated phospho-Akt levels by 50 % [Fig. 4.3].
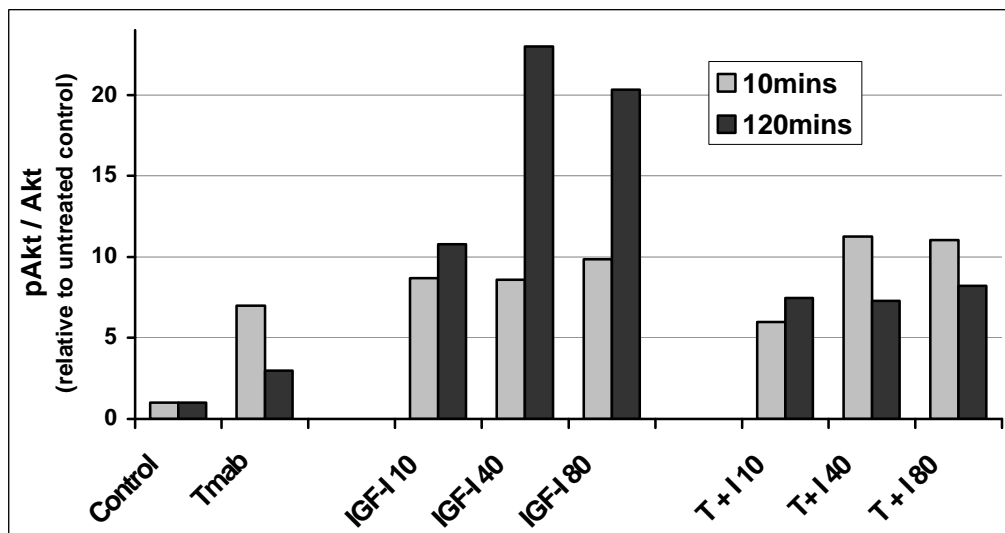
Figure 4.3 Phosphorylated Akt levels in MCF7-HER2 cells. Cells were serum-starved for 24 hours and then treated alone or in combination with trastuzumab (T, Tmab) (100 nM) and IGF-I (I) (10, 40 or 80 ng/ml). Phospho-Akt was measured by western blot at 10 and 120 minutes. Levels were normalised against total Akt levels, and are expressed relative to untreated control.

4.4   TRASTUZUMAB-CONDITIONED CELLS ARE MORE RESISTANT TO TRASTUZUMAB

BT474 and SKBR3 cells were continuously maintained in media containing 700 nM (100 µg/ml) trastuzumab for 18 months. After this time, conditioned cells (BT474/Tr and SKBR3/Tr) were less responsive to trastuzumab. 100 nM trastuzumab inhibited proliferation by 25.4 % in BT474/Tr cells, compared to 65.6 % in parental BT474 cells, and 24.1 % in SKBR3/Tr cells compared to 42.6 % in parental SKBR3 cells. When trastuzumab was removed from the growth media of conditioned cells for up to 12 weeks, conditioned cells maintained their relative resistance [Fig. 4.4].
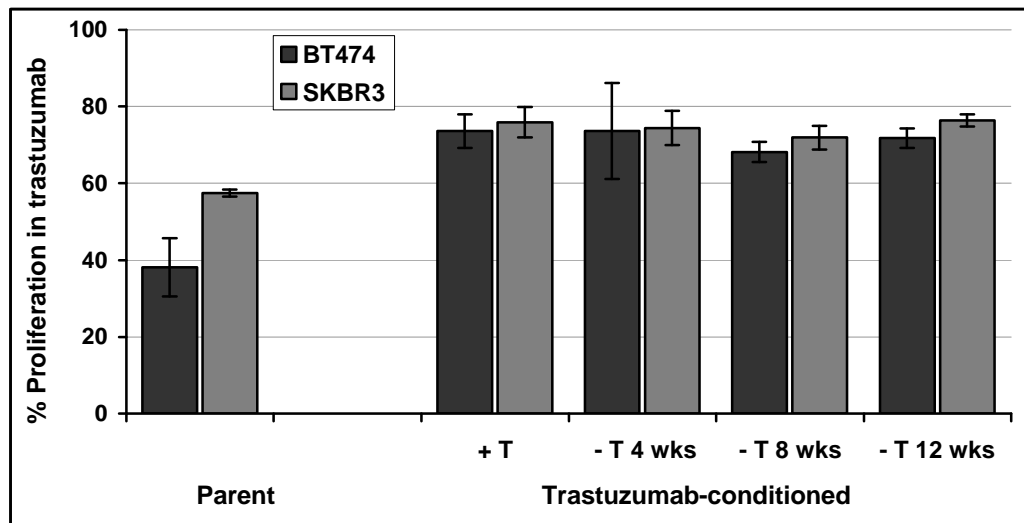
Figure 4.4 Proliferation of BT474 and SKBR3 parental and trastuzumab-conditioned treated with trastuzumab (100 nM). Trastuzumab-conditioned cells were maintained in media with (+T) or without trastuzumab (-T) for up to 12 weeks. Proliferation was measured after five days by cell counting and is expressed relative to untreated control. Error bars represent standard deviation of triplicate experiments.

4.5   HER-2, EGFR AND IGF-IR IN TRASTUZUMAB-RESISTANT CELLS

HER-2, IGF-IR, EGFR and phosphorylated HER-2, IGF-IR and EGFR levels were quantified by ELISAs in parental and trastuzumab-resistant BT474 and SKBR3 cells [Table 4.1].   HER-2 and phospho-HER-2 levels were not significantly altered in trastuzumab-resistant SKBR3 cells, but were significantly increased in the BT474/Tr cells compared to parental cells (T-test: HER-2, p = 0.041; p-HER-2, p = 0.044). While total EGFR results where similar in SKBR3 and SKBR3/Tr cells, SKBR3/Tr had significantly decreased phospho-EGFR levels compared to parental SKBR3 cells (p = 0.002), while both total and phospho- EGFR levels were significantly elevated in BT474/Tr compared to BT474 cells (EGFR, p = 0.003; p-EGFR, p = 0.002). IGF-IR levels were significantly higher in the SKBR3/Tr cells than in parental SKBR3 cells (p = 0.029), while they were unchanged in BT474/Tr cells [Table 4.1]. HER-2, phospho-HER-2 and EGFR ELISA results were confirmed by immunoblotting [Fig. 4.5].

_____
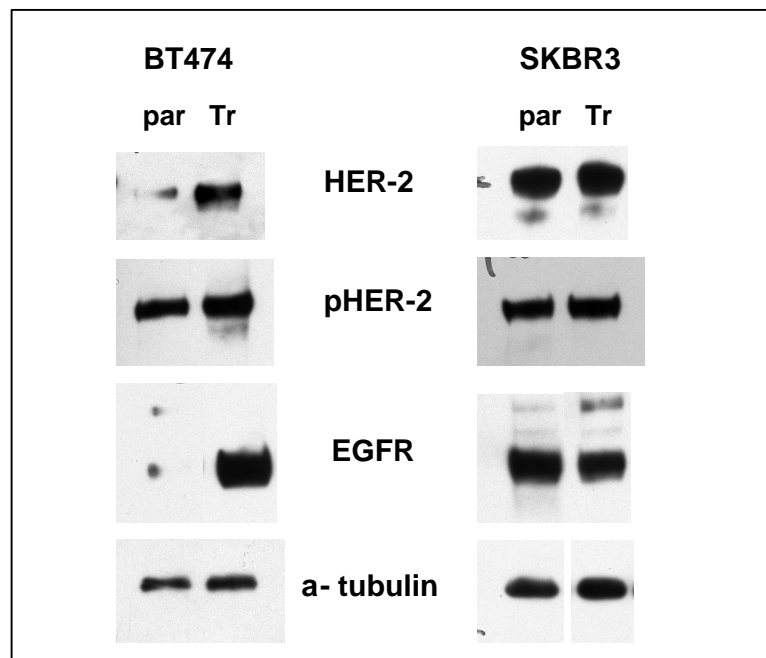
Figure 4.5   Western blot of HER-2, phospho-HER-2 and EGFR protein expression in parental (par) and trastuzumab-resistant (Tr) BT474 and SKBR3 cells. a-tubulin was used as a loading control.

_____

_____

Table 4.1 Expression and phosphorylation levels of HER-2, IGF-1R and EGFR and sensitivity to trastuzumab (T) (100 nM) in parental and trastuzumab-resistant BT474 and SKBR3 cells. Protein levels were measured by ELISA; phospho-HER-2, phospho-IGF-IR and phospho-EGFR levels are expressed as arbitrary units, relative to the cell line with the highest ELISA optical density reading, which was assigned a value of 1 (± standard error). Cell proliferation was measured by cell counting after 5 days treatment, and % growth was calculated relative to untreated control (± standard deviation).

	% GROWTH IN T	HER-2 NG/MG	P-HER-2	IGF-IR NG/MG	P-IGF-1R	EGFR NG/MG	P-EGFR
BT474	38.1 ± 7.6	147.9 ± 13.3	0.44 ± 0.05	3.6 ± 0.5	0.50 ± 0.03	3.18 ± 0.13	0.38 ± 0.01
BT474/TR	$73.6 \pm 4.4^*$	$411.4 \pm 78.2^*$	$0.62 \pm 0.05^*$	3.1 ± 0.4	0.57 ± 0.09	$13.16 \pm 0.34^{**}$	$1.00 \pm 0.00^{**}$
SKBR3	57.4 ± 0.9	228.1 ± 37.6	0.34 ± 0.02	0.7 ± 0.1	0.30 ± 0.04	2.41 ± 0.22	0.56 ± 0.01
SKBR3/TR	$75.9 \pm 4.0^*$	184.7 ± 16.8	0.34 ± 0.06	$1.8 \pm 0.3^*$	0.31 ± 0.03	2.56 ± 0.25	$0.20 \pm 0.01^{**}$

* indicates $p<0.05$; ** indicates $p<0.001$ for comparisons of resistant cell lines with parental cell lines, as determined by the Student's t-test.

_____

4.6   DIMERISATION BETWEEN HER-2 AND IGF-IR

Immunoprecipitation (IP) of IGF-IR protein and subsequent western blotting for HER-2 were performed in order to investigate HER-2/IGF-IR heterodimerisation in parental and trastuzumab-conditioned BT474 and SKBR3 cells. HER-2 co-precipitated with IGF-IR in parental and conditioned cells treated with trastuzumab (100 nM) for 24 hours, but not in untreated samples [Fig. 4.6]. However, in control IP experiments, without antibody present, HER-2 was also detected, suggesting that trastuzumab itself immunoprecipitated HER-2 in these samples [Fig. 4.6].   IP of HER-2 protein followed by western blotting for IGF-IR protein was then attempted to investigate if IGF-IR co-immunoprecipitates with HER-2 in any of the cell line samples. However, the results of this experiment were unclear, due to problems detecting low amounts of immunoprecipitated IGF-IR protein. Numerous antibodies were tested, but as BT474 and SKBR3 cells express relatively low levels of IGF-IR protein, none of the western blots were successful. Fig 4.7B shows a western blot of MCF7-HER2 cell protein after IGF-IR IP along side total IGF-IR; as IGF-IR was undetectable after IP in this cell line, which expresses high levels of IGF-IR, it is unlikely that IGF-IR could be detected in immunoprecipitated BT474 or SKBR3 cell lysates.
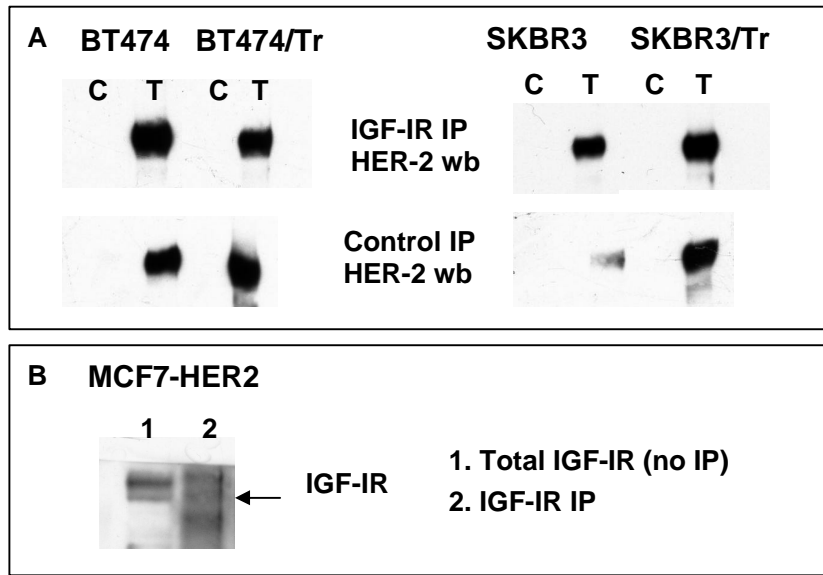
Figure 4.6 Immunoprecipitation (IP) -western blots (wb). **A.** HER-2 protein levels in parental and trastuzumab-resistant BT474 and SKBR3 cells after IGF-IR IP, and control IP, which was performed with no antibody present. Cells were treated with and without (C) trastuzumab (100 nM) (T) for 24 hours. **B.** IGF-IR levels in MCF7-HER-2 without any IP (lane 1) and after IGF-IR IP (lane 2).

4.7   AKT AND MAPK SIGNALLING IN TRASTUZUMAB-RESISTANT CELLS

While Akt and MAPK protein expression are unaltered in conditioned cells, BT474/Tr cells have significantly reduced phosphorylation of Akt and MAPK compared to BT474 cells [Fig 4.7].   Phospho-Akt levels were also reduced in SKBR3/Tr compared to parental SKBR3 cells. SKBR3/Tr cells displayed no alteration in phospho-MAPK levels.   Changes in phospho-Akt and phospho-MAPK levels in response to 100 nM trastuzumab treatment were investigated in SKBR3 and SKBR3/Tr cells over 5 days [Fig. 4.8]. A similar response to trastuzumab was seen in both cell lines: while at 16 hours, both phospho-Akt and phospho-MAPK levels were reduced; however, by 5 days, phosphoprotein levels were again upregulated.
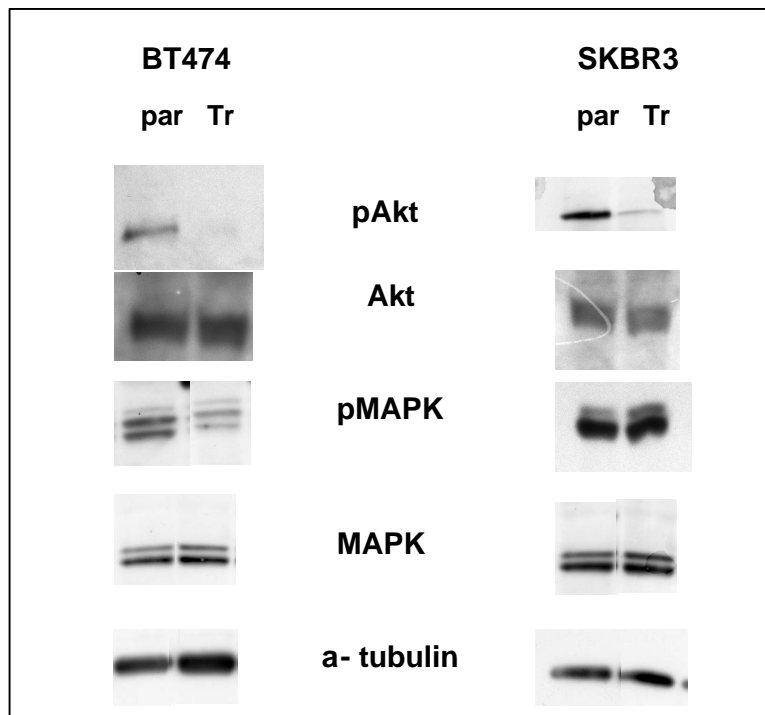
Figure 4.7   Western blot of Akt, phospho-Akt, MAPK and phospho-MAPK protein expression in parental (par) and trastuzumab-resistant (Tr) BT474 and SKBR3 cells. a-tubulin was used as a loading control.
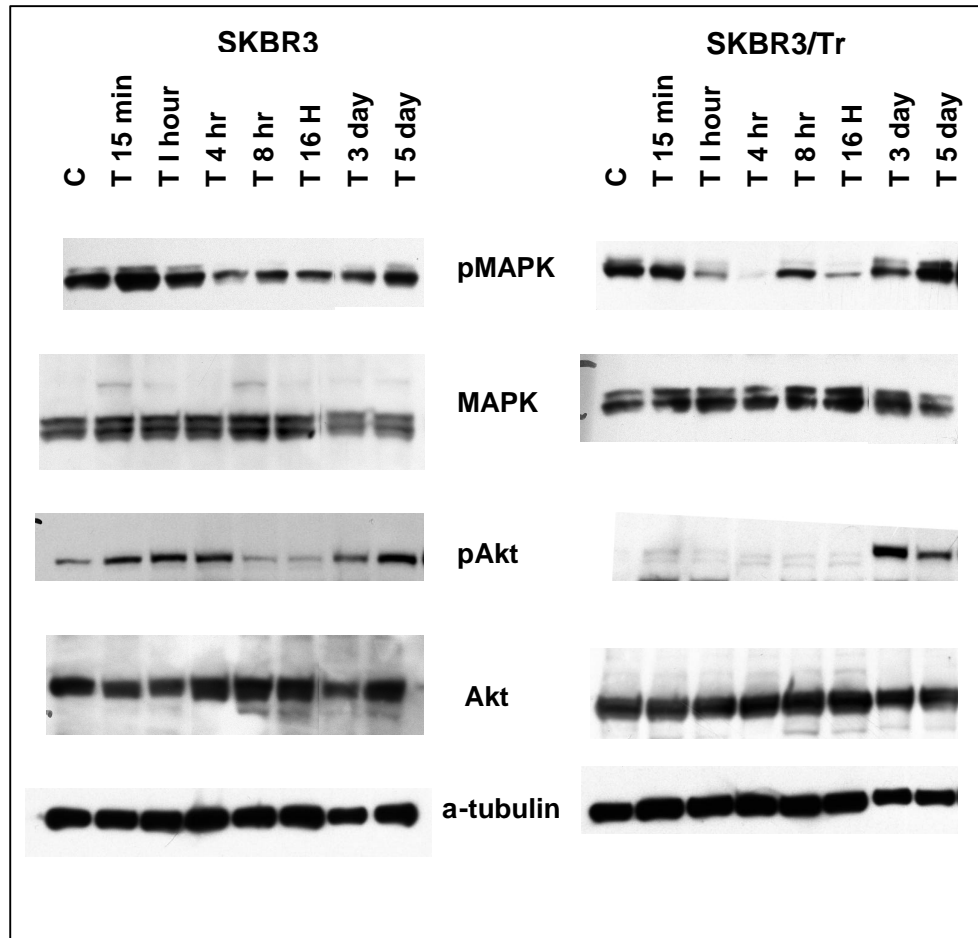
Figure 4.8 Western blot of Akt, phospho-Akt, MAPK and phospho-MAPK protein expression in SKBR3 and SKBR3/Tr cells after trastuzumab treatment (100 nM) for up to 5 days, compared to control untreated cells (C). a-tubulin was used as a loading control.

4.8   RESPONSE TO LAPATINIB IN TRASTUZUMAB-RESISTANT CELLS

In order to examine cross-resistance, response to lapatinib was measured in parental and trastuzumab-resistant SKBR3 and BT474 cells [Fig. 4.9]. BT474 and BT474/Tr cells were equally sensitive to lapatinib at concentrations lower than 100 nM, with IC_{50} concentrations of 27.0 ± 2.8 nM and 27.5 ± 9.2 nM, respectively. However, at higher concentrations, BT474/Tr cells were more sensitive to lapatinib, though this did not reach statistical significance. SKBR3/Tr cells were significantly less responsive to lapatinib than parental SKBR3 cells with an IC_{50} of 174 ± 40.2 nM, compared to 71.3 ± 18.0 nM in parental cells (t-test, $p = 0.009$)
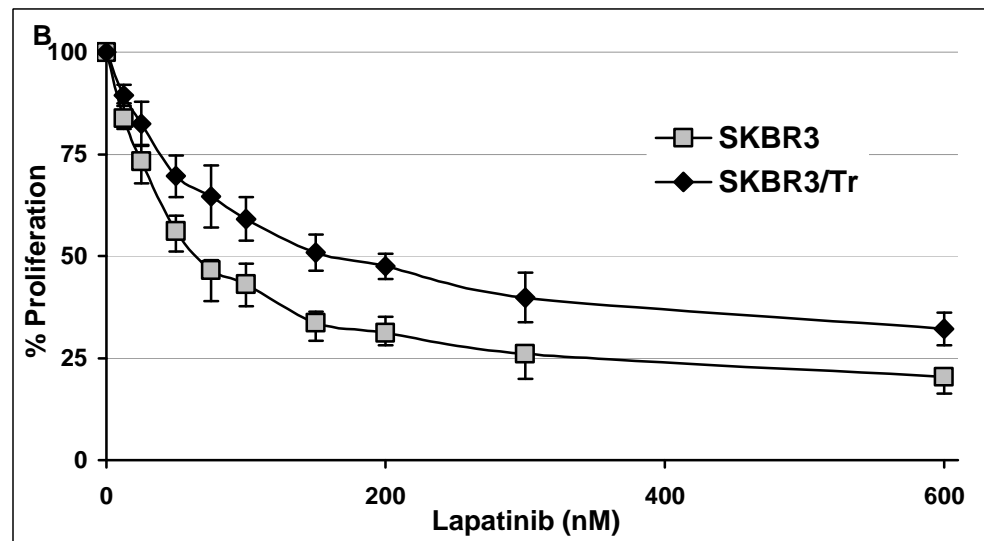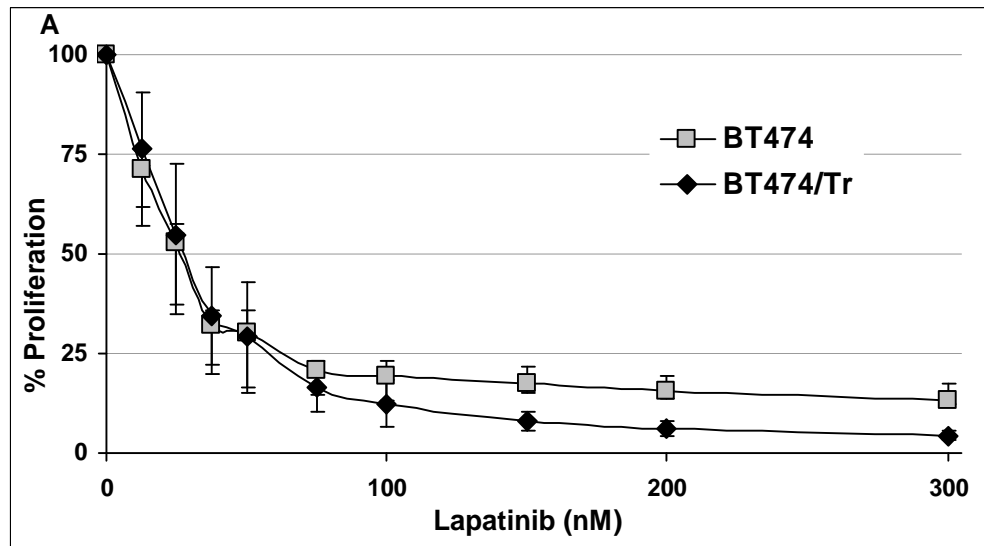
Figure 4.9 Proliferation of **A.** BT474 and **B.** SKBR3 parental and trastuzumab-resistant cells treated with increasing doses of lapatinib. Proliferation was measured after five days by the acid phosphatase method and is expressed relative to untreated control. Error bars represent standard deviation of at least duplicate experiments.

Chapter 5

INHIBITION OF IGF-IR IN TRASTUZUMAB RESISTANT CELLS

5.1 IGF-BINDING PROTEIN 3 (IGFBP3) AND ANTI-IGF-IR ANTIBODY aIR3

IGF-stimulated IGF-IR signalling was targeted using two molecules; IGFBP3 to reduce available ligand, and aIR3 to block the ligand-binding domain of IGF-IR. Neither molecule inhibited proliferation nor enhanced the inhibitory effects of trastuzumab in parental or trastuzumab-resistant BT474 and SKBR3 cells [Fig. 5.1]. The activity of IGFBP3 and aIR3 against IGF-I/IGF-IR signalling was confirmed with MCF7 cells, in which both molecules inhibited IGF-I-stimulated growth [Fig. 5.2].
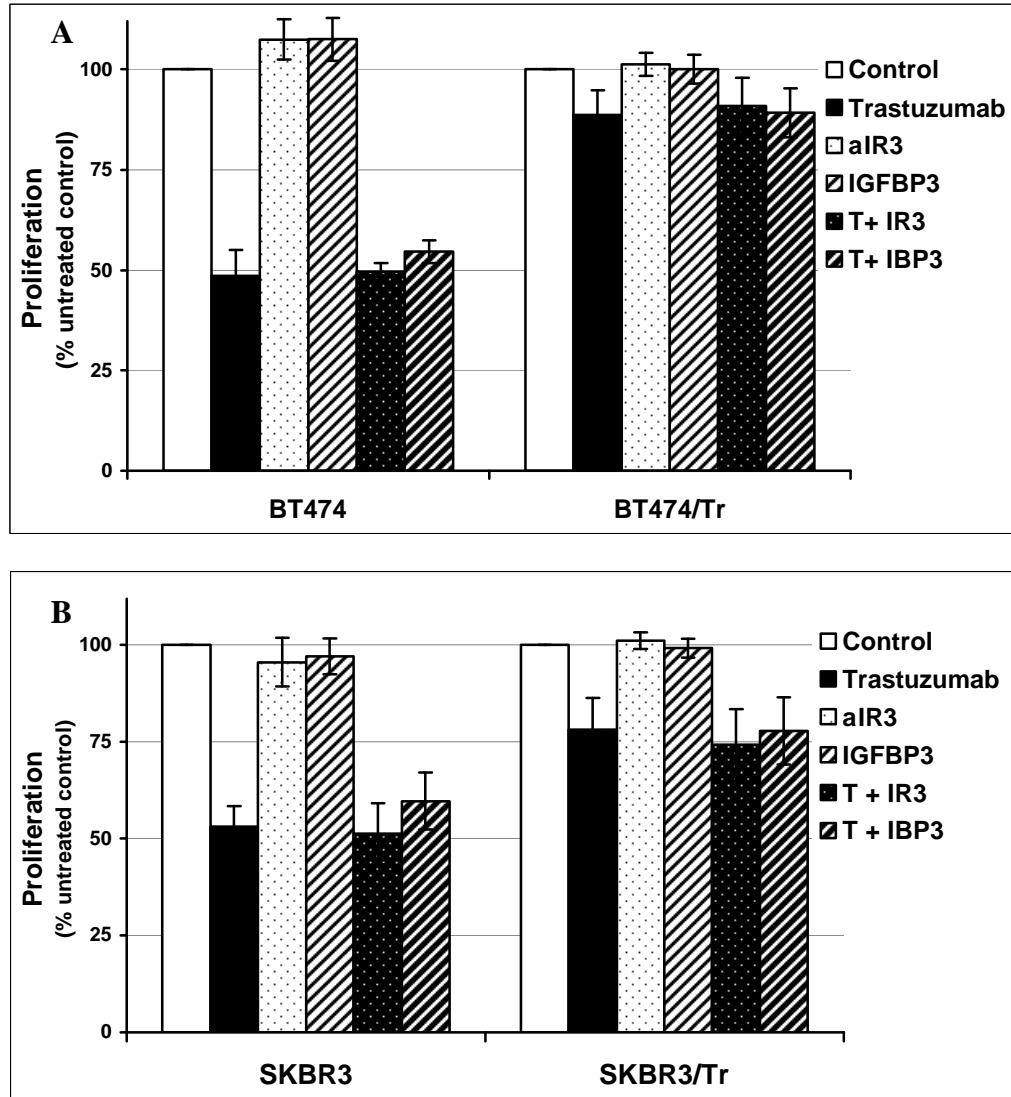
Figure 5.1 Proliferation of **A.** BT474 and **B.** SKBR3 parental and trastuzumab-resistant cells. Cells were cultured in the presence of 5 % serum and treated alone or in combinations with trastuzumab (T) (100 nM), aIR3 (1 µg/ml) and IGFBP3 (1 µg/ml). Proliferation was measured after five days by the acid phosphatase method, and is expressed relative to untreated control. Error bars represent standard deviation of triplicate experiments.

_____
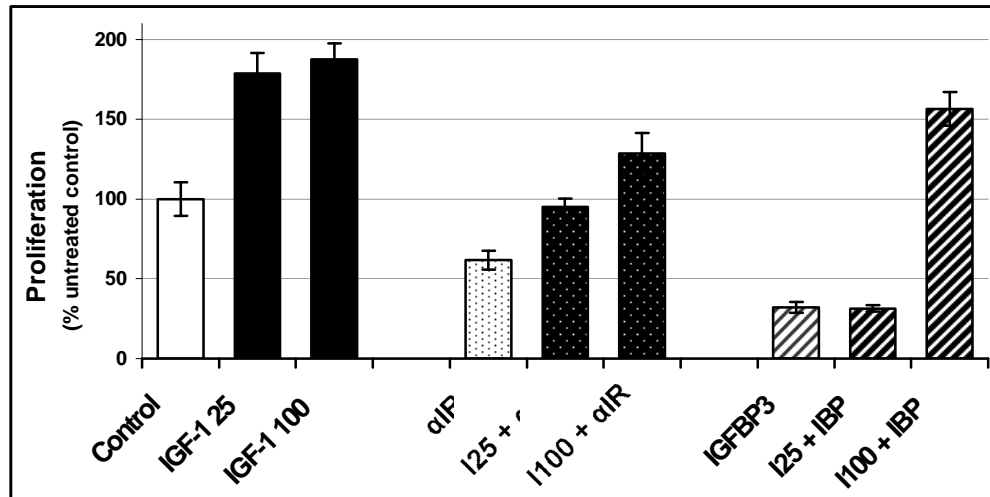
Figure 5.2 Proliferation of MCF7 cells. Cells were cultured in the presence of 1 %
serum and treated alone or in combinations with IGF-I (25 or 100 ng/ml) (I), aIR3 (1
µg/ml) and IGFBP3 (1 µg/ml) (IBP). Proliferation was measured after five days by the
acid phosphatase method, and is expressed relative to untreated control. Error bars
represent standard deviation of replicate wells (single experiment).

5.2 IGF-IR SMALL INTERFERING RNA (siRNA) ENHANCES THE INHIBITORY EFFECTS OF TRASTUZUMAB

Transfection with an anti-IGF-IR siRNA molecule reduced IGF-IR protein levels by 33.8 ± 3.5 % in SKBR3 cells, 11.2 ± 4.1 % in SKBR3/Tr cells, 24.0 ± 2.5 % in BT474 cells, and 20.6 ± 5.3 % in BT474/Tr cells, as quantified by IGF-IR ELISA. The IGF-IR siRNA also reduced proliferation of each of the cell lines [Fig. 5.3 and Fig. 5.4]. While combined treatment with IGF-IR siRNA and trastuzumab did not improve response compared to trastuzumab alone in BT474 cells, the combination inhibited significantly more growth than trastuzumab alone in BT474/Tr cells [Fig. 5.3]. The combined treatment also significantly enhanced response, compared to siRNA treatment alone in SKBR3 cells, and compared to either treatment alone, in SKBR3/Tr cells [Fig. 5.4]. Two other siRNA molecules, targeting different exons of the IGF-IR gene, were also studied in SKBR3/Tr cells; both reduced expression of IGF-IR (by 49.2 ± 10.6 % and 34.2 ± 3.2 %), inhibited proliferation, and enhanced response when combined with trastuzumab [Fig. 5.5]. IGF-IR protein knockdown was confirmed in SKBR3 and SKBR3/Tr cells by western blotting [Fig. 5.6].
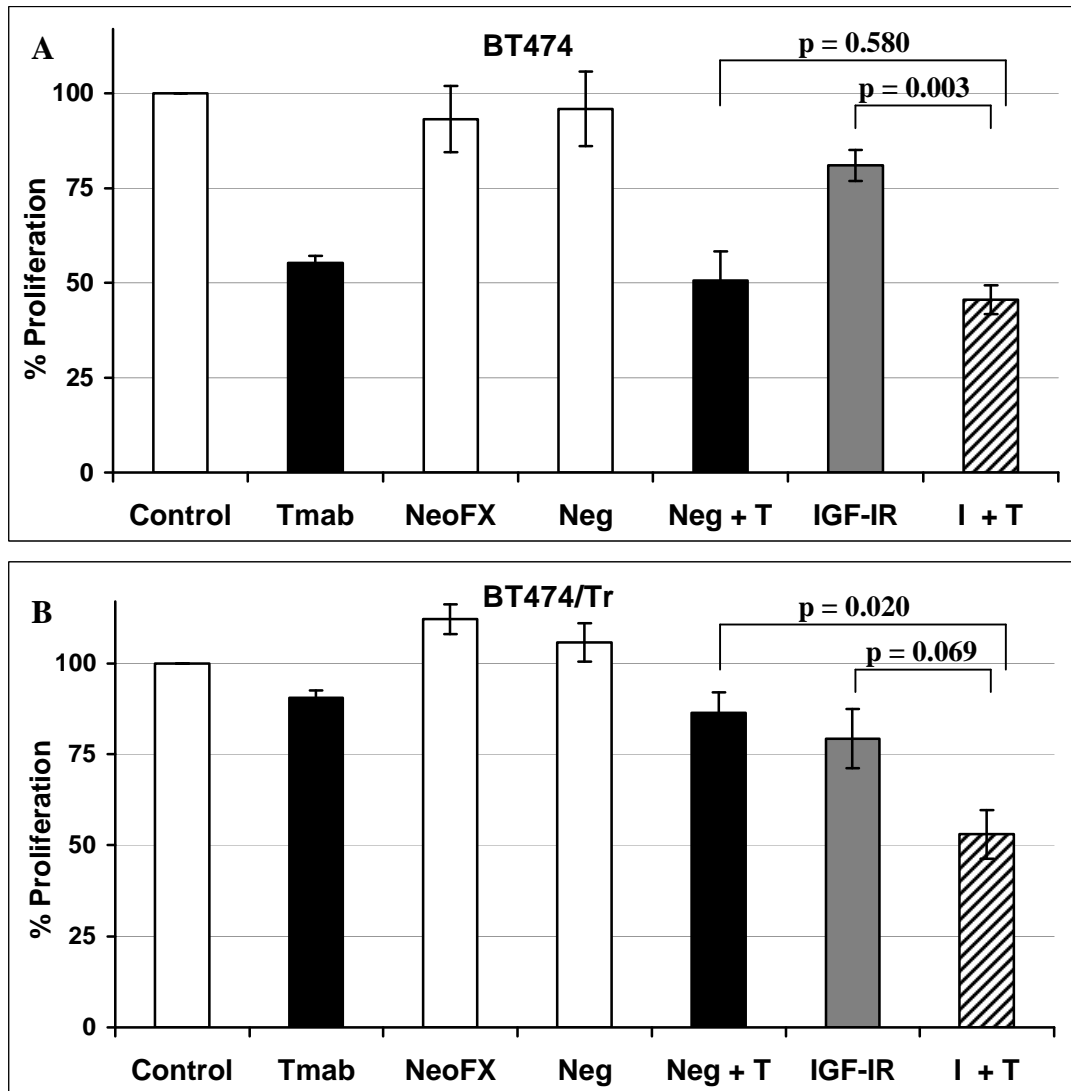
Figure 5.3 Proliferation of **A.** BT474 and **B.** BT474/Tr cells treated with and without trastuzumab (Tmab, T) (100 nM) and anti-IGF-IR siRNA (I) (30 nM). NeoFx transfection reagent, and a scrambled siRNA molecule (Neg) were used as negative controls. Proliferation was measured by cell counting after four days, and is expressed relative to untreated control. Student's t-test was performed to determine significance. Error bars represent standard error of triplicate experiments.
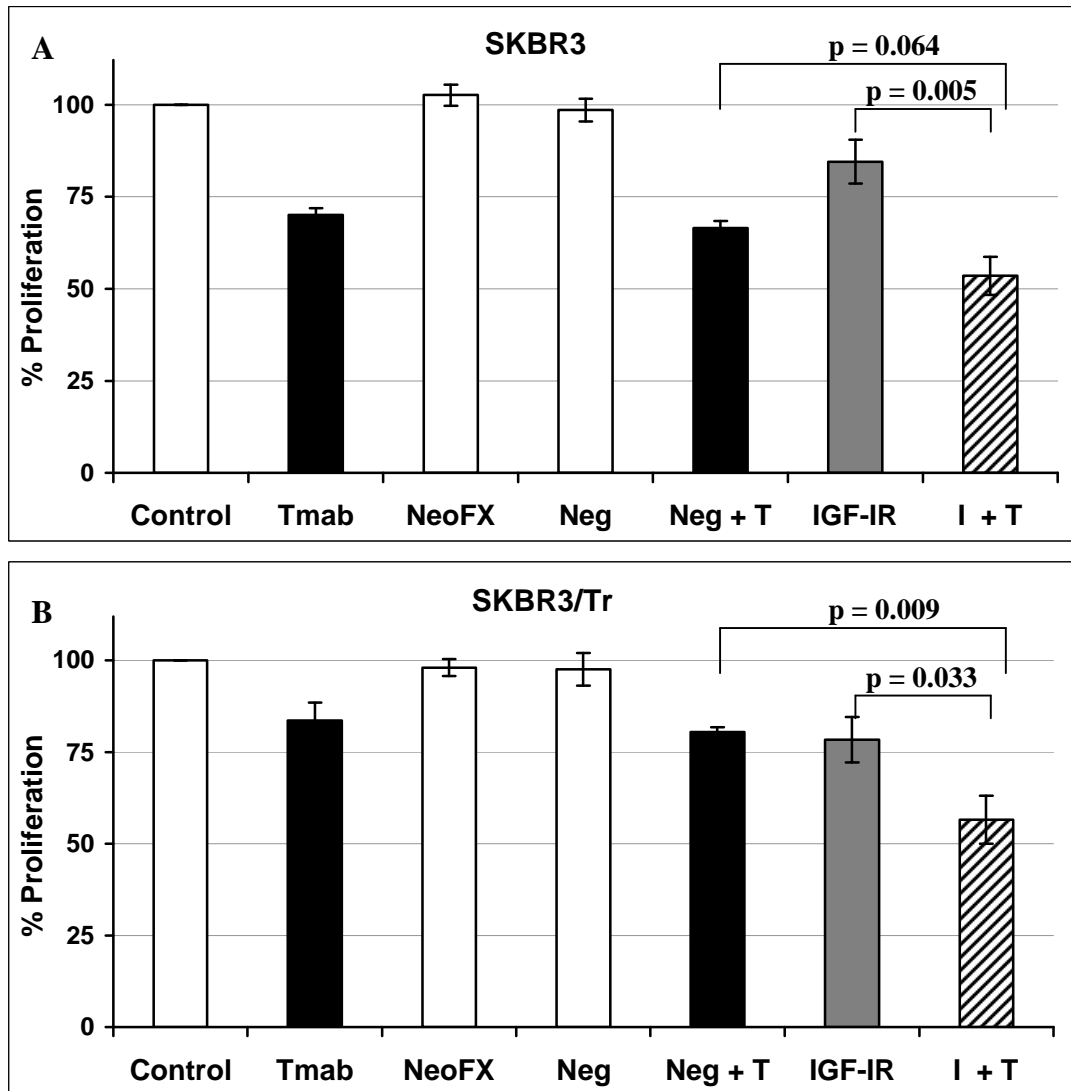
Figure 5.4 Proliferation of **A.** SKBR3 and **B.** SKBR3/Tr cells treated with and without trastuzumab (Tmab, T) (100 nM) and anti-IGF-IR siRNA (I) (30 nM). NeoFx transfection reagent, and a scrambled siRNA molecule (Neg) were used as negative controls. Proliferation was measured by cell counting after four days, and is expressed relative to untreated control. Student's t-test was performed to determine significance. Error bars represent standard error of triplicate experiments.
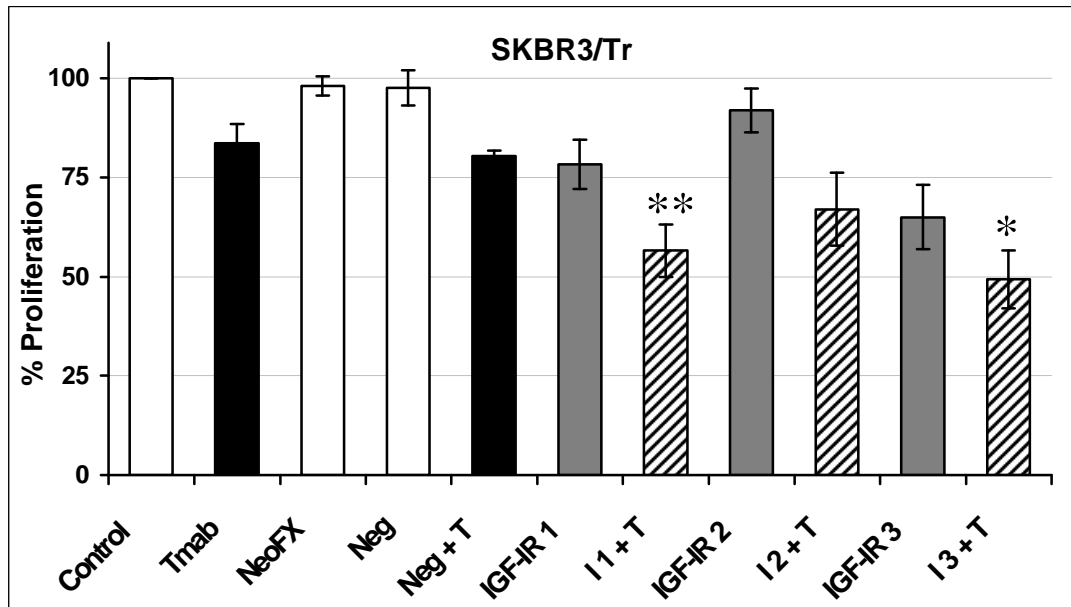
Figure 5.5 Proliferation of SKBR3/Tr cells treated with and without trastuzumab (Tmab, T) (100 nM) and three anti-IGF-IR siRNA molecules 1-3 (30nM). siRNA molecule 1 was also used to treat SKBR3, BT474 and BT474/Tr cells (see Figs. 5.4 and 5.5). NeoFx transfection reagent, and scrambled siRNA (Neg) were used as negative transfection controls. Proliferation was measured by cell counting after four days, and is expressed relative to untreated control. Student's t-test was performed to determine significance: * denotes $p < 0.05$; ** denotes $p < 0.01$, when comparing combined treatment with trastuzumab alone. Error bars represent standard error of three experiments.

_____
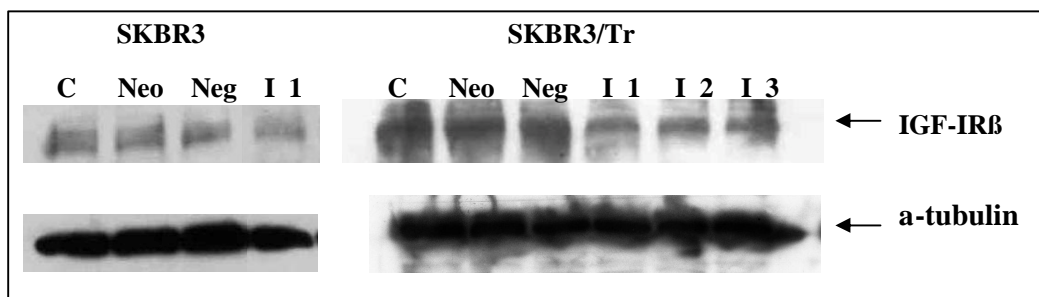
Figure 5.6 Western blot of SKBR3 and SKBR3/Tr cells transfected with anti-IGF-IR siRNA molecules no.s 1, 2 and 3. Untreated cells (C), NeoFx transfection reagent treated (Neo), and scrambled siRNA treated (Neg) cells were used as controls. Cells were lysed after 72 hours treatment. a-tubulin was used as a loading control.

_____

117

5.3 IGF-IR TYROSINE KINASE INHBITORS ENHANCE RESPONSE TO TRASTUZUMAB

5.3.1 IGF-IR tyrosine kinase inhibitors inhibit growth of trastuzumab-sensitive and -resistant cells

Two IGF-IR tyrosine kinase inhibitors (TKIs) were used to target IGF-IR tyrosine kinase signalling. Neither NVP-AEW541 nor BMS-536924 significantly inhibited the proliferation of BT474 or BT474/Tr cells [Fig. 5.7]. However, combined treatment with trastuzumab and each TKI inhibited more growth than treatment with either trastuzumab or TKI in BT474/Tr cells; the combination of trastuzumab and NVP-AEW541 had significantly enhanced effects compared to trastuzumab alone (p = 0.042), while the combination of trastuzumab and BMS-536924 did not reach statistical significance (p = 0.066) [Fig. 5.7]. NVP-AEW541 inhibited the growth of both SKBR3 and SKBR3/Tr cells, while BMS-536924 alone had no effects on the proliferation of these cells [Fig. 5.8]. Combined treatment with trastuzumab and NVP-AEW541 inhibited significantly more growth than trastuzumab alone in both SKBR3 and SKBR3/Tr cells (SKBR3, p = 0.010; SKBR3/Tr, p = 0.00002). The combination of trastuzumab with BMS-536924 had no inhibitory advantage over trastuzumab alone in these cells [Fig. 5.8]. To confirm the activity of the two TKIs, MCF7 cells (which express high levels of IGF-IR and low levels of HER-2) were also treated with combinations of trastuzumab and TKIs. Each inhibitor alone decreased growth of MCF7 cells by over 80 % [Fig. 5.9 A]. HER-2-transfected MCF7 cells, MCF7-HER2, which are resistant to trastuzumab, were also treated; each inhibitor alone decreased less than 25 % of cell growth, and the addition of trastuzumab to TKI treatment reduced these effects [Fig. 5.9 B].

Protein lysates of SKBR3 and SKBR3/Tr cells were prepared from cells treated for 24 hours with trastuzumab, NVP-AEW541 and BMS-536924. While trastuzumab treatment decreased phospho-Akt and phospho-MAPK levels in both cell lines, no change in levels of phosphoprotein were observed with either inhibitor alone [Fig. 5.10]. Combining trastuzumab with either NVP-AEW541 or BMS-536924 had a similar effect on phospho-Akt and phospho-MAPK levels to trastuzumab alone.
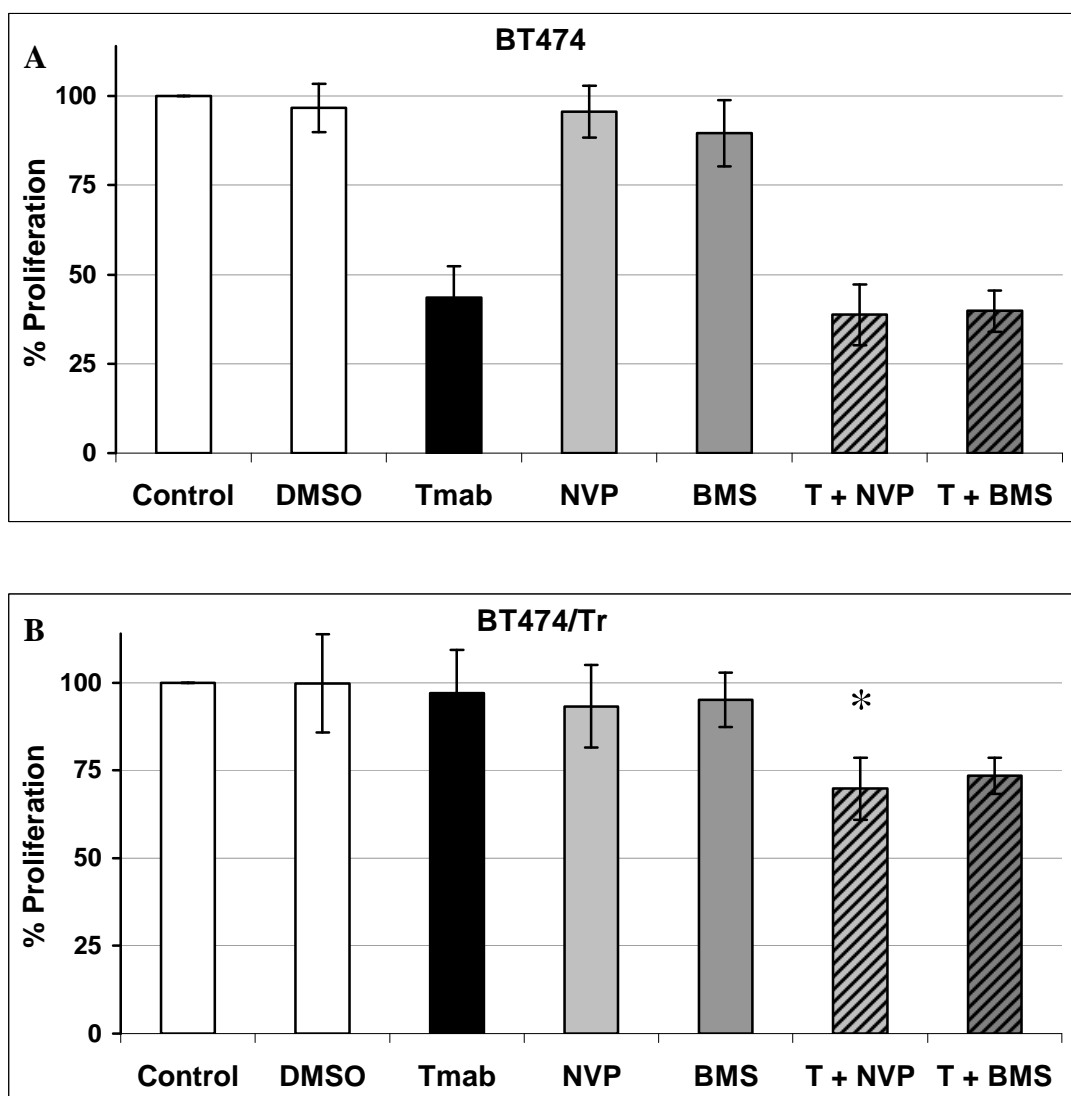
Figure 5.7 Proliferation of **A.** BT474 and **B.** BT474/Tr cells treated with and without trastuzumab (Tmab, T) (100 nM) and IGF-IR TKIs NVP-AEW541 (NVP) (1 μM) and BMS-536924 (BMS) (1 μM). Cells were grown in 2 % serum, and proliferation was measured after five days by the acid phosphatase method. Percent proliferation is expressed relative to untreated control. DMSO-containing media was included as a control. Student's t-test was performed to determine significance of the difference in response to treatment: * denotes $p < 0.05$ when comparing combined treatment with trastuzumab alone. Error bars represent standard deviation of triplicate experiments.
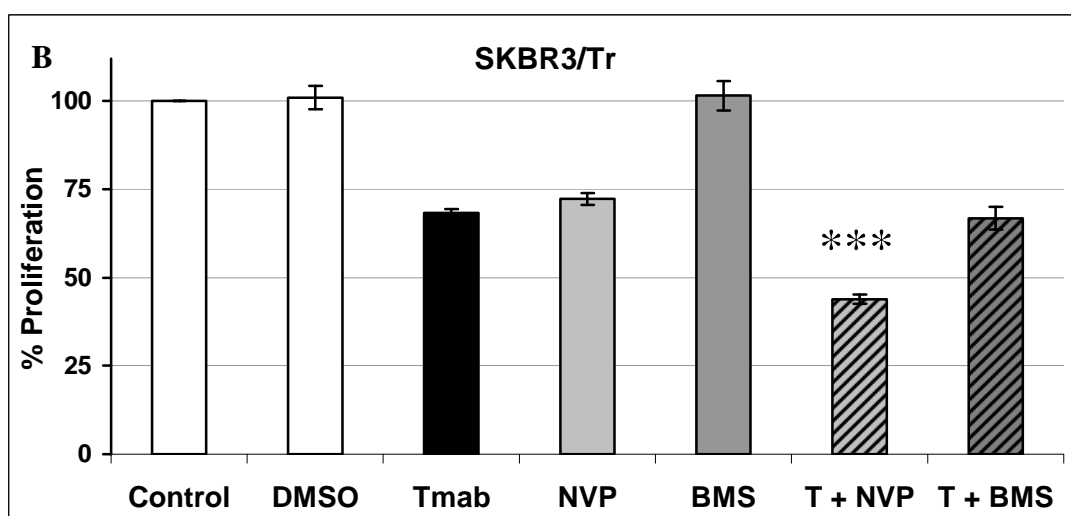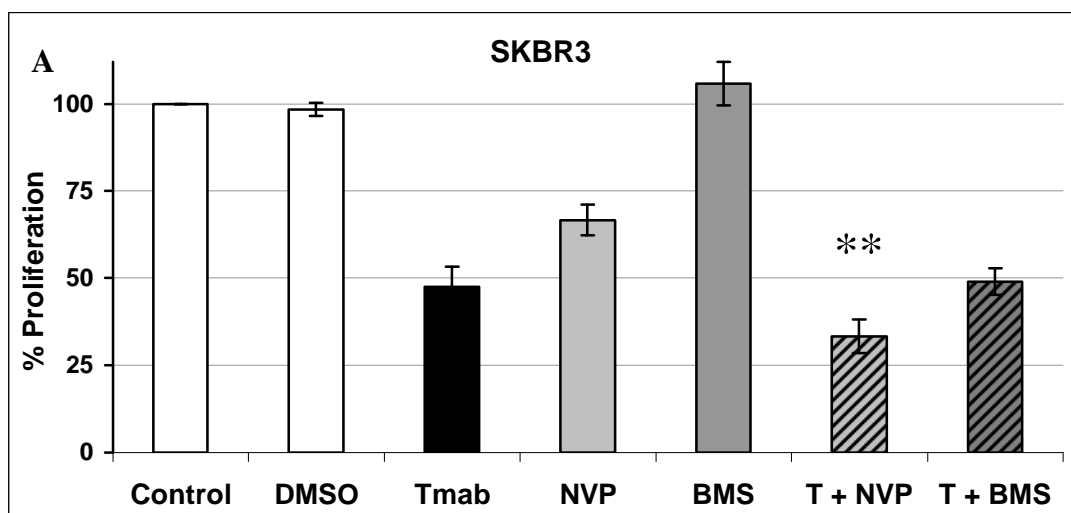
Figure 5.8 Proliferation of **A.** SKBR3 and **B.** SKBR3/Tr cells treated with and without trastuzumab (Tmab, T) (100 nM) and IGF-IR TKIs NVP-AEW541 (NVP) (1 µM) and BMS-536924 (BMS) (1 µM). Cells were grown in 2 % serum, and proliferation was measured after five days by the acid phosphatase method. Percent proliferation is expressed relative to untreated control. DMSO-containing media was included as a control. Student's t-test was performed to determine significance of the difference in response to treatment: ** denotes $p < 0.01$; *** denotes $p < 0.001$ when comparing combined treatment with trastuzumab alone. Error bars represent standard deviation of triplicate experiments.

_____

Figure 5.9 Proliferation of **A.** MCF7 and **B.** MCF7-HER2 cells treated with and without trastuzumab (Tmab, T) (100 nM) and IGF-IR TKIs NVP-AEW541 (NVP) (1 µM) and BMS-536924 (BMS) (1 µM). Cells were grown in 2 % serum, and proliferation was measured after five days by the acid phosphatase method. Percent proliferation is expressed relative to untreated control. DMSO-containing media was included as a control. Error bars represent standard deviation of triplicate experiments.

_____

SKBR3

C T N B T+N T+B

SKBR3/Tr

C T N B T+N T+B

pMAPK

MAPK

pAkt

Akt

a-tubulin
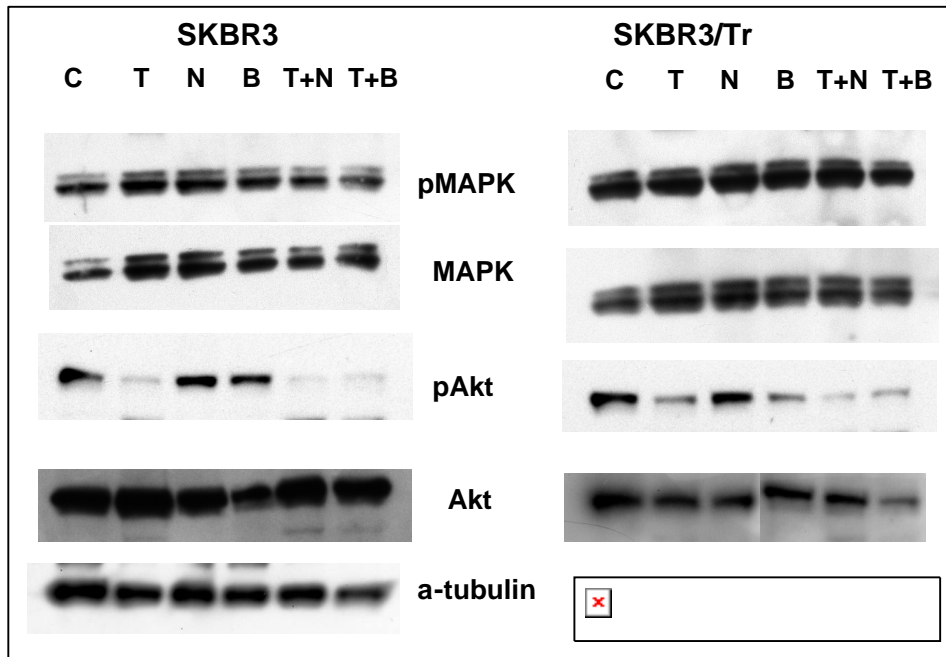
Figure 5.10 Western blot of MAPK, phospho-MAPK, Akt and phosho-Akt expression in SKBR3 and SKBR3/Tr cells that were untreated (C) or treated with trastuzumab (100 nM) (T), NVP-AEW541 (1 µM) (N), BMS-536924 (1 µM) (B), or combined trastuzumab plus NVP-AEW541 or BMS-536924, in 2 % serum for 24 hours. a-tubulin was used as a loading control.

5.3.2 NVP-AEW541 induces cell cycle arrest in trastuzumab-resistant cells

The effects of NVP-AEW541 on cell cycle progression were investigated in SKBR3 and SKBR3/Tr cells [Figs. 5.11 – 5.13]. While NVP-AEW541 alone had no significant effect on cell cycle progression in SKBR3 cells, treatment of SKBR3/Tr cells with NVP-AEW541 significantly increased the percentage of cells in the G1 (Gap 1) phase of the cell cycle (p = 0.040) [Fig. 5.11]. Trastuzumab induces G1 arrest, and this was demonstrated in SKBR3 (p = 0.019), and to a lesser extent, in SKBR3/Tr (p = 0.040) cells. NVP-AEW541 also increased the number of cells in G1 in both cell lines, and this effect was statistically significant in SKBR3/Tr cells (p = 0.040). The combination of trastuzumab and NVP-AEW541significantly increased the percentage of cell in G1 in both cells (SKBR3, p = 0.023; SKBR3/Tr, p = 0.006, compared to DMSO control). The combination had a greater effect than either treatment alone in SKBR3/Tr cells; however, this effect did not reach statistical significance (p = 0.106).

While single agent treatment had no significant effect on the number of cells in the synthesis (S) phase of the cell cycle, the combined treatment significantly decreased the proportion of cells in S phase in both SKBR3 and SKBR3/Tr cells (SKBR3, p = 0.039; SKBR3/Tr, p = 0.016, compared to DMSO control).
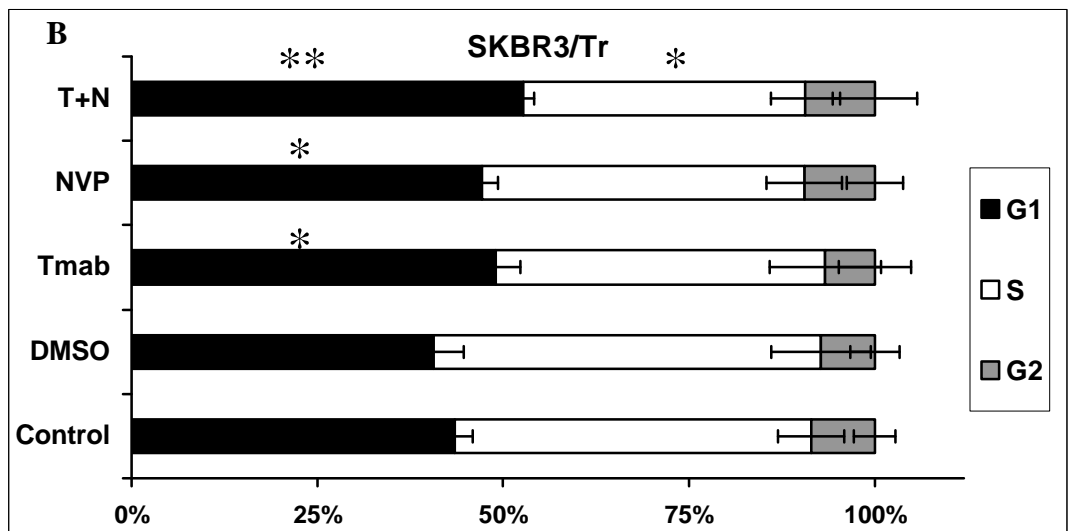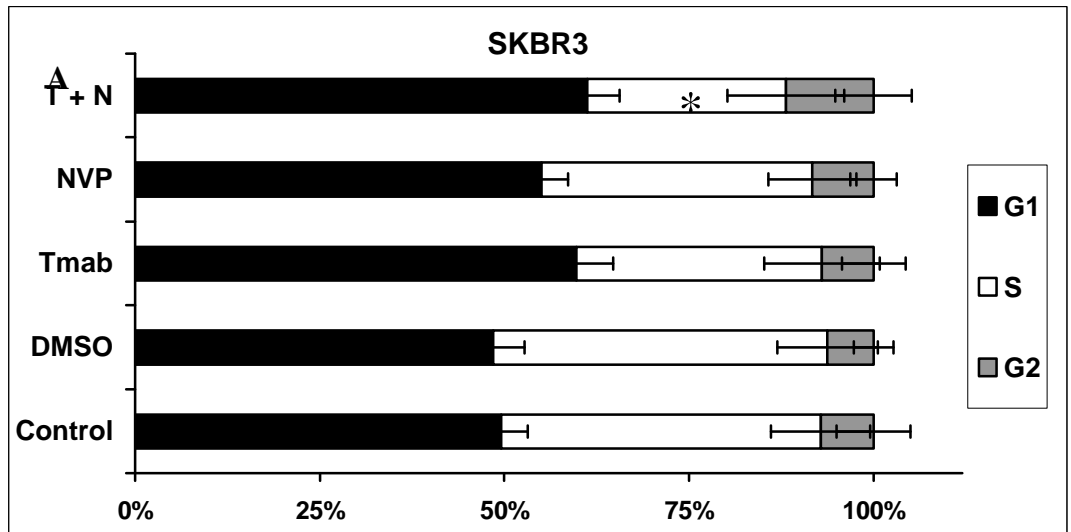
Figure 5.11 Percentage of diploid cells in G1, G2 and S phases of the cell cycle in **A.** SKBR3 and **B.** SKBR3/Tr cells. Cells were treated with trastuzumab (Tmab, T) (100 nM) and IGF-IR TKI NVP-AEW541 (NVP, N) (1 µM), alone and in combination. Cells were grown in 2 % serum, and were fixed after three days. Cell cycle analysis was performed using the Guava EasyCyte. Student's t-test was performed to determine significance: * denotes $p < 0.05$; ** denotes $p < 0.01$, when comparing combined treatment with control or DMSO control. Error bars represent standard deviation of triplicate experiments.
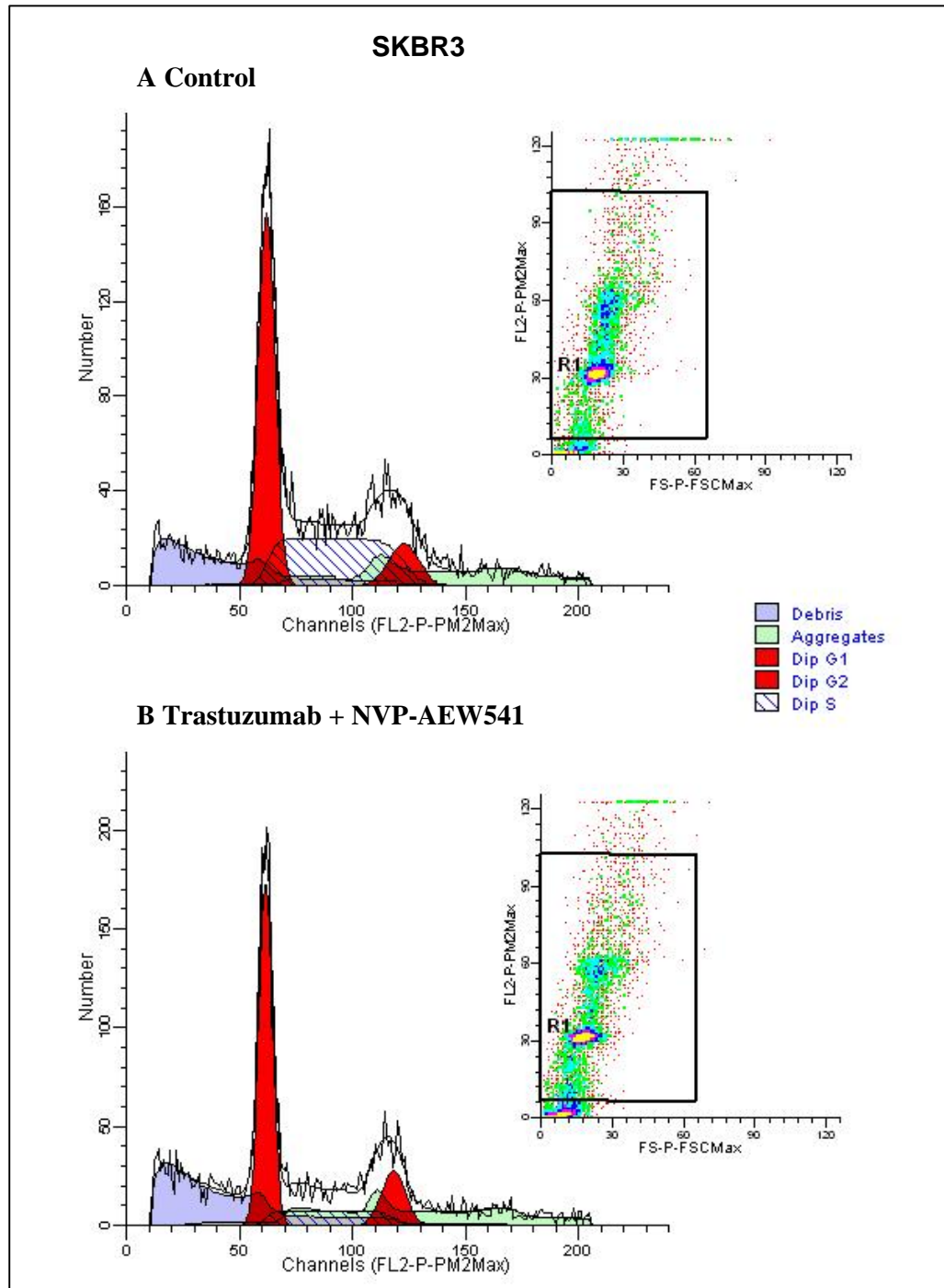
Figure 5.12 Sample graphs of **A.** control and **B.** trastuzumab (100 nM) + NVP-AEW541 (1 µM) treated SKBR3 cells analysed using ModFit software. This software calculates numbers of diploid (Dip) cells in G1, G2 and S phases of the cell cycle, as well as cell debris and cell aggregates.
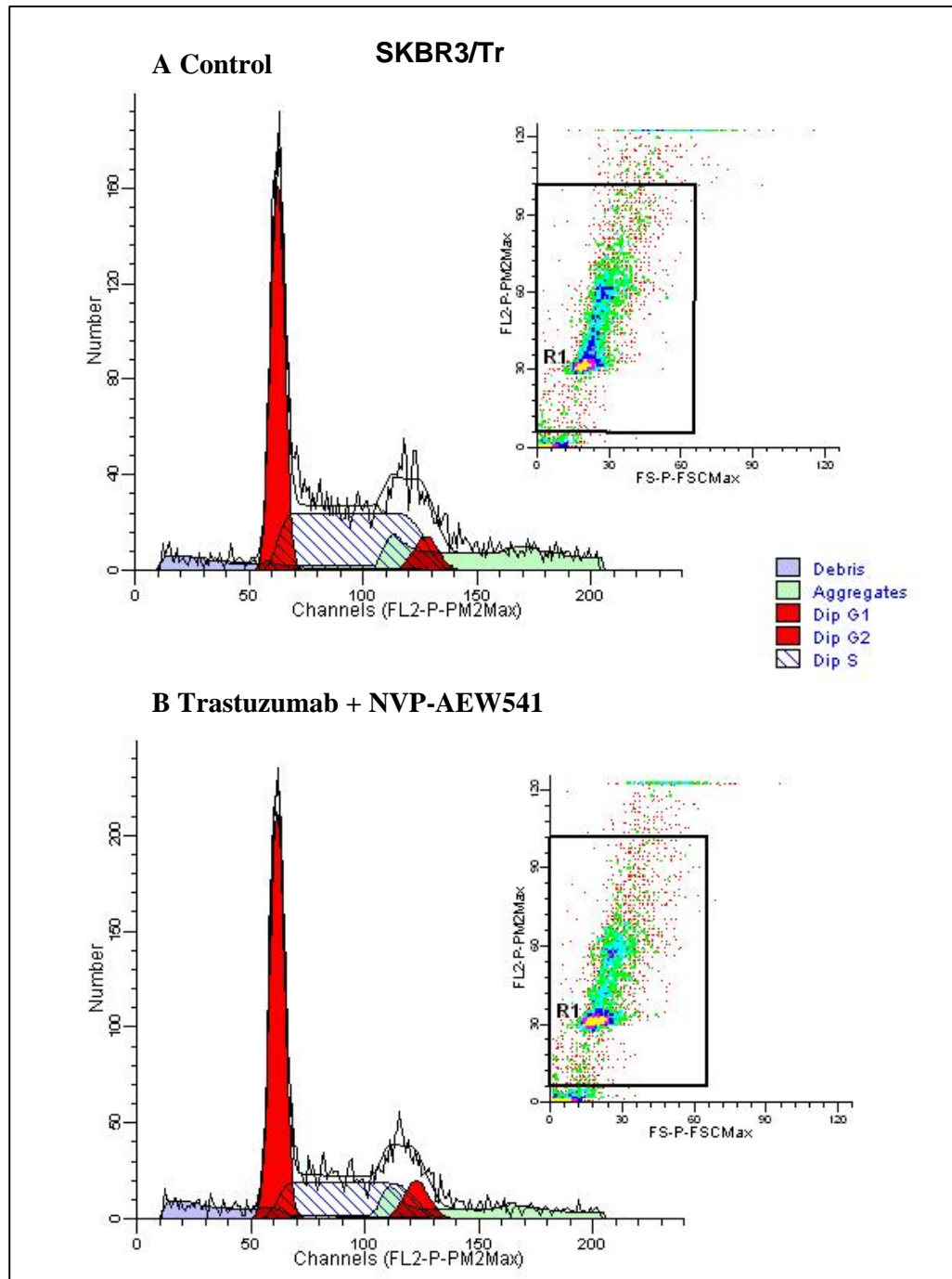
Figure 5.13 Sample graphs of **A.** control and **B.** trastuzumab (100 nM) and NVP-AEW541 (1 µM) treated SKBR3/Tr cells analysed using ModFit software. This software calculates numbers of diploid (Dip) cells in G1, G2 and S phases of the cell cycle, as well as cell debris and cell aggregates.

_____

Chapter 6

DEVELOPMENT AND CHARACTERISATION OF LAPATINIB- AND TRASTUZUMAB- CONDITIONED CELLS

6.1 DEVELOPMENT OF TRASTUZUMAB- AND LAPATINIB-CONDITIONED CELLS

SKBR3 cells, which are sensitive to trastuzumab, and SKBR3/Tr and HCC1419 cells, which are both relatively resistant to trastuzumab, were chosen to be conditioned in lapatinib-containing media. Lapatinib dose-response assays were performed in order to choose concentrations of lapatinib that inhibit approximately 70 – 80 % of cell growth [Fig. 4.9. and Fig. 6.1]. SKBR3 cells were also conditioned in media containing trastuzumab, and media containing trastuzumab and lapatinib. Table 6.1 shows the concentrations used to condition each cell line, and the names assigned for each new conditioned cell line. After four weeks of treatment, SKBR3-L and SKBR3-TL cells had visibly altered morphology compared to parental SKBR3 cells; however, by six months, the conditioned cells resembled the parental cells once again [Fig. 6.2].
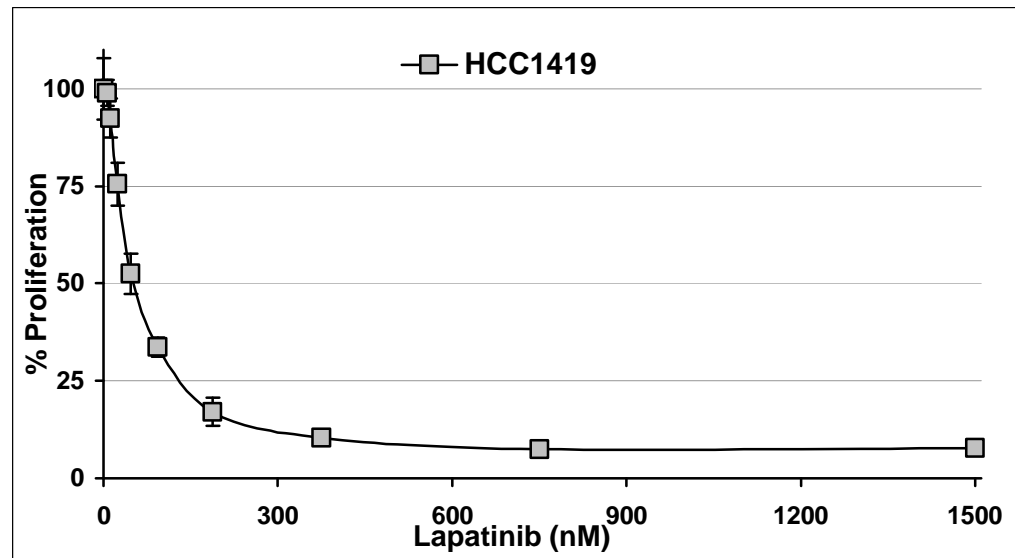
Figure 6.1 Proliferation of HCC1419 resistant cells treated with increasing doses of lapatinib. Proliferation was measured after five days by the acid phosphatase method and is expressed relative to untreated control. These results are from a single experiment.

_____

Table 6.1 List of parental and conditioned cell lines and the treatment in which they were conditioned for six months. The concentration of lapatinib in SKBR3-L cells was increased from 200 nM to 250 nM after two months of exposure.

Parent cell line	Conditioned cell line	Treatment
SKBR3	SKBR3	-
	SKBR3-T	Trastuzumab 10 ug/ml
	SKBR3-L	Lapatinib 200-250 nM
	SKBR3-TL	T 5 ug/ml + L 100 nM
SKBR3/Tr	SKBR3/Tr	-
	SKBR3/Tr-L	Lapatinib 400 nM
HCC1419	HCC1419	-
	HCC1419-L	Lapatinib 250 nM

_____
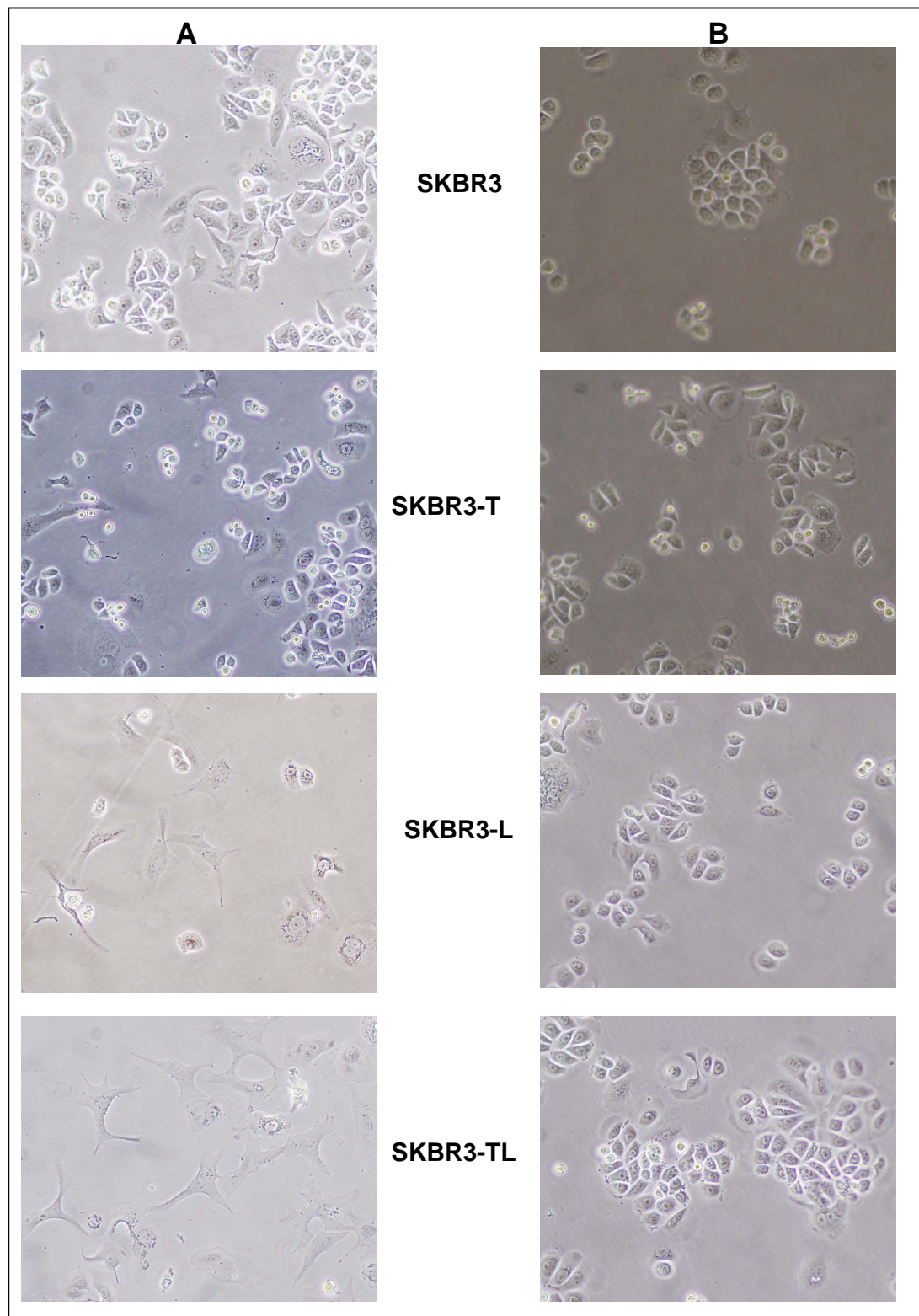
Figure 6.2 Images (100x) of SKBR3, SKBR3-T, SKBR3-L and SKBR3-TL cells after **A.** one month, and **B.** six months of conditioning.
_____

6.2 TRASTUZUMAB- AND LAPATINIB-CONDITIONED SKBR3 CELLS ARE MORE RESISTANT TO TRASTUZUMAB AND LAPATINIB

6.2.1 Proliferation assays

After six months of conditioning, SKBR3-T, SKBR3-L and SKBR3-TL were significantly more resistant to trastuzumab than parental SKBR3 cells [Fig. 6.3]. SKBR3/Tr-L cells also had significantly reduced response to trastuzumab compared to SKBR3/Tr cells [Fig. 6.3].

SKBR3-L, SKBR3-TL and SKBR3/Tr-L cells were also significantly more resistant to inhibition by lapatinib than the parental cells [Fig. 6.3 and Fig. 6.4]. Exposure of SKBR3 cells to trastuzumab alone (SKBR3-T) did not result in resistance to lapatinib.

The combination of lapatinib and trastuzumab treatment in SKBR3 cells inhibits significantly more growth than either treatment alone (T-test comparing combination versus lapatinib alone, $p = 0.0083$). SKBR3-TL cells showed significantly reduced response to the combination compared to parental SKBR3 cells (T-test, $p = 0.0035$), and the combination treatment did not improve response compared to either treatment alone in these cells [Fig. 6.5].

After six months of conditioning, SKBR3, SKBR3-T, SKBR3-L and SKBR3-TL cells were frozen in liquid nitrogen and thawed one month later. After one further month of growth, the stability of resistance was investigated by repeating proliferation assays with trastuzumab and lapatinib treatments. Each cell line showed a similar response to previous results [Fig. 6.6].
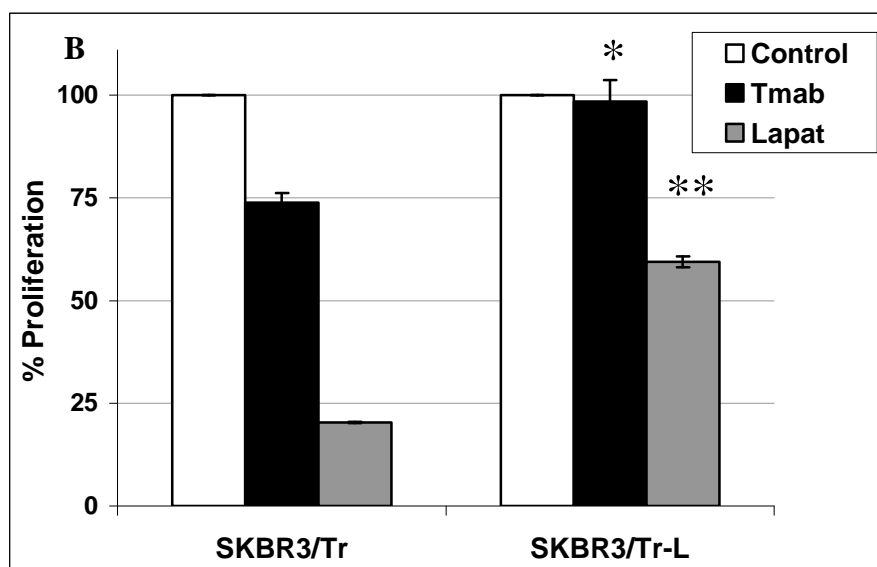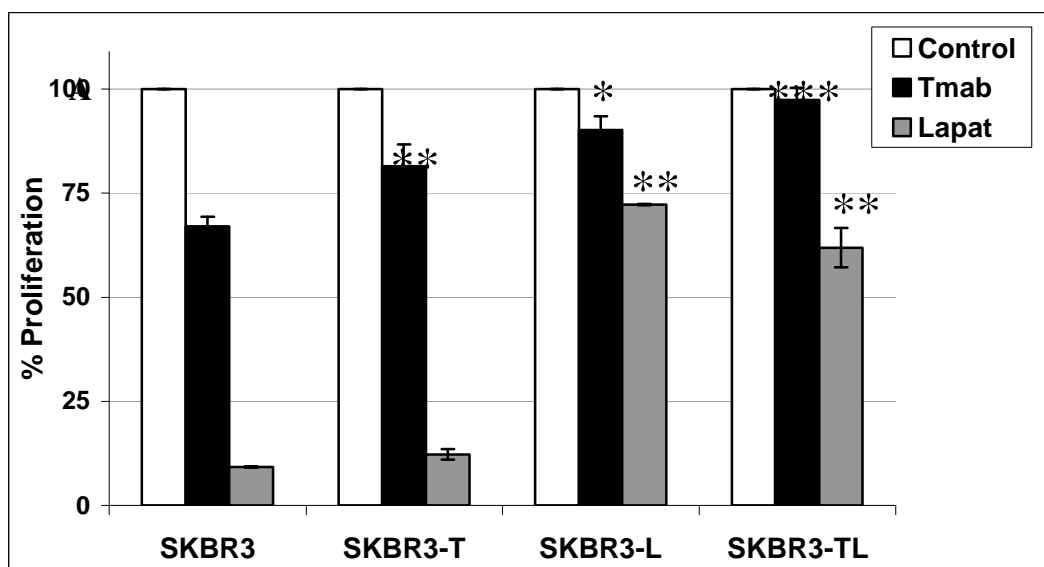
Figure 6.3 Proliferation of conditioned **A.** SKBR3 cells and **B.** SKBR3/Tr cells treated with trastuzumab (Tmab) (100 nM) and lapatinib (Lapat) (1 μM). Proliferation was measured after five days by the acid phosphatase method and is expressed relative to untreated control. Student's t-test was performed to determine significance of the difference in response to treatment: * denotes $p < 0.05$; ** denotes $p < 0.01$; *** denotes $p < 0.001$ when comparing response in conditioned cells with response in parental cells. Error bars represent standard deviation of triplicate experiments.
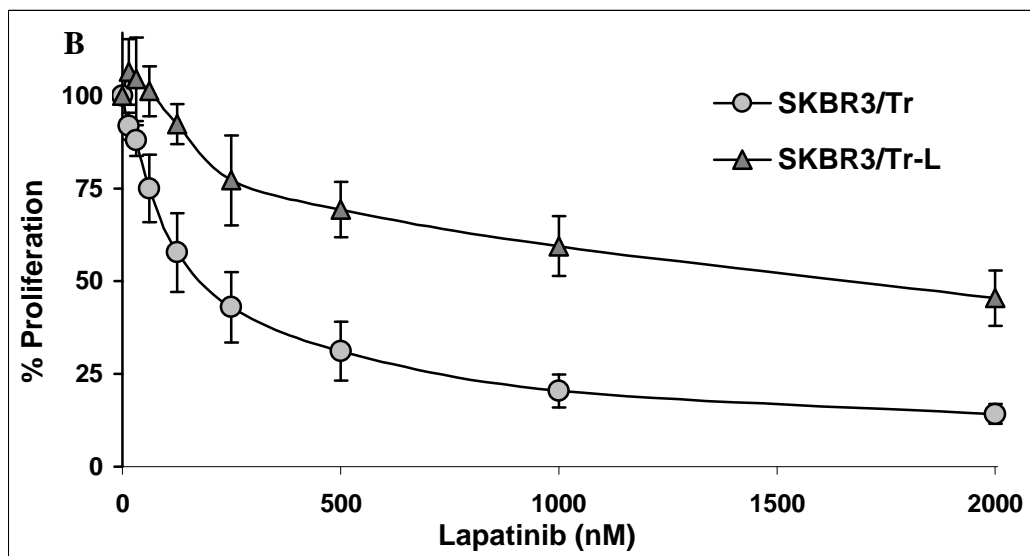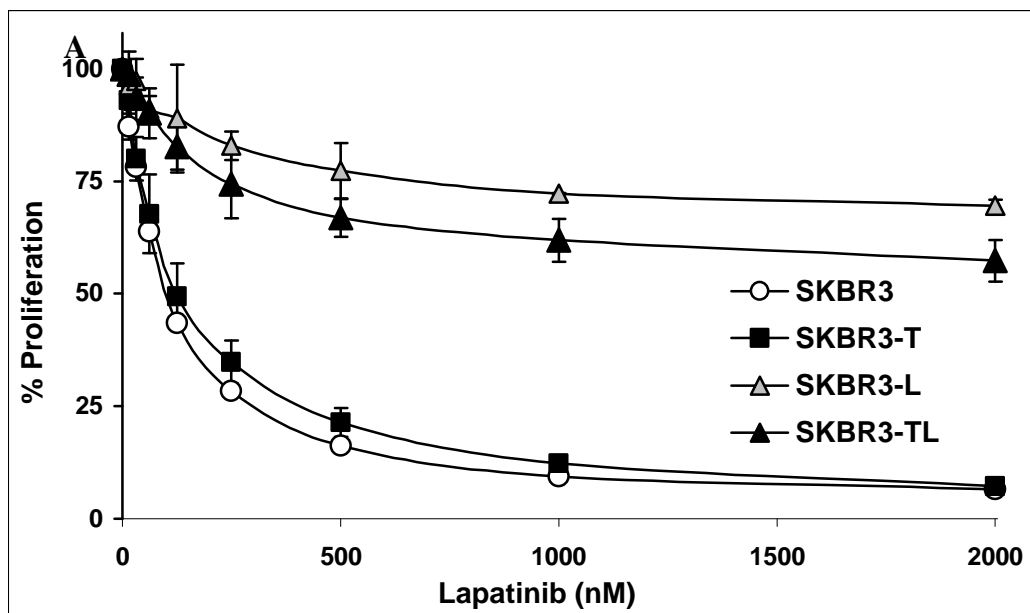
Figure 6.4 Proliferation of conditioned **A.** SKBR3 cells and **B.** SKBR3/Tr cells treated with increasing concentrations of lapatinib. Proliferation was measured after five days by the acid phosphatase method and is expressed relative to untreated control. Error bars represent standard deviation of triplicate experiments.
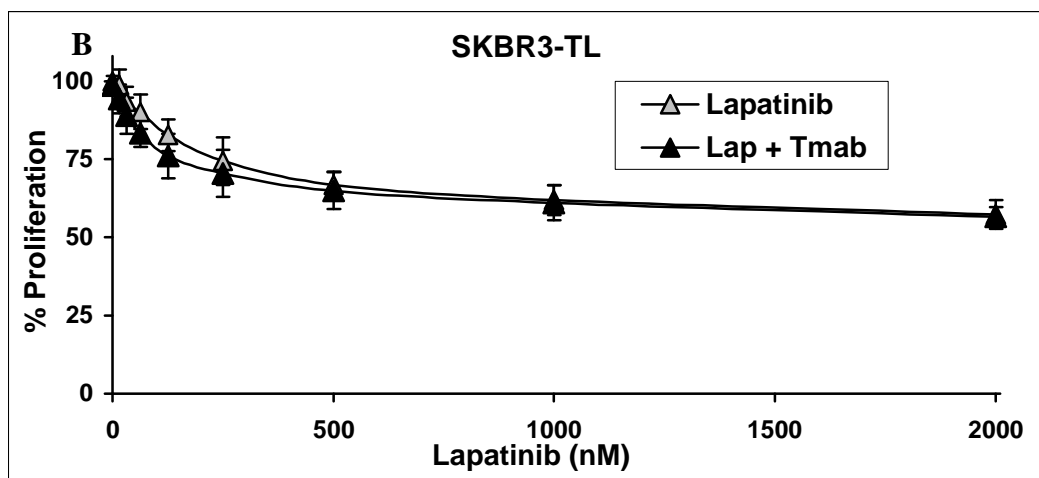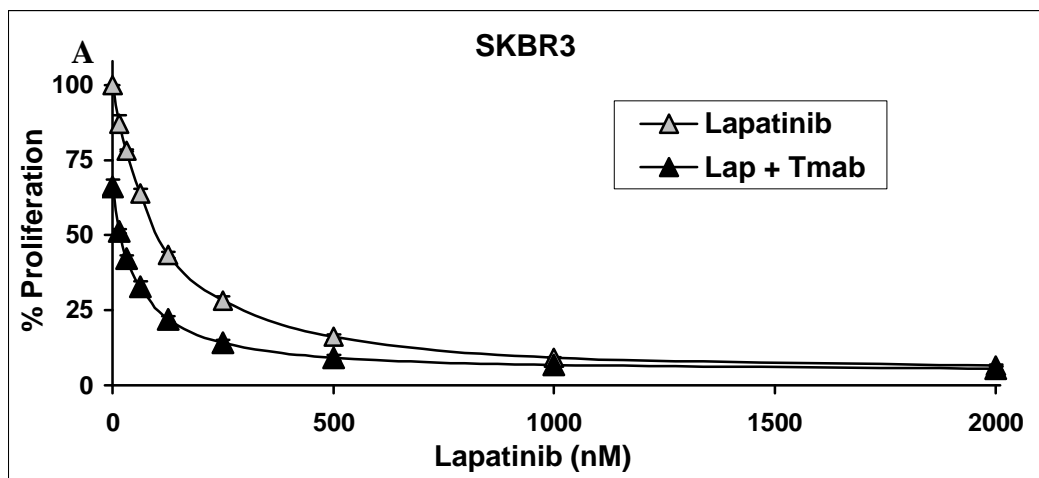
Figure 6.5 Proliferation of **A.** SKBR3 cells and **B.** SKBR3-TL cells treated with a combination of trastuzumab (Tmab) (100 nM) and increasing concentrations of lapatinib (Lap). Proliferation was measured after five days by the acid phosphatase method and is expressed relative to untreated control. Error bars represent standard deviation of triplicate experiments.
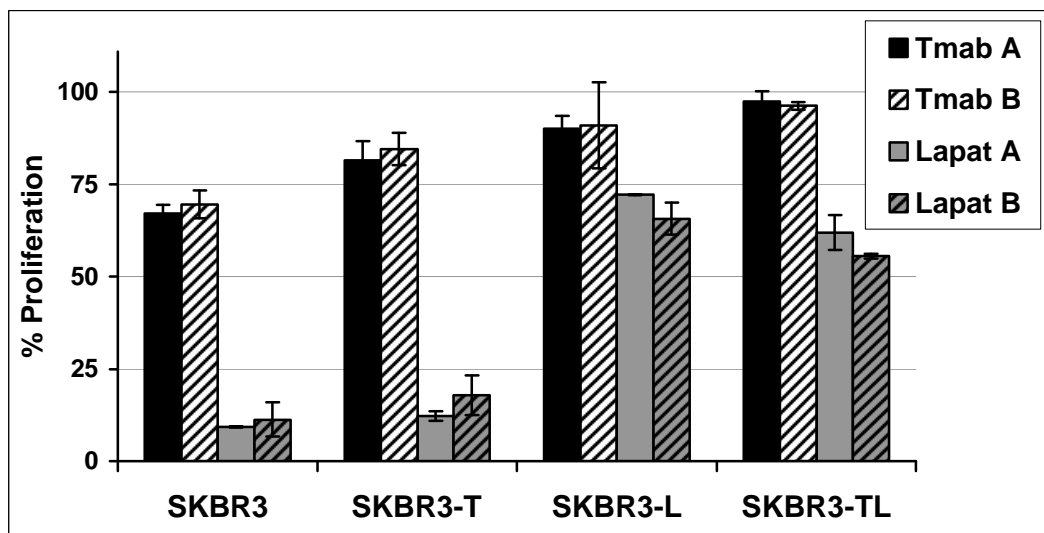
Figure 6.6 Proliferation of conditioned SKBR3 cells treated with trastuzumab (Tmab) (100 nM) or lapatinib (Lapat) (1 µM) before (A) and after (B) freeze-thawing of cells. Proliferation was measured after five days by the acid phosphatase method and is expressed relative to untreated control. Error bars represent standard deviation of triplicate experiments.

_____

6.2.2 Doubling time assays

Twenty-four-well plate assays were used to investigate cell growth rate over seven days with and without trastuzumab or lapatinib treatment of SKBR3, SKBR3-T, SKBR3-L and SKBR3-TL cells. Cell doubling times were determined for each cell line, and the alteration in growth rate caused by each treatment was calculated. Trastuzumab treatment significantly slowed the growth rate of SKBR3 cells only (p = 0.0006) [Fig. 6.7 and Table 6.2]. Lapatinib treatment significantly slowed the growth rate of both SKBR3 and SKBR3-T cells (SKBR3, p = 0.0037; SKBR3-T, p = 0.0010), while it did not affect the rate of proliferation of the two lapatinib-conditioned SKBR3-L and SKBR3-TL cells [Fig. 6.8 and Table 6.2].
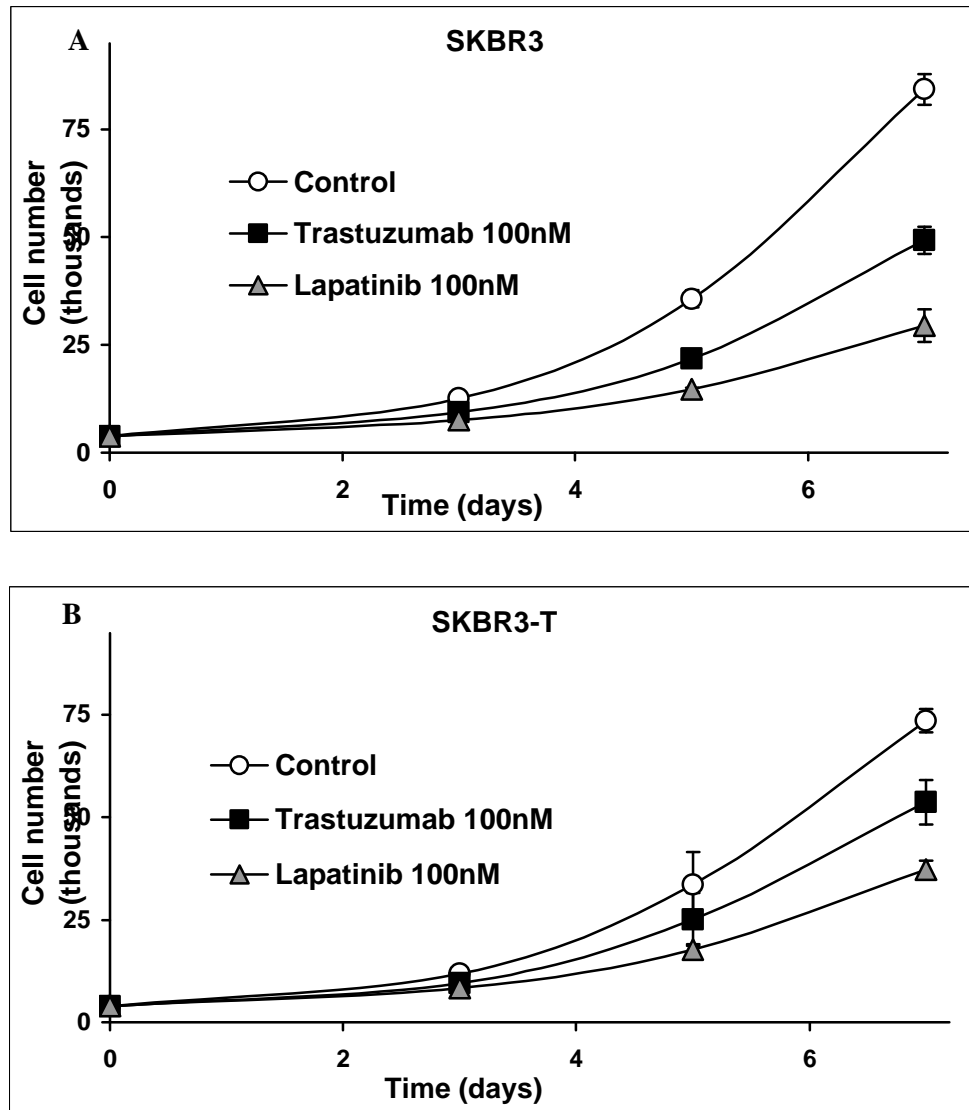
Figure 6.7 Proliferation of **A.** SKBR3 cells and **B.** SKBR3-T cells treated with trastuzumab or lapatinib for 7 days. Cells were plated in 24-well plates and proliferation was measured at days 3, 5 and 7 by cell counting. Error bars represent standard deviation of triplicate experiments.

_____
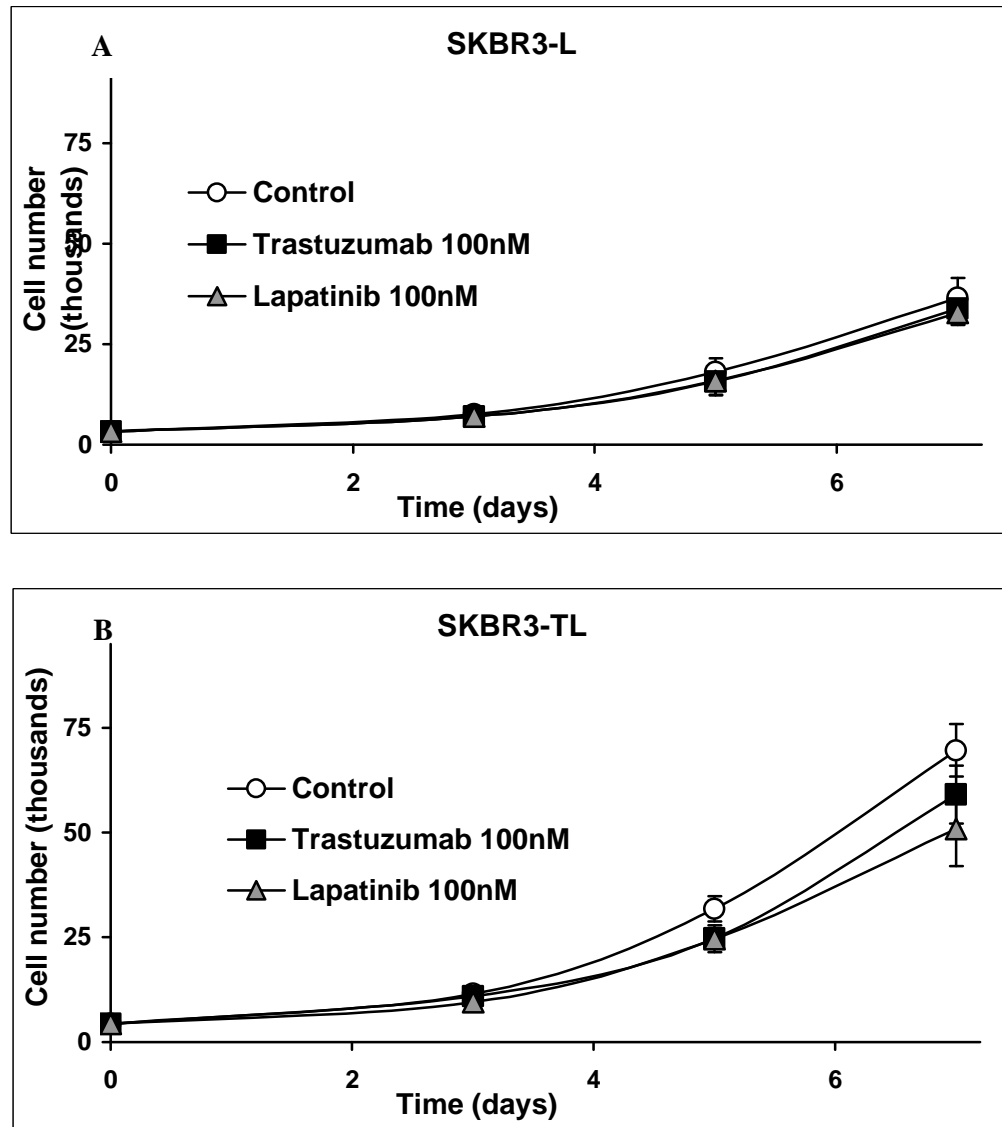
Figure 6.8 Proliferation of **A.** SKBR3-L cells and **B.** SKBR3-TL cells treated with trastuzumab or lapatinib for 7 days. Cells were plated in 24-well plates and proliferation was measured at days 3, 5 and 7 by cell counting. Error bars represent standard deviation of triplicate experiments.

_____

138

Table 6.2 Doubling times (hours) of conditioned SKBR3 cells with and without trastuzumab (Tmab) (100 nM) or lapatinib (Lap) (100 nM) treatment. ($\pm$ standard deviation of triplicate experiments). Student's t-test was performed to determine significance of the response to treatment: ** denotes $p < 0.01$; *** denotes $p < 0.001$ when comparing doubling time in treated compared to untreated cells. The growth rate of each was calculated relative to untreated parental SKBR3 cells.

		Control	**Tmab**	**Lap**
SKBR3	Doubling time (hrs)	35.0 ± 0.6	40.0 ± 0.4 ***	44.7 ± 1.5 **
	Growth rate (%)	*100.0*	*87.5*	*78.3*
SKBR3-T	Doubling time (hrs)	36.6 ± 1.3	38.7 ± 1.9	44.6 ± 2.0 **
	Growth rate (%)	*95.8*	*90.5*	*78.6*
SKBR3-L	Doubling time (hrs)	43.3 ± 7.4	42.5 ± 3.9	43.5 ± 3.1
	Growth rate (%)	*80.9*	*82.4*	*80.6*
SKBR3-TL	Doubling time (hrs)	37.1 ± 3.8	39.6 ± 3.1	39.5 ± 4.6
	Growth rate (%)	*94.5*	*88.5*	*88.7*

6.3   LAPATINIB-CONDITIONED HCC1419 CELLS REMAIN SENSITIVE TO LAPATINIB

After six months of conditioning HCC1419 cells in lapatinib-containing media, lapatinib treatment was discontinued and the cells were grown in growth media without lapatinib. However, HCC1419-L cells did not actively proliferate for over three months. After three months, their growth rate began to increase, and at six months, a sufficient number of cells were available to perform a proliferation assay. HCC1419-L cells were equally sensitive to both trastuzumab and lapatinib as parental HCC1419 cells [Fig. 6.9].
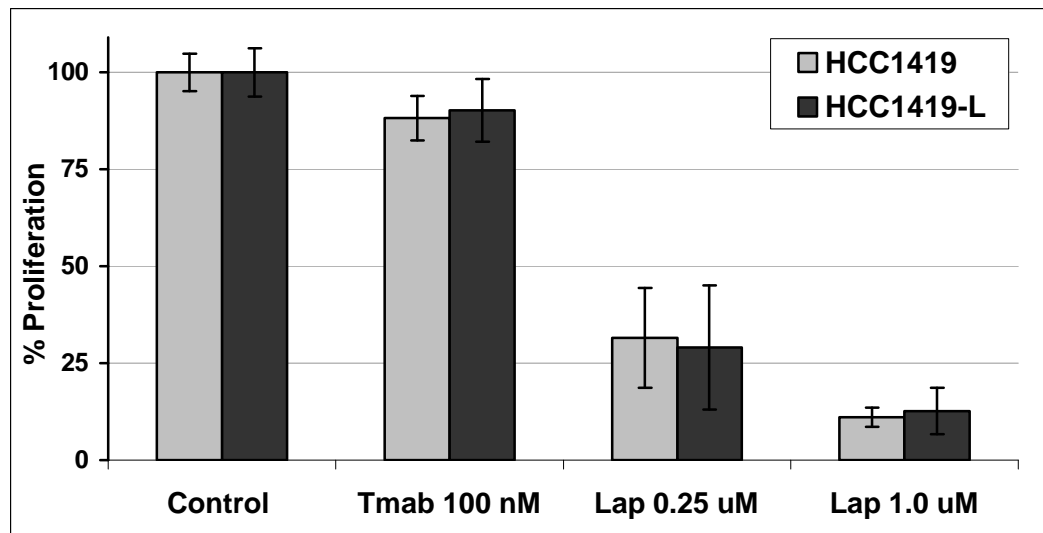
Figure 6.9 Proliferation of parental HCC1419 and lapatinib-conditioned HCC1419-L cells treated with trastuzumab (Tmab) (100 nM) and lapatinib (Lap) (0.25 µm and 1 µM). Proliferation was measured after 5 days and is expressed relative to untreated control. Error bars represent standard deviation of replicate wells in a single experiment.

6.4.1 HER-2, pHER-2, EGFR AND Pgp expression

HER-2, EGFR and phosphorylated HER-2, levels were determined by western blotting in conditioned SKBR3 and SKBR3/Tr cells. HER-2, phospho-HER-2 and EGFR levels were not significantly altered in any conditioned SKBR3 cells. However, SKBR3/Tr-L cells appear to have higher levels of HER-2 phosphorylation compared to SKBR3/Tr cells [Fig. 6.10 A]. IGF-IR and P-glycoprotein (Pgp) expression levels were also measured in the conditioned SKBR3 cells. Pgp levels were undetectable in each of the cell lines. IGF-IR expression was elevated in SKBR3-T, SKBR3-L and SKBR3-TL cells compared to parental SKBR3 cells [Fig. 6.10 B].
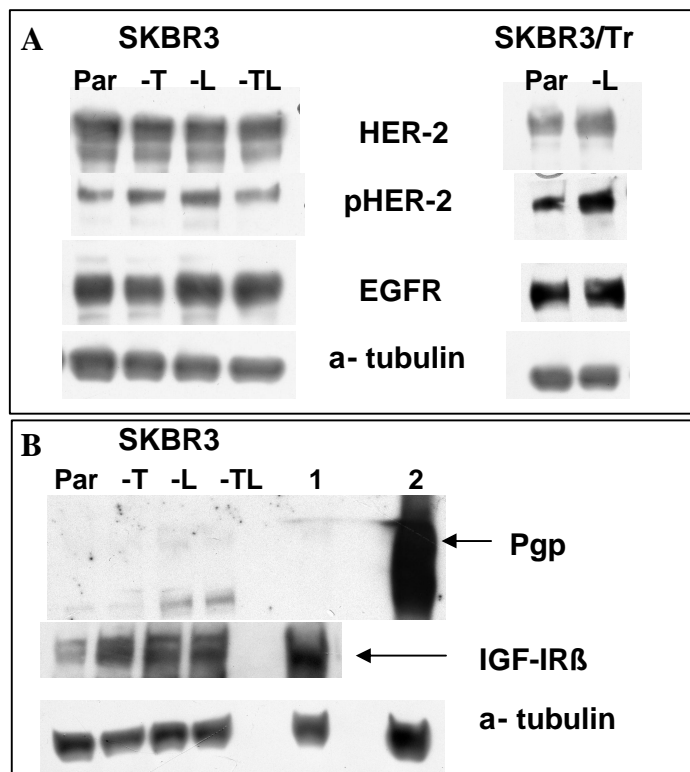
Figure 6.10 **A.** Western blot of HER-2, phospho-HER-2 and EGFR protein expression in parental SKBR3 (par), and SKBR3-T, SKBR3-L, SKBR3-TL cells, and parental and lapatinib conditioned SKBR3/Tr and SKBR3/Tr-L cells. **B.** Western blot of IGF-IR and Pgp in parental SKBR3 (par), and SKBR3-T, SKBR3-L, SKBR3-TL cells T47D (1) and DLKP-A (2) cell lysates were used as positive controls for IGF-IR and Pgp, respectively. a-tubulin was used as a loading control in each western blot.

6.4.2 Akt and MAPK signalling in SKBR3-L cells

As SKBR3-L cells were most resistant to both lapatinib and trastuzumab, this cell line was chosen for further analysis to study the mechanisms of resistance. Phosphorylation of Akt and MAPK was assessed in the SKBR3-L cells compared to the parental SKBR3 cells. Phospho-MAPK levels were slightly elevated in SKBR3-L cells compared to parental SKBR3 cells while phospho-Akt levels were unchanged in the SKBR3-L cells [Fig. 6.11].

_____
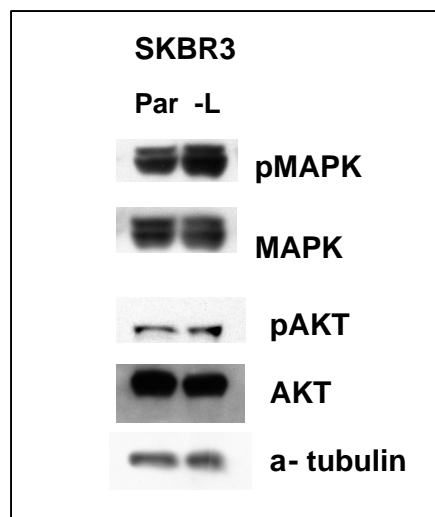
Figure 6.11   Western blot of phospho-MAPK, MAPK, phospho-Akt and Akt in parental SKBR3 (par) and SKBR3-L (-L) cells. a-tubulin was used as a loading control in each western blot.
_____

6.4.3 Response to trastuzumab and lapatinib in SKBR3-L cells

Protein lysates from SKBR3 and SKBR3-L cells were prepared in order to characterise alterations in phosphoprotein signalling in response to trastuzumab and lapatinib treatment. Trastuzumab treatment (5 µg/ml and 10 µg/ml) induced phosphorylation of HER-2 in both SKBR3 and SKBR3-L cells [Fig. 6.12]. Lapatinib treatment (1 µM) decreased phospho-HER-2 levels in both SKBR3 and SKBR3-L cells. While lapatinib slightly reduced EGFR levels in parental SKBR3 cells, EGFR levels were increased by lapatinib treatment in SKBR3-L cells [Fig. 6.12].
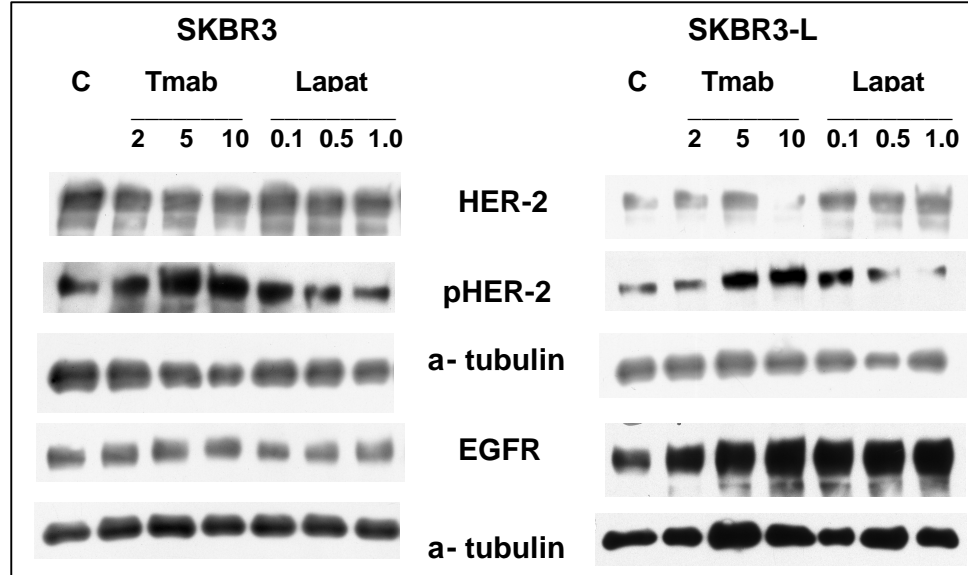
Figure 6.12 Western blot of HER-2, phospho-HER-2 and EGFR protein expression in SKBR3 and SKBR3-L cells untreated (C) or treated with trastuzumab (T) (2, 5 and 10 µg/ml) and lapatinib (L) (0.1, 0.5 and 1.0 µM). a-tubulin was used as a loading control in each western blot.

6.5 PHOSPHOPROTEOMIC ANALYSIS OF LAPATINIB-RESISTANCE

6.5.1 2-D DIGE analysis

Protein lysates were prepared from parental SKBR3 cells and SKBR3-L cells untreated and treated with trastuzumab (10 µg/ml) and lapatinib (1 µM). Phosphoprotein enrichment was performed, and the yield of phosphoprotein was approximately 10 % of total protein. Proteomic analysis was performed on the phosphoprotein samples as described in chapter 2 (section 2.13). 2,500 spots were detected on the DIGE gels, and each was assigned a unique ID number [Fig. 6.13]. The results of each set of replicate gels were analysed using the DeCyder differential in-gel analysis (DIA) module, and the difference in protein expression between two samples is expressed as fold-change. The DeCyder software produces 3-D images of protein abundance, and constructs graphs of relative protein abundance of each of the samples analysed [Fig. 6.14].
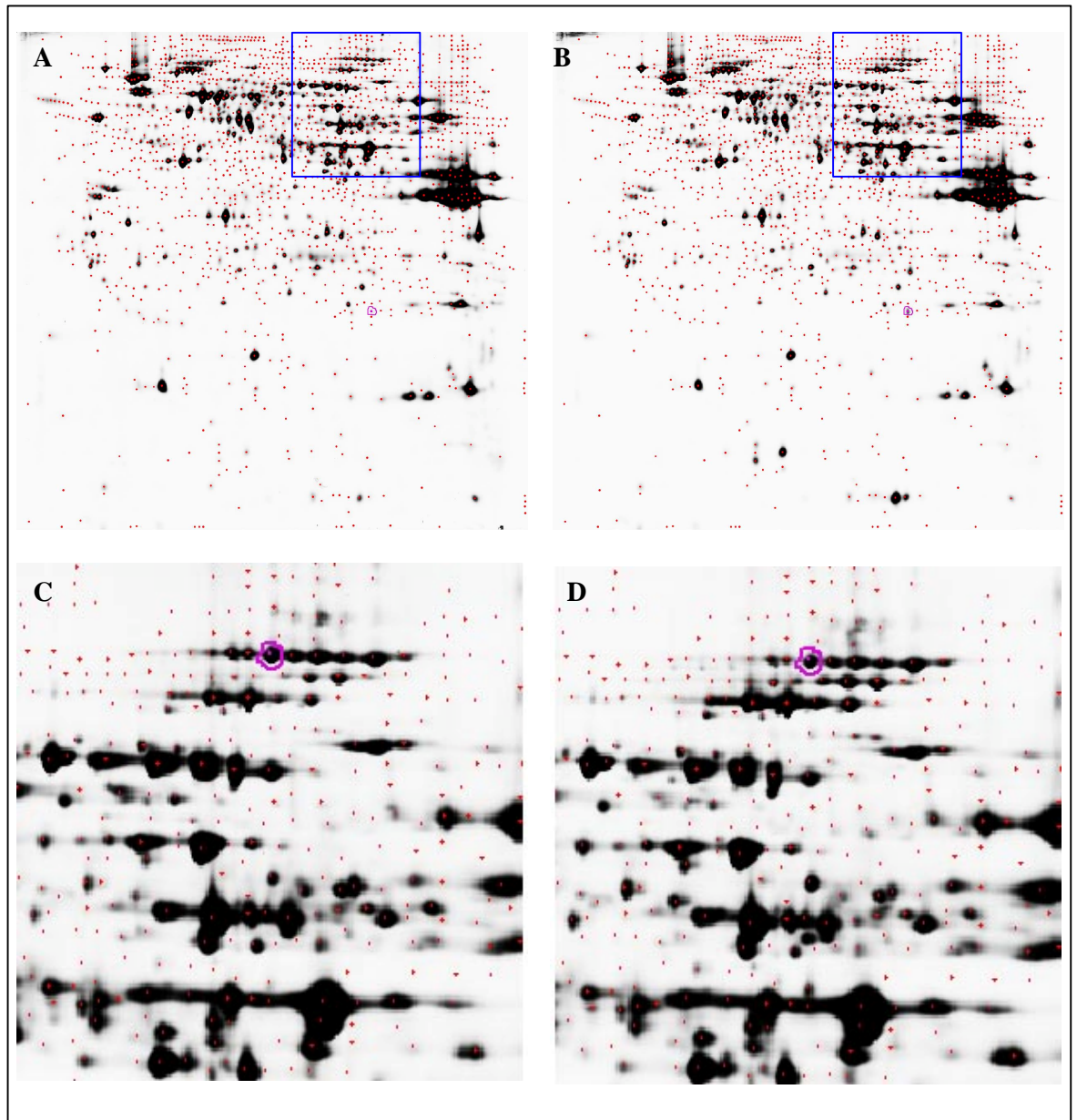
Figure 6.13 Example of DIGE gel pictures from Gel no. 1 scanned at different wavelengths to reveal spots from **A.** Cy3-labelled parental SKBR3 cells, **B.** Cy5-labelled SKBR3-L cells. The spots detected by the DeCyder software are marked with red dots. **C.** and **D.** are cropped pictures of A and B, respectively, focusing on the upper region of the gel, with the location of spot ID 350 circled.

_____
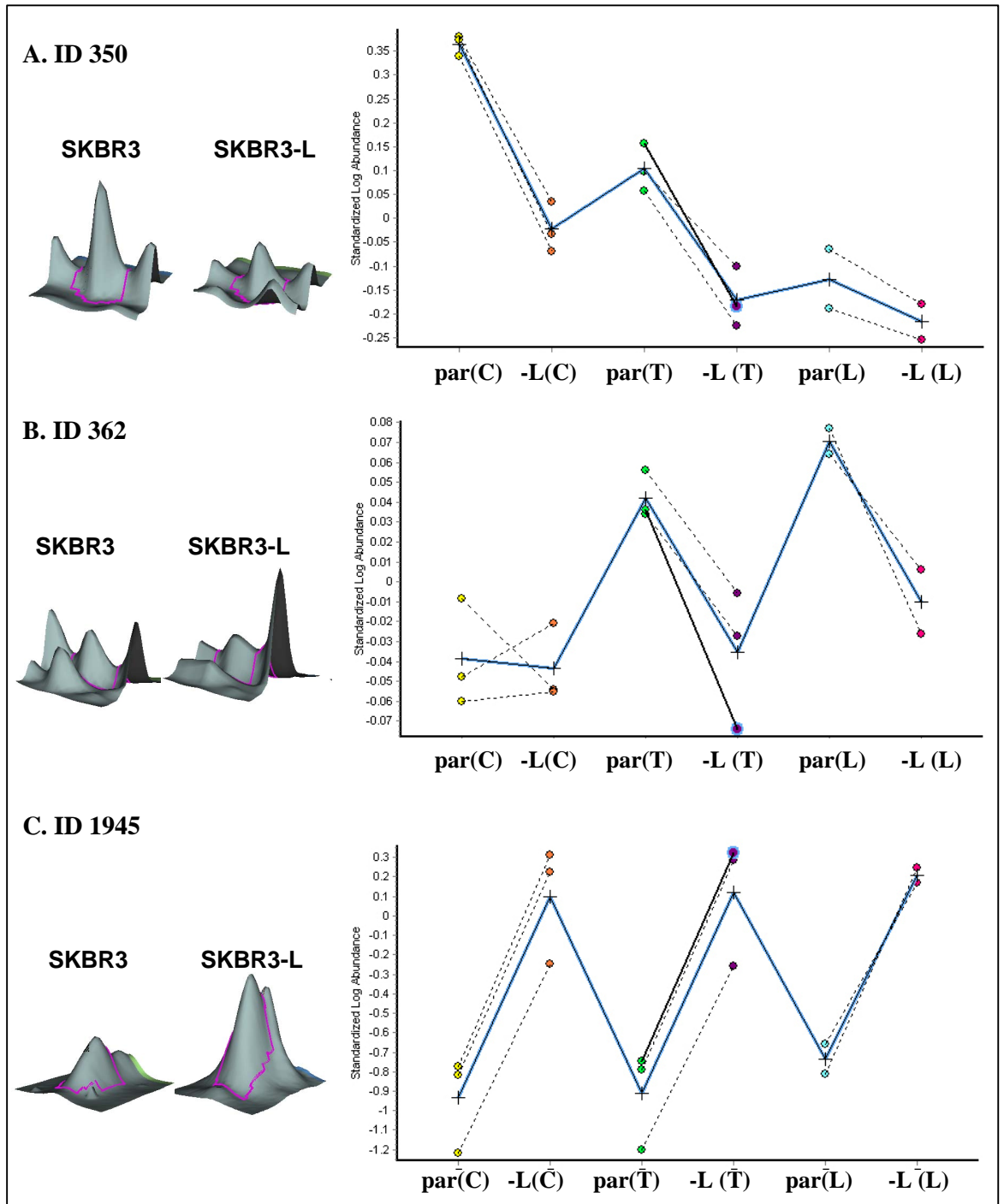
Figure 6.14 Examples of 3-D view of protein abundance in untreated SKBR3 ad SKBR3-L cells, and graphs of protein abundance in untreated (C), trastuzumab-treated (T) and lapatinib-treated (L) parental SKBR3 (par) and SKBR3-L cells, analysed by the DeCyder software. The solid line in the graph is the average of three replicate measurements (dotted lines) of protein abundance. **A.** ID no. 350, Eukaryotic translation elongation factor 2; **B.** ID no. 362, Eukaryotic translation elongation factor 2; **C.** ID no. 1945, aB-crystallin.

6.5.2 Phosphoprotein identification by MS

Of 2,500 spots detected on the DIGE gels, 81 spots were picked for identification by MALDI-ToF-MS. The DeCyder differential in-gel analysis (DIA) module analysed the difference in phosphoprotein levels between each set of two samples, and this difference is expressed as fold-change. Replicate results were analysed by ANOVA. Proteins which demonstrated a fold-change of = 1.2 and had an ANOVA p value = 0.05 were analysed. Student t-tests were also performed for the comparison of phosphoprotein levels in SKBR3-L compared to SKBR3 cells; proteins with a t-test p value = 0.05 were included in the analysis. A second cut-off of = 1.99-fold change was also applied to this comparison to select phosphoproteins with the greatest fold change.

The comparisons performed between SKBR3 and SKBR3-L cells with and without trastuzumab or lapatinib treatment are listed in Table 6.3 and the phosphoproteins identified are listed in Tables 6.4 - 6.11.

Table 6.3 Summary of the comparisons performed and displayed in Tables 6.4-6.11.

Comparison	Table
SKBR3-L versus SKBR3	Table 6.4 – 6.6
SKBR3 +/- trastuzumab	Table 6.7
SKBR3 +/- lapatinib	Table 6.8
SKBR3-L +/- trastuzumab	Table 6.9
SKBR3-L +/- lapatinib	Table 6.10
Trastuzumab treated SKBR3 versus SKBR3-L	Table 6.11
Lapatinib treated SKBR3 versus SKBR3-L	Table 6.12

Of the 81 phosphoproteins identified, 20 were significantly higher and 21 were significantly lower in SKBR3-L compared to parental SKBR3 cells [Tables 6.4 and 6.5]. Using a higher cut-off of = 1.99-fold difference combined with a significant T-test, 14 phosphoproteins which are significantly altered in SKBR3-L compared to parental SKBR3 cells were identified [Table 6.6].

In trastuzumab-treated (10 µg/ml) SKBR3 cells, levels of eight of the identified phosphoproteins were higher, while a further eight were lower in trastuzumab-treated compared to untreated SKBR3 cells [Table 6.7]. In lapatinib-treated (1 µM) SKBR3 cells, 11 identified phosphoproteins were upregulated, and 21 were downregulated compared to untreated SKBR3 cells [Table 6.8].

In SKBR3-L cells, eight identified phosphoproteins showed altered levels in trastuzumab-treated (10 µg/ml) compared to untreated cells: two were upregulated and six were downregulated [Table 6.9]. In lapatinib-treated (1 µM) SKBR3-L cells, 16 phosphoproteins were differentially regulated: four were upregulated and 12 were downregulated [Table 6.10].

Comparisons in response to each drug between SKBR3 and SKBR3-L were performed with the aid of Venn diagrams [Fig. 6.15]. Five phosphoproteins had altered levels in response to trastuzumab in both SKBR3 and SKBR3-L cells. However, 11 phosphoproteins had altered levels only in SKBR3 cells; these proteins may mediate response to trastuzumab [Table 6.11A]. Three phosphoproteins were altered only in SKBR3-L; these may be contributing to the trastuzumab-resistant phenotype of SKBR3-L cells [Table 6.11B].

13 phosphoproteins had altered levels in response to lapatinib in both SKBR3 and SKBR3-L cells. 19 phosphoproteins had altered levels only in SKBR3 cells; these proteins may mediate response to lapatinib [Table 6.12A]. Three phosphoproteins were altered only in SKBR3-L and may be contributing to the lapatinib-resistant phenotype of SKBR3-L cells [Table 6.12B].

7 phosphoproteins were altered only in parental SKBR3 cells in response to both trastuzumab and lapatinib, and may be mediators of response to both HER-2 antagonists [Table 6.13].

The proteins identified that may play a role in response or resistance to trastuzumab and/or lapatinib included a number of heat shock proteins (e.g. Hsp27, αβ−crystallin, HSPA1A (Hsp70), gp96, stress-induced-phosphoprotein 1), proteins involved in protein translation and degradation (e.g. translation elongation factor 2, translation initiation factor 4A, and ubiquitin activating enzyme E1), actin related proteins (e.g. adseverin, actinin) and proteins involved in metabolism (e.g. catalase, enoyl-CoA hydratase).

Table 6.4 List of identified phosphoproteins with = 1.2-fold increase in levels in SKBR3-L compared to SKBR3 cells. Fold change: protein abundance in SKBR3-L compared to SKBR3. ANOVA and Students' t-tests were performed to determine the significance of the results.

ID	Protein ID	Fold change	t-test p	ANOVA p
1945	Crystallin; alpha B	11.26	0.010	0.000
1921	Crystallin; alpha B	7.74	0.002	0.000
2203	S100 calcium binding protein A8 (calgranulin A)	3.97	0.009	0.000
2166	Chain H; Crystal structure of Mrp14 complexed with chaps	3.67	0.005	0.000
2152	Chain H; Crystal structure of Mrp14 complexed with chaps	3.61	0.015	0.000
2213	S100 calcium binding protein A8 (calgranulin A)	3.46	0.009	0.000
2145	Chain H; Crystal structure of Mrp14 complexed with chaps	3.24	0.007	0.000
580	Adseverin	2.57	0.012	0.000
1797	Heat shock 27kDa protein 1	2.38	0.037	0.004
461	Tumor rejection antigen (gp96) 1	2.16	0.005	0.000
366	Tumor rejection antigen (gp96) 1	1.92	0.016	0.000
1789	High-mobility group box 1	1.67	0.014	0.004
925	FK506 binding protein 4	1.60	0.006	0.000
1467	Uracil DNA glycosylase	1.52	0.014	0.000
1462	Uracil DNA glycosylase	1.46	0.003	0.000
951	FK506 binding protein 4	1.45	0.018	0.000
1647	Lactamase; beta 2	1.44	0.014	0.000
1486	Glyceraldehyde-3-phosphate dehydrogenase	1.35	0.032	0.002
1688	Methylthioadenosine phosphorylase	1.33	0.014	0.000
369	Eukaryotic translation elongation factor 2	1.22	0.040	0.005

Table 6.5 List of identified phosphoproteins with = 1.2-fold decrease in levels in SKBR3-L compared to SKBR3 cells. Fold change: protein abundance in SKBR3-L compared to SKBR3. ANOVA and Students' t-tests were performed to determine the significance of the results.

ID	Protein ID	Fold change	t-test p	ANOVA p
1720	PSMA4 protein	-1.21	0.015	0.009
1750	Proteasome (prosome; macropain) subunit; alpha type; 3	-1.24	0.006	0.005
1909	Proteasome subunit Y	-1.26	0.000	0.038
1774	Proteasome (prosome; macropain) subunit; alpha type; 7	-1.28	0.003	0.006
844	Stress-induced-phosphoprotein 1(Hsp70/90-organizing protein)	-1.31	0.040	0.000
1816	Proteasome (prosome; macropain) subunit; beta type; 4	-1.34	0.043	0.005
1135	Proteasome (prosome; macropain) 26S subunit; ATPase; 2	-1.34	0.004	0.001
783	HSPA1A protein; HSPA1A protein	-1.36	0.012	0.007
1701	PSMB7 protein	-1.37	0.016	0.004
982	Glucose-6-phosphate dehydrogenase	-1.41	0.034	0.000
361	Eukaryotic translation elongation factor 2	-1.46	0.005	0.000
1484	Putative sialoglycoprotease	-1.48	0.015	0.012
985	Glucose-6-phosphate dehydrogenase	-1.64	0.020	0.000
338	Eukaryotic translation elongation factor 2	-1.68	0.001	0.004
354	Eukaryotic translation elongation factor 2	-1.68	0.000	0.000
1006	Glucose-6-phosphate dehydrogenase	-1.72	0.010	0.000
948	Adenylyl cyclase-associated protein	-1.98	0.003	0.000
1659	Chain D; Crystal structure of human Dt-Diaphorase	-1.99	0.026	0.002
340	Eukaryotic translation elongation factor 2	-1.99	0.000	0.000
341	Eukaryotic translation elongation factor 2	-2.00	0.002	0.000
350	Eukaryotic translation elongation factor 2	-2.42	0.000	0.000

Table 6.6 List of identified phosphoproteins with = 1.99-fold change in levels in SKBR3-L compared to SKBR3 cells. Fold change: protein abundance in SKBR3-L to SKBR3. ANOVA and Students' t-tests were performed to determine the significance of the results.

ID	Protein ID	Fold change	t-test p	ANOVA p
1945	Crystallin; alpha B	11.26	0.010	0.000
1921	Crystallin; alpha B	7.74	0.002	0.000
2203	S100 calcium binding protein A8 (calgranulin A)	3.97	0.009	0.000
2166	Chain H; Crystal structure of Mrp14 complexed with chaps	3.67	0.005	0.000
2152	Chain H; Crystal structure of Mrp14 complexed with chaps	3.61	0.015	0.000
2213	S100 calcium binding protein A8 (calgranulin A)	3.46	0.009	0.000
2145	Chain H; Crystal structure of Mrp14 complexed with chaps	3.24	0.007	0.000
580	Adseverin	2.57	0.012	0.000
1797	Heat shock 27kDa protein 1	2.38	0.037	0.004
461	Tumor rejection antigen (gp96) 1	2.16	0.005	0.000
1659	Chain D; Crystal structure of human Dt-Diaphorase	-1.99	0.026	0.002
340	Eukaryotic translation elongation factor 2	-1.99	0.000	0.000
341	Eukaryotic translation elongation factor 2	-2.00	0.002	0.000
350	Eukaryotic translation elongation factor 2	-2.42	0.000	0.000

Table 6.7 List of identified phosphoproteins with = 1.2-fold change in levels in trastuzumab-treated (10 µg/ml) compared to untreated SKBR3 cells. Fold change: protein abundance in trastuzumab-treated to untreated SKBR3 cells. ANOVA was performed to determine the significance of the results.

ID	Protein ID	Fold Change	ANOVA p
369	Eukaryotic translation elongation factor 2	**1.53**	0.0047
375	Eukaryotic translation elongation factor 2	**1.51**	0.0017
713	Enoyl-CoA hydratase/3-hydroxyacyl-CoA dehydrogenase	**1.50**	0.0046
461	Tumor rejection antigen (gp96) 1	**1.28**	0.0001
1797	Heat shock 27kDa protein 1	**1.28**	0.0037
366	Tumor rejection antigen (gp96) 1	**1.27**	0.0005
1921	Crystallin; alpha B	**1.21**	0.0000
362	Eukaryotic translation elongation factor 2	**1.20**	0.0011
2203	S100 calcium binding protein A8 (calgranulin A)	**-1.21**	0.0002
387	Actinin; alpha 4	**-1.26**	0.0120
783	HSPA1A protein	**-1.27**	0.0065
354	Eukaryotic translation elongation factor 2	**-1.31**	0.0000
338	Eukaryotic translation elongation factor 2	**-1.38**	0.0035
341	Eukaryotic translation elongation factor 2	**-1.61**	0.0000
340	Eukaryotic translation elongation factor 2	**-1.63**	0.0001
350	Eukaryotic translation elongation factor 2	**-1.82**	0.0000

Table 6.8 List of identified phosphoproteins with = 1.2-fold change in levels in lapatinib-treated (1 µM) compared to untreated SKBR3 cells. Fold-change: protein abundance in lapatinib-treated to untreated SKBR3 cells. ANOVA was performed to determine the significance of the results.

ID	Protein ID	Fold Change	ANOVA *p*
713	Enoyl-CoA hydratase/3-hydroxyacyl-CoA dehydrogenase	2.00	0.0046
1721	Platelet-activating factor acetylhydrolase	1.73	0.0004
1557	Inorganic pyrophosphatase 2	1.63	0.0043
1921	Crystallin; alpha B	1.63	0.0000
580	Adseverin	1.61	0.0002
892	Catalase	1.56	0.0035
375	Eukaryotic translation elongation factor 2	1.50	0.0017
1945	Crystallin; alpha B	1.47	0.0005
369	Eukaryotic translation elongation factor 2	1.45	0.0047
362	Eukaryotic translation elongation factor 2	1.29	0.0011
1736	Tryptophan 5-monooxgenase activation protein	1.26	0.0340
925	FK506 binding protein 4	-1.23	0.0000
948	Adenylyl cyclase-associated protein	-1.24	0.0000
390	Ubiquitin activating enzyme E1	-1.27	0.0034
2152	Chain H; Crystal Structure of Mrp14 Complexed With Chaps	-1.29	0.0001
1124	Protein disulfide isomerase-related protein 5	-1.34	0.0009
783	HSPA1A protein	-1.35	0.0065
826	Stress-induced-phosphoprotein 1(Hsp70/90-organizing protein)	-1.39	0.0021
420	Eukaryotic translation elongation factor 2	-1.40	0.0160
951	FK506 binding protein 4	-1.40	0.0000
1484	Putative sialoglycoprotease	-1.41	0.0120
1116	Protein disulfide isomerase-related protein 5	-1.45	0.0270
1197	Eukaryotic translation initiation factor 4A; isoform 1	-1.46	0.0010
1134	OTTHUMP00000017054	-1.48	0.0029
844	Stress-induced-phosphoprotein 1(Hsp70/90-organizing protein)	-1.59	0.0001
361	Eukaryotic translation elongation factor 2	-1.62	0.0000
387	Actinin; alpha 4	-1.63	0.0120
354	Eukaryotic translation elongation factor 2	-1.67	0.0000
338	Eukaryotic translation elongation factor 2	-1.80	0.0035
340	Eukaryotic translation elongation factor 2	-2.13	0.0001
341	Eukaryotic translation elongation factor 2	-2.68	0.0000
350	Eukaryotic translation elongation factor 2	-3.07	0.0000

Table 6.9 List of identified phosphoproteins with = 1.2-fold change in levels in trastuzumab-treated (10 µg/ml) compared to untreated SKBR3-L cells. Fold change: protein abundance in trastuzumab-treated to untreated SKBR3-L cells. ANOVA was performed to determine the significance of the results.

ID	Protein ID	Fold Change	ANOVA p
1736	Tryptophan 5-monooxgenase activation protein	1.22	0.0340
1266	Brain creatine kinase	1.21	0.0078
354	Eukaryotic translation elongation factor 2	-1.21	0.0000
341	Eukaryotic translation elongation factor 2	-1.23	0.0000
340	Eukaryotic translation elongation factor 2	-1.28	0.0001
2203	S100 calcium binding protein A8 (calgranulin A)	-1.28	0.0002
350	Eukaryotic translation elongation factor 2	-1.40	0.0000
420	Eukaryotic translation elongation factor 2	-1.42	0.0160

Table 6.10 List of identified phosphoproteins with = 1.2-fold change in levels in lapatinib-treated (1 µM) compared to untreated SKBR3-L cells. Fold change: protein abundance in lapatinib-treated to control treated SKBR3-L cells. ANOVA was performed to determine the significance of the results.

ID	Protein ID	Fold Change	ANOVA *p*
1721	Platelet-activating factor acetylhydrolase	1.37	0.0004
713	Enoyl-CoA hydratase/3-hydroxyacyl-CoA dehydrogenase	1.33	0.0046
580	Adseverin	1.24	0.0002
1736	Tryptophan 5-monooxgenase activation protein	1.22	0.0340
354	Eukaryotic translation elongation factor 2	-1.22	0.0000
2166	Chain H; Crystal Structure of Mrp14 complexed with chaps	-1.24	0.0000
826	Stress-induced-phosphoprotein 1(Hsp70/90-organizing protein)	-1.25	0.0021
844	Stress-induced-phosphoprotein 1(Hsp70/90-organizing protein)	-1.26	0.0001
361	Eukaryotic translation elongation factor 2	-1.29	0.0000
340	Eukaryotic translation elongation factor 2	-1.33	0.0001
2145	Chain H; Crystal Structure of Mrp14 complexed with chaps	-1.34	0.0000
341	Eukaryotic translation elongation factor 2	-1.36	0.0000
420	Eukaryotic translation elongation factor 2	-1.37	0.0160
2152	Chain H; Crystal Structure of Mrp14 complexed with chaps	-1.40	0.0001
2203	S100 calcium binding protein A8 (calgranulin A)	-1.55	0.0002
350	Eukaryotic translation elongation factor 2	-1.57	0.0000

A **Trastuzumab-treated**

SKBR3   SKBR3-L

11   5   3

Table 6.11 A   Table 6.11 B

B **Lapatinib-treated**

SKBR3   SKBR3-L

19   13   3

Table 6.12 A   Table 6.12 B
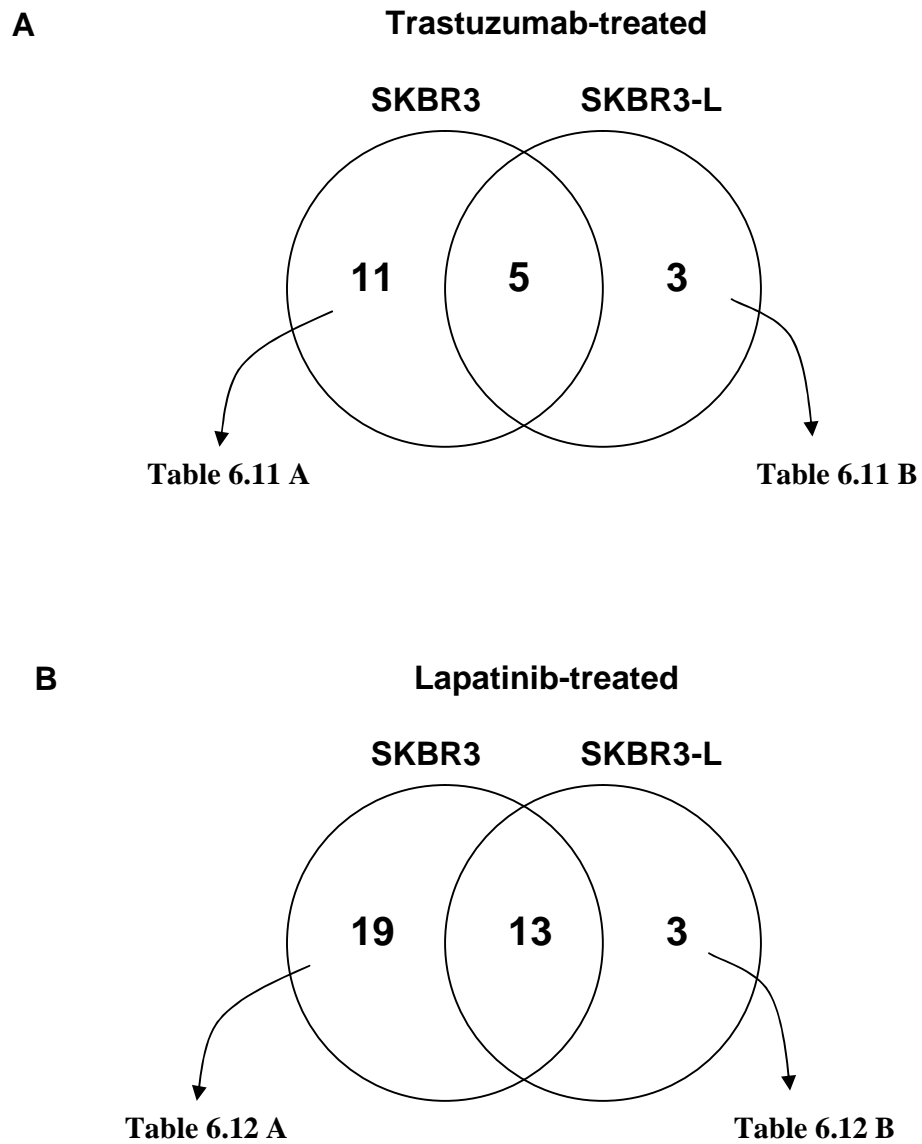
Figure 6.15 Venn diagrams showing the number of identified phosphoproteins with altered levels in response to **A.** trastuzumab (100 nM) and **B.** lapatinib (1 µM) treatment in SKBR3 compared to SKBR3-L cells.

Table 6.11 List of identified phosphoproteins that had altered levels only in **A.** SKBR3 cells and **B.** SKBR3-L cells in response trastuzumab (100 nM) treatment. ANOVA was performed to determine the significance of the results.

A

ID	Protein ID	Fold change	ANOVA p
369	Eukaryotic translation elongation factor 2	1.53	0.005
375	Eukaryotic translation elongation factor 2	1.51	0.002
713	Enoyl-CoA hydratase/3-hydroxyacyl-CoA dehydrogenase	1.50	0.005
461	Tumor rejection antigen (gp96) 1	1.28	0.000
1797	Heat shock 27kDa protein 1	1.28	0.004
366	Tumor rejection antigen (gp96) 1	1.27	0.000
1921	Crystallin; alpha B	1.21	0.000
362	Eukaryotic translation elongation factor 2	1.20	0.001
387	Actinin; alpha 4	-1.26	0.012
783	HSPA1A protein	-1.27	0.007
338	Eukaryotic translation elongation factor 2	-1.38	0.004

B

ID	Protein ID	Fold change	ANOVA p
1736	Tryptophan 5-monooxgenase activation protein	1.22	0.034
1266	Brain creatine kinase	1.21	0.008
420	Eukaryotic translation elongation factor 2	-1.42	0.016

Table 6.12 List of identified phosphoproteins that had altered levels only in **A.** SKBR3 cells and **B.** SKBR3-L cells in response lapatinib (1 µM) treatment. ANOVA was performed to determine the significance of the results.

A

ID	Protein ID	Fold change	ANOVA *p*
1557	Inorganic pyrophosphatase 2	1.63	0.004
1921	Crystallin; alpha B	1.63	0.000
892	Catalase	1.56	0.004
375	Eukaryotic translation elongation factor 2	1.50	0.002
1945	Crystallin; alpha B	1.47	0.000
369	Eukaryotic translation elongation factor 2	1.45	0.005
362	Eukaryotic translation elongation factor 2	1.29	0.001
925	FK506 binding protein 4	-1.23	0.000
948	Adenylyl cyclase-associated protein	-1.24	0.000
390	Ubiquitin activating enzyme E1	-1.27	0.003
1124	Protein disulfide isomerase-related protein 5	-1.34	0.001
783	HSPA1A protein	-1.35	0.007
951	FK506 binding protein 4	-1.40	0.000
1484	Putative sialoglycoprotease	-1.41	0.012
1116	Protein disulfide isomerase-related protein 5	-1.45	0.027
1197	Eukaryotic translation initiation factor 4A; isoform 1	-1.46	0.001
1134	OTTHUMP00000017054	-1.48	0.003
387	Actinin; alpha 4	-1.63	0.012
338	Eukaryotic translation elongation factor 2	-1.80	0.004

B

ID	Protein ID	Fold change	ANOVA *p*
2166	Chain H; Crystal Structure of Mrp14 Complexed With Chaps	-1.24	0.000
2145	Chain H; Crystal Structure of Mrp14 Complexed With Chaps	-1.34	0.000
2203	S100 calcium binding protein A8 (calgranulin A)	-1.55	0.000

Table 6.13 List of identified phosphoproteins that had altered levels only in SKBR3 cells after both trastuzumab (100 nM) and lapatinib (1 µM) treatment. ANOVA was performed to determine the significance of the results.

ID	Protein ID	Fold change	ANOVA *p*
369	Eukaryotic translation elongation factor 2	1.53	0.005
375	Eukaryotic translation elongation factor 2	1.51	0.002
1921	Crystallin; alpha B	1.21	0.000
362	Eukaryotic translation elongation factor 2	1.20	0.001
387	Actinin; alpha 4	-1.26	0.012
783	HSPA1A protein	-1.27	0.007
338	Eukaryotic translation elongation factor 2	-1.38	0.004

6.5.5 Identification of phosphorylated peptides

The MALDI-ToF-MS analysis also provides information on the amount of the total protein sequence, or the percent coverage, that was identified for each protein, and on post-translational modifications of the identified proteins, such as the presence of phosphate groups. Of the proteins that were identified, the average percent coverage was 45.4 %.

A MASCOT score is calculated for each protein identified and reflects the level of confidence in the identification. Fig 6.15 shows an example of an identified protein sequence; protein ID no. 783 (HSPA1A/ Hsp70), which had a high MASCOT score of 953, and 60 % protein coverage. Each individual peptide sequenced is also given an ion score, which indicates the level of homology between the peptide sequence and the protein identified [Fig 6.15].

_____

```
    1 MAKAAAIGID LGTTYSCVGV FQHGKVEIIA NDQGNRTTPS YVAFTDTERL
   51 IGDAAKNQVA LNPQNTVFDA KRLIGRKFGD PVVQSDMKHW PFQVINDGDK
  101 PKVQVSYKGE TKAFYPEEIS SMVLTKMKEI AEAYLGYPVT NAVITVPAYF
  151 NDSQRQATKD AGVIAGLNVL RIINEPTAAA IAYGLDRTGK GERNVLIFDL
  201 GGGTFDVSIL TIDDGIFEVK ATAGDTHLGG EDFDNRLVNH FVEEFKRKHK
  251 KDISQNKRAV RRLRTACERA KRTLSSSTQA SLEIDSLFEG IDFYTSITRA
  301 RFEELCSDLF RSTLEPVEKA LRDAKLDKAQ IHDLVLVGGS TRIPKVQKLL
  351 QDFFNGRDLN KSINPDEAVA YGAAVQAAIL MGDKSENVQD LLLLDVAPLS
  401 LGLETAGGVM TALIKRNSTI PTKQTQIFTT YSDNQPGVLI QVYEGERAMT
  451 KDNNLLGRFE LSGIPPAPRG VPQIEVTFDI DANGILNVTA TDKSTGKANK
  501 ITITNDKGRL SKEEIERMVQ EAEKYKAEDE VQRERVSAKN ALESYAFNMK
  551 SAVEDEGLKG KISEADKKKV LDKCQEVISW LDANTLAEKD EFEHKRKELE
  601 QVCNPIISGL YQGAGGPGPG GFGAQGPKGG SGSGPTIEEV D
```

Figure 6.15 Protein sequence of protein ID no. 783 (HSPA1A/ Hsp70), which had 60 % protein coverage. The matched peptide sequences are in red. The outlined peptide sequence corresponds to amino acids 221 – 236, and this peptide fragment had a high ion score of 131, indicating a high level of homology.

_____

60 of the identified proteins were further analysed for post-translational modifications. Between 1 and 12 phosphorylation sites were identified on 44 of the 60 proteins. Table 6.12A shows a comparison of the phosphorylation sites found on peptide sequences in six identified forms of eukaryotic elongation translation factor 2 (eEF2) that were downregulated in SKBR3-L compared to parental SKBR3 cells. Table 6.12B shows a comparison of the phosphorylation sites found on peptide sequences in three identified forms of eukaryotic Mrp14 (S100A9/Calgranulin B) that were upregulated in SKBR3-L compared to parental SKBR3 cells.

_____

Table 6.12 Matched peptide information for identified phosphorylated isoforms of **A.** eEF2 and **B.** Mrp14/S100A9 proteins, showing MASCOT scores, % coverage and highest ion score obtained for the matched peptides. The peptide sequences with identified phosphorylation groups are listed, and the no. of phosphorylation sites found on each sequence, as well as the total no. of phosphorylation sites identified, is shown for each protein ID.

A

Protein ID	338	340	341	350	354	361
Fold change	- 1.68	- 1.99	- 2.00	- 2.42	- 1.68	- 1.46
MASCOT Score	105	300	247	72	393	90
% Coverage	22	34	29	24	33	20
Highest ion score	19	42	52	18	61	26
Total no. phosphate groups identified	0	6	3	3	7	7
Peptide sequences and no. phosphate groups identified						
33 - 50 K.STLTDSLVCKAGIIASAR.A	0	0	0	0	**2**	0
43 - 50 K.AGIIASAR.A	0	0	**1**	**1**	**1**	**1**
51 - 61 R.AGETRFTDTR.K	0	**2**	**1**	0	**1**	0
163 - 180 R.ALLELQLEPEELYQTFQR.I	0	0	**1**	**1**	**1**	0
392 - 409 K.GPLMMYISKMVPTSDKGR.F	0	**3**	0	0	**3**	**3**
408 - 415 K.GRFYAFGR.V	0	0	0	0	0	**1**
450 - 456 R.TILMMGR.Y	0	**1**	0	0	0	0
482 - 498 K.TGTITTFEHAHNMRVMK.F	0	0	0	0	0	**2**
648 - 667 R.KIWCFGPDGTGPNILTDITK.G	0	0	0	**1**	0	0

B

Protein ID	2145	2152	2166
Fold change	3.24	3.61	3.67
MASCOT Score	242	349	350
% Coverage	74	72	75
Total no. phosphate groups identified	**1**	**1**	**0**
Peptide sequences and no. phosphate goups identified			
72 - 84 K.QLSFEEFIMLMAR.L	0	**1**	0
93 - 113 K.MHEGDEGPGHHHKPGLGEGTP.	**1**	0	0

Chapter 7

HER-2 AND IGF-IR
IMMUNOHISTOCHEMISTRY (IHC)
IN PATIENT SAMPLES

7.1 HER-2 AND IGF-IR IMMUNOHISTOCHEMISTRY (IHC)

HER-2 levels were scored using the DAKO HercepTest[M] scoring guidelines, and were assigned scores of 0, 1+ (both HER-2-negative), 2+ (weakly positive) or 3+ (strongly positive) based on membrane staining intensity [Fig. 71]. Membrane IGF-IR (mIGF-IR) and cytoplasmic IGF-IR (cIGF-IR) staining were scored separately; mIGF-IR was scored as positive or negative, while cIGF-IR levels were assigned scores of 0 (negative), 1+ (weakly positive), 2+ (moderately positive), or 3+ (strongly positive) [Fig. 7.2].

Two different studies were performed. Study 1 was an analysis of HER-2 and IGF-IR expression in 93 unselected breast cancer patients from St. Vincent's University Hospital. Study 2 was an analysis of HER-2 and IGF-IR expression in 150 HER-2-positive breast cancer patients from St. Vincent's University Hospital and St. James' Hospital. Results of each study will be presented separately in Sections 7.2 and 7.3.
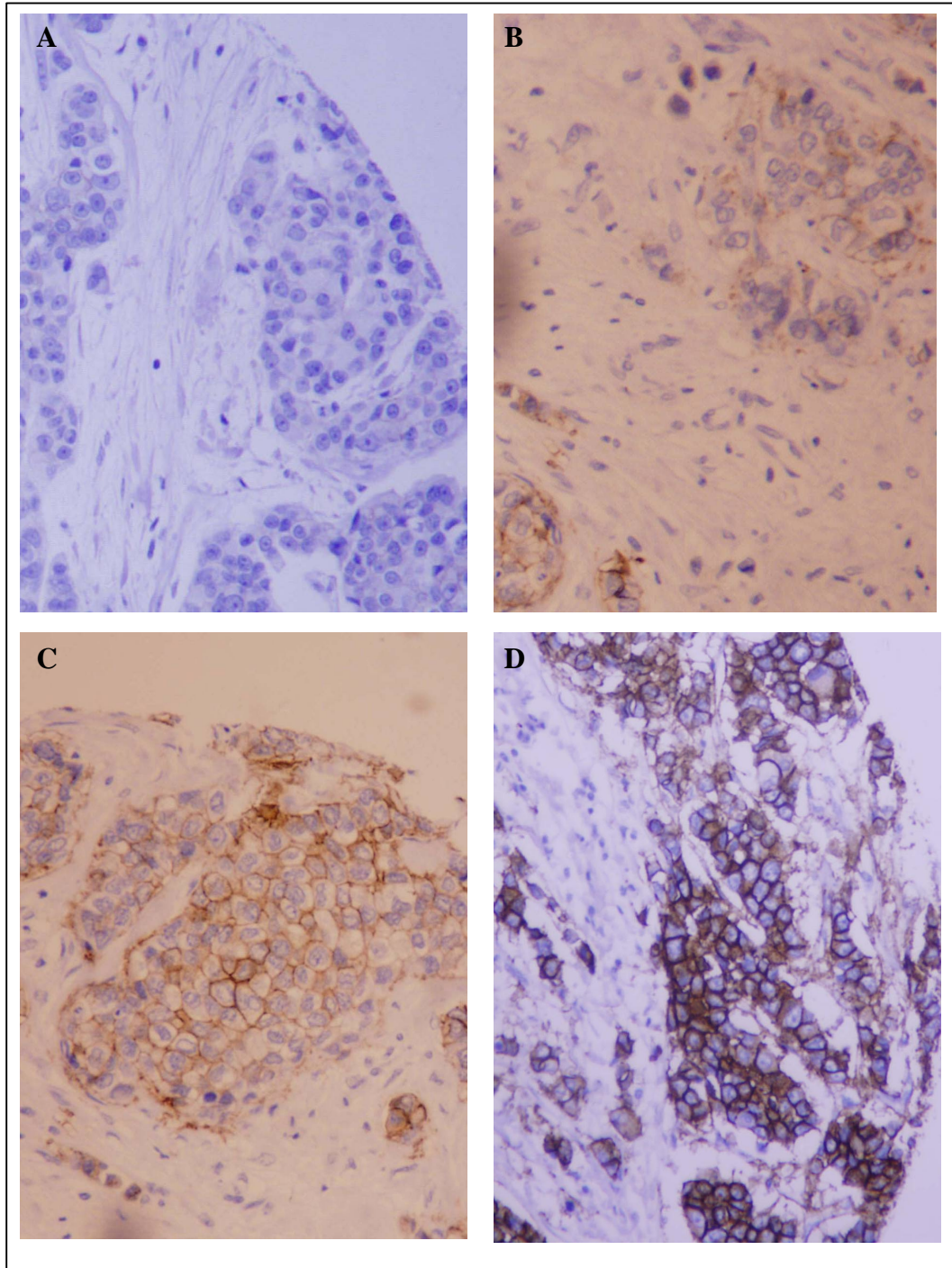
Figure 7.1 Representative pictures of HER-2 staining with different scores:
A. HER-2 negative; **B.** HER-2 1+; **C.** HER-2 2+ and **D.** HER-2 3+.

_____
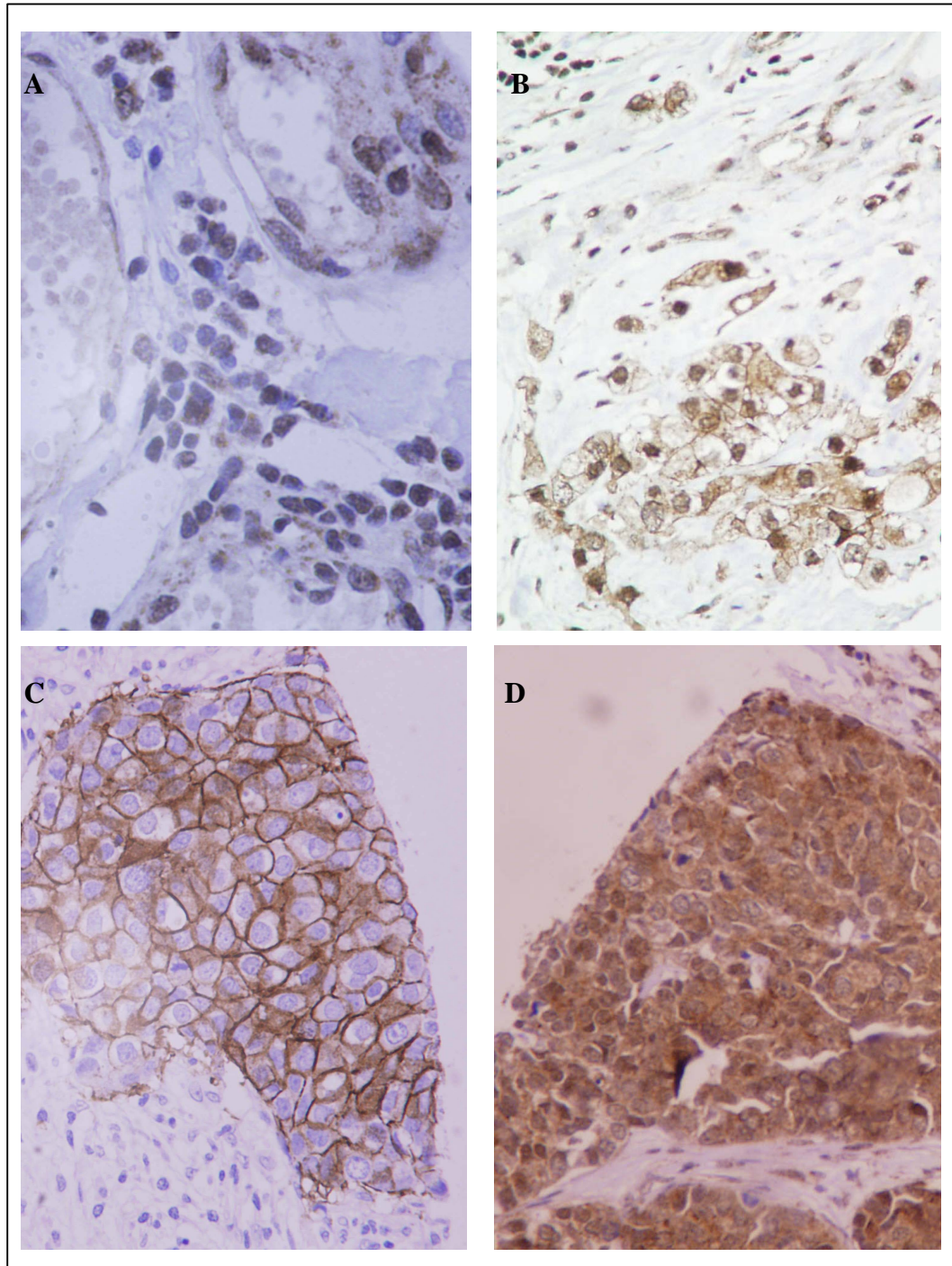
Figure 7.2 Representative pictures of IGF-IR staining with different membrane and cytoplasmic scores: **A.** IGF-IR membrane negative, cytoplasm 0; **B.** IGF-IR membrane positive, cytoplasm 1+; **C.** IGF-IR membrane positive, cytoplasm 2+, and **D.** IGF-IR membrane negative, cytoplasm 3+.

_____

7.2 STUDY 1: HER-2 AND IGF-IR EXPRESSION IN UNSELECTED BREAST CANCER PATIENTS

7.2.1 HER-2 and IGF-IR IHC scores

Tissue microarrays (TMAs) containing 93 breast tumour samples were obtained and were stained for HER-2, membrane IGF-IR and cytoplasmic IGF-IR expression [Table 7.1]. Consistent with previous reports, 20% of the breast tumours were HER-2 positive (2+ or 3+). All of the breast tumours, except one, were positive for cytoplasmic staining of IGF-IR, whereas only 34.4% were positive for IGF-IR membrane staining.

_____

Table 7.1 HER-2 and IGF-IR scores in 93 patient samples, as measured by IHC.

	n	%
HER-2		
0	70	77.8
1+	2	2.2
2+	4	4.4
3+	14	15.6
Unknown	3	
IGF-IR cytoplasm		
0	1	1.1
1+	14	15.6
2+	64	71.1
3+	11	12.2
Unknown	3	
IGF-IR membrane		
Negative	59	65.6
Positive	31	34.4
Unknown	3	

_____

7.2.2 HER-2 and IGF-IR correlation with prognostic indicators

Table 7.2 outlines the histopathological characteristics of the 93 patients studied.

No significant correlation was observed between HER-2 expression and patient age at diagnosis, tumour size, nodal status, histological type, or ER or PR status [Table 7.3]. However, HER-2 expression was significantly associated with tumour grade (Chi-squared test, p = 0.031); while the majority of HER-2-negative tumours were grade 2 (41/69, 59 %), the majority of HER-2 3+ tumours were grade 3 (11/14, 79 %) [Fig. 7.3].

Cytoplasmic expression of IGF-IR was not associated with patient age at diagnosis, tumour size, nodal status, histological type, or ER or PR status [Table 7.4]. However, a significant correlation was observed between cytoplasmic expression of IGF-IR and tumour grade (Chi-squared test, p = 0.046) [Fig. 7.3]; grade 3 tumours had a higher proportion of 2+ or 3+ cytoplasmic IGF-IR staining than lower grade tumours.

No correlation was observed between membrane IGF-IR expression and patient age at diagnosis, tumour size, tumour grade, or ER or PR status [Table 7.5]. A significant correlation was observed between membrane IGF-IR staining and histological type (Mann-Whitney test, p = 0.005) [Fig. 7.5]. No IGF-IR membrane staining was detected in lobular tumours, while 39 % of ductal tumours were membrane IGF-IR-positive and 61 % were membrane IGF-IR-negative. An inverse association was also observed between membrane IGF-IR expression and the number of positive nodes detected, although this association did not reach significance (Mann-Whitney test, p = 0.079) [Fig. 7.6].

No correlation was observed between HER-2 expression and membrane or cytoplasmic IGF-IR expression in this group of patients.

Table 7.2 Characteristics of the breast cancer patients analysed in Study 1 (n = 93).

	n	*%*
Age at diagnosis		
< 50 years	26	28.0
= 50 years	64	68.8
Unknown	3	3.2
Tumour size		
= 2 cm	25	26.9
> 2 cm	68	73.1
Unknown	0	0.0
Nodal status		
Neg	37	39.8
Pos	53	57.0
Unknown	3	3.2
Grade		
1	6	6.5
2	46	49.5
3	39	41.9
Unknown	2	2.2
Histology		
Ductal	79	84.9
Lobular	13	14.0
Unknown	1	1.1
ER status		
Negative	27	29.0
Positive	60	64.5
Unknown	6	6.5
PR status		
Negative	42	45.2
Positive	46	49.5
Unknown	5	5.4

Table 7.3 Relationship between HER-2 levels and patient prognostic indicators.

	HER-2 staining				
	0	1+	2+	3+	***p***
Age (years)					
< 50 *(n=26)*	18 (69.2%)	0 (0%)	1 (3.8%)	7 (26.9%)	0.2994
= 50 *(n=62)*	51 (82.3%)	1 (1.6%)	3 (4.8%)	7 (11.3%)	
Size (cm)					
= 2 *(n=24)*	20 (83.3%)	0 (0%)	1 (4.2%)	3 (12.5%)	0.8854
> 2 *(n=66)*	51 (77.3%)	1 (1.5%)	3 (4.5%)	11 (16.7%)	
Nodal status					
Neg *(n=35)*	28 (80.0%)	1 (2.9%)	2 (5.7%)	4 (11.4%)	0.5455
Pos *(n=52)*	41 (78.8%)	0 (0%)	2 (3.8%)	9 (17.3%)	
Grade					
1 *(n=5)*	4 (80%)	0 (0%)	1 (20.0%)	0 (0%)	
2 *(n=45)*	41 (91.1%)	0 (0%)	1 (2.2%)	3 (6.7%)	**0.0314**
3 *(n=38)*	24 (63.2%)	1 (2.6%)	2 (5.3%)	11 (28.9%)	
Histology					
D *(n=77)*	58 (75.3%)	1 (1.3%)	4 (5.2%)	14 (18.2%)	0.2880
L *(n=12)*	12 (100%)	0 (0%)	0 (0%)	0 (0%)	
ER status					
Neg *(n=26)*	18 (69.2%)	0 (0%)	1 (3.8%)	7 (26.9%)	0.3441
Pos *(n=59)*	48 (81.4%)	1 (1.7%)	3 (5.1%)	7 (11.9%)	
PR status					
Neg *(n=41)*	28 (68.3%)	0 (0%)	3 (7.3%)	10 (24.4%)	0.1021
Pos *(n=45)*	39 (86.7%)	1 (2.2%)	1 (2.2%)	4 (8.9%)	
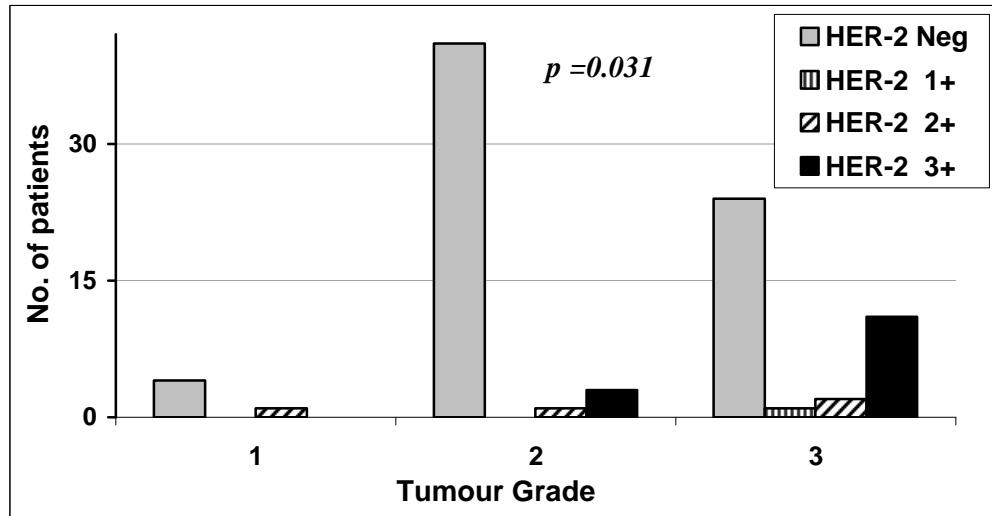
Figure 7.3 Number of patients divided by HER-2 status in grade 1, 2 and 3 tumours. The relationships were analysed by the Chi-squared test.

Table 7.4 Relationship between cytoplasmic IGF-IR levels and patient prognostic indicators.

	IGF-IR cytoplasmic staining				
	0	1+	2+	3+	*p*
Age (years)					
< 50 *(n=26)*	1 (3.8%)	3 (11.5%)	17 (65.4%)	5 (19.2%)	0.4206
= 50 *(n=61)*	0 (0%)	8 (13.1%)	37 (60.7%)	16 (26.2%)	
Size (cm)					
= 2 *(n=24)*	0 (0%)	1 (4.2%)	16 (66.7%)	7 (29.2%)	0.4512
> 2 *(n=66)*	1 (1.5%)	10 (15.2%)	41 (62.1%)	14 (21.2%)	
Nodal status					
Neg *(n=36)*	1 (2.8%)	4 (11.1%)	23 (63.9%)	8 (22.2%)	0.6466
Pos *(n=51)*	0 (0%)	7 (13.7%)	31 (60.8%)	13 (25.5%)	
Grade					
1 *(n=5)*	0 (0%)	1 (20.0%)	4 (80.0%)	0 (0%)	
2 *(n=44)*	0 (0%)	10 (22.7%)	23 (52.3%)	11 (25.0%)	**0.0459**
3 *(n=39)*	1 (2.6%)	1 (2.6%)	28 (71.8%)	10 (25.6%)	
Histology					
D *(n=76)*	1 (1.3%)	8 (10.5%)	47 (61.8%)	20 (26.3%)	0.3457
L *(n=13)*	0 (0%)	3 (23.1%)	9 (69.2%)	1 (7.7%)	
ER status					
Neg *(n=26)*	1 (3.8%)	4 (15.4%)	17 (65.4%)	4 (15.4%)	0.2466
Pos *(n=59)*	0 (0%)	5 (8.5%)	38 (64.4%)	16 (27.1%)	
PR status					
Neg *(n=41)*	0 (0%)	6 (14.6%)	29 (70.7%)	6 (14.6%)	0.1873
Pos *(n=44)*	1 (2.3%)	4 (9.1%)	25 (56.8%)	14 (31.8%)	
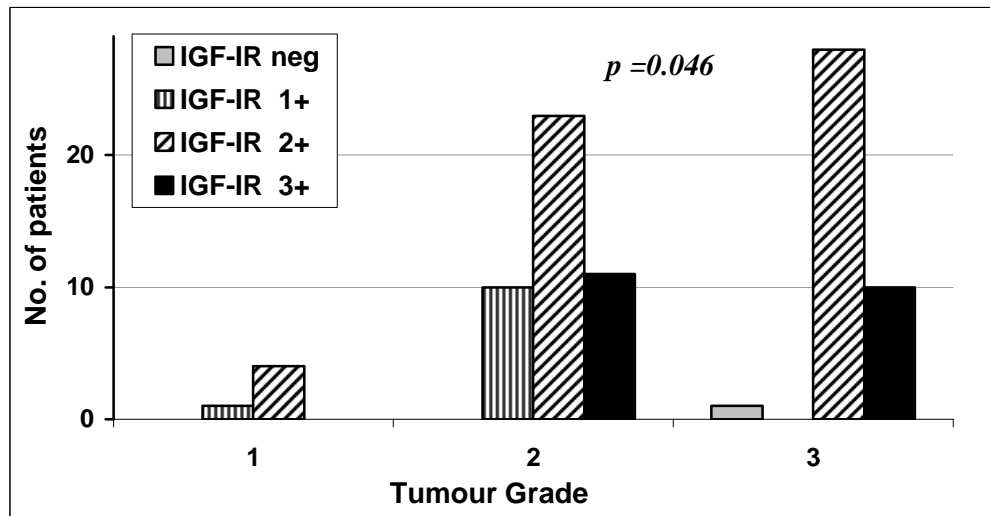
Figure 7.4 Number of patients divided by cytoplasmic IGF-IR status in grade 1, 2 and 3 tumours. The relationships were analysed by the Chi-squared test.

_____

Table 7.5 Relationship between membrane IGF-IR staining and patient prognostic indicators.

	n	No. positive	%	***p***
		IGF-IR membrane staining		
Age (years)				
< 50	*26*	10	38.5	0.6102
= 50	*61*	20	32.8	
Size (cm)				
= 2	*24*	9	37.5	0.7103
> 2	*66*	22	33.3	
Nodal status				
Neg	*36*	16	44.4	0.1493
Pos	*51*	15	29.4	
Grade				
1	*5*	2	40.0	
2	*44*	17	38.6	0.5817
3	*39*	11	28.2	
Histology				
D	*76*	30	39.5	**0.0054**
L	*13*	0	0.0	
ER status				
Neg	*26*	7	26.9	0.4332
Pos	*59*	21	35.6	
PR status				
Neg	*41*	14	34.1	0.9957
Pos	*44*	15	34.1	

_____
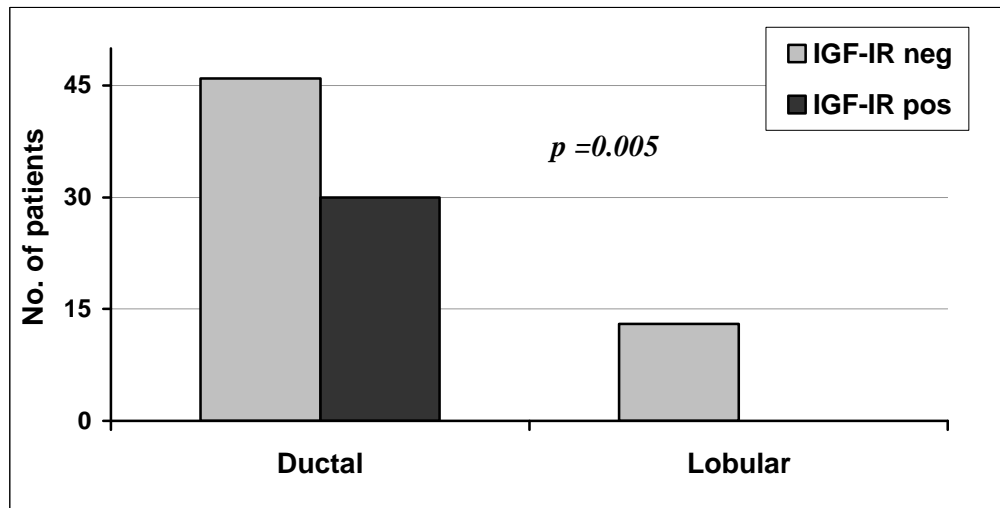
Figure 7.5 Number of patients with membrane IGF-IR staining in ductal and lobular tumours. The relationships were analysed by the Chi-squared test.
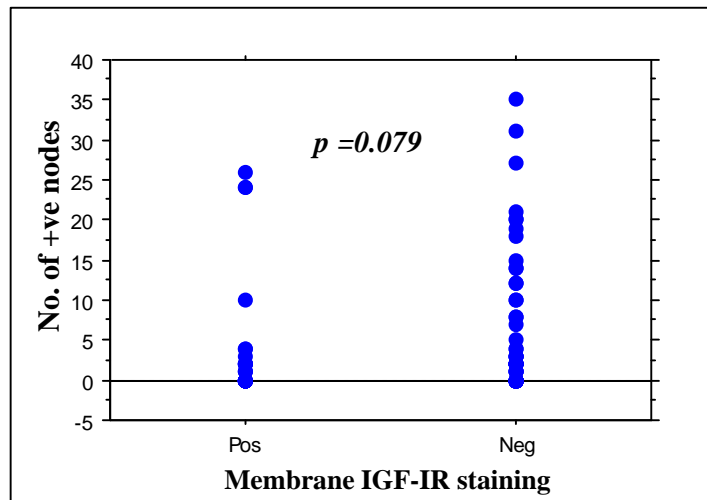
Figure 7.6 Number of positive nodes detected in patients with tumours positive and negative for membrane-IGF-IR. The relationship was analysed by the Mann-Whitney test.

7.3 STUDY 2: HER-2 AND IGF-IR EXPRESSION IN HER-2-POSITIVE BREAST CANCER PATIENTS

7.3.1 HER-2 and IGF-IR IHC scores

We constructed TMAs from 223 tumours, which had previously tested positive for HER-2 in hospital laboratories, by immunohistochemistry or FISH analysis. For patients where treatment details were available, approximately 83% (158/190) received trastuzumab, with the majority receiving trastuzumab in the adjuvant setting. The TMAs were stained for HER-2, membrane IGF-IR and cytoplasmic IGF-IR expression [Table 7.6]. Although all these tumours were believed to be HER-2 positive only 105 of 182 samples stained were either HER-2 2+ or HER-2 3+. All of the tumour samples showed some degree of IGF-IR cytoplasmic staining, with the majority being 2+ (143/187), whereas only approximately 20% were positive for IGF-IR membrane staining (38/187).

_____

Table 7.6 HER-2 and IGF-IR scores in 223 patient samples measured by IHC.

Protein	*n*	%
HER-2		
0	62	34.1
1+	15	8.2
2+	21	11.5
3+	84	46.2
Unknown	41	
IGF-IR cytoplasm		
0	0	0.0
1+	18	9.6
2+	143	76.5
3+	26	13.9
Unknown	36	
IGF-IR membrane		
Negative	149	79.7
Positive	38	20.3
Unknown	36	

_____

7.3.2 HER-2 and IGF-IR correlation with patient characteristics

Table 7.7 shows the histopathological characteristics of the 223 patients studied.

No correlation was observed between HER-2 expression and membrane or cytoplasmic IGF-IR expression in these tumour samples.

No significant correlation was observed between HER-2 expression and patient age at diagnosis, tumour size, nodal status, or PR status [Table 7.8]. However, a significant positive association was observed between HER-2 expression and tumour grade (Chi-squared test, p = 0.004) [Fig. 7.7]. HER-2 expression was also significantly higher in ductal compared to lobular tumours (Chi-squared test, p = 0.033) [Fig. 7.8]. A significant inverse relationship was also observed between HER-2 expression and ER status (Chi-squared test, p = 0.033) [Fig. 7.9].

A significant correlation was also observed between HER-2 IHC levels quantified on the TMAs with HER-2 IHC staining as scored by the hospital histopathology laboratories (Chi-squared test, p = 0.016). However, 41 of the tumour samples were scored as HER-2 0 and 15 as HER-2 1+. This discordance in results may be due to tumour heterogeneity and the small size of the tumour samples represented in the TMA cores (0.6 mm).

Cytoplasmic IGF-IR levels did not correlate with any of the histopathological characteristics studied [Table 7.9]. Membrane IGF-IR staining was not associated with patient age at diagnosis, nodal status, tumour grade, or histopathological type [Table 7.10]. However, membrane IGF-IR was detected significantly more frequently in ER-positive tumours than ER negative tumours (Chi-squared test, p = 0.0002) [Fig. 7.10]. Membrane IGF-IR expression was also found more frequently in PR-positive tumours, with this association was approaching statistical significance (Chi-squared test, p = 0.055). A trend towards a correlation between positive membrane IGF-IR staining and tumour size was also observed, however, this association did not reach statistical significance (Chi-squared test, p = 0.094) [Table 7.10].

No correlation was observed between HER-2 expression and membrane or cytoplasmic IGF-IR expression in these tumour samples.

Table 7.7 Characteristics of the breast cancer patients analysed in Study 2 (n = 223).

	n	%
Menopausal status		
Pre	71	31.8
Peri	4	1.8
Post	88	39.5
Unknown	60	26.9
Tumour size		
≤ 2 cm	57	25.6
> 2 cm	147	65.9
Unknown	19	8.5
Nodal status		
Neg	83	37.2
Pos	132	59.2
Unknown	8	3.6
Grade		
1	7	3.1
2	44	19.7
3	163	73.1
Unknown	9	4.0
Histology		
D	206	92.4
L	8	3.6
D+L	2	0.9
Other	3	1.3
Unknown	4	1.8
ER		
Neg	87	39.0
Pos	129	57.8
Unknown	7	3.1
PR		
Neg	70	31.4
Pos	34	15.2
Unknown	119	53.4
HER-2 FISH		
Neg	1	0.4
Pos	79	35.4
Unknown	143	64.1
HER-2 Status (3+ IHC or FISH)		
Neg	1	0.4
Pos	202	90.6
Unknown	20	9.0

Table 7.8 Relationship between HER-2 levels and patient prognostic indicators.

	HER-2 Staining				
	0	1+	2+	3+	*p*
Menopausal status					
Pre *(n=55)*	19 (34.5%)	5 (9.1%)	7 (12.7%)	24 (43.6%)	0.5259
Peri *(n=3)*	0 (0%)	1 (33.3%)	0 (0%)	2 (66.7%)	
Post *(n=74)*	21 (28.4%)	5 (6.8%)	8 (10.8%)	40 (54.1%)	
Tumour size (cm)					
≤ 2 *(n=47)*	22 (46.8%)	3 (6.4%)	5 (10.6%)	17 (36.2%)	0.2495
> 2 *(n=125)*	38 (30.4%)	12 (9.6%)	16 (12.8%)	59 (47.2%)	
Nodal status					
Neg *(n=66)*	26 (39.4%)	4 (6.1%)	10 (15.2%)	26 (39.4%)	0.3605
Pos	35 (31.5%)	11 (9.9%)	11 (9.9%)	54 (48.6%)	
Grade					
1 *(n=4)*	1 (25.0%)	0 (0%)	3 (75.0%)	0 (0%)	
2 *(n=39)*	13 (33.3%)	6 (15.4%)	4 (10.3%)	16 (41.0%)	**0.0044**
3 *(n=133)*	47 (36.3%)	9 (6.8%)	14 (10.5%)	63 (47.4%)	
Histology					
D *(n=169)*	56 (33.1%)	13 (7.7%)	21 (12.4%)	79 (46.7%)	
L *(n=7)*	4 (57.1%)	1 (14.3%)	0 (0%)	2 (28.6%)	**0.0331**
D+L *(n=1)*	0 (0%)	1 (100%)	0 (0%)	0 (0%)	
ER					
Neg *(n=71)*	19 (26.8%)	3 (4.2%)	5 (7.0%)	44 (62.0%)	**0.0033**
Pos	42 (39.3%)	12 (11.2%)	16 (14.9%)	37 (34.6%)	
PR					
Neg *(n=58)*	14 (24.1%)	4 (6.9%)	7 (12.1%)	33 (56.9%)	0.3731
Pos *(n=28)*	11 (39.3%)	2 (7.1%)	1 (3.6%)	14 (50.0%)	
HER-2 IHC					
2+ *(n=18)*	10 (55.6%)	4 (22.2%)	0 (0%)	4 (22.2%)	**0.0156**
3+ *(n=110)*	31 (28.2%)	11 (10.0%)	15 (13.6%)	53 (48.2%)	
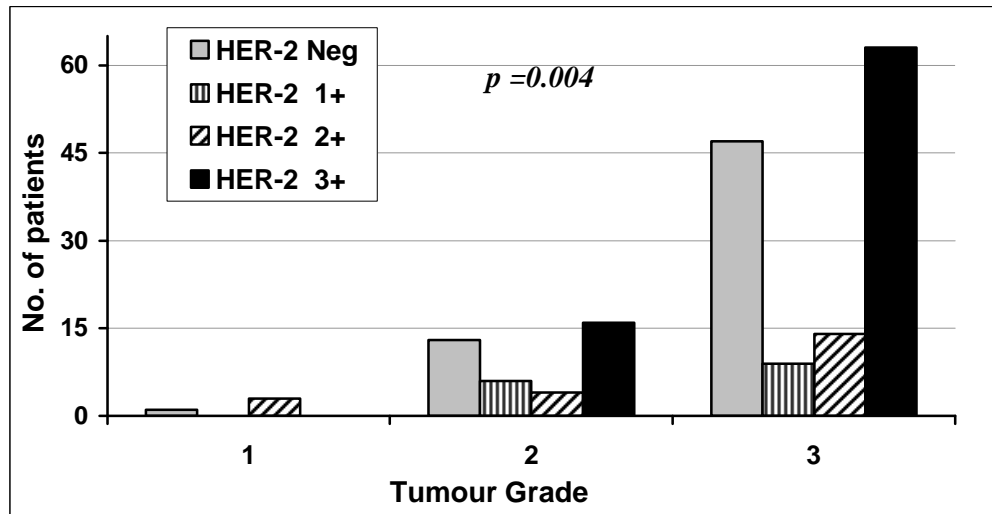
Fig 7.7 Number of patients divided by HER-2 status in grade 1, 2 and 3 tumours. The relationships were analysed by the Chi-squared test.

___
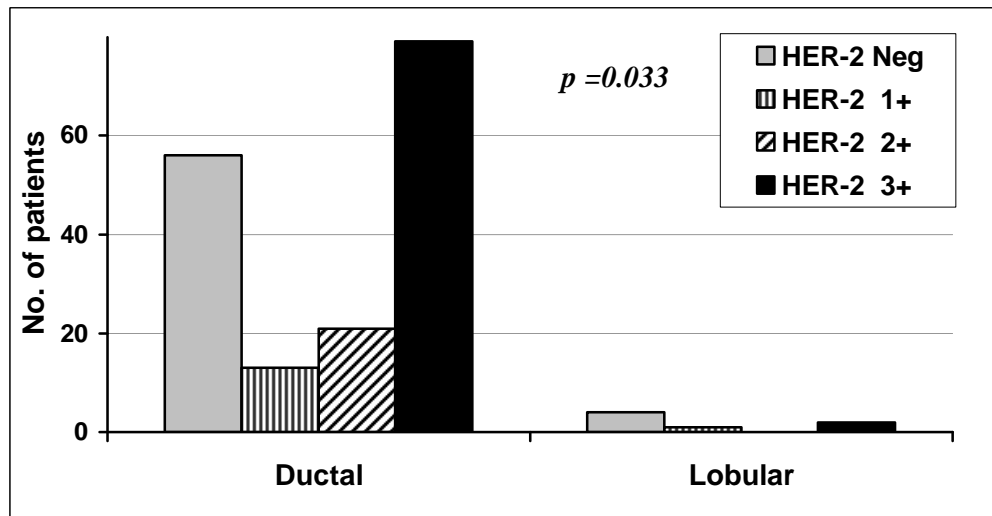
Fig 7.8 Number of patients divided by HER-2 status in ductal and lobular tumour histological groups. The relationships were analysed by the Chi-squared test.

___
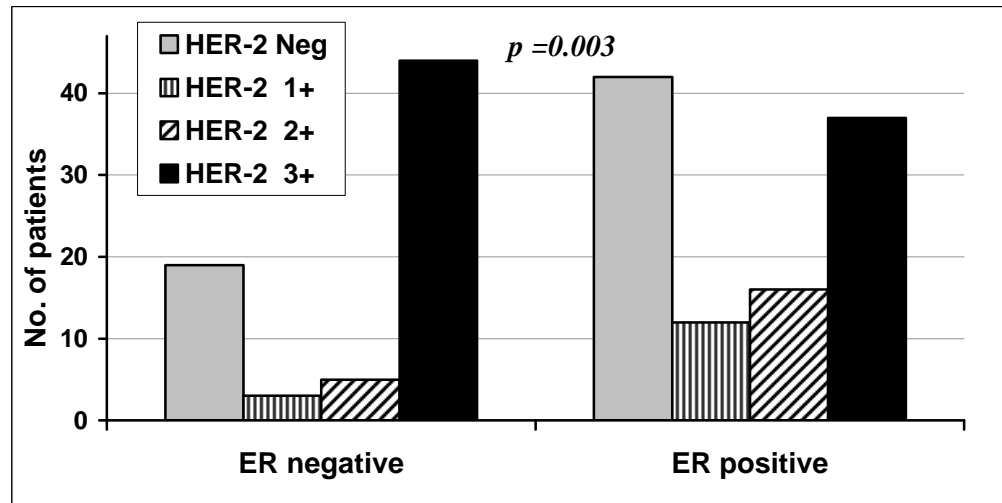
Fig 7.9 Number of patients divided by HER-2 status in ER-positive and -negative tumours. The relationships were analysed by the Chi-squared test.

_____

Table 7.9 Relationship between cytoplasmic IGF-IR levels and patient prognostic indicators.

	TMA IGF-IR Cytoplasmic staining			
	1+	2+	3+	***p***
Menopausal status				
Pre *(n=56)*	5 (8.9%)	43 (76.8%)	8 (14.3%)	0.6174
Peri *(n=3)*	0 (0%)	2 (66.7%)	1 (33.3%)	
Post *(n=77)*	11 (14.3%)	58 (75.3%)	8 (10.4%)	
Tumour size (cm)				
≤ 2 *(n=48)*	3 (6.2%)	38 (79.2%)	7 (14.6%)	0.5951
> 2 *(n=129)*	15 (11.6%)	99 (76.7%)	15 (11.6%)	
Nodal status				
Neg *(n=67)*	6 (9.0%)	53 (79.1%)	8 (11.9%)	0.9032
Pos *(n=115)*	12 (10.4%)	87 (75.7%)	16 (13.9%)	
Grade				
1 *(n=4)*	0 (0%)	4 (100%)	0 (0%)	
2 *(n=40)*	5 (12.5%)	28 (70.0%)	7 (17.5%)	0.7209
3 *(n=137)*	13 (9.5%)	107 (78.1%)	17 (12.4%)	
Histology				
D *(n=174)*	17 (9.8%)	133 (76.4%)	24 (13.8%)	
L *(n=7)*	1 (14.3%)	5 (71.4%)	1 (14.3%)	0.9723
D+L *(n=1)*	0 (0%)	1 (100%)	0 (0%)	
ER				
Neg *(n=74)*	10 (13.5%)	57 (77.0%)	7 (9.5%)	0.1906
Pos *(n=108)*	8 (7.4%)	84 (77.8%)	16 (14.8%)	
PR				
Neg *(n=61)*	11 (18.0%)	42 (68.9%)	8 (13.1%)	0.3084
Pos *(n=29)*	5 (17.2%)	23 (79.3%)	1 (3.4%)	
HER-2 IHC				
2+ *(n=20)*	3 (15.0%)	15 (75.0%)	2 (10.0%)	0.9693
3+ *(n=112)*	10 (8.9%)	89 (79.5%)	13 (11.6%)	

_____

Table 7.10 Relationship between membrane IGF-IR staining and patient prognostic indicators.

		TMA IGF-IR Membrane staining		
	n	No. positive	%	***p***
Menopausal status				
Pre	*56*	15	26.8	0.2323
Peri	*2*	1	50.0	
Post	*66*	12	18.2	
Tumour size				
≤ 2 cm	*48*	6	12.5	**0.0935**
> 2 cm	*129*	31	24.0	
Nodal status				
Neg	*67*	16	23.9	0.4470
Pos	*115*	22	19.1	
Grade				
1	*4*	0	0.0	
2	*40*	8	20.0	0.5615
3	*137*	30	21.9	
Histology				
D	*174*	37	21.3	
L	*7*	0	0.0	0.3438
D+L	*1*	0	0.0	
ER				
Neg	*74*	5	6.8	**0.0002**
Pos	*108*	32	29.6	
PR				
Neg	*61*	7	11.5	**0.0553**
Pos	*29*	8	27.6	
HER-2 IHC				
2+	*20*	4	20.0	0.9564
3+	*112*	23	20.5	
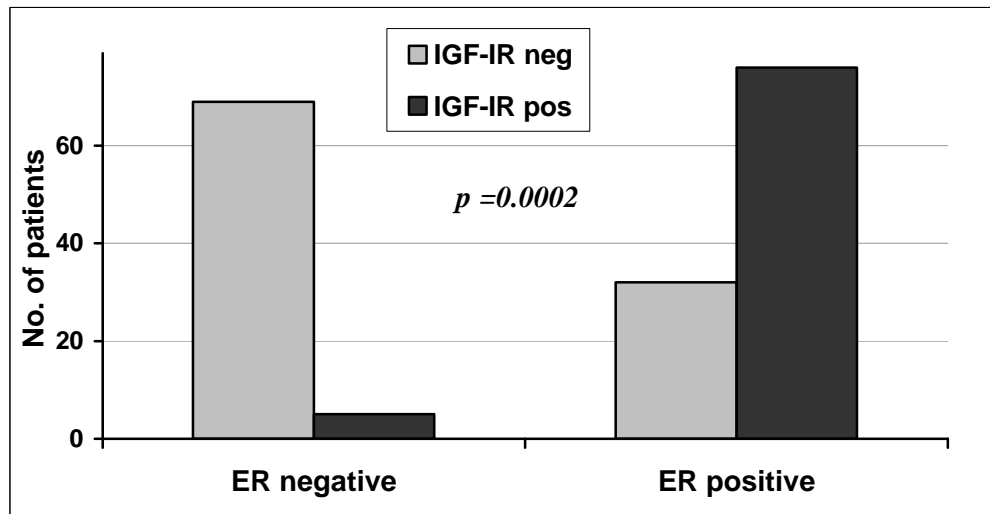
Fig 7.10 Number of patients and with membrane IGF-IR-positive and –negative
staining in ER-positive and –negative tumour groups. The relationships were analysed
by the Chi-squared test.

_____

7.4   POOLED ANALYSIS OF HER-2 AND IGF-IR IN STUDY 1 AND STUDY 2

Although no correlation between HER-2 and IGF-IR expression was observed in either study, pooled analysis of IGF-IR and HER-2 staining from study 1 and study 2 shows that there is a significant inverse correlation between membrane IGF-IR and HER-2 expression, with HER-2 score 0 tumours showing the highest frequency of IGF-IR membrane staining (32.3%,   42/130) and HER-2 3+ tumours having the lowest frequency of IGF-IR membrane staining (15.3%, 15/98) (Chi-squared test, $p = 0.025$) [Fig. 7.11].

_____
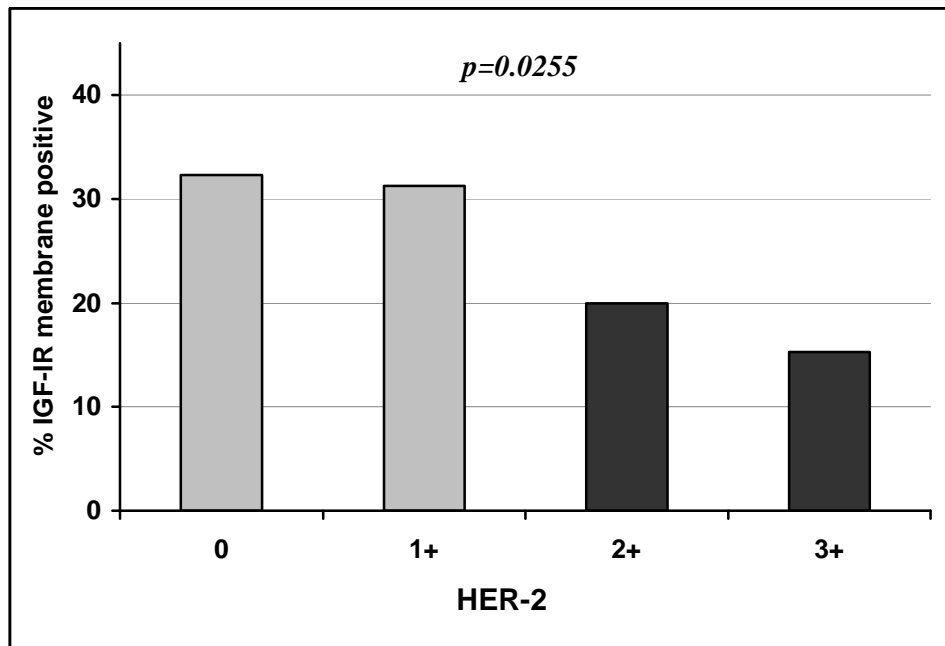
Figure 7.11 Number of patients with membrane IGF-IR staining in HER-2 0, 1+, 2+ and 3+ tumours in both study 1 and study 2. The relationships were analysed by the Chi-squared test.

_____

Chapter 8

DISCUSSION

HER-2, EGFR and IGF-IR signalling in breast cancer cells and response to trastuzumab

Long-term response rates to trastuzumab monotherapy in HER-2-overexpressing breast cancer patients are low, ranging from 12-34%, and with median response durations of only 9–12 months [133, 134]. Data has been emerging to suggest the role of alternative receptor tyrosine kinase (RTK) signalling, such as IGF-IR or EGFR signalling, in trastuzumab-resistance [163, 164, 177, 180]. In this study, response to trastuzumab was investigated in a panel of 14 HER-2-overexpressing breast cancer cell lines. HER-2 expression or activity levels did not correlate with response to trastuzumab. IGF-IR expression or phosphorylation also did not correlate with response. EGFR protein levels and phosphorylation levels were also analysed, and no correlation with response was observed. These data suggest that alternative signalling via IGF-IR or EGFR does not play a key role in innate trastuzumab resistance in HER-2 positive breast cancer.

When the relationships between total protein expression and phosphorylation of each of the three receptors were analysed, no correlation was observed between receptor expression and phosphorylation of HER-2, IGF-IR or EGFR. However, both HER-2 and phospho-HER-2 levels correlated positively with phospho-IGF-IR, and a trend was also observed between IGF-IR and phospho-EGFR levels. These results are consistent with previous reports of cross-talk between IGF-IR and EGFR/HER-2 signalling pathways. Stimulated EGFR can transactivate IGF-IR, and IGF-IR in turn can cause transactivation of EGFR [306, 346, 347]. Targeting EGFR with the tyrosine kinase inhibitor (TKI) gefitinib reduced IGF-I-stimulated Erk activity in normal mammary epithelial cells [349], and elevated IGF-IR signalling has been implicated in resistance to gefitinib and erlotinib, another EGFR TKI [307, 351]. Previous studies also reported interactions between HER-2 and IGF-IR signalling; Balana *et al* [353] reported that knockdown of IGF-IR protein inhibited HER-2-stimulated proliferation in mammary tumour primary cells, and decreased phosphorylation of HER-2 [182]. They also found that suppression of HER-2 expression had no effect on IGF-IR phosphorylation, suggesting a hierarchical interaction, whereby IGF-IR directs HER-2 phosphorylation. Here, we confirmed previous reports [354] that overexpression of HER-2 inhibits IGF-I-stimulated MAPK signalling in MCF7 cells, suggesting that HER-2 sends proliferative signals through the MAPK pathway in an IGF-IR-independent manner. Previous reports have shown that HER-2-overexpression does not affect IGF-IR-mediated Akt signalling

[354], and in HER-2 overexpressing cells in culture, Akt is predominantly activated by serum elements [356], suggesting that Akt signalling in HER-2-overexpressing cells may be directed by IGF-IR. We also found that HER-2 overexpression did not significantly alter Akt phosphorylation in response to IGF treatment in MCF-7-HER-2 cells. However, trastuzumab treatment of MCF7-HER2-cells reduced IGF-I-stimulated phosphorylation of Akt. Therefore, though an increase in HER-2 expression does not alter IGF-IR-Akt signalling, inhibition of HER-2 signalling does; this suggests that HER-2 may also regulate IGF-IR-Akt activity. Overall, these data suggest that HER-2 proliferation signals may be independent of IGF-IR, while its survival signalling may interact with that of IGF-IR in a complex manner.

Lu *et al* [177] reported that reduction of IGF-IR signalling in MCF7/HER-2-18 cells by reducing the serum content of the growth media restores sensitivity to trastuzumab. In this study, also in an MCF7 HER2-transfected cell line, reduction of serum in the growth media did not sensitise cells to trastuzumab; these cells were in fact less responsive in these conditions. This may be explained by the fact that the cells grew at a slower rate in reduced serum. Trastuzumab inhibits proliferation in growing cells; if proliferation has diminished, the inhibitory effects of trastuzumab are also likely to be reduced. Perhaps the MCF7/HER-2-18 cells studied by Lu *et al* [177] have a higher level of transfected HER-2, which could result in phenotypically different cells, possibly with a different growth rate. Those cells could, therefore, be less dependent on serum elements for growth, and this may explain the different results obtained. Differences in the growth factor content of the serum used in the two studies could also contribute to the inconsistency in results.

HER-2, EGFR and IGF-IR in acquired trastuzumab resistance
SKBR3 and BT474 parental and trastuzumab-conditioned cell lines were obtained from Dr. Slamon's laboratory, UCLA. We confirmed that the conditioned cells had acquired resistance to trastuzumab relative to parental cells, and that this resistance was stable after trastuzumab was removed from the growth media for up to three months. Molecular differences between parental and resistant cells were then investigated. HER-2, phospho-HER2, EGFR and phospho-EGFR levels were significantly elevated in BT474/Tr compared to parental BT474 cells, while no alteration in IGF-IR

expression or phosphorylation was observed. These results are consistent with recent reports of trastuzumab-resistant BT474 models. Ritter *et al* [429] developed a trastuzumab-resistant cell model from BT474 xenografts treated with trastuzumab. These cells retained HER-2 amplification and trastuzumab-binding, and had increased levels of EGFR, phospho-EGFR, and EGFR ligands [163]. Higher levels of EGFR/HER-2 heterodimers were detected in the resistant cells, suggesting that this could be a possible mechanism of resistance, as trastuzumab does not have the ability to block heterodimerisation [163]. Therefore, our BT474/Tr cells, which have elevated HER-2 and EGFR levels and signalling, may be less responsive to trastuzumab due to increased heterodimerisation between HER-2 and EGFR.

SKBR3/Tr cells showed no change in HER-2 expression or phosphorylation compared to parental cells; however, phospho-EGFR levels were significantly reduced. SKBR3/Tr cells also have significantly elevated IGF-IR levels compared to parental cells. Previous studies have reported that transfection of IGF-IR into SKBR3 cells confers resistance to trastuzumab, and that increased IGF-IR signalling mediates trastuzumab resistance [177, 180]. However, phospho-IGF-IR levels were not altered in SKBR3/Tr compared to parental SKBR3 cells. Perhaps investigation of IGF-IR response to stimulation would reveal differences in IGF-IR activity in these cells. In this model, cells were treated with fresh growth media 24 hours before protein lysis. A previous report has shown that IGF-I stimulation of IGF-IR causes maximal phosphorylation of IRS-1 within 1-2 minutes [178]. It is possible that differences in IGF-IR activity between parental and resistant cells would be apparent at earlier timepoints following stimulation, but that by 24 hours, IGF-IR activity has returned to basal levels in both cell lines.

Given that there appears to be increased HER-2 and EGFR signalling in BT474/Tr cells, one would expect to find elevated levels of Akt and MAPK signalling. However, the BT474/Tr cells have reduced phospho-Akt and phospho-MAPK levels compared to parental cells. This reduced signalling could be due to an increase in EGFR-containing receptor dimers, caused by the increase in EGFR expression. HER-2 has the strongest kinase activity of the HER family [16], and increased formation of EGFR/HER-2 heterodimers, accompanied by a reduction in HER-2 homodimerisation, could cause an overall reduction in HER intracellular signalling. It is also possible that HER signalling

through alternative pathways has increased to compensate for reduced Akt and MAPK activity; investigation of other signalling pathways, such as the PKC signalling pathway, would be required to determine if this is the case.

SKBR3/Tr cells have reduced EGFR activity, but unaltered phospho-MAPK levels, compared to parental SKBR3 cells. In a study mentioned above [349], IGF-I-stimulated Erk activity was regulated by EGFR signalling in normal mammary cells; however, targeting EGFR had no effect on IGF-IR signalling in MCF7 and CAL-51 breast cancer cells [349], which have high IGF-IR levels. Perhaps cells with increased IGF-IR expression, such as SKBR3/Tr, are no longer dependent on EGFR for MAPK signalling.

SKBR3/Tr cells have reduced phospho-Akt levels compared to SKBR3 cells. However, trastuzumab treatment had similar effects on phospho-Akt and phospho-MAPK levels in SKBR3 and SKBR3/Tr cells, as measured by immunoblotting. This suggests that alterations in Akt and MAPK signalling may not be playing a central role in resistance to trastuzumab in this model. In fact, Smith et al [185] analysed both phospho-Akt and phospho-MAPK levels in trastuzumab-treated breast cancer patient samples, and found no correlation between response and levels of either phospho-protein. However, response to trastuzumab in SKBR3/Tr cells is not completely diminished compared to parental cells; therefore, a similar, but reduced, effect on intracellular signalling in response to trastuzumab might be expected. The reduction in phospho-Akt and phospho-MAPK levels appear similar by western blotting but more subtle alterations may not be observed by this technique, and might be detected by a more sensitive method of detection, such as ELISA.

Overall, these data suggest differences in the mechanisms of resistance to trastuzumab in BT474/Tr and SKBR3/Tr cells, characterised by different receptor activity and different signalling pathways. Consistently, a previous study reported that HER-2 signalling via Akt had different effects in SKBR3 and BT474 cells; inhibition of HER-2/Akt signalling using trastuzumab and an Akt inhibitor increased the susceptibility of SKBR3 cells to TRAIL-induced apoptosis, but decreased the susceptibility of BT474 cells [430].

Nahta *et al* [181] reported that HER-2 and IGF-IR heterodimerise in trastuzumab-resistant SKBR3/HerR cells, and not in parental SKBR3 cells, and suggested that heterodimerisation contributes to trastuzumab resistance. IGF-I also stimulated phosphorylation of HER-2 only in the resistant cells, while a specific IGF-IR tyrosine kinase inhibitor decreased phosphorylation, again only in the resistant cells. Earlier studies, however, have shown that HER-2 and IGF-IR heterodimerise in response to IGF-I or heregulin in MCF7 cells [182], and that knocking out IGF-IR expression in breast cancer cells and xenografts also reduced HER-2 phosphorylation [182, 183]. Furthermore, in our study, HER-2 and phospho-HER-2 levels correlated with phospho-IGF-IR levels in the panel of cell lines, which contained both trastuzumab-sensitive and –resistant cells. Heterodimerisation and activation of HER-2 by IGF-IR, therefore, does not appear to be exclusively a characteristic of trastuzumab resistant cells. We immunoprecipitated (IP) IGF-IR protein from SKBR3 and BT474 parental and resistant cell lysates, and immunoblotted for HER-2 protein, to investigate if HER-2 co-precipitated with IGF-IR. Trastuzumab was removed from the growth media of resistant cells for at least seven days before protein lysate preparation. HER-2 was detected in parental and resistant immunoprecipitated samples, only when the cells had been treated with trastuzumab for 24 hours, suggesting that trastuzumab treatment may induce dimerisation. However, in control IPs without antibody, HER-2 was also precipitated, suggesting that trastuzumab itself immunoprecipitated HER-2 in these samples. Attempts were also made to immunoprecipitate HER-2 and investigate the co-precipitation of IGF-IR. However, the IP for IGF-IR was not successful. In a control experiment, IGF-IR was immunoprecipitated from MCF7-HER-2 cells, (which express high IGF-IR levels) and IGF-IR immunoblotting was subsequently performed; however, IGF-IR could not be detected. A number of IGF-IR antibodies were tested, without success. Therefore we were unable to confirm the presence of HER-2/IGF-IR heterodimers. Perhaps the development of more sensitive and specific anti-IGF-IR antibodies will aid such investigations in the future.

Inhibition of IGF-IR in HER-2-positive breast cancer cells
Previous studies have reported that inhibition of IGF-I/IGF-IR signalling sensitises trastuzumab-resistant cells to trastuzumab [180, 181]. However, we found that blocking IGF-IR stimulation with IGFBP3 or aIR3 antibody did not sensitise SKBR3/Tr or

BT474/Tr cells to trastuzumab. Although SKBR3/Tr cells have elevated IGF-IR levels, targeting ligand-activation of the receptor has no effect on proliferation. Perhaps resistant cells have developed ligand-independent mechanisms of IGF-IR signalling; an intracellular mechanism of IGF-IR activation has been reported [431].

In contrast, knockdown of IGF-IR expression with siRNA inhibited proliferation in both parental and trastuzumab-resistant BT474 and SKBR3 cells. The combination of anti-IGF-IR siRNA and trastuzumab had significantly greater inhibitory effects than either treatment alone in the two resistant cell lines. This enhanced effect was also seen in parental SKBR3 cells. IGF-IR signalling was also targeted in these cells with IGF-IR TKIs BMS-536924 and NVP-AEW541. Each inhibitor alone had little effect on the proliferation of BT474 or BT474/Tr cells. BT474 cells are estrogen-receptor (ER)-positive, while SKBR3 cells are ER-negative. Cross-talk between IGF-IR and ER signalling pathways has been reported, and ER signalling enhances IGF-IR signalling in breast cancer cells [334]; ER upregulation of IGF-IR signalling could therefore compensating for IGF-IR tyrosine kinase inhibition in BT474 cells. A recent study reported synergistic effects when combining NVP-AEW541 with an ER inhibitor in MCF7 and T474D breast cancer cells [432]. However, in BT474/Tr cells, combined treatment of each TKI with trastuzumab inhibited significantly more growth than single treatments. BT474/Tr cells have elevated EGFR signalling. EGFR has also been shown to heterodimerise with IGF-IR in breast cancer cells [349]; perhaps BT474Tr cells have increased levels of EGFR heterodimerisation with both HER-2 and IGF-IR; so while targeting HER-2 or IGF-IR alone has little effect, co-targeting HER-2 and IGF-IR inhibits signalling from HER-2/HER-2, IGF-IR/IGF-IR and IGF-IR/EGFR dimers, resulting in enhanced inhibitory effects.

SKBR3 and SKBR3/Tr cells were unresponsive to BMS-536924, either alone or in combination with trastuzumab. NVP-AEW541, however, inhibited proliferation by approximately 30 % in both SKBR3 and SKBR/Tr cells. Combined treatment of NVP-AEW541 and trastuzumab had significantly enhanced inhibitory effects compared to either treatment alone in both cell lines. In cell cycle assays, NVP-AEW541 increased the number of cells in the G1 phase in both SKBR3 and SKBR3/Tr cells, and combined treatment with NVP-AEW541 and trastuzumab significantly increased the number of cells in G1, and significantly decreased the number of cells in the synthesis phase

compared to untreated cells, suggesting that both NVP-AEW541 and trastuzumab may induce G1 arrest. These data support the potential for co-targeting HER-2 and IGF-IR in the clinical setting, both in trastuzumab-sensitive patients, and those who have developed resistance.

The differences in protein expression and phosphorylation, and response to IGF-IR inhibition, in BT474/Tr and SKBR3/Tr cells suggest that these two cell models differ in their RTK dependency for growth and survival, and that the role of IGF-IR or other RTKs in the development of trastuzumab resistance may vary by cell line, or by patient.

Response to lapatinib in trastuzumab-resistant cells

In order to study cross-resistance between trastuzumab and other HER-2 antagonists, response to lapatinib, a dual HER-2/EGFR TKI, was examined in parental and trastuzumab-resistant BT474 and SKBR3 cells. Lapatinib inhibited similar levels of proliferation in BT474 and BT474/Tr cells, with IC_{50} values of 23 nM and 26 nM, respectively. SKBR3/Tr cells were less responsive to lapatinib than parental SKBR3 cells, with an IC_{50} of 132 nM, compared to 62 nM in parental cells, suggesting some level of cross-resistance to lapatinib in the trastuzumab-resistant cells. Comparing these results to published data, each of the four cell lines is considered sensitive to lapatinib [113]. Again, these results suggest that SKBR3/Tr and BT474/Tr cells may have different mechanisms of resistance to trastuzumab; SKBR3/Tr cells display some cross-resistance to lapatinib, while BT474/Tr cells do not. BT474/Tr cells have elevated HER-2 and EGFR signalling, and may therefore be expected to be more sensitive to HER-2/EGFR tyrosine kinase inhibition. The increase in EGFR activity, however, may not significantly affect response to lapatinib; in a phase II study of lapatinib in breast cancer patients grouped into HER-2-postive and EGFR-positive/HER-2-negative patients, the response rates were 62 % in the HER-2-positive group, and only 8 % in the EGFR-positive/HER-2-negative group [187], suggesting that response to lapatinib is determined more by HER-2 than by EGFR expression. Though the IC_{50} concentrations were similar for BT474 and BT474/Tr the maximum growth inhibition achieved in BT474/Tr cells (95.7 %) was higher than in BT474 cells (86.7 %), although not significantly; this effect could be related to higher levels of HER-2 expression in BT474/Tr. Overall, the results with lapatinib suggest that HER-2-overexpressing

patients that have developed resistance to trastuzumab would benefit from lapatinib treatment. Work in this and other laboratories has shown synergistic inhibitory effects with combinations of lapatinib and trastuzumab *in vitro* [113], and lapatinib has also shown clinical efficacy alone or in combination with trastuzumab against breast cancer in phase II and III clinical trials [187].

Lapatinib and trastuzumab resistance in breast cancer cells

One study of *in vitro* acquired lapatinib resistance has been reported [196]. In a BT474 model of lapatinib resistance, a switch from dependence on HER-2 signalling to co-dependence on HER-2 and ER signalling was observed. We conditioned trastuzumab-sensitive and -resistant HER-2-overexpressing, ER negative cells in lapatinib-containing growth media, to investigate the development of lapatinib resistance in ER negative breast cancer. SKBR3 (trastuzumab-sensitive), and HCC1419 (trastuzumab-resistant) cells were conditioned in lapatinib for six months. SKBR3 cells were also conditioned with trastuzumab alone, and trastuzumab combined with lapatinib, to investigate development of resistance to the co-treatment, SKBR3-TL, compared to the single agents, SKBR3-T and SKBR3-L. The trastuzumab-resistant SKBR3/Tr cells from UCLA were also conditioned in lapatinib-containing media in order to develop a model for lapatinib treatment in patients who have progressed on trastuzumab treatment.

SKBR3-L, SKBR3-TL and SKBR3/Tr-L cells developed resistance to both trastuzumab and lapatinib, as demonstrated by standard proliferation assays and doubling time assays. SKBR3-T cells are resistant to trastuzumab yet retain their sensitivity to lapatinib. This is consistent with clinical findings; HER-2-positive patients who have progressed on trastuzumab benefit from lapatinib treatment [187]. However, lapatinib-resistant SKBR3-L cells demonstrate cross-resistance to trastuzumab, and are in fact more resistant to inhibition by trastuzumab than trastuzumab-resistant SKBR3-T cells. SKBR3-TL cells are also resistant to inhibition by the combined treatment of trastuzumab and lapatinib. These data may have important clinical implications. While lapatinib has shown clinical efficacy in combination with trastuzumab [187], these results suggest that patients on the combination therapy may develop resistance to both agents. Scheduling of treatment could be important to maximise clinical benefit. If patients progress on trastuzumab treatment, they may still benefit from lapatinib

treatment; however, if patients were treated with lapatinib first and progress, they may also be resistant to trastuzumab treatment.

Lapatinib-conditioned HCC1419-L cells did not develop resistance to lapatinib. This model may also have clinical relevance. The concentration of lapatinib used to condition the cells initially inhibited approximately 80 % of cell growth. The remaining cells maintained their viability, but did not actively proliferate during lapatinib treatment. When lapatinib treatment was discontinued after six months, the cells remained quiescent for a further three months. After this time, the cells began to proliferate again, and a proliferation assay showed that they had retained their sensitivity to lapatinib. This may suggest that some patients who relapse after completion of lapatinib treatment may benefit from further lapatinib treatment.

HER-2, phospho-HER-2 and EGFR levels were not altered in the conditioned SKBR3 cells, suggesting that alterations in other cellular pathways may be responsible for resistance. A number of TKIs are substrates for drug efflux pumps, such as p-glycoprotein (P-gp), and elevated levels of drug efflux pumps have been implicated in resistance to a number of number of anti-cancer agents [433]. Lapatinib is a P-gp substrate [434] and P-gp levels were therefore measured in the lapatinib-resistant SKBR3-L and SKBR3-TL cells; however, no detectable increase in P-gp levels was observed in these cells.

IGF-IR levels were also measured in the conditioned SKBR3 cells, and each of SKBR3-T, SKBR3-L and SKBR3-TL cells had elevated IGF-IR expression. IGF-IR has been implicated in resistance to EGFR TKIs erlotinib and gefitinib in breast cancer cells [307, 351]. However, using our ELISA data, our collaborators in UCLA found a positive correlation between phospho-IGF-IR levels and response to lapatinib in a panel of breast cancer cell lines [O'Brien *et al*, manuscript in preparation]. Furthermore, a recent phase II clinical trial also reported a positive correlation between IGF-IR expression and response to lapatinib monotherapy in 30 HER-2-positive breast cancer patients [108]. It is possible that IGF-IR signalling could play different roles in acquired and intrinsic lapatinib resistance.

As SKBR3-L cells displayed the highest level of resistance to both trastuzumab and lapatinib, downstream phosphoprotein signalling was investigated in these cells. No alteration in phospho-Akt or phospho-MAPK, as measured by immunoblotting, was observed in SKBR3-L compared to parental SKBR3 cells.

Phosphoproteomic analysis was performed in order to further investigate differences in protein phosphorylation, and thus signalling, between parental SKBR3 and lapatinib-resistant SKBR3-L cells. Phosphoproteins which were differentially regulated in SKBR3-L compared to SKBR3 cells, and in response to either trastuzumab or lapatinib were identified.

Many phosphorylated forms of heat shock proteins (Hsp) were found to be differentially regulated in SKBR3 and SKBR3-L cells. Hsp proteins are activated by phosphorylation, and are regulated by both Akt and MAPK signalling pathways [435]. Two phosphorylated forms of aB-crystallin were 11.26- and 7.74-fold more abundant in SKBR3-L cells. aB-crystallin is a small Hsp family member that is constitutively expressed in many tissues [436]. aB-crystallin is a negative regulator of apoptosis, and has been reported as a specific marker for basal-like breast cancer, and a predictor of poor clinical outcome [437, 438]. Expression of aB-crystallin was also found at a low frequency (16 %) in HER-2-positive breast cancers [439]. Overexpression of aB-crystallin was recently correlated with resistance to neoadjuvant trastuzumab and vinorelbine in a study of 48 HER-2-positive breast cancer patients [440]. Perhaps cells with higher aB-crystallin activity have become less dependent on HER signalling, and are therefore less sensitive to HER-2 inhibition. Inhibition of apoptosis by aB-crystallin could contribute to lapatinib resistance in SKBR3-L cells. In fact, phospho-aB-crystallin levels were increased 1.63-fold in lapatinib-treated parental cells, suggesting that increasing this regulator of apoptosis could be one cellular mechanism of opposing the cytotoxic effects of lapatinib.

A phosphorylated form of closely related family member Hsp27 was also found to be upregulated 2.38-fold in SKBR3-L cells. Hsp27 expression is associated with increased invasiveness and resistance to chemotherapeutic drugs, and with poor prognosis in breast cancer [441]. Hsp27 protects from apoptosis by a number of mechanisms, including direct interaction with cytochrome C, and with both Akt and MAPK [442].

Higher Hsp27 expression was found in gefitinib-resistant compared to gefitinib-responsive colorectal cancer cell lines studied by proteomics [443], suggesting that increased interaction between Hsp27 and Akt and MAPK could be protecting these pathways from downregulation by HER-2/EGFR family inhibitors.

Expression of a phosphorylated form of another Hsp, glycoprotein 96 (gp96/tumor rejection antigen) was also significantly increased (2.16-fold) in SKBR3-L cells. Gp96 has been related to resistance to chemotherapeutic drugs [444], and has been found to be expressed on the surface of breast cancer cells [445]. Gp96 is known to have immune-stimulatory properties and its potential for use in cancer therapeutics has been acknowledged [445].

Expression of a phosphorylated form of Hsp70 (HSPA1A) was downregulated (1.36-fold) in SKBR3-L cells compared to parental SKBR3 cells. The Hsp70 family are chaperone proteins that form a complex with Hsp90 proteins, regulating the maturation, stability and activity of numerous cellular proteins, including hormone receptors, and RTKs such as HER-2 [446]. Hsp70 also has important anti-apoptotic functions, interacting with the intrinsic and extrinsic apoptotic pathways at multiple steps, and can protect cells from apoptosis-induction by chemotherapy [436]. Elevated levels of Hsp70 have been reported in breast and other cancers, where they are associated with worse prognosis [446-448]. Both trastuzumab and lapatinib treatment of parental SKBR3 caused decreases in phospho-Hsp70 levels (1.27- and 1.35-fold, respectively). This suggests that downregulation of Hsp70 activity may play a role in response to these inhibitors. Lapatinib-resistant cells have decreased phospho-Hsp70 levels, and may therefore be less reliant on Hsp70 activity for survival.

A number of phosphorylated forms of the protein eukaryotic translation elongation factor 2 (eEF2) were significantly differentially regulated in SKBR3-L compared to parental SKBR3 cells. eEF2 is an enzyme that plays an important role in protein synthesis, where it mediates ribosomal translocation during peptide chain elongation. The activity of eEF2 is inhibited by its phosphorylation (at Thr^{56} and Thr^{58}) by eEF2 kinase (eEF2K), which in turn is regulated by mTOR and p70 ribosomal S6 kinase (p70S6K) [449]. One form of phosphorylated eEF2 was upregulated in SKBR3-L,

while six were downregulated. This suggests that there are higher levels of eEF2 activity in SKBR3-L cells, and therefore a greater level of protein synthesis, and this may be a mechanism of resistance to inhibitors of HER-2 signalling.

Between five and seven forms of phospho-eEF2 are downregulated in response to trastuzumab or lapatinib in both parental SKBR3 and SKBR3-L cell lines. However, three phospho-eEF2 isoforms are significantly upregulated in parental cells treated with either drug, and are not affected by either treatment in SKBR3-L cells. Downregulation of the phosphorylation of these three isoforms may therefore play a role in response to HER-2-antagonism in these cells. Recent studies reported that eEF2 phosphorylation accompanied inhibition of protein synthesis by a farnesyltransferase inhibitor (FTI) induced in head and neck cancer cell lines, and by a new mTOR inhibitor in multiple human cancer cell lines [450, 451].

Multiple phosphorylation sites were identified on five forms of eEF2 which are downregulated in SKBR3-L cells. Three had one or two phospho-sites identified on the peptide sequence ranging from amino acids 51 – 61. This peptide region contains Thr^{56} and Thr^{58}; therefore, downregulation of phosphorylation of eEF2 at these sites in resistant cells, which would enhance eEF2 activity and promote protein synthesis, may be contributing to the resistant phenotype of these cells. Components upstream of eEF2 have recently been implicated in lapatinib resistance. Lapatinib-resistant MCF7-HER-2 cells had significantly elevated phosphorylation and activity of p70S6K1, and treatment with rapamycin, which targets mTOR, decreased phosphorylation, and re-sensitised these cells to lapatinib [452]. Together, these data suggest that alterations in the mTOR/p70S6K/eEF2 pathway could play a role in resistance to lapatinib. It would also be interesting, therefore, to examine expression or activity of other components of this pathway in the resistant cell lines. Inhibitors of this pathway could also be used to further investigate its role in these cells.

A phosphorylated form of another protein of the translation machinery, eukaryotic initiation factor 4A (eIF4A) was also found to be significantly downregulated by lapatinib treatment in parental cells and not in SKBR3-L cells. eIF4A is a RNA helicase that forms part of a complex that binds the cap structure of mRNA, facilitating mRNA ribosome binding. eIF4A overexpression has been reported in human melanoma cells

and in primary hepatocellular carcinomas [453, 454]. eIF4A is regulated by the transformation repressor programmed cell death 4 gene (PDCD4) which inhibits eIF4A activity. Afonja *et al* [455] observed that trastuzumab induced PDCD4 expression in T47D breast cancer cells, suggesting that PDCD4 inhibition of protein translation may play a role in trastuzumab-mediated growth inhibition. Inhibition of eIF4A activity may also play a role in response to lapatinib in SKBR3 cells.

Two members of the S100 family of calcium-binding proteins were also found to be differentially regulated in SKBR3-L cells compared to parental cells. This large group of proteins is expressed in various tissues and is implicated in the immune response, differentiation, cytoskeleton dynamics, enzyme activity, Ca2+ homeostasis and growth [456]. A phosphorylated form of S100A8 (calgranulin A), and three forms of phosphorylated S100A9 (Mrp14/calgranulin B) are significantly upregulated in SKBR3-L cells. S100A8 and S100A9 form a complex called calprotectin, which is found at high levels at sites of inflammation [457]. Phosphorylation of S100A9 promotes calcium-binding, and upregulates its translocation from the cytoplasm to the plasma membrane and the cytoskeleton [458]. Phosphorylation sites were detected on two of the three S100A9 isoforms identified; increased phosphorylation at these sites may therefore be increasing calprotectin activity in SKBR3-L cells, and may contribute to lapatinib resistance in this model. S100A8 and S100A9 have been implicated in a number of cancers; they are both overexpressed in breast cancer [457], where a recent study reported highest expression in triple negative tumours [459]. Increased expression of both proteins was also found in three antiestrogen-resistant breast cancer cell lines [460]. Perhaps the antiestrogen-resistant cells, and our anti-HER-2-resistant SKBR3-L cells, are developing a phenotype resembling that of triple-negative or basal-like breast cancers, with reduced requirements for ER and HER-2 signalling. As mentioned above, SKBR3-L cells also have a significant increase in phosphorylated aB-crystallin, which is a recognised marker for basal-like breast cancer. Indeed, Harris et al [440] showed that HER-2 positive breast cancers with a basal-like phenotype were more likely to be resistant to the neoadjuvant combination of trastuzumab and vinorelbine. These results suggest that it may be interesting to examine expression of other markers of the basal-like phenotype, such as basal cytokeratins (CK 14/15, CK 5 and CK 17) in our resistant cell lines.

Phosphoproteomic analysis also identified a number of proteins that are involved in cytoskeleton modelling. Phosphorylated adseverin (scinderin), an actin-bundling protein, is upregulated in SKBR3-L cells, while phosphorylated forms of adenylylcyclase-associated protein (CAP1), and actinin-4, also actin-binding proteins, were downregulated in response to trastuzumab or lapatinib treatment in SKBR3 cells. Actinin-4 has been associated with cancer cell motility and invasion [461], and is overexpressed in a number of human cancers [462, 463].

A phosphorylated form of ubiquitin activating enzyme (E1) was also differentially regulated in response to lapatinib treatment in SKBR3 cells. This enzyme plays a role in the ubiquitin-proteosome pathway (UPP), where it catalyses the ubiquitination of protein substrates, which is the initial step in targeting proteins to the proteosome for degradation. A number of cancer-associated proteins are regulated by the UPP; these include p53, p27 and cell surface receptors including HER-2 and EGFR [464]. Response to lapatinib in SKBR3 cells may involve promoting the degradation of HER-2, or other cellular proteins such as p27, and this response could be mediated by E1. Dysregulation in the ubiquitin-proteosome pathway could contribute to irregular protein expression and activity in cells, and inhibitors of different components of this pathway, including E1 [465], are being investigated for use in human cancers.

A phosphorylated isoform of tryptophan 5-monooxygenase activation protein, otherwise known as 14-3-3, was upregulated 1.22-fold in SKBR3-L cells in response to trastuzumab, but was not altered in parental SKBR3 cells. 14-3-3 proteins are a family of cytosolic proteins that play key roles in a range of cellular processes including mitogenic and cell survival signalling, cell cycle control, apoptosis, vesicular trafficking, and cellular migration (reviewed in [466]). Both growth promoting and tumour suppressing actions have been demonstrated for 14-3-3; these are mediated via direct interactions with a number of cellular proteins, such as Raf, Bcr-Abl, IGF-IR, IRS-1, PI3K, p53, p27^{kip1}, p21^{waf1}, integrins and ADAM22 [466]. Studies have reported that phosphorylation at specific serine residues, including Ser^{58} can interfere with its ability to dimerize with target proteins [467]. Aberrant 14-3-3 activity has been implicated in breast cancer [468], where a role in the transcriptional regulation of HER-2 has been demonstrated [469], as well as an association with chemoresistance [470].

In our phosphoproteomic analysis, 14-3-3 levels were not altered in SKBR3-L cells compared to parental SKBR3 cells; however, levels of one phosphorylated form of this protein were altered in response to trastuzumab in SKBR3-L cells, and not in SKBR3 cells. This may suggest that altered 14-3-3 activity could be contributing to the trastuzumab-resistant phenotype of these cells.

Many phosphoproteins with potential roles in response or resistance to HER-2 antagonists have been identified. Examination of phosphoprotein levels by immunoblotting would confirm the observed alterations. Further work may then determine their specific roles in response or resistance. Stimulating or inhibiting phosphorylation of proteins of interest and investigating cellular responses such as proliferation, apoptosis induction, protein synthesis or degradation, or response to therapy would help to elucidate their roles.

HER-2 and IGF-IR expression in breast cancer patient samples

Analysis of HER-2 and IGF-IR expression in two groups of patient samples were performed. Study 1 was an analysis of 93 unselected breast cancer patients, and Study 2 was an analysis of HER-2 and IGF-IR expression in 223 HER-2-positive breast cancer patients. In study 1, HER-2-overexpression (scores of 2+ or 3+) was detected in 18 out of 90 patients (20.0%). This is consistent with published reports of HER-2 gene amplification or overexpression in 15-30% of invasive human breast cancers, where its expression is correlated with poor prognostic paramaters [53, 92]. In both TMA studies, HER-2 expression correlated positively with tumour grade. In Study 2, HER-2 expression was also significantly higher in ductal compared to lobular tumours, which is also consistent with previous reports [471]. A significant inverse association was observed between HER-2 expression and ER status, which has also been reported [92]. These data confirm the value of HER-2 overexpression as a predictor of poor prognosis in breast cancer.

Cytoplasmic IGF-IR expression was detected in over 99 % of the tumour samples studied. In Study 1, membrane IGF-IR expression was detected in 34 % of samples. Previous studies of IGF-IR have reported that IGF-IR is expressed in 39-93% of breast cancers [283, 288]. The variation in expression levels detected may be related to

measurement of either membrane or cytoplasmic IGF-IR. In study 1, cytoplasmic IGF-IR expression was significantly correlated with higher tumour grade. Reports of the prognostic significance of IGF-IR expression in breast cancer have been inconsistent and correlation with tumour grade has not been reported [278]. Correlation of IGF-IR with higher grade might suggest IGF-IR as an indicator of poor prognosis. However, an association was also observed between membrane IGF-IR expression and a lower number of positive nodes detected, suggesting IGF-IR expression as a predictor of positive outcome. Previous studies have also found an association between IGF-IR expression and negative nodal status [285]. IGF-IR is a membrane RTK, and its cellular localisation in breast cancer cells may, therefore, be an important determinant of its activity. Cytoplasmic and membrane IGF-IR expression, therefore, could have different prognostic significance in breast cancer. Further analysis into patient outcome in this cohort may determine the prognostic value of IGF-IR expression and localisation. Membrane expression of IGF-IR was not observed in any of the lobular tumours, suggesting that IGF-IR signalling may not play as central a role in cell signalling in these tumours, although the number of lobular tumours was small (n=13). Previous studies have also reported a lower frequency of IGF-IR expression in lobular than ductal tumours [273].

No association was observed between HER-2 and cytoplasmic or membrane IGF-IR expression in either TMA study. In Study 2, cytoplasmic IGF-IR expression was not associated with any of the prognostic parameters studied. Membrane IGF-IR expression was detected in 20 % of tumours in this group. Compared to membrane IGF-IR staining in 34 % of unselected breast cancer patients, this suggests that IGF-IR expression may be down-regulated in HER-2-positive tumours. Indeed, in the pooled analysis of study 1 and study 2, IGF-IR staining was detected significantly less frequently in HER-2-positive tumours. This relationship between IGF-IR and HER-2 expression in breast cancer has not previously been reported. However, membrane IGF-IR expression was recently correlated with lower response rates to neoadjuvant trastuzumab and vinorelbine in HER-2-positive patients [440]. The cellular localisation of IGF-IR may therefore be a determining factor in its involvement in trastuzumab response. Functional analysis of the cellular localisation of IGF-IR has not been reported, though the cytoplasmic form of IGF-IR is suggested to represent a bound form, internalised following ligand-stimulated activation [440].

Membrane IGF-IR expression was also detected significantly more frequently in ER-positive tumours than ER-negative tumours. Cross-talk between IGF-IR and ER signalling has been described in breast cancer cells, and previous studies have reported correlations between IGF-IR and both ER and PR expression in breast cancer patients [273]. Positive ER status is independently associated with better outcome in breast cancer, and in a study of patients with HER-2-positive breast cancer, those with tumours that also express ER had longer overall survival than those without ER [98]. Membrane IGF-IR expression, therefore, may also be associated with better outcome in HER-2-positive patients. However, a trend was also observed between positive membrane IGF-IR staining and tumour size in this group, suggesting a correlation between IGF-IR and disease progression in HER-2-positive breast cancer. Many of these patients have received trastuzumab treatment; further analysis of patient response and survival will be performed to determine correlations between IGF-IR cytoplasmic and membrane expression and patient outcome.

Summary and conclusion

In summary, these data show that HER family signalling pathways cross-talk with IGF-IR signalling in breast cancer cells. Signalling through alternative RTKs such as EGFR and IGF-IR does not seem to play a role in innate resistance to trastuzumab, but elevated IGF-IR or EGFR expression may play a role in acquired trastuzumab resistance. Targeting IGF-IR protein expression or tyrosine kinase activity improves response to trastuzumab in both trastuzumab-sensitive and -resistant cells.

Cytoplasmic IGF-IR was detected in 100 % of the HER-2-positive tumours analysed in this study. Membrane IGF-IR expression was detected significantly less frequently in HER-2-positive tumours. Further analysis of patient response to trastuzumab and overall patient survival may determine the role of IGF-IR expression and localisation in HER-2-overexpressing breast cancers, and in response to trastuzumab.

Thus, despite the fact that IGF-IR does not predict response to trastuzumab in the panel of cell lines, inhibiting both HER-2 and IGF-IR in HER-2-positive cells results in an

enhanced response; therefore, the combination of anti-IGF-IR therapy with trastuzumab may be clinically beneficial in patients with HER-2-overexpressing breast cancer.

Trastuzumab-resistant BT474, SKBR3 and HCC1419 cells are sensitive to the dual EGFR and HER-2 tyrosine kinase inhibitor lapatinib. Resistance to lapatinib, however, can also occur; in this study we present an ER-negative model of cells with stable resistance to both lapatinib and trastuzumab. It is likely that resistance to trastuzumab and/or lapatinib does not have a single cause, but rather, aberrations in multiple signalling pathways, caused by irregular activity of a number of cellular proteins, may be contributing to the resistant phenotype. The identification of such proteins is an important step in elucidating mechanisms of resistance. In this study, phosphoproteomic analysis revealed that SKBR3-L cells are characterised by many alterations in their phosphoproteome. This is the first reported study of phospho-proteomic profiling of lapatinib or trastuzumab resistant cells and we have identified a number of phosphoproteins with potential involvement in trastuzumab and/or lapatinib resistance. These include phosphoproteins involved in protein translation, maturation, and degradation, and in a wide range of cellular processes such as cell proliferation, apoptosis and migration. A number of these phosphoproteins represent rational targets for resistance to HER-2 antagonists and warrant further investigation. We anticipate that validation and functional analysis of these targets will lead to novel therapeutic targets and/or biomarkers for HER-2 resistant breast cancer.

REFERENCES

References

1. Sorlie, T., et al., *Repeated observation of breast tumor subtypes in independent gene expression data sets.* Proc Natl Acad Sci U S A, 2003. **100**(14): p. 8418-23.

2. Hu, Z., et al., *The molecular portraits of breast tumors are conserved across microarray platforms.* BMC Genomics, 2006. **7**: p. 96.

3. Sorlie, T., et al., *Gene expression patterns of breast carcinomas distinguish tumor subclasses with clinical implications.* Proc Natl Acad Sci U S A, 2001. **98**(19): p. 10869-74.

4. Akiyama, T., et al., *The product of the human c-erbB-2 gene: a 185-kilodalton glycoprotein with tyrosine kinase activity.* Science, 1986. **232**(4758): p. 1644-6.

5. Stern, D.F., P.A. Heffernan, and R.A. Weinberg, *p185, a product of the neu proto-oncogene, is a receptorlike protein associated with tyrosine kinase activity.* Mol Cell Biol, 1986. **6**(5): p. 1729-40.

6. Yarden, Y. and A. Ullrich, *Growth factor receptor tyrosine kinases.* Annu Rev Biochem, 1988. **57**: p. 443-78.

7. Citri, A., K.B. Skaria, and Y. Yarden, *The deaf and the dumb: the biology of ErbB-2 and ErbB-3.* Exp Cell Res, 2003. **284**(1): p. 54-65.

8. Hynes, N.E. and H.A. Lane, *ERBB receptors and cancer: the complexity of targeted inhibitors.* Nat Rev Cancer, 2005. **5**(5): p. 341-54.

9. Garrett, T.P., et al., *Crystal structure of a truncated epidermal growth factor receptor extracellular domain bound to transforming growth factor alpha.* Cell, 2002. **110**(6): p. 763-73.

10. Ogiso, H., et al., *Crystal structure of the complex of human epidermal growth factor and receptor extracellular domains.* Cell, 2002. **110**(6): p. 775-87.

11. Cho, H.S. and D.J. Leahy, *Structure of the extracellular region of HER3 reveals an interdomain tether.* Science, 2002. **297**(5585): p. 1330-3.

12. Garrett, T.P., et al., *The crystal structure of a truncated ErbB2 ectodomain reveals an active conformation, poised to interact with other ErbB receptors.* Mol Cell, 2003. **11**(2): p. 495-505.

13. Guy, P.M., et al., *Insect cell-expressed p180erbB3 possesses an impaired tyrosine kinase activity.* Proc Natl Acad Sci U S A, 1994. **91**(17): p. 8132-6.

14. Graus-Porta, D., et al., *ErbB-2, the preferred heterodimerization partner of all ErbB receptors, is a mediator of lateral signaling.* Embo J, 1997. **16**(7): p. 1647-55.

15. Tzahar, E., et al., *A hierarchical network of interreceptor interactions determines signal transduction by Neu differentiation factor/neuregulin and epidermal growth factor.* Mol Cell Biol, 1996. **16**(10): p. 5276-87.

16. Yarden, Y., *The EGFR family and its ligands in human cancer. signalling mechanisms and therapeutic opportunities.* Eur J Cancer, 2001. **37 Suppl 4**: p. S3-8.

17. Citri, A. and Y. Yarden, *EGF-ERBB signalling: towards the systems level.* Nat Rev Mol Cell Biol, 2006. **7**(7): p. 505-16.

18. Olayioye, M.A., et al., *ErbB-1 and ErbB-2 acquire distinct signaling properties dependent upon their dimerization partner.* Mol Cell Biol, 1998. **18**(9): p. 5042-51.

19. Marmor, M.D., K.B. Skaria, and Y. Yarden, *Signal transduction and oncogenesis by ErbB/HER receptors.* Int J Radiat Oncol Biol Phys, 2004. **58**(3): p. 903-13.

20. Sweeney, C. and K.L. Carraway, 3rd, *Ligand discrimination by ErbB receptors: differential signaling through differential phosphorylation site usage.* Oncogene, 2000. **19**(49): p. 5568-73.

21. Obermeier, A., et al., *Identification of Trk binding sites for SHC and phosphatidylinositol 3'-kinase and formation of a multimeric signaling complex.* J Biol Chem, 1993. **268**(31): p. 22963-6.

22. Yokote, K., et al., *Direct interaction between Shc and the platelet-derived growth factor beta-receptor.* J Biol Chem, 1994. **269**(21): p. 15337-43.

23. Pronk, G.J., et al., *Insulin-induced phosphorylation of the 46- and 52-kDa Shc proteins.* J Biol Chem, 1993. **268**(8): p. 5748-53.

24. Craparo, A., T.J. O'Neill, and T.A. Gustafson, *Non-SH2 domains within insulin receptor substrate-1 and SHC mediate their phosphotyrosine-dependent interaction with the NPEY motif of the insulin-like growth factor I receptor.* J Biol Chem, 1995. **270**(26): p. 15639-43.

25. De Meyts, P., et al., *Structural biology of insulin and IGF-1 receptors.* Novartis Found Symp, 2004. **262**: p. 160-71; discussion 171-6, 265-8.

26. Chan, T.O., S.E. Rittenhouse, and P.N. Tsichlis, *AKT/PKB and other D3 phosphoinositide-regulated kinases: kinase activation by phosphoinositide-dependent phosphorylation.* Annu Rev Biochem, 1999. **68**: p. 965-1014.

27. Chan, T.O. and P.N. Tsichlis, *PDK2: a complex tail in one Akt.* Sci STKE, 2001. **2001**(66): p. PE1.

28. Kulik, G., A. Klippel, and M.J. Weber, *Antiapoptotic signalling by the insulin-like growth factor I receptor, phosphatidylinositol 3-kinase, and Akt.* Mol Cell Biol, 1997. **17**(3): p. 1595-606.

29. Maehama, T. and J.E. Dixon, *The tumor suppressor, PTEN/MMAC1, dephosphorylates the lipid second messenger, phosphatidylinositol 3,4,5-trisphosphate.* J Biol Chem, 1998. **273**(22): p. 13375-8.

30. Datta, S.R., et al., *Akt phosphorylation of BAD couples survival signals to the cell-intrinsic death machinery.* Cell, 1997. **91**(2): p. 231-41.

31. Zha, J., et al., *Serine phosphorylation of death agonist BAD in response to survival factor results in binding to 14-3-3 not BCL-X(L).* Cell, 1996. **87**(4): p. 619-28.

32. Schulze, W.X., L. Deng, and M. Mann, *Phosphotyrosine interactome of the ErbB-receptor kinase family.* Mol Syst Biol, 2005. **1**: p. 2005 0008.

33. Lenferink, A.E., et al., *ErbB2/neu kinase modulates cellular p27(Kip1) and cyclin D1 through multiple signaling pathways.* Cancer Res, 2001. **61**(17): p. 6583-91.

34. Britsch, S., et al., *The ErbB2 and ErbB3 receptors and their ligand, neuregulin-1, are essential for development of the sympathetic nervous system.* Genes Dev, 1998. **12**(12): p. 1825-36.

35. Erickson, S.L., et al., *ErbB3 is required for normal cerebellar and cardiac development: a comparison with ErbB2-and heregulin-deficient mice.* Development, 1997. **124**(24): p. 4999-5011.

36. Morris, J.K., et al., *Rescue of the cardiac defect in ErbB2 mutant mice reveals essential roles of ErbB2 in peripheral nervous system development.* Neuron, 1999. **23**(2): p. 273-83.

37. Lee, K.F., et al., *Requirement for neuregulin receptor erbB2 in neural and cardiac development.* Nature, 1995. **378**(6555): p. 394-8.

38. Meyer, D. and C. Birchmeier, *Multiple essential functions of neuregulin in development.* Nature, 1995. **378**(6555): p. 386-90.

39.	Gassmann, M., et al., *Aberrant neural and cardiac development in mice lacking the ErbB4 neuregulin receptor.* Nature, 1995. **378**(6555): p. 390-4.

40.	Goodearl, A., A. Viehover, and T. Vartanian, *Neuregulin-induced association of Sos Ras exchange protein with HER2(erbB2)/HER3(erbB3) receptor complexes in Schwann cells through a specific Grb2-HER2(erbB2) interaction.* Dev Neurosci, 2001. **23**(1): p. 25-30.

41.	Nebigil, C.G., et al., *Serotonin 2B receptor is required for heart development.* Proc Natl Acad Sci U S A, 2000. **97**(17): p. 9508-13.

42.	Hertig, C.M., et al., *Synergistic roles of neuregulin-1 and insulin-like growth factor-I in activation of the phosphatidylinositol 3-kinase pathway and cardiac chamber morphogenesis.* J Biol Chem, 1999. **274**(52): p. 37362-9.

43.	Russell, K.S., et al., *Neuregulin activation of ErbB receptors in vascular endothelium leads to angiogenesis.* Am J Physiol, 1999. **277**(6 Pt 2): p. H2205-11.

44.	Andrechek, E.R., D. White, and W.J. Muller, *Targeted disruption of ErbB2/Neu in the mammary epithelium results in impaired ductal outgrowth.* Oncogene, 2005. **24**(5): p. 932-7.

45.	Press, M.F., C. Cordon-Cardo, and D.J. Slamon, *Expression of the HER-2/neu proto-oncogene in normal human adult and fetal tissues.* Oncogene, 1990. **5**(7): p. 953-62.

46.	Bast, R.C., Jr., et al., *Coexpression of the HER-2 gene product, p185HER-2, and epidermal growth factor receptor, p170EGF-R, on epithelial ovarian cancers and normal tissues.* Hybridoma, 1998. **17**(4): p. 313-21.

47.	Danova, M., et al., *HER-2/neu oncogene expression and DNA ploidy in normal human kidney and renal cell carcinoma.* Eur J Histochem, 1992. **36**(3): p. 279-88.

48.	Wiley, H.S., *Trafficking of the ErbB receptors and its influence on signaling.* Exp Cell Res, 2003. **284**(1): p. 78-88.

49.	Citri, A., B.S. Kochupurakkal, and Y. Yarden, *The achilles heel of ErbB-2/HER2: regulation by the Hsp90 chaperone machine and potential for pharmacological intervention.* Cell Cycle, 2004. **3**(1): p. 51-60.

50.	Sidera, K., et al., *A Critical Role for HSP90 in Cancer Cell Invasion Involves Interaction with the Extracellular Domain of HER-2.* J Biol Chem, 2008. **283**(4): p. 2031-41.

51.	Azios, N.G., et al., *Expression of herstatin, an autoinhibitor of HER-2/neu, inhibits transactivation of HER-3 by HER-2 and blocks EGF activation of the EGF receptor.* Oncogene, 2001. **20**(37): p. 5199-209.

52.	Lee, H., et al., *A naturally occurring secreted human ErbB3 receptor isoform inhibits heregulin-stimulated activation of ErbB2, ErbB3, and ErbB4.* Cancer Res, 2001. **61**(11): p. 4467-73.

53.	Zhang, H., et al., *ErbB receptors: from oncogenes to targeted cancer therapies.* J Clin Invest, 2007. **117**(8): p. 2051-8.

54.	Slamon, D.J., et al., *Studies of the HER-2/neu proto-oncogene in human breast and ovarian cancer.* Science, 1989. **244**(4905): p. 707-12.

55.	Pegram, M.D., G. Konecny, and D.J. Slamon, *The molecular and cellular biology of HER2/neu gene amplification/overexpression and the clinical development of herceptin (trastuzumab) therapy for breast cancer.* Cancer Treat Res, 2000. **103**: p. 57-75.

56. Chazin, V.R., et al., *Transformation mediated by the human HER-2 gene independent of the epidermal growth factor receptor.* Oncogene, 1992. **7**(9): p. 1859-66.

57. Di Fiore, P.P., et al., *erbB-2 is a potent oncogene when overexpressed in NIH/3T3 cells.* Science, 1987. **237**(4811): p. 178-82.

58. Hudziak, R.M., J. Schlessinger, and A. Ullrich, *Increased expression of the putative growth factor receptor p185HER2 causes transformation and tumorigenesis of NIH 3T3 cells.* Proc Natl Acad Sci U S A, 1987. **84**(20): p. 7159-63.

59. Kokai, Y., et al., *Synergistic interaction of p185c-neu and the EGF receptor leads to transformation of rodent fibroblasts.* Cell, 1989. **58**(2): p. 287-92.

60. Zhang, K., et al., *Transformation of NIH 3T3 cells by HER3 or HER4 receptors requires the presence of HER1 or HER2.* J Biol Chem, 1996. **271**(7): p. 3884-90.

61. Benz, C.C., et al., *Estrogen-dependent, tamoxifen-resistant tumorigenic growth of MCF-7 cells transfected with HER2/neu.* Breast Cancer Res Treat, 1992. **24**(2): p. 85-95.

62. Muthuswamy, S.K., et al., *ErbB2, but not ErbB1, reinitiates proliferation and induces luminal repopulation in epithelial acini.* Nat Cell Biol, 2001. **3**(9): p. 785-92.

63. Asanuma, H., et al., *Survivin expression is regulated by coexpression of human epidermal growth factor receptor 2 and epidermal growth factor receptor via phosphatidylinositol 3-kinase/AKT signaling pathway in breast cancer cells.* Cancer Res, 2005. **65**(23): p. 11018-25.

64. Woods Ignatoski, K.M., et al., *The role of phosphatidylinositol 3'-kinase and its downstream signals in erbB-2-mediated transformation.* Mol Cancer Res, 2003. **1**(7): p. 551-60.

65. Woods Ignatoski, K.M., et al., *p38MAPK induces cell surface alpha4 integrin downregulation to facilitate erbB-2-mediated invasion.* Neoplasia, 2003. **5**(2): p. 128-34.

66. Moasser, M.M., *The oncogene HER2: its signaling and transforming functions and its role in human cancer pathogenesis.* Oncogene, 2007. **26**(45): p. 6469-87.

67. Penuel, E., et al., *Structural requirements for ErbB2 transactivation.* Semin Oncol, 2001. **28**(6 Suppl 18): p. 36-42.

68. Zhan, L., B. Xiang, and S.K. Muthuswamy, *Controlled activation of ErbB1/ErbB2 heterodimers promote invasion of three-dimensional organized epithelia in an ErbB1-dependent manner: implications for progression of ErbB2-overexpressing tumors.* Cancer Res, 2006. **66**(10): p. 5201-8.

69. Yarden, Y. and M.X. Sliwkowski, *Untangling the ErbB signalling network.* Nat Rev Mol Cell Biol, 2001. **2**(2): p. 127-37.

70. Petit, A.M., et al., *Neutralizing antibodies against epidermal growth factor and ErbB-2/neu receptor tyrosine kinases down-regulate vascular endothelial growth factor production by tumor cells in vitro and in vivo: angiogenic implications for signal transduction therapy of solid tumors.* Am J Pathol, 1997. **151**(6): p. 1523-30.

71. Slamon, D.J., et al., *Human breast cancer: correlation of relapse and survival with amplification of the HER-2/neu oncogene.* Science, 1987. **235**(4785): p. 177-82.

72. Ross, J.S., et al., *The Her-2/neu gene and protein in breast cancer 2003: biomarker and target of therapy.* Oncologist, 2003. **8**(4): p. 307-25.

73. Press, M.F., et al., *Evaluation of HER-2/neu gene amplification and overexpression: comparison of frequently used assay methods in a molecularly characterized cohort of breast cancer specimens.* J Clin Oncol, 2002. **20**(14): p. 3095-105.

74. Sinczak-Kuta, A., et al., *Evaluation of HER2/neu gene amplification in patients with invasive breast carcinoma. Comparison of in situ hybridization methods.* Pol J Pathol, 2007. **58**(1): p. 41-50.

75. Gupta, D., et al., *Comparison of fluorescence and chromogenic in situ hybridization for detection of HER-2/neu oncogene in breast cancer.* Am J Clin Pathol, 2003. **119**(3): p. 381-7.

76. Dietel, M., et al., *Comparison of automated silver enhanced in situ hybridisation (SISH) and fluorescence ISH (FISH) for the validation of HER2 gene status in breast carcinoma according to the guidelines of the American Society of Clinical Oncology and the College of American Pathologists.* Virchows Arch, 2007. **451**(1): p. 19-25.

77. Ni, R., et al., *PGDS, a novel technique combining chromogenic in situ hybridization and immunohistochemistry for the assessment of ErbB2 (HER2/neu) status in breast cancer.* Appl Immunohistochem Mol Morphol, 2007. **15**(3): p. 316-24.

78. Revillion, F., J. Bonneterre, and J.P. Peyrat, *ERBB2 oncogene in human breast cancer and its clinical significance.* Eur J Cancer, 1998. **34**(6): p. 791-808.

79. Mirza, A.N., et al., *Prognostic factors in node-negative breast cancer: a review of studies with sample size more than 200 and follow-up more than 5 years.* Ann Surg, 2002. **235**(1): p. 10-26.

80. Goldhirsch, A., et al., *Progress and promise: highlights of the international expert consensus on the primary therapy of early breast cancer 2007.* Ann Oncol, 2007. **18**(7): p. 1133-44.

81. Goldhirsch, A., et al., *Meeting highlights: international expert consensus on the primary therapy of early breast cancer 2005.* Ann Oncol, 2005. **16**(10): p. 1569-83.

82. Sturgeon, C.M., et al., *National Academy of Clinical Biochemistry Laboratory Medicine Practice Guidelines for Use of Tumor Markers in Testicular, Prostate, Colorectal, Breast and Ovarian Cancers.* Clin Chem, in press.

83. Molina, R., et al., *Tumor markers in breast cancer- European Group on Tumor Markers recommendations.* Tumour Biol, 2005. **26**(6): p. 281-93.

84. Carney, W.P., et al., *Potential clinical utility of serum HER-2/neu oncoprotein concentrations in patients with breast cancer.* Clin Chem, 2003. **49**(10): p. 1579-98.

85. Ludovini, V., et al., *Evaluation of serum HER2 extracellular domain in early breast cancer patients: correlation with clinicopathological parameters and survival.* Ann Oncol, 2008.

86. Molina, M.A., et al., *NH(2)-terminal truncated HER-2 protein but not full-length receptor is associated with nodal metastasis in human breast cancer.* Clin Cancer Res, 2002. **8**(2): p. 347-53.

87. Xia, W., et al., *Truncated ErbB2 receptor (p95ErbB2) is regulated by heregulin through heterodimer formation with ErbB3 yet remains sensitive to the dual EGFR/ErbB2 kinase inhibitor GW572016.* Oncogene, 2004. **23**(3): p. 646-53.

88. Saez, R., et al., *p95HER-2 predicts worse outcome in patients with HER-2-positive breast cancer.* Clin Cancer Res, 2006. **12**(2): p. 424-31.

89.   Thor, A.D., et al., *Activation (tyrosine phosphorylation) of ErbB-2 (HER-2/neu): a study of incidence and correlation with outcome in breast cancer.* J Clin Oncol, 2000. **18**(18): p. 3230-9.

90.   DiGiovanna, M.P., et al., *Active signaling by HER-2/neu in a subpopulation of HER-2/neu-overexpressing ductal carcinoma in situ: clinicopathological correlates.* Cancer Res, 2002. **62**(22): p. 6667-73.

91.   Cicenas, J., et al., *Phosphorylation of tyrosine 1248-ERBB2 measured by chemiluminescence-linked immunoassay is an independent predictor of poor prognosis in primary breast cancer patients.* Eur J Cancer, 2006. **42**(5): p. 636-45.

92.   Menard, S., et al., *Role of HER2 gene overexpression in breast carcinoma.* J Cell Physiol, 2000. **182**(2): p. 150-62.

93.   Ross, J.S., et al., *Targeted therapy in breast cancer: the HER-2/neu gene and protein.* Mol Cell Proteomics, 2004. **3**(4): p. 379-98.

94.   Ferretti, G., et al., *HER2/neu role in breast cancer: from a prognostic foe to a predictive friend.* Curr Opin Obstet Gynecol, 2007. **19**(1): p. 56-62.

95.   Konecny, G., et al., *Quantitative association between HER-2/neu and steroid hormone receptors in hormone receptor-positive primary breast cancer.* J Natl Cancer Inst, 2003. **95**(2): p. 142-53.

96.   Stoica, G.E., et al., *Heregulin-beta1 regulates the estrogen receptor-alpha gene expression and activity via the ErbB2/PI 3-K/Akt pathway.* Oncogene, 2003. **22**(14): p. 2073-87.

97.   Stoica, G.E., et al., *Estradiol rapidly activates Akt via the ErbB2 signaling pathway.* Mol Endocrinol, 2003. **17**(5): p. 818-30.

98.   Ferrero-Pous, M., et al., *Relationship between c-erbB-2 and other tumor characteristics in breast cancer prognosis.* Clin Cancer Res, 2000. **6**(12): p. 4745-54.

99.   Zhang, J. and Y. Liu, *HER2 over-expression and response to different chemotherapy regimens in breast cancer.* J Zhejiang Univ Sci B, 2008. **9**(1): p. 5-9.

100.   Muss, H.B., et al., *c-erbB-2 expression and response to adjuvant therapy in women with node-positive early breast cancer.* N Engl J Med, 1994. **330**(18): p. 1260-6.

101.   Carlomagno, C., et al., *c-erb B2 overexpression decreases the benefit of adjuvant tamoxifen in early-stage breast cancer without axillary lymph node metastases.* J Clin Oncol, 1996. **14**(10): p. 2702-8.

102.   Baselga, J., et al., *Phase II study of weekly intravenous recombinant humanized anti-p185HER2 monoclonal antibody in patients with HER2/neu-overexpressing metastatic breast cancer.* J Clin Oncol, 1996. **14**(3): p. 737-44.

103.   Slamon, D.J., et al., *Use of chemotherapy plus a monoclonal antibody against HER2 for metastatic breast cancer that overexpresses HER2.* N Engl J Med, 2001. **344**(11): p. 783-92.

104.   Arnould, L., et al., *Pathologic complete response to trastuzumab-based neoadjuvant therapy is related to the level of HER-2 amplification.* Clin Cancer Res, 2007. **13**(21): p. 6404-9.

105.   Scaltriti, M., et al., *Expression of p95HER2, a truncated form of the HER2 receptor, and response to anti-HER2 therapies in breast cancer.* J Natl Cancer Inst, 2007. **99**(8): p. 628-38.

106.   Harris, L., et al., *American Society of Clinical Oncology 2007 update of recommendations for the use of tumor markers in breast cancer.* J Clin Oncol, 2007. **25**(33): p. 5287-312.

107.   Bilancia, D., et al., *Lapatinib in breast cancer.* Ann Oncol, 2007. **18 Suppl 6**: p. vi26-30.

108.   Johnston, S., et al., *Phase II Study of Predictive Biomarker Profiles for Response Targeting Human Epidermal Growth Factor Receptor 2 (HER-2) in Advanced Inflammatory Breast Cancer With Lapatinib Monotherapy.* J Clin Oncol, 2008.

109.   Tokuda, Y., et al., *In vitro and in vivo anti-tumour effects of a humanised monoclonal antibody against c-erbB-2 product.* Br J Cancer, 1996. **73**(11): p. 1362-5.

110.   Kamath, S. and J.K. Buolamwini, *Targeting EGFR and HER-2 receptor tyrosine kinases for cancer drug discovery and development.* Med Res Rev, 2006. **26**(5): p. 569-94.

111.   Walshe, J.M., et al., *A phase II trial with trastuzumab and pertuzumab in patients with HER2-overexpressed locally advanced and metastatic breast cancer.* Clin Breast Cancer, 2006. **6**(6): p. 535-9.

112.   Nahta, R., M.C. Hung, and F.J. Esteva, *The HER-2-targeting antibodies trastuzumab and pertuzumab synergistically inhibit the survival of breast cancer cells.* Cancer Res, 2004. **64**(7): p. 2343-6.

113.   Konecny, G.E., et al., *Activity of the dual kinase inhibitor lapatinib (GW572016) against HER-2-overexpressing and trastuzumab-treated breast cancer cells.* Cancer Res, 2006. **66**(3): p. 1630-9.

114.   Burris, H.A., 3rd, et al., *Phase I safety, pharmacokinetics, and clinical activity study of lapatinib (GW572016), a reversible dual inhibitor of epidermal growth factor receptor tyrosine kinases, in heavily pretreated patients with metastatic carcinomas.* J Clin Oncol, 2005. **23**(23): p. 5305-13.

115.   Moasser, M.M., *Targeting the function of the HER2 oncogene in human cancer therapeutics.* Oncogene, 2007. **26**(46): p. 6577-92.

116.   Meric-Bernstam, F. and M.C. Hung, *Advances in targeting human epidermal growth factor receptor-2 signaling for cancer therapy.* Clin Cancer Res, 2006. **12**(21): p. 6326-30.

117.   Yeon, C.H. and M.D. Pegram, *Anti-erbB-2 antibody trastuzumab in the treatment of HER2-amplified breast cancer.* Invest New Drugs, 2005. **23**(5): p. 391-409.

118.   Austin, C.D., et al., *Endocytosis and sorting of ErbB2 and the site of action of cancer therapeutics trastuzumab and geldanamycin.* Mol Biol Cell, 2004. **15**(12): p. 5268-82.

119.   Nahta, R. and F.J. Esteva, *Herceptin: mechanisms of action and resistance.* Cancer Lett, 2006. **232**(2): p. 123-38.

120.   Gennari, R., et al., *Pilot study of the mechanism of action of preoperative trastuzumab in patients with primary operable breast tumors overexpressing HER2.* Clin Cancer Res, 2004. **10**(17): p. 5650-5.

121.   Delord, J.P., et al., *Selective inhibition of HER2 inhibits AKT signal transduction and prolongs disease-free survival in a micrometastasis model of ovarian carcinoma.* Ann Oncol, 2005. **16**(12): p. 1889-97.

122.   Nagata, Y., et al., *PTEN activation contributes to tumor inhibition by trastuzumab, and loss of PTEN predicts trastuzumab resistance in patients.* Cancer Cell, 2004. **6**(2): p. 117-27.

123. Christianson, T.A., et al., *NH2-terminally truncated HER-2/neu protein: relationship with shedding of the extracellular domain and with prognostic factors in breast cancer.* Cancer Res, 1998. **58**(22): p. 5123-9.

124. Hudelist, G., et al., *Her-2/neu-triggered intracellular tyrosine kinase activation: in vivo relevance of ligand-independent activation mechanisms and impact upon the efficacy of trastuzumab-based treatment.* Br J Cancer, 2003. **89**(6): p. 983-91.

125. Molina, M.A., et al., *Trastuzumab (herceptin), a humanized anti-Her2 receptor monoclonal antibody, inhibits basal and activated Her2 ectodomain cleavage in breast cancer cells.* Cancer Res, 2001. **61**(12): p. 4744-9.

126. Kostler, W.J., et al., *Monitoring of serum Her-2/neu predicts response and progression-free survival to trastuzumab-based treatment in patients with metastatic breast cancer.* Clin Cancer Res, 2004. **10**(5): p. 1618-24.

127. Esteva, F.J., et al., *Clinical utility of serum HER2/neu in monitoring and prediction of progression-free survival in metastatic breast cancer patients treated with trastuzumab-based therapies.* Breast Cancer Res, 2005. **7**(4): p. R436-43.

128. Valabrega, G., F. Montemurro, and M. Aglietta, *Trastuzumab: mechanism of action, resistance and future perspectives in HER2-overexpressing breast cancer.* Ann Oncol, 2007.

129. Yakes, F.M., et al., *Herceptin-induced inhibition of phosphatidylinositol-3 kinase and Akt Is required for antibody-mediated effects on p27, cyclin D1, and antitumor action.* Cancer Res, 2002. **62**(14): p. 4132-41.

130. Lane, H.A., et al., *Modulation of p27/Cdk2 complex formation through 4D5-mediated inhibition of HER2 receptor signaling.* Ann Oncol, 2001. **12 Suppl 1**: p. S21-2.

131. Le, X.F., et al., *The role of cyclin-dependent kinase inhibitor p27Kip1 in anti-HER2 antibody-induced G1 cell cycle arrest and tumor growth inhibition.* J Biol Chem, 2003. **278**(26): p. 23441-50.

132. Le, X.F., F. Pruefer, and R.C. Bast, Jr., *HER2-targeting antibodies modulate the cyclin-dependent kinase inhibitor p27Kip1 via multiple signaling pathways.* Cell Cycle, 2005. **4**(1): p. 87-95.

133. Vogel, C.L., et al., *Efficacy and safety of trastuzumab as a single agent in first-line treatment of HER2-overexpressing metastatic breast cancer.* J Clin Oncol, 2002. **20**(3): p. 719-26.

134. Mohsin, S.K., et al., *Neoadjuvant trastuzumab induces apoptosis in primary breast cancers.* J Clin Oncol, 2005. **23**(11): p. 2460-8.

135. Menard, S., et al., *Apoptosis induction by trastuzumab: possible role of the core biopsy intervention.* J Clin Oncol, 2005. **23**(28): p. 7238-40.

136. Lee, S., et al., *Enhanced sensitization to taxol-induced apoptosis by herceptin pretreatment in ErbB2-overexpressing breast cancer cells.* Cancer Res, 2002. **62**(20): p. 5703-10.

137. Henson, E.S., X. Hu, and S.B. Gibson, *Herceptin sensitizes ErbB2-overexpressing cells to apoptosis by reducing antiapoptotic Mcl-1 expression.* Clin Cancer Res, 2006. **12**(3 Pt 1): p. 845-53.

138. Cuello, M., et al., *Down-regulation of the erbB-2 receptor by trastuzumab (herceptin) enhances tumor necrosis factor-related apoptosis-inducing ligand-mediated apoptosis in breast and ovarian cancer cell lines that overexpress erbB-2.* Cancer Res, 2001. **61**(12): p. 4892-900.

139. Konecny, G.E., et al., *Association between HER-2/neu and vascular endothelial growth factor expression predicts clinical outcome in primary breast cancer patients.* Clin Cancer Res, 2004. **10**(5): p. 1706-16.

140. Laughner, E., et al., *HER2 (neu) signaling increases the rate of hypoxia-inducible factor 1alpha (HIF-1alpha) synthesis: novel mechanism for HIF-1-mediated vascular endothelial growth factor expression.* Mol Cell Biol, 2001. **21**(12): p. 3995-4004.

141. Yen, L., et al., *Heregulin selectively upregulates vascular endothelial growth factor secretion in cancer cells and stimulates angiogenesis.* Oncogene, 2000. **19**(31): p. 3460-9.

142. Izumi, Y., et al., *Tumour biology: herceptin acts as an anti-angiogenic cocktail.* Nature, 2002. **416**(6878): p. 279-80.

143. Klos, K.S., et al., *Combined trastuzumab and paclitaxel treatment better inhibits ErbB-2-mediated angiogenesis in breast carcinoma through a more effective inhibition of Akt than either treatment alone.* Cancer, 2003. **98**(7): p. 1377-85.

144. Klos, K.S., et al., *ErbB2 increases vascular endothelial growth factor protein synthesis via activation of mammalian target of rapamycin/p70S6K leading to increased angiogenesis and spontaneous metastasis of human breast cancer cells.* Cancer Res, 2006. **66**(4): p. 2028-37.

145. Pietras, R.J., et al., *Antibody to HER-2/neu receptor blocks DNA repair after cisplatin in human breast and ovarian cancer cells.* Oncogene, 1994. **9**(7): p. 1829-38.

146. Pegram, M.D., et al., *Rational combinations of trastuzumab with chemotherapeutic drugs used in the treatment of breast cancer.* J Natl Cancer Inst, 2004. **96**(10): p. 739-49.

147. Pietras, R.J., et al., *Monoclonal antibody to HER-2/neureceptor modulates repair of radiation-induced DNA damage and enhances radiosensitivity of human breast cancer cells overexpressing this oncogene.* Cancer Res, 1999. **59**(6): p. 1347-55.

148. Pietras, R.J., et al., *Remission of human breast cancer xenografts on therapy with humanized monoclonal antibody to HER-2 receptor and DNA-reactive drugs.* Oncogene, 1998. **17**(17): p. 2235-49.

149. Mayfield, S., J.P. Vaughn, and T.E. Kute, *DNA strand breaks and cell cycle perturbation in herceptin treated breast cancer cell lines.* Breast Cancer Res Treat, 2001. **70**(2): p. 123-9.

150. Kauraniemi, P., et al., *Effects of Herceptin treatment on global gene expression patterns in HER2-amplified and nonamplified breast cancer cell lines.* Oncogene, 2004. **23**(4): p. 1010-3.

151. Clynes, R.A., et al., *Inhibitory Fc receptors modulate in vivo cytoxicity against tumor targets.* Nat Med, 2000. **6**(4): p. 443-6.

152. Cobleigh, M.A., et al., *Multinational study of the efficacy and safety of humanized anti-HER2 monoclonal antibody in women who have HER2-overexpressing metastatic breast cancer that has progressed after chemotherapy for metastatic disease.* J Clin Oncol, 1999. **17**(9): p. 2639-48.

153. Tokunaga, E., et al., *Trastuzumab and breast cancer: developments and current status.* Int J Clin Oncol, 2006. **11**(3): p. 199-208.

154. Sawyer, D.B., et al., *Modulation of anthracycline-induced myofibrillar disarray in rat ventricular myocytes by neuregulin-1beta and anti-erbB2: potential mechanism for trastuzumab-induced cardiotoxicity.* Circulation, 2002. **105**(13): p. 1551-4.

155.   Piccart-Gebhart, M.J., *Adjuvant trastuzumab therapy for HER2-overexpressing breast cancer: what we know and what we still need to learn.* Eur J Cancer, 2006. **42**(12): p. 1715-9.

156.   Viani, G.A., et al., *Adjuvant trastuzumab in the treatment of her-2-positive early breast cancer: a meta-analysis of published randomized trials.* BMC Cancer, 2007. **7**: p. 153.

157.   Buzdar, A.U., et al., *Significantly higher pathologic complete remission rate after neoadjuvant therapy with trastuzumab, paclitaxel, and epirubicin chemotherapy: results of a randomized trial in human epidermal growth factor receptor 2-positive operable breast cancer.* J Clin Oncol, 2005. **23**(16): p. 3676-85.

158.   Nahta, R. and F.J. Esteva, *Trastuzumab: triumphs and tribulations.* Oncogene, 2007. **26**(25): p. 3637-43.

159.   Nagy, P., et al., *Decreased accessibility and lack of activation of ErbB2 in JIMT-1, a herceptin-resistant, MUC4-expressing breast cancer cell line.* Cancer Res, 2005. **65**(2): p. 473-82.

160.   Liu, P.C., et al., *Identification of ADAM10 as a major source of HER2 ectodomain sheddase activity in HER2 overexpressing breast cancer cells.* Cancer Biol Ther, 2006. **5**(6): p. 657-64.

161.   Cho, H.S., et al., *Structure of the extracellular region of HER2 alone and in complex with the Herceptin Fab.* Nature, 2003. **421**(6924): p. 756-60.

162.   Agus, D.B., et al., *Targeting ligand-activated ErbB2 signaling inhibits breast and prostate tumor growth.* Cancer Cell, 2002. **2**(2): p. 127-37.

163.   Ritter, C.A., et al., *Human breast cancer cells selected for resistance to trastuzumab in vivo overexpress epidermal growth factor receptor and ErbB ligands and remain dependent on the ErbB receptor network.* Clin Cancer Res, 2007. **13**(16): p. 4909-19.

164.   Diermeier, S., et al., *Epidermal growth factor receptor coexpression modulates susceptibility to Herceptin in HER2/neu overexpressing breast cancer cells via specific erbB-receptor interaction and activation.* Exp Cell Res, 2005. **304**(2): p. 604-19.

165.   du Manoir, J.M., et al., *Strategies for delaying or treating in vivo acquired resistance to trastuzumab in human breast cancer xenografts.* Clin Cancer Res, 2006. **12**(3 Pt 1): p. 904-16.

166.   Valabrega, G., et al., *TGFalpha expression impairs Trastuzumab-induced HER2 downregulation.* Oncogene, 2005. **24**(18): p. 3002-10.

167.   Chan, C.T., M.Z. Metz, and S.E. Kane, *Differential sensitivies of trastuzumab (Herceptin)-resistant human breast cancer cells to phosphoinositide-3 kinase (PI-3K) and epidermal growth factor receptor (EGFR) kinase inhibitors.* Breast Cancer Res Treat, 2005. **91**(2): p. 187-201.

168.   Fujita, T., et al., *PTEN activity could be a predictive marker of trastuzumab efficacy in the treatment of ErbB2-overexpressing breast cancer.* Br J Cancer, 2006. **94**(2): p. 247-52.

169.   Lu, C.H., et al., *Preclinical testing of clinically applicable strategies for overcoming trastuzumab resistance caused by PTEN deficiency.* Clin Cancer Res, 2007. **13**(19): p. 5883-8.

170.   Neve, R.M., et al., *A collection of breast cancer cell lines for the study of functionally distinct cancer subtypes.* Cancer Cell, 2006. **10**(6): p. 515-27.

171.   Berns, K., et al., *A functional genetic approach identifies the PI3K pathway as a major determinant of trastuzumab resistance in breast cancer.* Cancer Cell, 2007. **12**(4): p. 395-402.

172.   Saal, L.H., et al., *PIK3CA mutations correlate with hormone receptors, node metastasis, and ERBB2, and are mutually exclusive with PTEN loss in human breast carcinoma.* Cancer Res, 2005. **65**(7): p. 2554-9.

173.   Liang, J., et al., *PKB/Akt phosphorylates p27, impairs nuclear import of p27 and opposes p27-mediated G1 arrest.* Nat Med, 2002. **8**(10): p. 1153-60.

174.   Fujita, N., S. Sato, and T. Tsuruo, *Phosphorylation of p27Kip1 at threonine 198 by p90 ribosomal protein S6 kinases promotes its binding to 14-3-3 and cytoplasmic localization.* J Biol Chem, 2003. **278**(49): p. 49254-60.

175.   Nahta, R., et al., *P27(kip1) down-regulation is associated with trastuzumab resistance in breast cancer cells.* Cancer Res, 2004. **64**(11): p. 3981-6.

176.   Kute, T., et al., *Development of Herceptin resistance in breast cancer cells.* Cytometry A, 2004. **57**(2): p. 86-93.

177.   Lu, Y., et al., *Insulin-like growth factor-I receptor signaling and resistance to trastuzumab (Herceptin).* J Natl Cancer Inst, 2001. **93**(24): p. 1852-7.

178.   Camirand, A., Y. Lu, and M. Pollak, *Co-targeting HER2/ErbB2 and insulin-like growth factor-1 receptors causes synergistic inhibition of growth in HER2-overexpressing breast cancer cells.* Med Sci Monit, 2002. **8**(12): p. BR521-6.

179.   Lu, Y., X. Zi, and M. Pollak, *Molecular mechanisms underlying IGF-I-induced attenuation of the growth-inhibitory activity of trastuzumab (Herceptin) on SKBR3 breast cancer cells.* Int J Cancer, 2004. **108**(3): p. 334-41.

180.   Jerome, L., et al., *Recombinant human insulin-like growth factor binding protein 3 inhibits growth of human epidermal growth factor receptor-2-overexpressing breast tumors and potentiates herceptin activity in vivo.* Cancer Res, 2006. **66**(14): p. 7245-52.

181.   Nahta, R., et al., *Insulin-like growth factor-I receptor/human epidermal growth factor receptor 2 heterodimerization contributes to trastuzumab resistance of breast cancer cells.* Cancer Res, 2005. **65**(23): p. 11118-28.

182.   Balana, M.E., et al., *Activation of ErbB-2 via a hierarchical interaction between ErbB-2 and type I insulin-like growth factor receptor in mammary tumor cells.* Oncogene, 2001. **20**(1): p. 34-47.

183.   Salatino, M., et al., *Inhibition of in vivo breast cancer growth by antisense oligodeoxynucleotides to type I insulin-like growth factor receptor mRNA involves inactivation of ErbBs, PI-3K/Akt and p42/p44 MAPK signaling pathways but not modulation of progesterone receptor activity.* Oncogene, 2004. **23**(30): p. 5161-74.

184.   Kostler, W.J., et al., *Insulin-like growth factor-1 receptor (IGF-1R) expression does not predict for resistance to trastuzumab-based treatment in patients with Her-2/neu overexpressing metastatic breast cancer.* J Cancer Res Clin Oncol, 2006. **132**(1): p. 9-18.

185.   Smith, B.L., et al., *The efficacy of Herceptin therapies is influenced by the expression of other erbB receptors, their ligands and the activation of downstream signalling proteins.* Br J Cancer, 2004. **91**(6): p. 1190-4.

186.   Valabrega, G., F. Montemurro, and M. Aglietta, *Trastuzumab: mechanism of action, resistance and future perspectives in HER2-overexpressing breast cancer.* Ann Oncol, 2007. **18**(6): p. 977-84.

187.   Moy, B. and P.E. Goss, *Lapatinib: Current Status and Future Directions in Breast Cancer.* Oncologist, 2006. **11**(10): p. 1047-1057.

188. Spector, N.L., et al., *Study of the biologic effects of lapatinib, a reversible inhibitor of ErbB1 and ErbB2 tyrosine kinases, on tumor growth and survival pathways in patients with advanced malignancies.* J Clin Oncol, 2005. **23**(11): p. 2502-12.

189. Xia, W., et al., *Combining lapatinib (GW572016), a small molecule inhibitor of ErbB1 and ErbB2 tyrosine kinases, with therapeutic anti-ErbB2 antibodies enhances apoptosis of ErbB2-overexpressing breast cancer cells.* Oncogene, 2005. **24**(41): p. 6213-21.

190. Chu, I., et al., *The dual ErbB1/ErbB2 inhibitor, lapatinib (GW572016), cooperates with tamoxifen to inhibit both cell proliferation- and estrogen-dependent gene expression in antiestrogen-resistant breast cancer.* Cancer Res, 2005. **65**(1): p. 18-25.

191. Xia, W., et al., *Anti-tumor activity of GW572016: a dual tyrosine kinase inhibitor blocks EGF activation of EGFR/erbB2 and downstream Erk1/2 and AKT pathways.* Oncogene, 2002. **21**(41): p. 6255-63.

192. Blackwell, K.L., et al., *Determining relevant biomarkers from tissue and serum that may predict response to single agent lapatinib in trastuzumab refractory metastatic breast cancer.* J Clin Oncol, 2005. **23 (suppl 16)**: p. Abstract 3004.

193. Xia, W., et al., *Lapatinib Antitumor Activity Is Not Dependent upon Phosphatase and Tensin Homologue Deleted on Chromosome 10 in ErbB2-Overexpressing Breast Cancers.* Cancer Res, 2007. **67**(3): p. 1170-1175.

194. Spector, N.L., et al., *EGF103009, a phase II trial of lapatinib monotherapy in patients with relapsed/refractory inflammatory breast cancer (IBC): Clinical activity and biologic predictors of response.* J Clin Oncol, 2006. **18S**: p. 502.

195. Sergina, N.V., et al., *Escape from HER-family tyrosine kinase inhibitor therapy by the kinase-inactive HER3.* Nature, 2007. **445**(7126): p. 437-41.

196. Xia, W., et al., *A model of acquired autoresistance to a potent ErbB2 tyrosine kinase inhibitor and a therapeutic strategy to prevent its onset in breast cancer.* Proc Natl Acad Sci U S A, 2006. **103**(20): p. 7795-800.

197. Baserga, R., F. Peruzzi, and K. Reiss, *The IGF-1 receptor in cancer biology.* Int J Cancer, 2003. **107**(6): p. 873-7.

198. Jones, J.I. and D.R. Clemmons, *Insulin-like growth factors and their binding proteins: biological actions.* Endocr Rev, 1995. **16**(1): p. 3-34.

199. Nakae, J., Y. Kido, and D. Accili, *Distinct and overlapping functions of insulin and IGF-I receptors.* Endocr Rev, 2001. **22**(6): p. 818-35.

200. Resnik, J.L., et al., *Elevated insulin-like growth factor I receptor autophosphorylation and kinase activity in human breast cancer.* Cancer Res, 1998. **58**(6): p. 1159-64.

201. Renehan, A.G., M. Harvie, and A. Howell, *Insulin-like growth factor (IGF)-I, IGF binding protein-3, and breast cancer risk: eight years on.* Endocr Relat Cancer, 2006. **13**(2): p. 273-8.

202. Valentinis, B., et al., *Growth and differentiation signals by the insulin-like growth factor 1 receptor in hemopoietic cells are mediated through different pathways.* J Biol Chem, 1999. **274**(18): p. 12423-30.

203. Yakar, S., et al., *Normal growth and development in the absence of hepatic insulin-like growth factor I.* Proc Natl Acad Sci U S A, 1999. **96**(13): p. 7324-9.

204. Murphy, L.J. and H.G. Friesen, *Differential effects of estrogen and growth hormone on uterine and hepatic insulin-like growth factor I gene expression in the ovariectomized hypophysectomized rat.* Endocrinology, 1988. **122**(1): p. 325-32.

205. Sussenbach, J.S., et al., *Transcriptional and post-transcriptional regulation of the human IGF-II gene expression.* Adv Exp Med Biol, 1993. **343**: p. 63-71.

206. Walenkamp, M.J., et al., *Homozygous and heterozygous expression of a novel insulin-like growth factor-I mutation.* J Clin Endocrinol Metab, 2005. **90**(5): p. 2855-64.

207. Denley, A., et al., *Molecular interactions of the IGF system.* Cytokine Growth Factor Rev, 2005. **16**(4-5): p. 421-39.

208. Pollak, M.N., *Insulin-like growth factors and neoplasia.* Novartis Found Symp, 2004. **262**: p. 84-98; discussion 98-107, 265-8.

209. Adams, T.E., et al., *Structure and function of the type 1 insulin-like growth factor receptor.* Cell Mol Life Sci, 2000. **57**(7): p. 1050-93.

210. Brandt, J., A.S. Andersen, and C. Kristensen, *Dimeric fragment of the insulin receptor alpha-subunit binds insulin with full holoreceptor affinity.* J Biol Chem, 2001. **276**(15): p. 12378-84.

211. Schaefer, E.M., K. Siddle, and L. Ellis, *Deletion analysis of the human insulin receptor ectodomain reveals independently folded soluble subdomains and insulin binding by a monomeric alpha-subunit.* J Biol Chem, 1990. **265**(22): p. 13248-53.

212. Kasuga, M., et al., *The structure of insulin receptor and its subunits. Evidence for multiple nonreduced forms and a 210,000 possible proreceptor.* J Biol Chem, 1982. **257**(17): p. 10392-9.

213. De Meyts, P. and J. Whittaker, *Structural biology of insulin and IGF1 receptors: implications for drug design.* Nat Rev Drug Discov, 2002. **1**(10): p. 769-83.

214. Garrett, T.P., et al., *Crystal structure of the first three domains of the type-1 insulin-like growth factor receptor.* Nature, 1998. **394**(6691): p. 395-9.

215. Hubbard, S.R., et al., *Crystal structure of the tyrosine kinase domain of the human insulin receptor.* Nature, 1994. **372**(6508): p. 746-54.

216. Hubbard, S.R., *Crystal structure of the activated insulin receptor tyrosine kinase in complex with peptide substrate and ATP analog.* Embo J, 1997. **16**(18): p. 5572-81.

217. Favelyukis, S., et al., *Structure and autoregulation of the insulin-like growth factor 1 receptor kinase.* Nat Struct Biol, 2001. **8**(12): p. 1058-63.

218. Brzozowski, A.M., et al., *Structural origins of the functional divergence of human insulin-like growth factor-I and insulin.* Biochemistry, 2002. **41**(30): p. 9389-97.

219. Baker, E.N., et al., *The structure of 2Zn pig insulin crystals at 1.5 A resolution.* Philos Trans R Soc Lond B Biol Sci, 1988. **319**(1195): p. 369-456.

220. Kato, H., et al., *Role of tyrosine kinase activity in signal transduction by the insulin-like growth factor-I (IGF-I) receptor. Characterization of kinase-deficient IGF-I receptors and the action of an IGF-I-mimetic antibody (alpha IR-3).* J Biol Chem, 1993. **268**(4): p. 2655-61.

221. Rubin, J.B., M.A. Shia, and P.F. Pilch, *Stimulation of tyrosine-specific phosphorylation in vitro by insulin-like growth factor I.* Nature, 1983. **305**(5933): p. 438-40.

222. Frasca, F., et al., *Insulin receptor isoform A, a newly recognized, high-affinity insulin-like growth factor II receptor in fetal and cancer cells.* Mol Cell Biol, 1999. **19**(5): p. 3278-88.

223. Soos, M.A., C.E. Field, and K. Siddle, *Purified hybrid insulin/insulin-like growth factor-I receptors bind insulin-like growth factor-I, but not insulin, with high affinity.* Biochem J, 1993. **290 (Pt 2)**: p. 419-26.

224. Lowe, W.L., Jr., et al., *Regulation by fasting of rat insulin-like growth factor I and its receptor. Effects on gene expression and binding.* J Clin Invest, 1989. **84**(2): p. 619-26.

225. Kim, J.J. and D. Accili, *Signalling through IGF-I and insulin receptors: where is the specificity?* Growth Horm IGF Res, 2002. **12**(2): p. 84-90.

226. Liu, J.P., et al., *Mice carrying null mutations of the genes encoding insulin-like growth factor I (Igf-1) and type 1 IGF receptor (Igf1r).* Cell, 1993. **75**(1): p. 59-72.

227. Oshima, A., et al., *The human cation-independent mannose 6-phosphate receptor. Cloning and sequence of the full-length cDNA and expression of functional receptor in COS cells.* J Biol Chem, 1988. **263**(5): p. 2553-62.

228. Kornfeld, S., *Structure and function of the mannose 6-phosphate/insulinlike growth factor II receptors.* Annu Rev Biochem, 1992. **61**: p. 307-30.

229. Scott, C.D. and S.M. Firth, *The role of the M6P/IGF-II receptor in cancer: tumor suppression or garbage disposal?* Horm Metab Res, 2004. **36**(5): p. 261-71.

230. Firth, S.M. and R.C. Baxter, *Cellular actions of the insulin-like growth factor binding proteins.* Endocr Rev, 2002. **23**(6): p. 824-54.

231. Clemmons, D.R., *Use of mutagenesis to probe IGF-binding protein structure/function relationships.* Endocr Rev, 2001. **22**(6): p. 800-17.

232. Baxter, R.C., *Insulin-like growth factor (IGF)-binding proteins: interactions with IGFs and intrinsic bioactivities.* Am J Physiol Endocrinol Metab, 2000. **278**(6): p. E967-76.

233. Hwa, V., Y. Oh, and R.G. Rosenfeld, *The insulin-like growth factor-binding protein (IGFBP) superfamily.* Endocr Rev, 1999. **20**(6): p. 761-87.

234. Carrick, F.E., B.E. Forbes, and J.C. Wallace, *BIAcore analysis of bovine insulin-like growth factor (IGF)-binding protein-2 identifies major IGF binding site determinants in both the amino- and carboxyl-terminal domains.* J Biol Chem, 2001. **276**(29): p. 27120-8.

235. Standker, L., et al., *Partial IGF affinity of circulating N- and C-terminal fragments of human insulin-like growth factor binding protein-4 (IGFBP-4) and the disulfide bonding pattern of the C-terminal IGFBP-4 domain.* Biochemistry, 2000. **39**(17): p. 5082-8.

236. Frystyk, J., *Free insulin-like growth factors -- measurements and relationships to growth hormone secretion and glucose homeostasis.* Growth Horm IGF Res, 2004. **14**(5): p. 337-75.

237. Mohan, S. and D.J. Baylink, *IGF-binding proteins are multifunctional and act via IGF-dependent and -independent mechanisms.* J Endocrinol, 2002. **175**(1): p. 19-31.

238. Fang, P., V. Hwa, and R. Rosenfeld, *IGFBPs and cancer.* Novartis Found Symp, 2004. **262**: p. 215-30; discussion 230-4, 265-8.

239. Kato, H., et al., *Essential role of tyrosine residues 1131, 1135, and 1136 of the insulin-like growth factor-I (IGF-I) receptor in IGF-I action.* Mol Endocrinol, 1994. **8**(1): p. 40-50.

240. O'Connor, R., et al., *Identification of domains of the insulin-like growth factor I receptor that are required for protection from apoptosis.* Mol Cell Biol, 1997. **17**(1): p. 427-35.

241. Ward, C.W., et al., *Systematic mapping of potential binding sites for Shc and Grb2 SH2 domains on insulin receptor substrate-1 and the receptors for insulin,*

epidermal growth factor, platelet-derived growth factor, and fibroblast growth factor. J Biol Chem, 1996. **271**(10): p. 5603-9.

242. Xu, P., A.R. Jacobs, and S.I. Taylor, *Interaction of insulin receptor substrate 3 with insulin receptor, insulin receptor-related receptor, insulin-like growth factor-1 receptor, and downstream signaling proteins.* J Biol Chem, 1999. **274**(21): p. 15262-70.

243. Butler, A.A., et al., *Insulin-like growth factor-I receptor signal transduction: at the interface between physiology and cell biology.* Comp Biochem Physiol B Biochem Mol Biol, 1998. **121**(1): p. 19-26.

244. Chow, J.C., G. Condorelli, and R.J. Smith, *Insulin-like growth factor-I receptor internalization regulates signaling via the Shc/mitogen-activated protein kinase pathway, but not the insulin receptor substrate-1 pathway.* J Biol Chem, 1998. **273**(8): p. 4672-80.

245. Sasaoka, T., et al., *Shc is the predominant signaling molecule coupling insulin receptors to activation of guanine nucleotide releasing factor and p21ras-GTP formation.* J Biol Chem, 1994. **269**(14): p. 10734-8.

246. Peruzzi, F., et al., *Multiple signaling pathways of the insulin-like growth factor 1 receptor in protection from apoptosis.* Mol Cell Biol, 1999. **19**(10): p. 7203-15.

247. Jiang, Y., et al., *Effect of tyrosine mutations on the kinase activity and transforming potential of an oncogenic human insulin-like growth factor I receptor.* J Biol Chem, 1996. **271**(1): p. 160-7.

248. Blakesley, V.A., et al., *Tumorigenic and mitogenic capacities are reduced in transfected fibroblasts expressing mutant insulin-like growth factor (IGF)-I receptors. The role of tyrosine residues 1250, 1251, and 1316 in the carboxy-terminus of the IGF-I receptor.* Endocrinology, 1996. **137**(2): p. 410-7.

249. Hernandez-Sanchez, C., et al., *The role of the tyrosine kinase domain of the insulin-like growth factor-I receptor in intracellular signaling, cellular proliferation, and tumorigenesis.* J Biol Chem, 1995. **270**(49): p. 29176-81.

250. Hongo, A., et al., *Mutational analysis of the mitogenic and transforming activities of the insulin-like growth factor I receptor.* Oncogene, 1996. **12**(6): p. 1231-8.

251. Yakar, S., D. Leroith, and P. Brodt, *The role of the growth hormone/insulin-like growth factor axis in tumor growth and progression: Lessons from animal models.* Cytokine Growth Factor Rev, 2005. **16**(4-5): p. 407-20.

252. Aimaretti, G., et al., *Diagnostic reliability of a single IGF-I measurement in 237 adults with total anterior hypopituitarism and severe GH deficiency.* Clin Endocrinol (Oxf), 2003. **59**(1): p. 56-61.

253. Krajcik, R.A., et al., *Insulin-like growth factor I (IGF-I), IGF-binding proteins, and breast cancer.* Cancer Epidemiol Biomarkers Prev, 2002. **11**(12): p. 1566-73.

254. Schernhammer, E.S., et al., *Circulating levels of insulin-like growth factors, their binding proteins, and breast cancer risk.* Cancer Epidemiol Biomarkers Prev, 2005. **14**(3): p. 699-704.

255. Platz, E.A., et al., *Plasma insulin-like growth factor-1 and binding protein-3 and subsequent risk of prostate cancer in the PSA era.* Cancer Causes Control, 2005. **16**(3): p. 255-62.

256. Hankinson, S.E., et al., *Circulating concentrations of insulin-like growth factor-I and risk of breast cancer.* Lancet, 1998. **351**(9113): p. 1393-6.

257. Toniolo, P., et al., *Serum insulin-like growth factor-I and breast cancer.* Int J Cancer, 2000. **88**(5): p. 828-32.

258. Allen, N.E., et al., *A prospective study of serum insulin-like growth factor-I (IGF-I), IGF-II, IGF-binding protein-3 and breast cancer risk.* Br J Cancer, 2005. **92**(7): p. 1283-7.

259. Li, H., et al., *Growth hormone induces bone morphogenetic proteins and bone-related proteins in the developing rat periodontium.* J Bone Miner Res, 2001. **16**(6): p. 1068-76.

260. Renehan, A.G., et al., *Insulin-like growth factor (IGF)-I, IGF binding protein-3, and cancer risk: systematic review and meta-regression analysis.* Lancet, 2004. **363**(9418): p. 1346-53.

261. Jenkins, P.J. and S.A. Bustin, *Evidence for a link between IGF-I and cancer.* Eur J Endocrinol, 2004. **151 Suppl 1**: p. S17-22.

262. Del Giudice, M.E., et al., *Insulin and related factors in premenopausal breast cancer risk.* Breast Cancer Res Treat, 1998. **47**(2): p. 111-20.

263. Vadgama, J.V., et al., *Plasma insulin-like growth factor-I and serum IGF-binding protein 3 can be associated with the progression of breast cancer, and predict the risk of recurrence and the probability of survival in African-American and Hispanic women.* Oncology, 1999. **57**(4): p. 330-40.

264. Li, B.D., et al., *Free insulin-like growth factor-I and breast cancer risk.* Int J Cancer, 2001. **91**(5): p. 736-9.

265. Holdaway, I.M., et al., *Serum levels of insulin-like growth factor binding protein-3 in benign and malignant breast disease.* Aust N Z J Surg, 1999. **69**(7): p. 495-500.

266. Bruning, P.F., et al., *Insulin-like growth-factor-binding protein 3 is decreased in early-stage operable pre-menopausal breast cancer.* Int J Cancer, 1995. **62**(3): p. 266-70.

267. Bohlke, K., et al., *Insulin-like growth factor-I in relation to premenopausal ductal carcinoma in situ of the breast.* Epidemiology, 1998. **9**(5): p. 570-3.

268. Hirose, K., et al., *Insulin, insulin-like growth factor-I and breast cancer risk in Japanese women.* Asian Pac J Cancer Prev, 2003. **4**(3): p. 239-46.

269. Petridou, E., et al., *Leptin and insulin growth factor I in relation to breast cancer (Greece).* Cancer Causes Control, 2000. **11**(5): p. 383-8.

270. Yu, H., et al., *Insulin-like growth factors and breast cancer risk in Chinese women.* Cancer Epidemiol Biomarkers Prev, 2002. **11**(8): p. 705-12.

271. Agurs-Collins, T., et al., *Insulin-like growth factor-1 and breast cancer risk in postmenopausal African-American women.* Cancer Detect Prev, 2000. **24**(3): p. 199-206.

272. Rollison, D.E., et al., *Premenopausal levels of circulating insulin-like growth factor I and the risk of postmenopausal breast cancer.* Int J Cancer, 2006. **118**(5): p. 1279-84.

273. Happerfield, L.C., et al., *The localization of the insulin-like growth factor receptor 1 (IGFR-1) in benign and malignant breast tissue.* J Pathol, 1997. **183**(4): p. 412-7.

274. Papa, V., et al., *Insulin-like growth factor-I receptors are overexpressed and predict a low risk in human breast cancer.* Cancer Res, 1993. **53**(16): p. 3736-40.

275. Peyrat, J.P., et al., *Insulin-like growth factor 1 receptors (IGF1-R) and IGF1 in human breast tumors.* J Steroid Biochem Mol Biol, 1990. **37**(6): p. 823-7.

276. Jammes, H., et al., *Insulin-like growth factor 1 receptors in human breast tumour: localisation and quantification by histo-autoradiographic analysis.* Br J Cancer, 1992. **66**(2): p. 248-53.

277. Nielsen, T.O., et al., *Expression of the insulin-like growth factor I receptor and urokinase plasminogen activator in breast cancer is associated with poor survival: potential for intervention with 17-allylamino geldanamycin.* Cancer Res, 2004. **64**(1): p. 286-91.

278. Shimizu, C., et al., *Expression of insulin-like growth factor 1 receptor in primary breast cancer: immunohistochemical analysis.* Hum Pathol, 2004. **35**(12): p. 1537-42.

279. Ueda, S., et al., *Alternative tyrosine phosphorylation of signaling kinases according to hormone receptor status in breast cancer overexpressing the insulin-like growth factor receptor type 1.* Cancer Sci, 2006. **97**(7): p. 597-604.

280. Shin, A., et al., *Expression patterns of insulin-like growth factor 1 (IGF-I) and its receptor in mammary tissues and their associations with breast cancer survival.* Breast Cancer Res Treat, 2006.

281. Chong, Y.M., et al., *Insulin-like growth factor 1 (IGF-1) and its receptor mRNA levels in breast cancer and adjacent non-neoplastic tissue.* Anticancer Res, 2006. **26**(1A): p. 167-73.

282. Nardon, E., et al., *Insulin-like growth factor system gene expression in women with type 2 diabetes and breast cancer.* J Clin Pathol, 2003. **56**(8): p. 599-604.

283. Voskuil, D.W., et al., *Insulin-like growth factor (IGF)-system mRNA quantities in normal and tumor breast tissue of women with sporadic and familial breast cancer risk.* Breast Cancer Res Treat, 2004. **84**(3): p. 225-33.

284. Schnarr, B., et al., *Down-regulation of insulin-like growth factor-I receptor and insulin receptor substrate-1 expression in advanced human breast cancer.* Int J Cancer, 2000. **89**(6): p. 506-13.

285. Koda, M., et al., *Expression of the insulin-like growth factor-I receptor in primary breast cancer and lymph node metastases: correlations with estrogen receptors alpha and beta.* Horm Metab Res, 2003. **35**(11-12): p. 794-801.

286. LeRoith, D. and C.T. Roberts, Jr., *The insulin-like growth factor system and cancer.* Cancer Lett, 2003. **195**(2): p. 127-37.

287. Sperandio, S., I. de Belle, and D.E. Bredesen, *An alternative, nonapoptotic form of programmed cell death.* Proc Natl Acad Sci U S A, 2000. **97**(26): p. 14376-81.

288. Koda, M., et al., *Expression of insulin-like growth factor-I receptor, estrogen receptor alpha, Bcl-2 and Bax proteins in human breast cancer.* Oncol Rep, 2005. **14**(1): p. 93-8.

289. De Leon, D.D., et al., *Demonstration of insulin-like growth factor (IGF-I and -II) receptors and binding protein in human breast cancer cell lines.* Biochem Biophys Res Commun, 1988. **152**(1): p. 398-405.

290. Rubin, R. and R. Baserga, *Insulin-like growth factor-I receptor. Its role in cell proliferation, apoptosis, and tumorigenicity.* Lab Invest, 1995. **73**(3): p. 311-31.

291. Pandini, G., et al., *Insulin and insulin-like growth factor-I (IGF-I) receptor overexpression in breast cancers leads to insulin/IGF-I hybrid receptor overexpression: evidence for a second mechanism of IGF-I signaling.* Clin Cancer Res, 1999. **5**(7): p. 1935-44.

292. Surmacz, E., *Function of the IGF-I receptor in breast cancer.* J Mammary Gland Biol Neoplasia, 2000. **5**(1): p. 95-105.

293. Rocha, R.L., et al., *Insulin-like growth factor binding protein-3 and insulin receptor substrate-1 in breast cancer: correlation with clinical parameters and disease-free survival.* Clin Cancer Res, 1997. **3**(1): p. 103-9.

294.   Koda, M., et al., *Expression of insulin receptor substrate 1 in primary breast cancer and lymph node metastases.* J Clin Pathol, 2005. **58**(6): p. 645-9.

295.   DeAngelis, T., et al., *Transformation by the simian virus 40 T antigen is regulated by IGF-I receptor and IRS-1 signaling.* Oncogene, 2006. **25**(1): p. 32-42.

296.   Byron, S.A., et al., *Insulin receptor substrates mediate distinct biological responses to insulin-like growth factor receptor activation in breast cancer cells.* Br J Cancer, 2006. **95**(9): p. 1220-8.

297.   Nagle, J.A., et al., *Involvement of insulin receptor substrate 2 in mammary tumor metastasis.* Mol Cell Biol, 2004. **24**(22): p. 9726-35.

298.   Zhang, X. and D. Yee, *Tyrosine kinase signalling in breast cancer: insulin-like growth factors and their receptors in breast cancer.* Breast Cancer Res, 2000. **2**(3): p. 170-5.

299.   Resnicoff, M., et al., *Growth inhibition of human melanoma cells in nude mice by antisense strategies to the type 1 insulin-like growth factor receptor.* Cancer Res, 1994. **54**(18): p. 4848-50.

300.   Resnicoff, M., et al., *Rat glioblastoma cells expressing an antisense RNA to the insulin-like growth factor-1 (IGF-1) receptor are nontumorigenic and induce regression of wild-type tumors.* Cancer Res, 1994. **54**(8): p. 2218-22.

301.   D'Ambrosio, C., et al., *A soluble insulin-like growth factor I receptor that induces apoptosis of tumor cells in vivo and inhibits tumorigenesis.* Cancer Res, 1996. **56**(17): p. 4013-20.

302.   Reiss, K., et al., *Inhibition of tumor growth by a dominant negative mutant of the insulin-like growth factor I receptor with a bystander effect.* Clin Cancer Res, 1998. **4**(11): p. 2647-55.

303.   Yanochko, G.M. and W. Eckhart, *Type I insulin-like growth factor receptor over-expression induces proliferation and anti-apoptotic signaling in a three-dimensional culture model of breast epithelial cells.* Breast Cancer Res, 2006. **8**(2): p. R18.

304.   Dunn, S.E., et al., *Insulin-like growth factor 1 (IGF-1) alters drug sensitivity of HBL100 human breast cancer cells by inhibition of apoptosis induced by diverse anticancer drugs.* Cancer Res, 1997. **57**(13): p. 2687-93.

305.   Gooch, J.L., C.L. Van Den Berg, and D. Yee, *Insulin-like growth factor (IGF)-I rescues breast cancer cells from chemotherapy-induced cell death--proliferative and anti-apoptotic effects.* Breast Cancer Res Treat, 1999. **56**(1): p. 1-10.

306.   Gilmore, A.P., et al., *Activation of BAD by therapeutic inhibition of epidermal growth factor receptor and transactivation by insulin-like growth factor receptor.* J Biol Chem, 2002. **277**(31): p. 27643-50.

307.   Camirand, A., et al., *Inhibition of insulin-like growth factor-1 receptor signaling enhances growth-inhibitory and proapoptotic effects of gefitinib (Iressa) in human breast cancer cells.* Breast Cancer Res, 2005. **7**(4): p. R570-9.

308.   Nickerson, T., H. Huynh, and M. Pollak, *Insulin-like growth factor binding protein-3 induces apoptosis in MCF7 breast cancer cells.* Biochem Biophys Res Commun, 1997. **237**(3): p. 690-3.

309.   Gill, Z.P., et al., *Insulin-like growth factor-binding protein (IGFBP-3) predisposes breast cancer cells to programmed cell death in a non-IGF-dependent manner.* J Biol Chem, 1997. **272**(41): p. 25602-7.

310.   Rajah, R., B. Valentinis, and P. Cohen, *Insulin-like growth factor (IGF)-binding protein-3 induces apoptosis and mediates the effects of transforming growth*

factor-beta1 on programmed cell death through a p53- and IGF-independent mechanism. J Biol Chem, 1997. **272**(18): p. 12181-8.

311. Butt, A.J., et al., *Insulin-like growth factor-binding protein-3 modulates expression of Bax and Bcl-2 and potentiates p53-independent radiation-induced apoptosis in human breast cancer cells.* J Biol Chem, 2000. **275**(50): p. 39174-81.

312. Fowler, C.A., et al., *Insulin-like growth factor binding protein-3 (IGFBP-3) potentiates paclitaxel-induced apoptosis in human breast cancer cells.* Int J Cancer, 2000. **88**(3): p. 448-53.

313. Kim, H.S., et al., *Insulin-like growth factor-binding protein 3 induces caspase-dependent apoptosis through a death receptor-mediated pathway in MCF-7 human breast cancer cells.* Cancer Res, 2004. **64**(6): p. 2229-37.

314. Cantley, L.C. and B.G. Neel, *New insights into tumor suppression: PTEN suppresses tumor formation by restraining the phosphoinositide 3-kinase/AKT pathway.* Proc Natl Acad Sci U S A, 1999. **96**(8): p. 4240-5.

315. Engin, H., et al., *Expression of PTEN, cyclin D1, P27/KIP1 in invasive ductal carcinomas of the breast and correlation with clinicopathological parameters.* Bull Cancer, 2006. **93**(2): p. E21-6.

316. Bose, S., et al., *Allelic loss of chromosome 10q23 is associated with tumor progression in breast carcinomas.* Oncogene, 1998. **17**(1): p. 123-7.

317. Bose, S., et al., *Reduced expression of PTEN correlates with breast cancer progression.* Hum Pathol, 2002. **33**(4): p. 405-9.

318. Feilotter, H.E., et al., *Analysis of the 10q23 chromosomal region and the PTEN gene in human sporadic breast carcinoma.* Br J Cancer, 1999. **79**(5-6): p. 718-23.

319. Depowski, P.L., S.I. Rosenthal, and J.S. Ross, *Loss of expression of the PTEN gene protein product is associated with poor outcome in breast cancer.* Mod Pathol, 2001. **14**(7): p. 672-6.

320. Hwang, P.H., et al., *PTEN/MMAC1 enhances the growth inhibition by anticancer drugs with downregulation of IGF-II expression in gastric cancer cells.* Exp Mol Med, 2005. **37**(5): p. 391-8.

321. Tanno, S., et al., *AKT activation up-regulates insulin-like growth factor I receptor expression and promotes invasiveness of human pancreatic cancer cells.* Cancer Res, 2001. **61**(2): p. 589-93.

322. Yi, H.K., et al., *Impact of PTEN on the expression of insulin-like growth factors (IGFs) and IGF-binding proteins in human gastric adenocarcinoma cells.* Biochem Biophys Res Commun, 2005. **330**(3): p. 760-7.

323. Zhang, D. and P. Brodt, *Type 1 insulin-like growth factor regulates MT1-MMP synthesis and tumor invasion via PI 3-kinase/Akt signaling.* Oncogene, 2003. **22**(7): p. 974-82.

324. Zhao, H., et al., *Expression profile of genes associated with antimetastatic gene: nm23-mediated metastasis inhibition in breast carcinoma cells.* Int J Cancer, 2004. **109**(1): p. 65-70.

325. Samani, A.A., et al., *The Role of the IGF System in Cancer Growth and Metastasis: Overview and Recent Insights.* Endocr Rev, 2007.

326. Weng, L.P., et al., *PTEN inhibits insulin-stimulated MEK/MAPK activation and cell growth by blocking IRS-1 phosphorylation and IRS-1/Grb-2/Sos complex formation in a breast cancer model.* Hum Mol Genet, 2001. **10**(6): p. 605-16.

327. Weng, L.P., et al., *PTEN blocks insulin-mediated ETS-2 phosphorylation through MAP kinase, independently of the phosphoinositide 3-kinase pathway.* Hum Mol Genet, 2002. **11**(15): p. 1687-96.

328. Moorehead, R.A., et al., *Insulin-like growth factor-II regulates PTEN expression in the mammary gland.* J Biol Chem, 2003. **278**(50): p. 50422-7.

329. Martin, M.B. and A. Stoica, *Insulin-like growth factor-I and estrogen interactions in breast cancer.* J Nutr, 2002. **132**(12): p. 3799S-3801S.

330. Hamelers, I.H. and P.H. Steenbergh, *Interactions between estrogen and insulin-like growth factor signaling pathways in human breast tumor cells.* Endocr Relat Cancer, 2003. **10**(2): p. 331-45.

331. Clemons, M. and P. Goss, *Estrogen and the risk of breast cancer.* N Engl J Med, 2001. **344**(4): p. 276-85.

332. Stewart, A.J., et al., *Role of insulin-like growth factors and the type I insulin-like growth factor receptor in the estrogen-stimulated proliferation of human breast cancer cells.* J Biol Chem, 1990. **265**(34): p. 21172-8.

333. Maor, S., et al., *Estrogen receptor regulates insulin-like growth factor-I receptor gene expression in breast tumor cells: involvement of transcription factor Sp1.* J Endocrinol, 2006. **191**(3): p. 605-12.

334. Lee, A.V., et al., *Enhancement of insulin-like growth factor signaling in human breast cancer: estrogen regulation of insulin receptor substrate-1 expression in vitro and in vivo.* Mol Endocrinol, 1999. **13**(5): p. 787-96.

335. Oesterreich, S., et al., *Re-expression of estrogen receptor alpha in estrogen receptor alpha-negative MCF-7 cells restores both estrogen and insulin-like growth factor-mediated signaling and growth.* Cancer Res, 2001. **61**(15): p. 5771-7.

336. Surmacz, E. and M. Bartucci, *Role of estrogen receptor alpha in modulating IGF-I receptor signaling and function in breast cancer.* J Exp Clin Cancer Res, 2004. **23**(3): p. 385-94.

337. Jackson, J.G. and D. Yee, *IRS-1 expression and activation are not sufficient to activate downstream pathways and enable IGF-I growth response in estrogen receptor negative breast cancer cells.* Growth Horm IGF Res, 1999. **9**(5): p. 280-9.

338. Bartucci, M., et al., *Differential insulin-like growth factor I receptor signaling and function in estrogen receptor (ER)-positive MCF-7 and ER-negative MDA-MB-231 breast cancer cells.* Cancer Res, 2001. **61**(18): p. 6747-54.

339. Aronica, S.M. and B.S. Katzenellenbogen, *Stimulation of estrogen receptor-mediated transcription and alteration in the phosphorylation state of the rat uterine estrogen receptor by estrogen, cyclic adenosine monophosphate, and insulin-like growth factor-I.* Mol Endocrinol, 1993. **7**(6): p. 743-52.

340. Ignar-Trowbridge, D.M., et al., *Peptide growth factor cross-talk with the estrogen receptor requires the A/B domain and occurs independently of protein kinase C or estradiol.* Endocrinology, 1996. **137**(5): p. 1735-44.

341. Lee, A.V., et al., *Activation of estrogen receptor-mediated gene transcription by IGF-I in human breast cancer cells.* J Endocrinol, 1997. **152**(1): p. 39-47.

342. Kato, S., et al., *Activation of the estrogen receptor through phosphorylation by mitogen-activated protein kinase.* Science, 1995. **270**(5241): p. 1491-4.

343. Stoica, A., et al., *Role of insulin-like growth factor-I in regulating estrogen receptor-alpha gene expression.* J Cell Biochem, 2000. **76**(4): p. 605-14.

344. Morelli, C., et al., *Estrogen receptor-alpha regulates the degradation of insulin receptor substrates 1 and 2 in breast cancer cells.* Oncogene, 2003. **22**(26): p. 4007-16.

345. Zhang, S., et al., *Role of estrogen receptor (ER) alpha in insulin-like growth factor (IGF)-I-induced responses in MCF-7 breast cancer cells.* J Mol Endocrinol, 2005. **35**(3): p. 433-47.

346. Roudabush, F.L., et al., *Transactivation of the EGF receptor mediates IGF-1-stimulated shc phosphorylation and ERK1/2 activation in COS-7 cells.* J Biol Chem, 2000. **275**(29): p. 22583-9.

347. Burgaud, J.L. and R. Baserga, *Intracellular transactivation of the insulin-like growth factor I receptor by an epidermal growth factor receptor.* Exp Cell Res, 1996. **223**(2): p. 412-9.

348. Desbois-Mouthon, C., et al., *Impact of IGF-1R/EGFR cross-talks on hepatoma cell sensitivity to gefitinib.* Int J Cancer, 2006. **119**(11): p. 2557-66.

349. Ahmad, T., et al., *The mitogenic action of insulin-like growth factor I in normal human mammary epithelial cells requires the epidermal growth factor receptor tyrosine kinase.* J Biol Chem, 2004. **279**(3): p. 1713-9.

350. Morgillo, F., et al., *Heterodimerization of insulin-like growth factor receptor/epidermal growth factor receptor and induction of survivin expression counteract the antitumor action of erlotinib.* Cancer Res, 2006. **66**(20): p. 10100-11.

351. Jones, H.E., et al., *Insulin-like growth factor-I receptor signalling and acquired resistance to gefitinib (ZD1839; Iressa) in human breast and prostate cancer cells.* Endocr Relat Cancer, 2004. **11**(4): p. 793-814.

352. Ram, T.G., et al., *Insulin-like growth factor and epidermal growth factor independence in human mammary carcinoma cells with c-erbB-2 gene amplification and progressively elevated levels of tyrosine-phosphorylated p185erbB-2.* Mol Carcinog, 1996. **15**(3): p. 227-38.

353. Balana, M.E., et al., *Interactions between progestins and heregulin (HRG) signaling pathways: HRG acts as mediator of progestins proliferative effects in mouse mammary adenocarcinomas.* Oncogene, 1999. **18**(46): p. 6370-9.

354. Lu, Y., et al., *Overexpression of ErbB2 receptor inhibits IGF-I-induced Shc-MAPK signaling pathway in breast cancer cells.* Biochem Biophys Res Commun, 2004. **313**(3): p. 709-15.

355. Hermanto, U., C.S. Zong, and L.H. Wang, *ErbB2-overexpressing human mammary carcinoma cells display an increased requirement for the phosphatidylinositol 3-kinase signaling pathway in anchorage-independent growth.* Oncogene, 2001. **20**(51): p. 7551-62.

356. Tari, A.M. and G. Lopez-Berestein, *Serum predominantly activates MAPK and akt kinases in EGFR- and ErbB2-over-expressing cells, respectively.* Int J Cancer, 2000. **86**(2): p. 295-7.

357. Burfeind, P., et al., *Antisense RNA to the type I insulin-like growth factor receptor suppresses tumor growth and prevents invasion by rat prostate cancer cells in vivo.* Proc Natl Acad Sci U S A, 1996. **93**(14): p. 7263-8.

358. Hellawell, G.O., et al., *Chemosensitization of human prostate cancer using antisense agents targeting the type 1 insulin-like growth factor receptor.* BJU Int, 2003. **91**(3): p. 271-7.

359. Nakamura, K., et al., *Down-regulation of the insulin-like growth factor I receptor by antisense RNA can reverse the transformed phenotype of human cervical cancer cell lines.* Cancer Res, 2000. **60**(3): p. 760-5.

360. Neuenschwander, S., C.T. Roberts, Jr., and D. LeRoith, *Growth inhibition of MCF-7 breast cancer cells by stable expression of an insulin-like growth factor I receptor antisense ribonucleic acid.* Endocrinology, 1995. **136**(10): p. 4298-303.

361. Pavelic, J., et al., *Insulin-like growth factor family and combined antisense approach in therapy of lung carcinoma.* Mol Med, 2002. **8**(3): p. 149-57.

362. Scotlandi, K., et al., *Effectiveness of insulin-like growth factor I receptor antisense strategy against Ewing's sarcoma cells.* Cancer Gene Ther, 2002. **9**(3): p. 296-307.

363. Shapiro, D.N., et al., *Antisense-mediated reduction in insulin-like growth factor-I receptor expression suppresses the malignant phenotype of a human alveolar rhabdomyosarcoma.* J Clin Invest, 1994. **94**(3): p. 1235-42.

364. Macaulay, V.M., et al., *Downregulation of the type 1 insulin-like growth factor receptor in mouse melanoma cells is associated with enhanced radiosensitivity and impaired activation of Atm kinase.* Oncogene, 2001. **20**(30): p. 4029-40.

365. Chernicky, C.L., et al., *Treatment of human breast cancer cells with antisense RNA to the type I insulin-like growth factor receptor inhibits cell growth, suppresses tumorigenesis, alters the metastatic potential, and prolongs survival in vivo.* Cancer Gene Ther, 2000. **7**(3): p. 384-95.

366. Andrews, D.W., et al., *Results of a pilot study involving the use of an antisense oligodeoxynucleotide directed against the insulin-like growth factor type I receptor in malignant astrocytomas.* J Clin Oncol, 2001. **19**(8): p. 2189-200.

367. Bahr, C. and B. Groner, *The insulin like growth factor-1 receptor (IGF-1R) as a drug target: novel approaches to cancer therapy.* Growth Horm IGF Res, 2004. **14**(4): p. 287-95.

368. Bohula, E.A., et al., *The efficacy of small interfering RNAs targeted to the type 1 insulin-like growth factor receptor (IGF1R) is influenced by secondary structure in the IGF1R transcript.* J Biol Chem, 2003. **278**(18): p. 15991-7.

369. Elbashir, S.M., et al., *Duplexes of 21-nucleotide RNAs mediate RNA interference in cultured mammalian cells.* Nature, 2001. **411**(6836): p. 494-8.

370. Macaulay, V.M., *The IGF receptor as anticancer treatment target*, in *Biology of IGF-1: its interactin with insulin in health and malignant stages.* 2004, Wily, Chichester (Novartis Foundation Symposium 262). p. 235-246.

371. McVittie, C., et al., *Extended silencing of the insulin-like growth factor-I receptor gene in MCF-7 cells by serial transfection with siRNA.* Anal Biochem, 2006. **357**(2): p. 305-7.

372. Niu, J., et al., *siRNA-mediated type 1 insulin-like growth factor receptor silencing induces chemosensitization of a human liver cancer cell line with mutant P53.* Cell Biol Int, 2007. **31**(2): p. 156-64.

373. Qian, J., et al., *Suppression of Type 1 Insulin-like Growth Factor Receptor Expression by Small Interfering RNA Inhibits A549 Human Lung Cancer Cell Invasion in vitro and Metastasis in Xenograft Nude Mice.* Acta Biochim Biophys Sin (Shanghai), 2007. **39**(2): p. 137-47.

374. Zhang, H., et al., *Down-regulation of type I insulin-like growth factor receptor increases sensitivity of breast cancer cells to insulin.* Cancer Res, 2007. **67**(1): p. 391-7.

375. Filleur, S., et al., *SiRNA-mediated inhibition of vascular endothelial growth factor severely limits tumor resistance to antiangiogenic thrombospondin-1 and slows tumor vascularization and growth.* Cancer Res, 2003. **63**(14): p. 3919-22.

376.   Arteaga, C.L., et al., *Blockade of the type I somatomedin receptor inhibits growth of human breast cancer cells in athymic mice.* J Clin Invest, 1989. **84**(5): p. 1418-23.

377.   Sachdev, D. and D. Yee, *Disrupting insulin-like growth factor signaling as a potential cancer therapy.* Mol Cancer Ther, 2007. **6**(1): p. 1-12.

378.   Arteaga, C.L., *Interference of the IGF system as a strategy to inhibit breast cancer growth.* Breast Cancer Res Treat, 1992. **22**(1): p. 101-6.

379.   Jackson-Booth, P.G., et al., *Inhibition of the biologic response to insulin-like growth factor I in MCF-7 breast cancer cells by a new monoclonal antibody to the insulin-like growth factor-I receptor. The importance of receptor down-regulation.* Horm Metab Res, 2003. **35**(11-12): p. 850-6.

380.   Hailey, J., et al., *Neutralizing anti-insulin-like growth factor receptor 1 antibodies inhibit receptor function and induce receptor degradation in tumor cells.* Mol Cancer Ther, 2002. **1**(14): p. 1349-53.

381.   Maloney, E.K., et al., *An anti-insulin-like growth factor I receptor antibody that is a potent inhibitor of cancer cell proliferation.* Cancer Res, 2003. **63**(16): p. 5073-83.

382.   Li, S.L., et al., *Single-chain antibodies against human insulin-like growth factor I receptor: expression, purification, and effect on tumor growth.* Cancer Immunol Immunother, 2000. **49**(4-5): p. 243-52.

383.   Sachdev, D., et al., *A chimeric humanized single-chain antibody against the type I insulin-like growth factor (IGF) receptor renders breast cancer cells refractory to the mitogenic effects of IGF-I.* Cancer Res, 2003. **63**(3): p. 627-35.

384.   Wu, J.D., et al., *In vivo effects of the human type I insulin-like growth factor receptor antibody A12 on androgen-dependent and androgen-independent xenograft human prostate tumors.* Clin Cancer Res, 2005. **11**(8): p. 3065-74.

385.   Wang, Y., et al., *Inhibition of insulin-like growth factor-I receptor (IGF-IR) signaling and tumor cell growth by a fully human neutralizing anti-IGF-IR antibody.* Mol Cancer Ther, 2005. **4**(8): p. 1214-21.

386.   Cohen, B.D., et al., *Combination therapy enhances the inhibition of tumor growth with the fully human anti-type 1 insulin-like growth factor receptor monoclonal antibody CP-751,871.* Clin Cancer Res, 2005. **11**(5): p. 2063-73.

387.   Goetsch, L., et al., *A recombinant humanized anti-insulin-like growth factor receptor type I antibody (h7C10) enhances the antitumor activity of vinorelbine and anti-epidermal growth factor receptor therapy against human cancer xenografts.* Int J Cancer, 2005. **113**(2): p. 316-28.

388.   Lu, D., et al., *A fully human recombinant IgG-like bispecific antibody to both the epidermal growth factor receptor and the insulin-like growth factor receptor for enhanced antitumor activity.* J Biol Chem, 2005. **280**(20): p. 19665-72.

389.   Burgaud, J.L., M. Resnicoff, and R. Baserga, *Mutant IGF-I receptors as dominant negatives for growth and transformation.* Biochem Biophys Res Commun, 1995. **214**(2): p. 475-81.

390.   Brodt, P., et al., *Cooperative regulation of the invasive and metastatic phenotypes by different domains of the type I insulin-like growth factor receptor beta subunit.* J Biol Chem, 2001. **276**(36): p. 33608-15.

391.   Heron-Milhavet, L., et al., *Insulin-like growth factor-I (IGF-I) receptor activation rescues UV-damaged cells through a p38 signaling pathway. Potential role of the IGF-I receptor in DNA repair.* J Biol Chem, 2001. **276**(21): p. 18185-92.

392. Seely, B.L., G. Samimi, and N.J. Webster, *Retroviral expression of a kinase-defective IGF-I receptor suppresses growth and causes apoptosis of CHO and U87 cells in-vivo.* BMC Cancer, 2002. **2**: p. 15.

393. Scotlandi, K., et al., *Expression of an IGF-I receptor dominant negative mutant induces apoptosis, inhibits tumorigenesis and enhances chemosensitivity in Ewing's sarcoma cells.* Int J Cancer, 2002. **101**(1): p. 11-6.

394. Adachi, Y., et al., *Effects of genetic blockade of the insulin-like growth factor receptor in human colon cancer cell lines.* Gastroenterology, 2002. **123**(4): p. 1191-204.

395. Lee, C.T., et al., *Recombinant adenoviruses expressing dominant negative insulin-like growth factor-I receptor demonstrate antitumor effects on lung cancer.* Cancer Gene Ther, 2003. **10**(1): p. 57-63.

396. Min, Y., et al., *Genetic blockade of the insulin-like growth factor-I receptor: a promising strategy for human pancreatic cancer.* Cancer Res, 2003. **63**(19): p. 6432-41.

397. Dunn, S.E., et al., *A dominant negative mutant of the insulin-like growth factor-I receptor inhibits the adhesion, invasion, and metastasis of breast cancer.* Cancer Res, 1998. **58**(15): p. 3353-61.

398. Prager, D., et al., *Dominant negative inhibition of tumorigenesis in vivo by human insulin-like growth factor I receptor mutant.* Proc Natl Acad Sci U S A, 1994. **91**(6): p. 2181-5.

399. Sachdev, D., et al., *A dominant negative type I insulin-like growth factor receptor inhibits metastasis of human cancer cells.* J Biol Chem, 2004. **279**(6): p. 5017-24.

400. Liu, Y., et al., *Expression of the insulin-like growth factor I receptor C terminus as a myristylated protein leads to induction of apoptosis in tumor cells.* Cancer Res, 1998. **58**(3): p. 570-6.

401. Hongo, A., et al., *Inhibition of tumorigenesis and induction of apoptosis in human tumor cells by the stable expression of a myristylated COOH terminus of the insulin-like growth factor I receptor.* Cancer Res, 1998. **58**(11): p. 2477-84.

402. Zhang, X. and D. Yee, *Insulin-like growth factor binding protein-1 (IGFBP-1) inhibits breast cancer cell motility.* Cancer Res, 2002. **62**(15): p. 4369-75.

403. Figueroa, J.A., et al., *Recombinant insulin-like growth factor binding protein-1 inhibits IGF-I, serum, and estrogen-dependent growth of MCF-7 human breast cancer cells.* J Cell Physiol, 1993. **157**(2): p. 229-36.

404. Jerome, L., L. Shiry, and B. Leyland-Jones, *Deregulation of the IGF axis in cancer: epidemiological evidence and potential therapeutic interventions.* Endocr Relat Cancer, 2003. **10**(4): p. 561-78.

405. Shiry, L.J., et al., *Radiosensitizing effect of rhIGFBP-3 on MCF-7 breast cancer cells in vitro.* Hormone Research, 2002. **58**(266): p. (abstract P20).

406. Perks, C.M., et al., *A non-IGF binding mutant of IGFBP-3 modulates cell function in breast epithelial cells.* Biochem Biophys Res Commun, 2002. **294**(5): p. 988-94.

407. Lee, D.Y., et al., *Enhanced expression of insulin-like growth factor binding protein-3 sensitizes the growth inhibitory effect of anticancer drugs in gastric cancer cells.* Biochem Biophys Res Commun, 2002. **294**(2): p. 480-6.

408. Hochscheid, R., G. Jaques, and B. Wegmann, *Transfection of human insulin-like growth factor-binding protein 3 gene inhibits cell growth and tumorigenicity: a cell culture model for lung cancer.* J Endocrinol, 2000. **166**(3): p. 553-63.

409. Lee, H.Y., et al., *Insulin-like growth factor binding protein-3 inhibits the growth of non-small cell lung cancer.* Cancer Res, 2002. **62**(12): p. 3530-7.

410. Devi, G.R., et al., *Insulin-like growth factor binding protein-3 induces early apoptosis in malignant prostate cancer cells and inhibits tumor formation in vivo.* Prostate, 2002. **51**(2): p. 141-52.

411. Feng, Y., et al., *Novel human monoclonal antibodies to insulin-like growth factor (IGF)-II that potently inhibit the IGF receptor type I signal transduction function.* Mol Cancer Ther, 2006. **5**(1): p. 114-20.

412. Parrizas, M., et al., *Specific inhibition of insulin-like growth factor-1 and insulin receptor tyrosine kinase activity and biological function by tyrphostins.* Endocrinology, 1997. **138**(4): p. 1427-33.

413. Blum, G., A. Gazit, and A. Levitzki, *Development of new insulin-like growth factor-1 receptor kinase inhibitors using catechol mimics.* J Biol Chem, 2003. **278**(42): p. 40442-54.

414. Blum, G., A. Gazit, and A. Levitzki, *Substrate competitive inhibitors of IGF-1 receptor kinase.* Biochemistry, 2000. **39**(51): p. 15705-12.

415. Mitsiades, C.S., et al., *Inhibition of the insulin-like growth factor receptor-1 tyrosine kinase activity as a therapeutic strategy for multiple myeloma, other hematologic malignancies, and solid tumors.* Cancer Cell, 2004. **5**(3): p. 221-30.

416. Garcia-Echeverria, C., et al., *In vivo antitumor activity of NVP-AEW541-A novel, potent, and selective inhibitor of the IGF-IR kinase.* Cancer Cell, 2004. **5**(3): p. 231-9.

417. Scotlandi, K., et al., *Antitumor activity of the insulin-like growth factor-I receptor kinase inhibitor NVP-AEW541 in musculoskeletal tumors.* Cancer Res, 2005. **65**(9): p. 3868-76.

418. Hopfner, M., et al., *Blockade of IGF-1 receptor tyrosine kinase has antineoplastic effects in hepatocellular carcinoma cells.* Biochem Pharmacol, 2006. **71**(10): p. 1435-48.

419. Tanno, B., et al., *Down-regulation of insulin-like growth factor I receptor activity by NVP-AEW541 has an antitumor effect on neuroblastoma cells in vitro and in vivo.* Clin Cancer Res, 2006. **12**(22): p. 6772-80.

420. Warshamana-Greene, G.S., et al., *The insulin-like growth factor-I (IGF-I) receptor kinase inhibitor NVP-ADW742, in combination with STI571, delineates a spectrum of dependence of small cell lung cancer on IGF-I and stem cell factor signaling.* Mol Cancer Ther, 2004. **3**(5): p. 527-35.

421. Warshamana-Greene, G.S., et al., *The insulin-like growth factor-I receptor kinase inhibitor, NVP-ADW742, sensitizes small cell lung cancer cell lines to the effects of chemotherapy.* Clin Cancer Res, 2005. **11**(4): p. 1563-71.

422. Girnita, A., et al., *Cyclolignans as inhibitors of the insulin-like growth factor-1 receptor and malignant cell growth.* Cancer Res, 2004. **64**(1): p. 236-42.

423. Menu, E., et al., *Inhibiting the IGF-1 receptor tyrosine kinase with the cyclolignan PPP: an in vitro and in vivo study in the 5T33MM mouse model.* Blood, 2006. **107**(2): p. 655-60.

424. Stromberg, T., et al., *IGF-1 receptor tyrosine kinase inhibition by the cyclolignan PPP induces G2/M-phase accumulation and apoptosis in multiple myeloma cells.* Blood, 2006. **107**(2): p. 669-78.

425. Vasilcanu, D., et al., *The cyclolignan PPP induces activation loop-specific inhibition of tyrosine phosphorylation of the insulin-like growth factor-1 receptor. Link to the phosphatidyl inositol-3 kinase/Akt apoptotic pathway.* Oncogene, 2004. **23**(47): p. 7854-62.

426. Haluska, P., et al., *In vitro and in vivo antitumor effects of the dual insulin-like growth factor-I/insulin receptor inhibitor, BMS-554417.* Cancer Res, 2006. **66**(1): p. 362-71.

427. Wittman, M., et al., *Discovery of a (1H-benzoimidazol-2-yl)-1H-pyridin-2-one (BMS-536924) inhibitor of insulin-like growth factor I receptor kinase with in vivo antitumor activity.* J Med Chem, 2005. **48**(18): p. 5639-43.

428. Alban, A., et al., *A novel experimental design for comparative two-dimensional gel analysis: two-dimensional difference gel electrophoresis incorporating a pooled internal standard.* Proteomics, 2003. **3**(1): p. 36-44.

429. Ritter, C.A., et al., *Mechanisms of resistance development against trastuzumab (Herceptin) in an in vivo breast cancer model.* Int J Clin Pharmacol Ther, 2004. **42**(11): p. 642-3.

430. Dubska, L., L. Andera, and M.A. Sheard, *HER2 signaling downregulation by trastuzumab and suppression of the PI3K/Akt pathway: an unexpected effect on TRAIL-induced apoptosis.* FEBS Lett, 2005. **579**(19): p. 4149-58.

431. Peterson, J.E., et al., *c phosphorylation and activation of the IGF-I receptor in src-transformed cells.* J Biol Chem, 1994. **269**(44): p. 27315-21.

432. Lisztwan, J., et al., *The aromatase inhibitor letrozole and inhibitors of insulin-like growth factor I receptor synergistically induce apoptosis in in vitro models of estrogen-dependent breast cancer.* Breast Cancer Res, 2008. **10**(4): p. R56.

433. Kuo, M.T., *Roles of multidrug resistance genes in breast cancer chemoresistance.* Adv Exp Med Biol, 2007. **608**: p. 23-30.

434. Polli, J.W., et al., *The Role of Efflux and Uptake Transporters in Lapatinib (Tykerb, GW572016) Disposition and Drug Interactions.* Drug Metab Dispos, 2008.

435. Nadeau, S.I. and J. Landry, *Mechanisms of activation and regulation of the heat shock-sensitive signaling pathways.* Adv Exp Med Biol, 2007. **594**: p. 100-13.

436. Arya, R., M. Mallik, and S.C. Lakhotia, *Heat shock genes - integrating cell survival and death.* J Biosci, 2007. **32**(3): p. 595-610.

437. Kamradt, M.C., et al., *The small heat shock protein alpha B-crystallin is a novel inhibitor of TRAIL-induced apoptosis that suppresses the activation of caspase-3.* J Biol Chem, 2005. **280**(12): p. 11059-66.

438. Sitterding, S.M., et al., *AlphaB-crystallin: a novel marker of invasive basal-like and metaplastic breast carcinomas.* Ann Diagn Pathol, 2008. **12**(1): p. 33-40.

439. Ivanov, O., et al., *alphaB-crystallin is a novel predictor of resistance to neoadjuvant chemotherapy in breast cancer.* Breast Cancer Res Treat, 2007.

440. Harris, L.N., et al., *Predictors of resistance to preoperative trastuzumab and vinorelbine for HER2-positive early breast cancer.* Clin Cancer Res, 2007. **13**(4): p. 1198-207.

441. Lee, S.A., et al., *Expression of the Brn-3b transcription factor correlates with expression of HSP-27 in breast cancer biopsies and is required for maximal activation of the HSP-27 promoter.* Cancer Res, 2005. **65**(8): p. 3072-80.

442. Rane, M.J., et al., *Heat shock protein 27 controls apoptosis by regulating Akt activation.* J Biol Chem, 2003. **278**(30): p. 27828-35.

443. Loeffler-Ragg, J., et al., *Gefitinib-responsive EGFR-positive colorectal cancers have different proteome profiles from non-responsive cell lines.* Eur J Cancer, 2005. **41**(15): p. 2338-46.

444. Haverty, A.A., et al., *Interleukin-6 upregulates GP96 expression in breast cancer.* J Surg Res, 1997. **69**(1): p. 145-9.

445. Melendez, K., et al., *Heat shock protein 70 and glycoprotein 96 are differentially expressed on the surface of malignant and nonmalignant breast cells.* Cell Stress Chaperones, 2006. **11**(4): p. 334-42.

446. Havik, B. and C.R. Bramham, *Additive viability-loss following hsp70/hsc70 double interference and Hsp90 inhibition in two breast cancer cell lines.* Oncol Rep, 2007. **17**(6): p. 1501-10.

447. Vargas-Roig, L.M., et al., *Heat shock proteins and cell proliferation in human breast cancer biopsy samples.* Cancer Detect Prev, 1997. **21**(5): p. 441-51.

448. Ciocca, D.R., et al., *Heat shock protein hsp70 in patients with axillary lymph node-negative breast cancer: prognostic implications.* J Natl Cancer Inst, 1993. **85**(7): p. 570-4.

449. Connolly, E., et al., *Hypoxia inhibits protein synthesis through a 4E-BP1 and elongation factor 2 kinase pathway controlled by mTOR and uncoupled in breast cancer cells.* Mol Cell Biol, 2006. **26**(10): p. 3955-65.

450. Shor, B., et al., *A new pharmacologic action of CCI-779 involves FKBP12-independent inhibition of mTOR kinase activity and profound repression of global protein synthesis.* Cancer Res, 2008. **68**(8): p. 2934-43.

451. Ren, H., et al., *Farnesyltransferase inhibitor SCH66336 induces rapid phosphorylation of eukaryotic translation elongation factor 2 in head and neck squamous cell carcinoma cells.* Cancer Res, 2005. **65**(13): p. 5841-7.

452. Vazquez-Martin, A., et al., *Low-scale phosphoproteome analyses identify the mTOR effector p70 S6 kinase 1 as a specific biomarker of the dual-HER1/HER2 tyrosine kinase inhibitor lapatinib (Tykerb) in human breast carcinoma cells.* Ann Oncol, 2008. **19**(6): p. 1097-109.

453. Shuda, M., et al., *Enhanced expression of translation factor mRNAs in hepatocellular carcinoma.* Anticancer Res, 2000. **20**(4): p. 2489-94.

454. Eberle, J., K. Krasagakis, and C.E. Orfanos, *Translation initiation factor eIF-4A1 mRNA is consistently overexpressed in human melanoma cells in vitro.* Int J Cancer, 1997. **71**(3): p. 396-401.

455. Afonja, O., et al., *Induction of PDCD4 tumor suppressor gene expression by RAR agonists, antiestrogen and HER-2/neu antagonist in breast cancer cells. Evidence for a role in apoptosis.* Oncogene, 2004. **23**(49): p. 8135-45.

456. Emberley, E.D., L.C. Murphy, and P.H. Watson, *S100 proteins and their influence on pro-survival pathways in cancer.* Biochem Cell Biol, 2004. **82**(4): p. 508-15.

457. Cross, S.S., et al., *Expression of S100 proteins in normal human tissues and common cancers using tissue microarrays: S100A6, S100A8, S100A9 and S100A11 are all overexpressed in common cancers.* Histopathology, 2005. **46**(3): p. 256-69.

458. van den Bos, C., et al., *Phosphorylation of MRP14, an S100 protein expressed during monocytic differentiation, modulates Ca(2+)-dependent translocation from cytoplasm to membranes and cytoskeleton.* J Immunol, 1996. **156**(3): p. 1247-54.

459. Sanders, M.E., et al., *Differentiating proteomic biomarkers in breast cancer by laser capture microdissection and MALDI MS.* J Proteome Res, 2008. **7**(4): p. 1500-7.

460. Sommer, A., et al., *Studies on the development of resistance to the pure antiestrogen Faslodex in three human breast cancer cell lines.* J Steroid Biochem Mol Biol, 2003. **85**(1): p. 33-47.

461. Honda, K., et al., *Actinin-4, a novel actin-bundling protein associated with cell motility and cancer invasion.* J Cell Biol, 1998. **140**(6): p. 1383-93.

462. Yamamoto, S., et al., *Actinin-4 expression in ovarian cancer: a novel prognostic indicator independent of clinical stage and histological type.* Mod Pathol, 2007. **20**(12): p. 1278-85.

463. Honda, K., et al., *Actinin-4 increases cell motility and promotes lymph node metastasis of colorectal cancer.* Gastroenterology, 2005. **128**(1): p. 51-62.

464. Burger, A.M. and A.K. Seth, *The ubiquitin-mediated protein degradation pathway in cancer: therapeutic implications.* Eur J Cancer, 2004. **40**(15): p. 2217-29.

465. Yang, Y., et al., *Inhibitors of ubiquitin-activating enzyme (E1), a new class of potential cancer therapeutics.* Cancer Res, 2007. **67**(19): p. 9472-81.

466. Tzivion, G., et al., *14-3-3 proteins as potential oncogenes.* Semin Cancer Biol, 2006. **16**(3): p. 203-13.

467. Woodcock, J.M., et al., *The dimeric versus monomeric status of 14-3-3zeta is controlled by phosphorylation of Ser58 at the dimer interface.* J Biol Chem, 2003. **278**(38): p. 36323-7.

468. Horie-Inoue, K. and S. Inoue, *Epigenetic and proteolytic inactivation of 14-3-3sigma in breast and prostate cancers.* Semin Cancer Biol, 2006. **16**(3): p. 235-9.

469. Dillon, R.L., et al., *An EGR2/CITED1 transcription factor complex and the 14-3-3sigma tumor suppressor are involved in regulating ErbB2 expression in a transgenic-mouse model of human breast cancer.* Mol Cell Biol, 2007. **27**(24): p. 8648-57.

470. Chuthapisith, S., et al., *Proteomic profiling of MCF-7 breast cancer cells with chemoresistance to different types of anti-cancer drugs.* Int J Oncol, 2007. **30**(6): p. 1545-51.

471. Arpino, G., et al., *HER-2 amplification, HER-1 expression, and tamoxifen response in estrogen receptor-positive metastatic breast cancer: a southwest oncology group study.* Clin Cancer Res, 2004. **10**(17): p. 5670-6.